Dimeric histamine H_2 receptor agonists as molecular tools and genetically engineered HEK293T cells as an assay platform to unravel signaling pathways of hH_1R and hH_2R

Dissertation

zur Erlangung des Doktorgrades der Naturwissenschaften (Dr. rer. nat.)

an der Fakultät für Chemie und Pharmazie

der Universität Regensburg

vorgelegt von

Nicole Plank geb. Kagermeier

aus Straubing

2015

Die vorliegende Arbeit entstand in der Zeit von Mai 2011 bis Dezember 2014 unter der Anleitung von Herrn Prof. Dr. Armin Buschauer am Institut für Pharmazie der Naturwissenschaftlichen Fakultät IV – Chemie und Pharmazie – der Universität Regensburg.

Das Promotionsgesuch wurde eingereicht im April 2015.

Tag der mündlichen Prüfung: 30.04.2015

Prüfungsausschuss: Prof. Dr. A. Jacobi von Wangelin (Vorsitzender)
Prof. Dr. A. Buschauer (Erstgutachter)
Prof. Dr. G. Bernhardt (Zweitgutachter)
Prof. Dr. J. Heilmann (Drittprüfer)

Für Patrick

Danksagung

An dieser Stelle möchte ich mich ganz herzlich bedanken bei:

Meinem Doktorvater Herrn Prof. Dr. Armin Buschauer, der mir die Möglichkeit gegeben hat dieses Projekt zu verwirklichen, seine konstruktive Kritik bei der Durchsicht der Arbeit, die Aufnahme ins Graduiertenkolleg, seine Geduld und dass er trotz viel Arbeit stets ein offenes Ohr für mich hatte.

Herrn Professor Dr. Günther Bernhard für seine stetige Unterstützung im Laboralltag, seine fachliche Anleitung, das Durchsehen der Arbeit und natürlich auch für das schöne Sommerfest.

Herrn Professor Dr. Roland Seifert und Frau Kristin Werner für die Durchführung der Monozytenexperimente.

Herrn Professor Dr. Sigurd Elz und Frau PD Dr. Andrea Strasser für das Überlassen der H_1R Liganden.

Herrn Dr. Max Keller für die Hilfe bei der Synthese des Radioliganden und seine fachliche Kompetenz.

Herrn Dr. Paul Baumeister für seine Unterstützung bei der Testung und für die immer lustigen Unterhaltungen am Gang.

Frau Dita Fritsch und Frau Elvira Schreiber für die Hilfe der Durchführung vieler Assays.

Herrn Peter Richthammer für seine Hilfsbereitschaft und die netten Gespräche.

Frau Uta Hasselmann, Silvia Heinrich und Karin Reindl für die stets freundliche Unterstützung bei organisatorischen Angelegenheiten.

Dem Graduiertenkolleg 1910 für die Finanzierung interessanter Tagungen.

Meinen Bürokollegen: Frau Frauke Antoni, Frau Stefanie Dukorn und Herrn Andrea Pegoli (grazie buffo puffo).

„14.2.08“: Herrn Dr. Johannes Felixberger für sein enormes Wissen, seine unermüdliche Hilfsbereitschaft und die schöne Zeit auch außerhalb der Arbeit. Herrn Dr. Stefan Huber für die lustigen, aber manchmal auch fachlichen Diskussionen und seine Freundschaft. Herrn Dr. Uwe Nordemann für das Überlassen der HEK293T CRE Luc Zellen und sein unerschütterlich freundliches Gemüt.

Meinen ehemaligen Kolleginnen und Freundinnen Dr. Melanie Kaske, Dr. Carolin Meyer und Dr. Stefanie Rodler für die vielen sportlichen Aktivitäten und den schönen Abenden mit gutem Wein.

Bei Arminia Buschauer, insbesondere: Herrn Dr. Tobias Birnkammer, Herrn Dr. Roland Geyer, Herrn Dr. Tobias Holzammer, Herrn Kilian Kuhn, Herrn Sebastian Lieb, Herrn José Esteban Obreque-Balboa, Frau Dr. Miriam Pluym, Herrn Dr. Nicola Pluym, Herrn Steffen Pockes und Herrn Dr. David Wifling für die gute Zusammenarbeit und die angenehme Atmosphäre.

Zu guter letzt die Menschen, die mehr als Dank verdienen:

Alle meine Freunde außerhalb der Uni, die namentlich zu erwähnen den Rahmen sprengen würde.

Frau Maria Beer-Kroen für die enorme Unterstützung bei der Laborarbeit, die Süßigkeiten im Büro, die stets aufmunternden Worte und ihre nie endend wollende Hilfsbereitschaft.

Meine Schwiegereltern Gisela und Max für Ihre gute Laune und Ihre immerwährende Hilfsbereitschaft.

Meine Geschwister Peter und Ulrike für Ihre Unterstützung in allen Lebenslagen.

Meine Eltern auf die ich mich immer verlassen kann und ohne die es diese Arbeit sicher nicht geben würde.

Mein Mann Patrick für seine Liebe, seine unermessliche Geduld und unser kleines Igelchen.

Publications (published results prior to the submission of this thesis):

1. Kagermeier, N.; Werner, K.; Keller, M.; Baumeister, P.; Bernhardt, G.; Seifert, R.; Buschauer, A. Dimeric carbamoylguanidine-type histamine H_2 receptor ligands: A new class of potent and selective agonists. *Bioorg. Med. Chem.* **2015**.

2. Baumeister, P.; Erdmann, D.; Biselli, S.; Kagermeier, N.; Elz, S.; Bernhardt, G.; Buschauer, A. [^{3}H]UR-DE257: Development of a tritium-labeled squaramide-type selective histamine H_2 receptor antagonist. *ChemMedChem*. **2015**.

3. Kagermeier, N.; Nordemann, U.; Bernhardt, G.; König, G.; Buschauer, A. Differential Signaling Pathways of the hH_1R and the hH_2R. *Inflamm. Res*. **2014** (Abstract)

4. Birnkammer, T.; Spickenreither, A.; Brunskole, I.; Lopuch, M.; Kagermeier, N.; Bernhardt, G.; Dove, S.; Seifert, R., Elz, S.; Buschauer, A. The bivalent ligand approach leads to highly potent and selective acylguanidine-type histamine H_2 receptor agonists. *J. Med. Chem*. **2012**

Short lecture:

1. Kagermeier, N.: Differential Signaling Pathways of the hH_1R and the hH_2R. 43th Annual Meeting of the European Histamine Research Society in Lyon; **2014**.

Poster presentations:

09/11: 6th Summer School in Medicinal Chemistry, Regensburg.

Kagermeier, N.; Holzammer, T.; Bernhardt, G.; Dove, S.; Buschauer, A.: Thr^{190} in the human histamine H_2 receptor (hH_2R) contributes to binding of imidazole-type ligand**s.**

10/13: Annual meeting of the German Pharmaceutical Society (DPhG) in Freiburg.

Kagermeier, N.; Nordemann, U.; Bernhardt, G.; König, G.; Buschauer, A.: Alternative signaling pathways of the histamine H_1 (H_1R) and the histamine H_2 receptor (H_2R).

09/14: 13th International Symposium on Medicinal Chemistry (EFMC-ISMC) in Lisbon.

Kagermeier, N.; Keller, M.; Baumeister, P.; Bernhardt, G.; Buschauer, A.: Bivalent carbamoylguanidine-type H_2 receptor ligands: Potent and selective agonists, but inappropriate for radio- and fluorescence labeling.

09/14: 7th Summer School in Medicinal Chemistry, Regensburg.

Kagermeier, N.; Nordemann, U.; Felixberger, J.; Bernhardt, G.; König, G.; Buschauer, A.: Differential signaling pathways of the human histamine H_1R (hH_1R) and the human histamine H_2R (hH_2R).

Contents

1 General Introduction 1

1.1 G-protein coupled receptors 2
1.1.1 Brief history 2
1.1.2 GPCRs as drug targets 2
1.1.3 GPCR structure and classification 2
1.1.4 GPCR activation and signaling 3
1.1.4.1 Classical model 3
1.1.4.1.1 G-proteins 4
1.1.4.1.2 G-protein regulated effectors 4

1.2 Histamine and its receptors 6
1.2.1 The biogenic amine histamine 6
1.2.1.1 Brief history 6
1.2.1.2 Biosynthesis, metabolism and function 6
1.2.2 The four histamine receptors and their ligands 6
1.2.2.1 The histamine H_1R 6
1.2.2.2 The histamine H_2R 7
1.2.2.3 The histamine H_3R 9
1.2.2.4 The histamine H_4R 10

1.3 GPCR dimerization and bivalent ligands 11
1.3.1 GPCR dimerization 11
1.3.2 Bivalent ligands 12

1.4 Functional selectivity and G-protein independent signaling 13

1.5 References 15

2 Scope and Objectives 25

2.1 Dimeric carbamoylguanidine-type H_2 receptor ligands 26

2.2 Unraveling signaling pathways of the human histamine receptors H_1R and H_2R in HEK293T CRE Luc cells 26

3 Dimeric carbamoylguanidine-type H_2 receptor ligands: A new class of potent and selective agonists 27

3.1 Introduction 28

3.2 Chemistry 28
3.2.1 Homobivalent carbamoylguanidine-type H_2R ligands 28
3.2.2 Toward bivalent fluorescence- and radioligands 31

3.3 Results and Discussion 33
3.3.1 Stability of carbamoylguanidines compared to acylguanidines 33
3.3.2 Pharmacological results and discussion 34
3.3.2.1 H_2R agonism in the GTPγS binding assay 34
3.3.2.2 H_2R affinities and receptor subtype selectivities 35

3.3.2.3 Investigation of the fluorescence ligands **3.40-3.42** and the radioligand **3.43b** 36
3.3.2.4 Investigation of H_2R agonists in human monocytes[a] 40
3.3.2.5 Stability of selected carbamoylguanidines in plasma 42
3.3.2.6 Plasma protein binding 42
3.3.2.6.1 Equilibrium dialysis 42
3.3.2.6.2 Ultrafiltration 43
3.3.2.7 Cytotoxicity in the crystal violet based chemosensitivity assay 44

3.4 Summary and conclusion 46

3.5 Experimental section 47

3.5.1 General Experimental conditions 47
3.5.2 Chemistry: Experimental Protocols and Analytical data 47
3.5.3 Pharmacological Protocols 61
3.5.3.1 GTPγS binding assay 61
3.5.3.2 Competition binding experiments 61
3.5.3.3 Studies on human monocytes 61
3.5.3.4 EBAO staining 62
3.5.3.5 Stability in plasma 62
3.5.3.6 Plasma protein binding 62
3.5.3.6.1 Recovery after equillibrium dialysis 62
3.5.3.6.2 Ultrafiltration 63
3.5.3.7 Crystal violet based chemosensitivity assay 63

3.6 References 64

4 Unraveling signaling pathways of the human histamine receptors H_1R and H_2R in HEK293T CRE Luc cells 67

4.1 Introduction 68

4.2 Materials and Methods 69

4.2.1 Cell culture 69
4.2.2 Stable transfection of HEK293T CRE Luc cells with the pcDNA3.1(+)-hH_1R vector 69
4.2.3 Stable transfection of HEK293T CRE Luc cells with the pcDNA3.1(+)-hH_2R vector 70
4.2.4 Stable transfection of HEK293T CRE Luc hH_1R cells with the pcDNA3.1(-)mtAEQ plasmid 70
4.2.5 Stable transfection of HEK293T CRE Luc hH_2R cells with the pcDNA3.1(-)mtAEQ vector 70
4.2.6 Stable transfection of HEK293T CRE Luc-SF-hH_4R-His_6 with pGL4.29[luc2P/CRE/Hygro] plasmid 70
4.2.7 Whole cell radioligand binding assay 70
4.2.8 Luciferase reporter gene assay 71
4.2.9 Fura-2 Ca^{2+} assay 71
4.2.10 Aequorin assay 72
4.2.11 cAMP assay 72

4.3 Results and Discussion 73

4.3.1 Investigation of HEK293T CRE Luc cells expressing the hH_1R 73
4.3.1.1 Saturation binding assay using HEK293T CRE Luc hH_1R cells 73
4.3.1.2 Luciferase reporter gene assay using HEK293T CRE Luc hH_1R cells 73

4.3.1.2.1 Effect of $G\alpha_q$ inhibition on the H_1R dependent luciferase activity 74
4.3.1.2.2 Effect of pertussis toxin on the H_1R dependent luciferase activity 75
4.3.1.2.3 Effect of protein kinase A inhibitors on the H_1R dependent luciferase activity 77
4.3.1.2.4 Effect of the Gβγ inhibitor gallein on the H_1R dependent luciferase activity 78
4.3.1.3 Investigation of hH_1R expressing HEK293T cells in the fura-2 assay 79
4.3.1.4 Investigation of hH_1R expressing HEK293T cells in the aequorin assay 79
4.3.1.5 Investigation of hH_1R expressing HEK293T cells in a cAMP assay 81
4.3.1.5.1 Optimization of cAMP assay parameters 81
4.3.1.5.2 cAMP assay on HEK293T CRE Luc hH_1R cells 82
4.3.2 Investigation of HEK293T CRE Luc cells expressing the hH_2R 82
4.3.2.1 Saturation binding assay using HEK293T CRE Luc hH_2R cells 83
4.3.2.2 Luciferase reporter gene assay using HEK293T CRE Luc hH_2R cells 83
4.3.2.2.1 Effect of $G\alpha_q$ inhibition on the H_2R dependent luciferase activity 84
4.3.2.2.2 Effect of protein kinase A inhibitors on the H_2R stimulated luciferase activity 84
4.3.2.2.3 Effect of pertussis toxin on the H_2R stimulated luciferase activity 85
4.3.2.2.4 Effect of the Gβγ inhibitor gallein on the H_2R dependent luciferase activity 86
4.3.2.3 Investigation of hH_2R expressing HEK293T cells in the fura-2 assay 86
4.3.2.4 Investigation of hH_2R expressing HEK293T cells in the aequorin assay 86
4.3.2.5 Investigation of hH_2R expressing HEK293T cells in a cAMP assay 87

4.4 Summary and conclusion 88

4.5 References 90

5 Application of the established luciferase reporter gene assay for the functional investigation of hH_1R ligands 93

5.1 Introduction 94

5.2 Material and Methods 94

5.2.1 Cell culture 94
5.2.2 Stable transfection of HEK293T CRE Luc cells with the pcDNA3.1(+)-hH_1R vector 94
5.2.3 Luciferase reporter gene assay 94
5.2.4 Crystal violet based chemosensitivity assay 94
5.2.5 Selected test compounds 94
5.2.5.1 H_1R agonists 94
5.2.5.2 H_1R antagonists 95

5.3 Results and Discussion 96

5.3.1 Quantification of hH_1 receptors per cell 96
5.3.2 Optimization of the incubation period 96
5.3.3 Effect of the solvent on the luciferase activity 97
5.3.4 Functional characterization of H_1R ligands 97
5.3.5 Characterization of histaprodifen derivatives in the crystal violet based chemosensitivity assay 100

5.4 Summary and conclusion 101

5.5 References 102

6 Summary 103

7 Appendix 107

Chapter 1

General Introduction

1.1 G-protein coupled receptors

1.1.1 Brief history

It was in the early 20th century that binding of biologically active molecules to "specific sites on cells" was postulated for the first time by Langley and his student Dale. It is noteworthy that their studies included two of the most important families of receptors, the ion channel receptors and the G-protein coupled receptors (GPCRs).[1] Now we know that with about 800 genes, GPCRs, also refered to as seven-transmembrane domaine receptors or heptahelical receptors, represent the largest family of cell surface receptors encoded in the human genome, including approximately 400 chemosensory (olfactory and taste) receptors.[2,3]

Within the next 50 years the work of Langley and Dale was refined to the concept of classical receptor pharmacology by pioneers like e.g. Black and Furchgott.[4] The β_2-adrenergic receptor was the first GPCR to be cloned in 1986 and represents the starting point for a molecular understanding of GPCRs.[5] Another milestone in the field of GPCR research was achieved in 2000, when Palczewski and coworkers published the first high-resolution X-ray crystal structure of a GPCR, the bovine rhodopsin.[6] So far, high-resolution structures are available for 25 GPCRs, including β-adrenoceptors (avian β_1-AR[7] and human β_2-AR[8]), muscarinic acetylcholine receptors (human M_2R[9] and rat M_3R[10]), opioid receptors (human nociceptin receptor[11], human κ-OR[12], mouse μ-OR[13] and mouse δ-OR[14]) and the histamine H_1R.[15] The importance and significance of GPCRs in biomedical research was underlined in 2012 when Brian Kobilka and Robert Lefkowitz were awarded the Nobel Prize for their work in the GPCR field.

1.1.2 GPCRs as drug targets

Drugs binding to GPCRs show therapeutic benefit in a broad variety of indications, such as pain, bronchial asthma, cardiovascular diseases and neurological disorders. Although addressing only a small number of these membrane proteins,[16] more than 30 % of the approximately 500 most important approved drugs bind to GPCRs, making them the most successful therapeutic targets.[17] Endogenous ligands were identified for more than 200 GPCRs, including hormones and neurotransmitters.[18-20] The endogenous ligands of around 140 GPCRs are yet unidentified.[21] These so-called orphan GPCRs represent promising potential new drug targets.

1.1.3 GPCR structure and classification

Characteristic of all GPCRs are seven hydrophobic transmembrane (TM) domains, with an extracellular amino terminus and an intracellular carboxyl terminus (**Fig 1.1**). GPCRs share the highest homology within the TM domains, whereas the carboxyl terminus, the intracellular loop between TM5 and TM6 and the amino terminus represent the most variable structures.[22] The extracellular parts and the transmembrane regions are important for ligand binding, whereas the intracellular regions are crucial for signaling and for feedback modulation of receptor function.[23] Under evolutionary aspects, Fredriksson et al. classified GPCRs into five families: Glutamate, Rhodopsin, Adhesion, Frizzled/Taste2 and Secretin (GRAFS).[18] The rhodopsin family, by far the largest group, can be subdivided into four main groups: α, β, γ and δ. The histamine receptors belong to the α group. The rhodopsin family shows several characteristic features like the NSxxNPxxY motif in TM7, the DRY motif or

D(E)-R-Y(F) at the bottom of TM3, close to IL2.[18] Most ligands for the rhodopsin family receptors bind between the TM helices.[24]

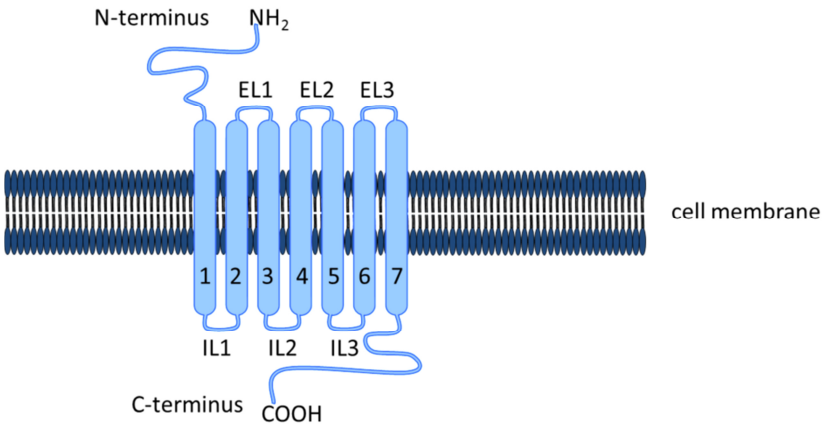

Figure 1.1. Schematic representation of a prototype class A GPCR (IL = intracellular loop; EL = extracellular loop; 1-7 = transmembrane domains)

1.1.4 GPCR activation and signaling

1.1.4.1 Classical model

Upon binding of an agonist, the receptor in its active form is functioning as a nucleotide exchange factor on the α subunit of heterotrimeric G-proteins, triggering the exchange of GDP by GTP. Thereby, the Gα subunit dissociates from the Gβγ subunit and both subunits interact with effector proteins, resulting in an increase or decrease in second messenger concentrations. The G-protein returns to its inactive state upon cleavage of GTP to GDP by the intrinsic GTPase activity of the Gα subunit (**Fig. 1.2**).[23]

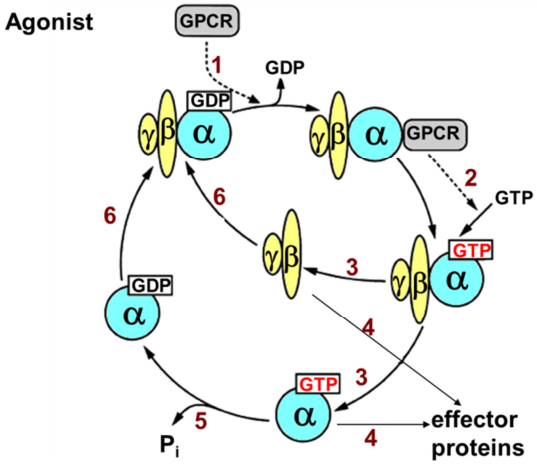

Figure 1.2. G-Protein cycle upon receptor activation by an agonist (adopted from Seifert et al. 2005).[25]

The classical model of activation of GPCRs is the ternary complex model.[26] This model was extended by the finding that numerous receptors are capable of activating G-proteins in the absence of agonists.[27] According to this extended ternary complex model (**Fig.1.3A**), the receptor exists in an inactive (R_i) and in an active (R_a) conformation. The level of basal

receptor activity is given by the equilibrium between the active and the inactive state. Ligands are classified according to their ability to shift the equilibrium. Agonists show higher affinity for R_a and stabilize the active conformation, leading to G-protein activation. Neutral antagonists bind to R_i and R_a with the same affinity and, therefore, they do not alter the equilibrium. In contrast, inverse agonists stabilize the inactive receptor conformation.[27,28]

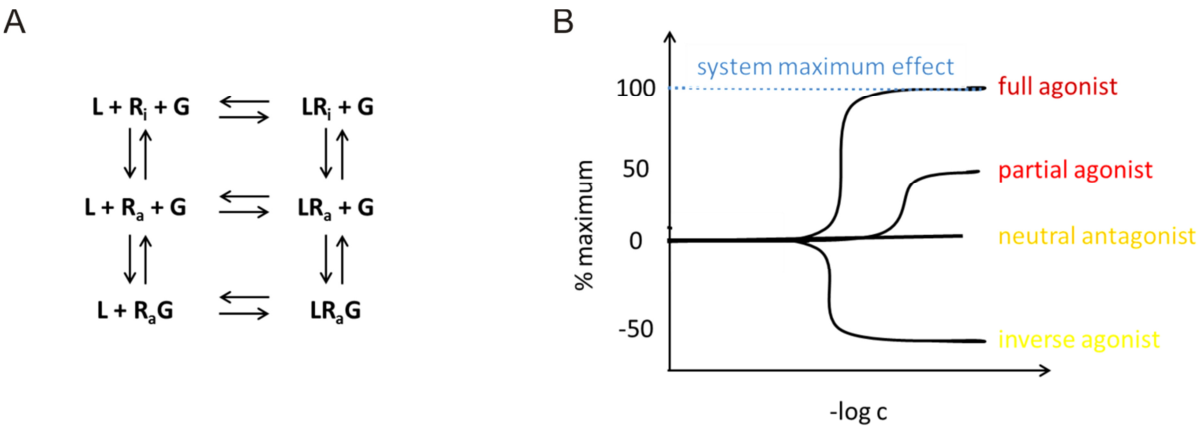

Figure 1.3. (A) Extended ternary complex model (L = ligand; R_a = active state of the receptor; R_i = inactive state of the receptor; G = G-protein) (adopted from Rajagopal et al.)[29] **(B)** Effects produced by different ligands in a biological system (adopted from Kenakin).[30]

1.1.4.1.1 G-proteins

Heterotrimeric G-proteins consist of a 39-52 kDa GTP-binding Gα subunit and a Gβγ subunit. In the inactive state, the Gβγ dimer is non-covalently bound to the Gα subunit. There are 16 known mammalian Gα subunits and they are grouped into four families ($G\alpha_{i/o}$, $G\alpha_s$, $G\alpha_{q/11}$ and $G\alpha_{12/13}$).[23] Furthermore, there are 5 known Gβ- and 12 known Gγ subunits. In vitro most Gβ and Gγ subunits can form stable heterodimers. In combination with the diversity of the Gα subunits, this provides the potential of numerous combinations to form functional heterotrimeric G-proteins. Still, the role of subunit diversity of G-proteins is not fully understood.[31]

1.1.4.1.2 G-protein regulated effectors

In principle, the interaction between receptor and G-protein is not strictly specific. G-protein mediated signaling can depend on the cellular background [31] and, moreover, some GPCRs are capable of coupling to multiple G-proteins.[32,33] An overview of typical signaling patterns of GPCRs is given in Figure **1.4**.

Activated G-proteins regulate the function of different effectors. The most widely studied effector are isoforms of adenylyl cyclase (AC). All of the nine ACs are activated by the $G\alpha_s$ subunit, resulting in an increase in intracellular cAMP. It is noteworthy that some of the ACs can additionally be influenced by Gβγ subunits via calcium-calmodulin.[23] The $G\alpha_s$ family includes the ubiquitously expressed $G\alpha_s$ subunit and the olfactory α subunit $G\alpha_{olf}$.

The G-proteins of the $G\alpha_{i/o}$ family are widely expressed, and the main function of the $G\alpha_i$ subunit is the inhibition of most of the ACs. The role of this family of G-proteins has extensively been studied with pertussis toxin (PTX), resulting in ADP-ribosylation and preventing the coupling of $G\alpha_i$ to the receptor.[34] Because of high expression, the activation of

$G\alpha_i$ leads to a release of high amounts of βγ subunits. Therefore, $G\alpha_i$ activation is believed to be the major pathway resulting in Gβγ mediated signaling.[35]

The $G\alpha_q$ and $G\alpha_{11}$ subunits are almost ubiquitously expressed, whereas $G\alpha_{14}$ and $G\alpha_{15/16}$ show a rather limited expression pattern.[35] $G\alpha_{q/11}$ coupled receptors do not discriminate between the $G\alpha_q$ and the $G\alpha_{11}$ subunit.[36,37] Both subunits are efficient activators of the isoforms β_1, β_3 and β_4 of PLC, but not of the β_2 isoform.[38] While the role of $G\alpha_q$ and $G\alpha_{11}$ in biological processes is well understood, the function of the other two members of the $G\alpha_{q/11}$ family is still unclear.[35]

The investigation of the function of the $G_{12/13}$ family is compromised by the lack of selective inhibitors. G_{12} and G_{13} are often stimulated by receptors simultaneously activating $G\alpha_{q/11}$. Studies revealed that G_{12}/G_{13} can alter a variety of downstream effectors including phospholipase A_2 (PLA_2) and the Na^+/H^+ exchanger.[39,40] Moreover, they regulate the formation of actomyosin-based structures and modulate their contractility by increasing the activity of the small GTPase RhoA (Ras homolog gene family, member A).[41]

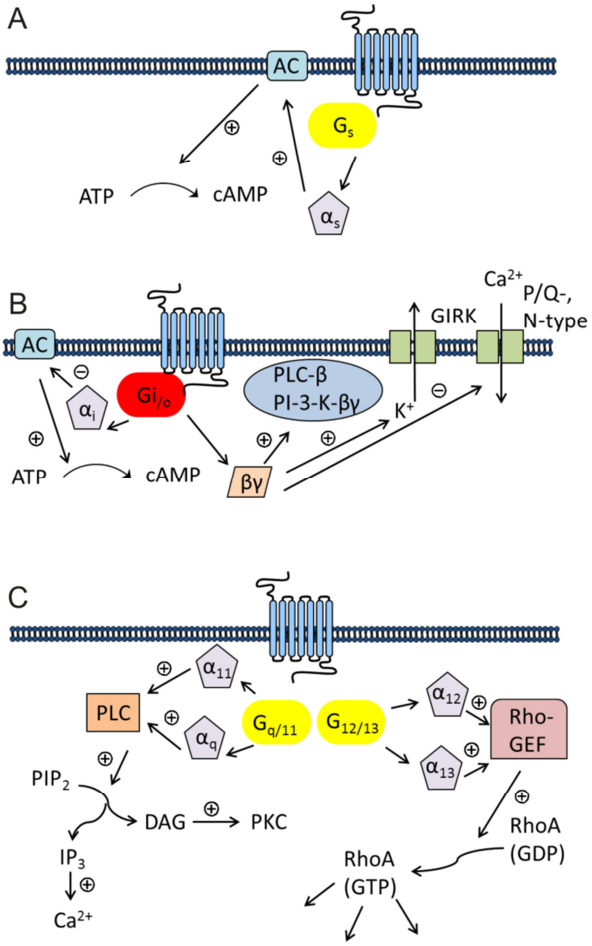

Figure 1.4. Typical pattern of GPCRs coupling. (**A**) G_s mediated signaling (AC = adenylyl cyclase; ATP = adenosine triphosphate; cAMP = cyclic adenosine monophosphate) (**B**) $G_{i/o}$ mediated signaling (GIRK = G-protein-regulated inward rectifier potassium channel; PI-3-K = phosphoinositide-3-kinase; PLC-ß = phospholipase C-β (**C**) $G_{q/11}$ and $G_{12/13}$ mediated signaling (DAG = diacylglycerol; GDP = guanosine diphosphate; GTP = guanosine triphosphate; IP_3 = inositol 1,4,5-trisphosphate; PIP_2 = phosphatidylinositol 4,5-bisphosphate; PKC = protein kinase C; Rho-GEF = Rho-guanine nucleotide exchange factor; RhoA = Ras homolog gene family, member A) (adopted and modified from Wettschureck et al. 2005).[35]

1.2 Histamine and its receptors

1.2.1 The biogenic amine histamine

1.2.1.1 Brief history

More than 100 years ago, the British physiologist Sir Henry Dale discovered histamine as a constituent of ergot. Subsequently, histamine was identified as endogenous substance in the body ("histos" = "tissue").[42] During the next decade, the pharmacological effects of histamine were extensively studied, and in 1937 the first antihistamines were synthesized by Daniel Bovet and Anne-Marie Staub.[43] Five years later, the first H_1R antagonists were introduced into therapy.

1.2.1.2 Biosynthesis, metabolism and function

In the body, histamine is formed from the amino acid L-histidine by the action of histidine decarboxylase (HDC).[44] After liberation, histamine is rapidly cleaved by histamine *N*-methyltransferase (HNMT)[45] or diamine oxidase (DAO).[46] As a neurotransmitter, histamine plays a crucial role in brain functions, including circadian rhythm, nociception and locomotor activity.[47] Furthermore, histamine regulates secretion of pituitary hormones, gastrointestinal and circulatory functions, and it is involved in inflammatory reactions and the modulation of the immune response.[47] Histamine is mainly stored in the granules of mast cells[48] and basophils[49] and can be released in large amounts upon degranulation in response to various stimuli. Another depot are the enterochromaffin-like (ECL) cells in the stomach. Histamine released from ECL cells, regulates gastric acid secretion from parietal cells.[50] The effects of histamine are mediated by four histamine receptor (H_xR) subtypes, termed H_1R, H_2R, H_3R and H_4R, all of them belonging to class A GPCRs.

1.2.2 The four histamine receptors and their ligands

1.2.2.1 The histamine H_1R

The H_1R is mainly expressed in mammalian brain, on smooth muscle and endothelium cells and on lymphocytes.[51] On immune cells, the H_1R is often co-expressed along with the H_2R, complicating detailed studies of both receptors due to the lack of selectivity of some ligands.[52] The H_1R preferentially couples to the $G\alpha_q$ protein, resulting in an increase in intracellular Ca^{2+}. H_1R-mediated biological effects comprise vasodilatation, bronchoconstriction, modulation of endothelial barrier function, as well as pain and itching as a consequence of insect stings.[53] The first H_1R antagonists, usually referred to as "classical antihistamines" (e.g. mepyramine, diphenhydramine) against allergic diseases, were already established in the 1940s. These 1st generation H_1R antagonists are highly lipophilic compounds, able to pass the blood brain barrier and to cause sedation. For that reason, antagonists such as cetirizine and loratadine were developed that cross the blood brain barrier to a much lower degree. This 2nd generation of antihistamines still represents blockbuster drugs for the treatment of allergic disorders (**Fig 1.5**).[54]

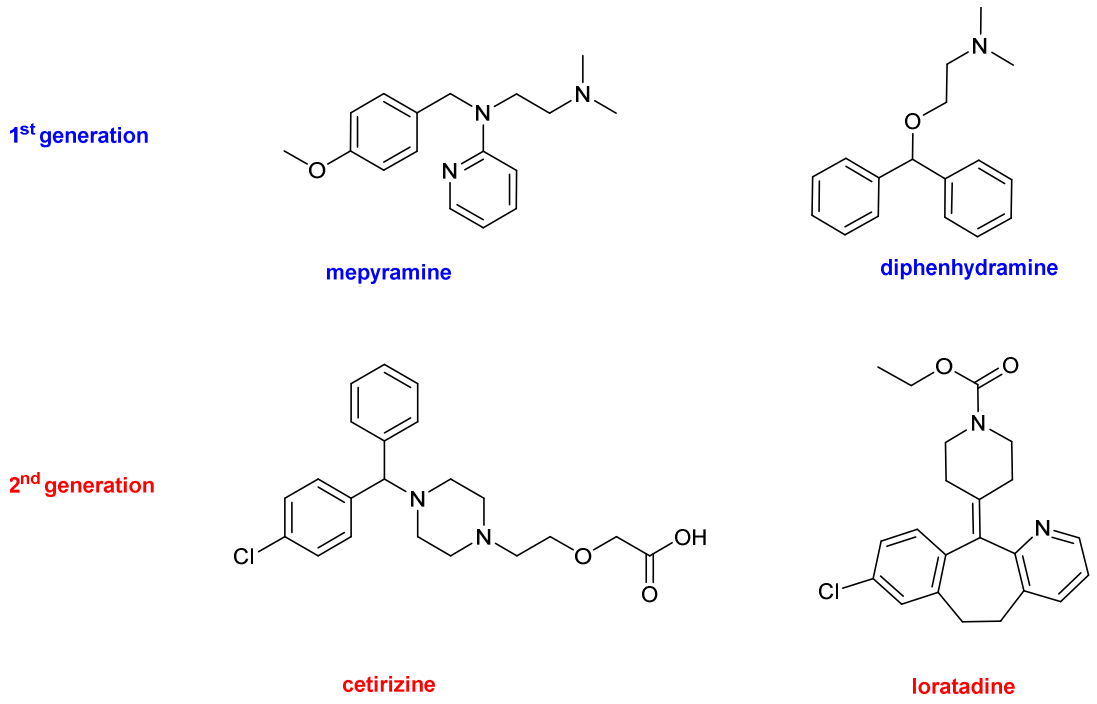

Fig. 1.5. Chemical structures of selected H_1R antagonists

The only H_1R agonist in clinical use is betahistine (**Fig. 1.6**), a drug for the treatment of Meniere`s disease.[55] Highly potent H_1R agonists were developed as pharmacological tools. Potent agonists, superior to histamine, were obtained by structural optimization of 2-phenylhistamines.[56,57] The most successful approach to potent and selective H_1R agonists resulted in histaprodifen derivatives, especially suprahistaprodifen.[58-61]

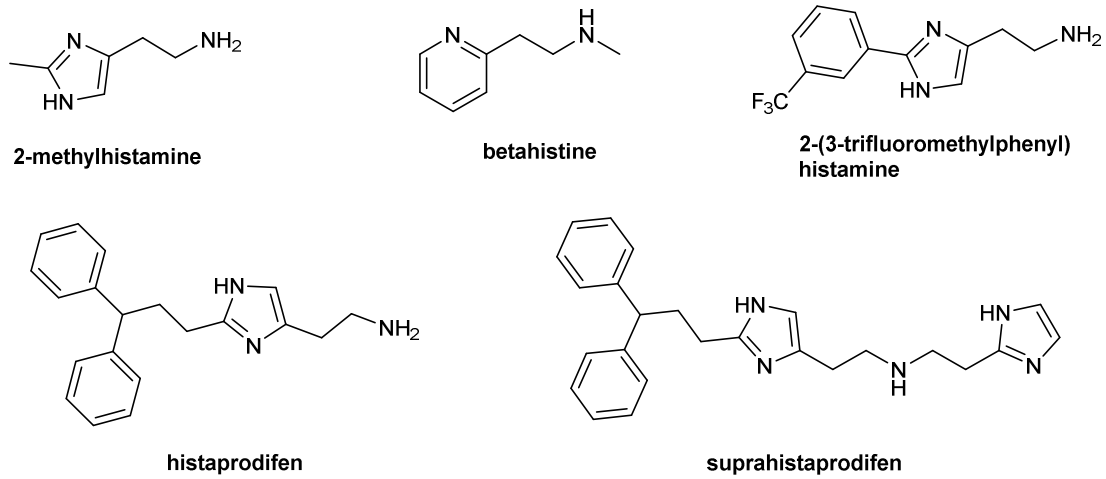

Figure 1.6. Chemical structures of selected H_1R agonists

1.2.2.2 The histamine H_2R

Up to the late 1940s, scientists had no explanation why some of the histamine-mediated effects, for example the positive chronotropic response and the stimulation of gastric acid secretion, could not be antagonized by the classical antihistamines.[62,63] In 1966, Ash and Schild postulated the existence of a second receptor subtype,[64] which was pharmacologically

characterized and termed H_2R in 1972 by the Nobel laureate Sir James Black.[65] The H_2R is located in mammalian brain, on parietal cells, on human neutrophils and eosinophils, in cardiac-, airways and uterus tissue.[52,66] The H_2R canonically couples to the $G\alpha_s$ protein resulting in the activation of PKA and in an increase in cAMP.[67] After burimamide,[65] the first antagonist used to define the H_2R, H_2R antagonists with increased affinity, e.g. cimetidine, famotidine and ranitidine, revolutionized the treatment of gastric and duodenal ulcer (**Fig. 1.7**).[68] Nowadays, these drugs have been replaced by proton pump inhibitors. Nevertheless, there is a great interest in CNS permeable H_2R ligands to elucidate the role of the H_2R in the CNS.[63]

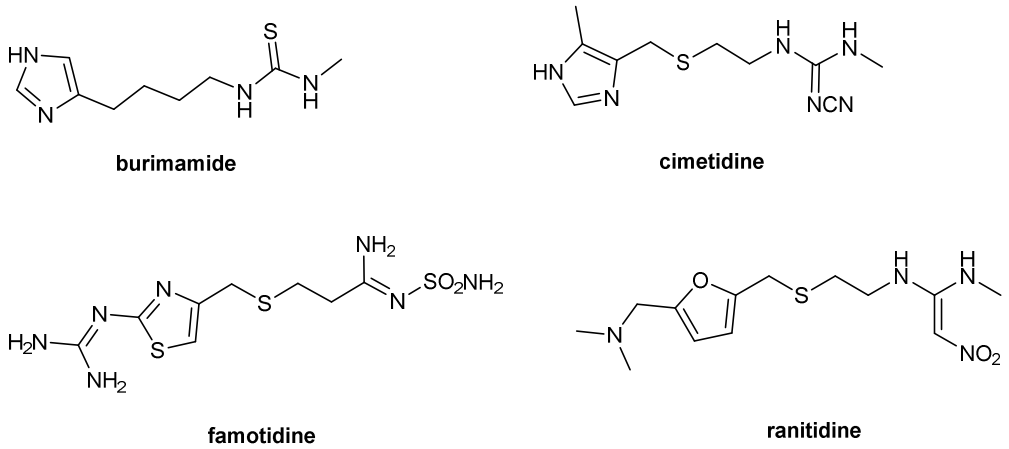

Figure 1.7. Chemical structures of selected H_2R antagonists

The guanidine derivative impromidine was the first highly potent H_2R agonist. A large number of impromidine analogues has been synthesized and characterized with respect to H_2R agonism.[69] Impromidine was the first H_2R agonist clinically tested in patients suffering from severe catecholamine-refractory congestive heart failure.[70,71] Structural modification of impromidine led to arpromidine, in which the cimetidine-like moiety was replaced by a more lipophilic pheniramine-like structure. Such compounds showed up to 400 times the potency of histamine.[72] With respect to oral bioavailability, the strongly basic guanidine (pK_a~13) was replaced by an acylguanidine (pK_a~8). Surprisingly, agonistic potency was retained or even increased (e.g. UR-Bit24).[73,74] A tremendous increase in potency was achieved according to the bivalent ligand approach. Bivalent H_2R agonists (e.g. UR-AK381) were up to 4000 times more potent than histamine and are the most potent H_2R agonists known so far (**Fig. 1.8**).[75] Highly selective H_2R agonists might be beneficial for patients suffering from acute myeloid leukemia (AML).[76,77] In myeloid cells histamine facilitates T-cell mediated killing of tumor cells and is therefore used as an orphan drug in combination with interleukin 2 (IL2) for maintenance treatment of AML.[78]

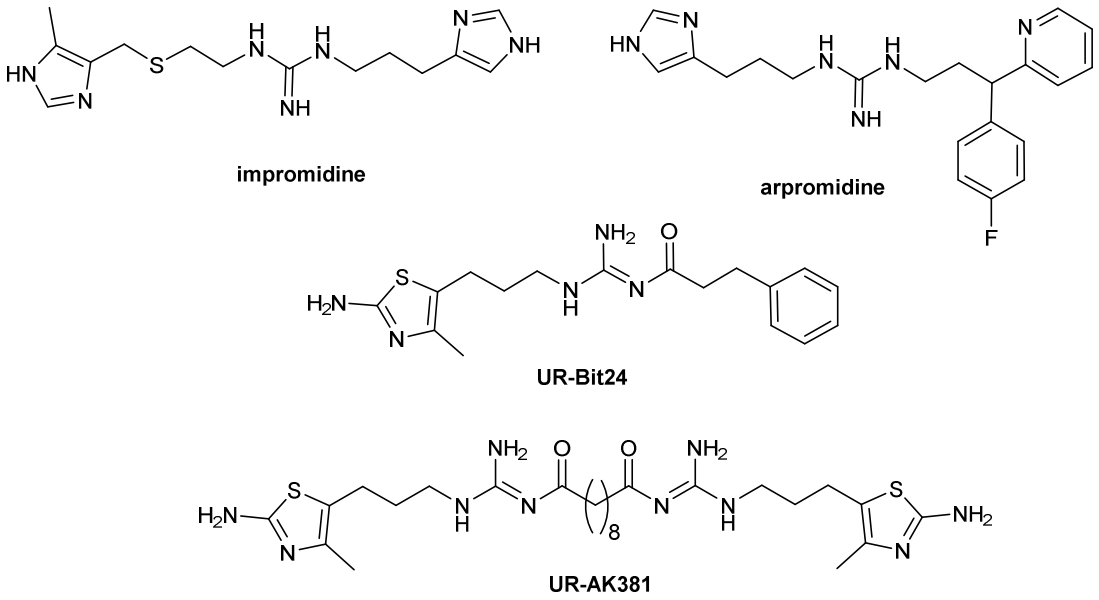

Figure 1.8. Chemical structures of selected H_2R agonists

1.2.2.3 The histamine H_3R

In 1983, Schwartz and coworkers suggested the existence of a third histamine receptor. They discovered that histamine was able to inhibit its own release from cerebral neurons and that this effect was antagonized by burimamide at nanomolar concentrations, which was far below the concentration necessary to block the H_2R.[79,80] The H_3R is predominantly located in neurons where it acts as an autoreceptor regulating the synthesis and release of histamine. Additionally, the H_3R also occurs as a hetero-receptor on non-histaminergic neurons, controlling the release of other neurotransmitters including dopamine, acetylcholine and GABA.[63] In the periphery, the receptor is expressed in the gastrointestinal tract, the airways and the cardiovascular system.[81] The H_3R couples to G_i proteins and has been shown to interfere with various transduction pathways apart from the modulation of the AC activity, for example activation of PLA_2 and inhibition of K^+-induced Ca^{2+} activation.[82] The first potent H_3R antagonists were thioperamide and clobenpropit, which turned out to be additionally highly potent H_4R ligands. Moreover, as imidazole-type ligands, these compounds harbor the risk of drug-drug interactions due to interactions with cytochrome P-450 enzymes. With the discovery of high constitutive activity, numerous H_3R antagonists had to be re-classified as inverse agonists. To reduce the off-target effects and to improve the drug-like properties, the imidazole ring was replaced mainly by a variety of secondary and tertiary amines, including cyclic amine moieties (e.g. piperazino, pyrrolidino and morpholino).[83] Potential therapeutic implications for H_3R antagonists (**Fig. 1.9**) include obesity and numerous CNS disorders such as schizophrenia, epilepsy and Alzheimer`s disease. Very recently, the first H_3R inverse agonist pitolisant was introduced as an orphan drug for patients suffering from narcolepsy.[84,85]

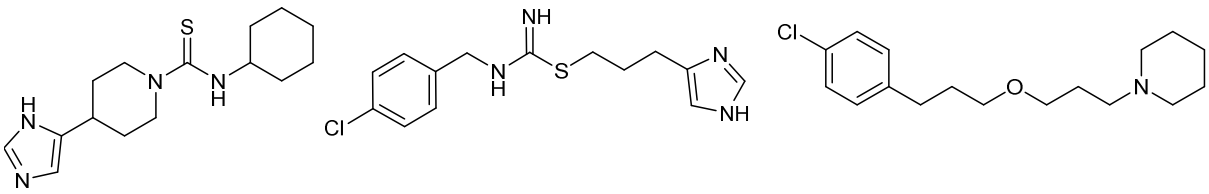

Fig 1.9. Chemical structures of selected H_3R antagonists/inverse agonists

Modifications of histamine by mono- or dimethyl substitution resulted in more potent and selective H_3R agonists (**Fig. 1.10**), such as (*R*)-α-methylhistamine. A further improvement regarding selectivity over the H_4R was achieved with immethridine[86] and methimepip[87]. All of the H_3R agonists represent histamine derivatives, which carry the risk of drug-drug interactions. Bioisosteric replacement of the imidazole moiety in H_3R agonists harbors a potential for new drugs, for example, for the treatment of migraine, ischemic arrhythmias, asthma or diabetes mellitus.[88,89]

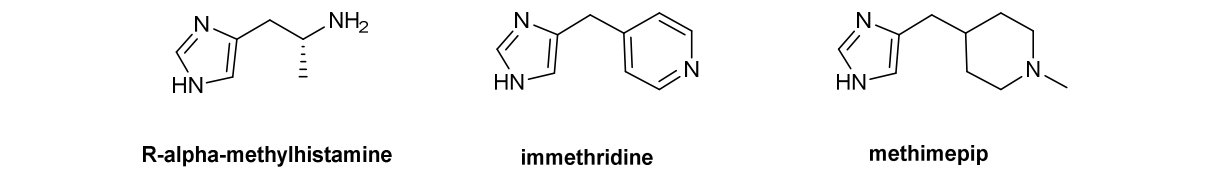

Figure 1.10. Chemical structures of selected H_3R agonists

1.2.2.4 The histamine H_4R

In 1994, Raible and coworkers suggested the existence of a novel histamine receptor on human eosinophils, based on a histamine induced calcium response.[90] This hypothesis was corroborated by several workgroups, which independently cloned the H_4R.[91-95] The H_4R was reported to be expressed in bone marrow and immunocytes, such as mast cells, eosinophils and monocytes.[52] The identification of the H_4R in the CNS[96] was not confirmed by several workgroups.[97] Additionally, according to a recently published study, there is no evidence for the expression of the H_4R in human monocytes.[98] Presumably, the erroneous detection of the H_4R in brain and monocytes was due to the use of unspecific antibodies and unreliable data on mRNA expression.[97-100] The H_4R is a G_i coupled receptor and mediates an increase in intracellular Ca^{2+} concentration. The indole derivative JNJ7777120 was the first selective and potent non-imidazole H_4R antagonist described in the literature and has been widely used as a reference compound in vitro and in vivo.[101] Surprisingly, JNJ7777120 turned out to be a biased agonist, stimulating H_4R mediated β-arrestin recruitment.[102] Five H_4R antagonists (e.g. UR-63325 [undisclosed structure], PF-3893787[103], JNJ39758979[104]) (**Fig.1.11**) entered clinical trials for the treatment of allergic rhinitis, allergic asthma, atopic dermatitis and rheumatoid arthritis.[105] Despite significantly antipruritic effects in human, the clinical trial of JNJ39758979 was terminated due to two agranulocytosis cases.[106,107]

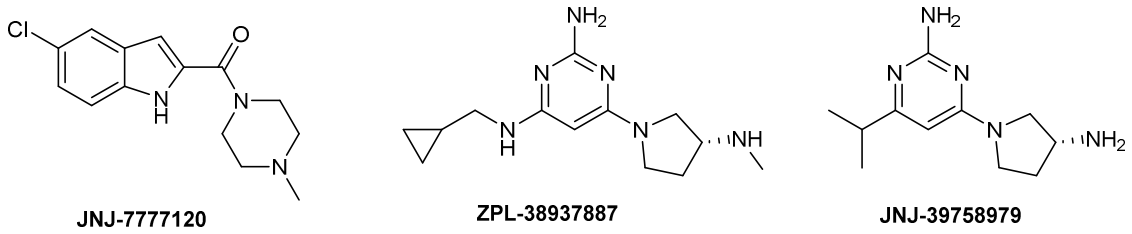

Figure 1.11. Chemical structures of selected H_4R antagonists

In contrast to H_4R antagonists, the potential therapeutic value of H_4R agonists (**Fig 1.12**) is still a matter of speculation. Regardless of that, further investigation of the (patho)physiological role of the H_4R requires selective and potent H_4R agonists as molecular tools. Due to the high sequence homology with the H_3R (~ 58 % identity in the TM regions)[94] the design of selective H_4R proved to be rather challenging. The cyanoguanidine OUP-16 was the first ligand with improved (approximately 30-fold) H_4R selectivity. Structural optimization of imidazolylalkylguanidines led to the highly potent and selective H_4R agonists, like e.g. UR-PI376.[108] One of the most potent H_4R agonists known so far was identified among a series of 2-arylbenzimidazoles.[109] Potencies and efficacies of numerous H_4R agonists are depending on the species considered.[110] In this context, oxime-type compounds, structurally derived from JNJ7777120, proved to be of special value. The Z-configured isomers have comparable agonist potencies on human and rodent H_4Rs.[111]

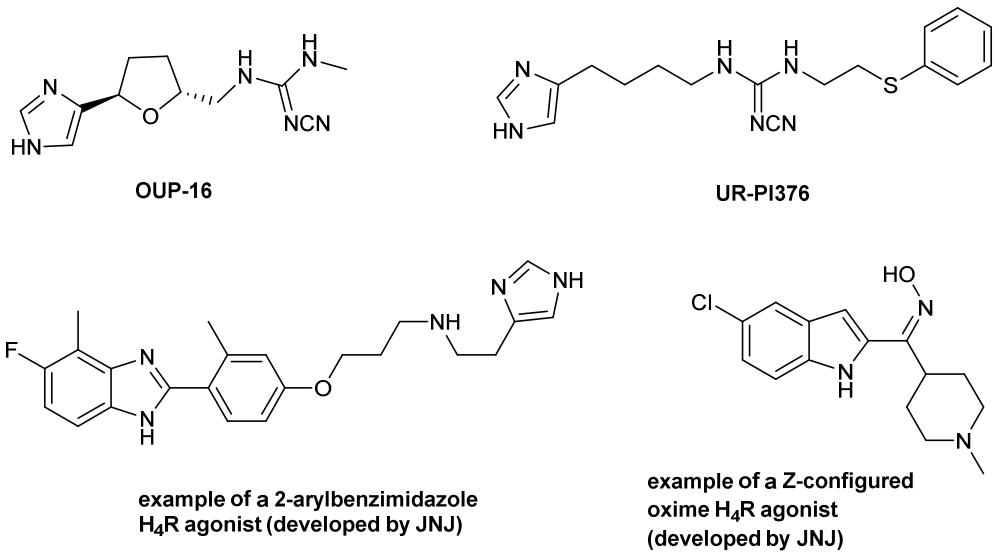

Figure 1.12. Chemical structures of selected H_4R agonists

1.3 GPCR dimerization and bivalent ligands

1.3.1 GPCR dimerization

Over a long period of time, it has been assumed that GPCRs exist and function as monomers. However, there is growing evidence that GPCRs are able to form dimers or oligomers. The first receptor shown to form dimers was the $GABA_B$ receptor. Only when coexpressed with $GABA_{B2}$, the $GABA_{B1}$ receptor is capable of forming a functional $GABA_B$

receptor.[112-114] Meanwhile, many GPCRs are known to form hetero- and homodimers, respectively (for reviews, cf. Agnati et al. 2003, Hiller et al. 2013).[115,116] Receptor dimerization can induce distinct ligand binding properties. For example, it was shown for δOR and μOR coexpressing cells that there was a significant increase in binding of μOR ligands in the presence of δOR antagonists.[117] This phenomenon can be explained by positive cooperativity: binding of one ligand to the first receptor molecule increases the interaction of the second ligand to the second receptor protomer (**Fig. 1.13A**). Receptor dimerization can alter signaling, e.g., induce a switch in G protein coupling. For example, the D_1R canonically couples to $G\alpha_s$, and the D_2R couples to $G\alpha_i$, whereas heterodimers of the two receptors preferentially activate $G\alpha_q$.[118] It is noteworthy that dimerization can also cause a switch from G-protein activation to β-arrestin signaling.[119] Furthermore, GPCR dimerization may have an influence on trafficking. For instance, coexpression of the α_{1D}- and the α_{1B} adrenoceptor led to a 10-fold increase in cell surface expression of the α_{1D}-AR, suggesting that heterodimerization enhances the transport of α_{1D}-AR to the cell membrane.[120] Drugs selectively targeting receptor dimers might possess higher affinity and selectivity and/or an improved pharmacokinetic profile resulting in reduced side effects.[121,122]

1.3.2 Bivalent ligands

One possibility to target GPCR dimers is the bivalent ligand approach. Typically, the term "bivalent ligands" refers to molecules composed of two pharmacophoric moieties linked through a spacer.[123] Based on the pioneering work of Porthogese and coworkers, who developed the first bivalent ligands for the investigation of the dimerization of opioid receptors,[124-126] the bivalent ligand approach was successfully adopted for many GPCRs, including e.g. serotonin, histamine and dopamine,[75,127-131] resulting in compounds with higher affinity and selectivity compared to their monovalent counterparts. The two pharmacophoric entities can either be structurally equal (homobivalent) or different (heterobivalent). Obviously, the length of the spacer is a key factor for bridging a receptor dimer (**Fig. 1.13B**). A very short or a very long spacer decreases the potential to bridge two vicinal receptor protomers.[132] Porthogese et al. observed highest agonist potency at a spacer length of 18 atoms (~20 Å).[133] However, newer studies revealed that the optimum spacer length for bivalent ligands targerting receptor dimers depends on the dimer interface, the structure of pharmacophores and topicity of the point of attachments.[116] Thus, bivalent ligands with clozapine as pharmacophore displayed highest affinity with a spacer length of 16 and 18 atoms.[134] Interestingly, the highest potency for bivalent H_2R agonists was achieved with compounds bearing an octa- or hexamethylene chain, rather indicating to an additional binding site at the same receptor molecule (**Fig. 1.13C**).[75]

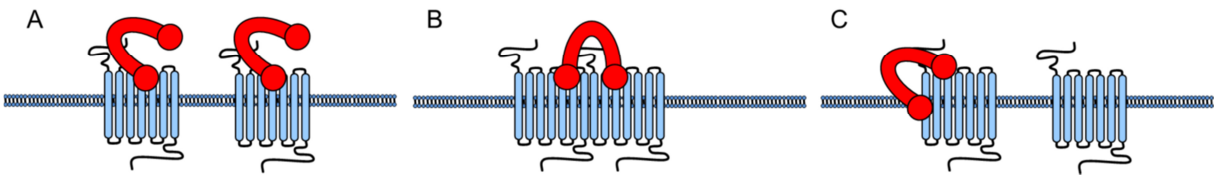

Figure 1.13. Possible binding modes of bivalent ligands. (**A**) Binding to two receptor protomers (**B**) Bridging of a receptor dimer (**C**) Simultaneous binding to an orthosteric and allosteric binding site of the same receptor molecule (bitopic or dualsteric binding mode) (adopted and modified from Bonger et al. 2007).[135]

Previously, our workgroup applied the guanidine – acylguanidine bioisosteric approach to imidazolylpropylguanidine-type histamine H_2 receptor (H_2R) agonists[73,136] and explored the bivalent ligand approach, taking into consideration the hypothesis that GPCRs, including histamine receptor subtypes, can form functionally active dimers. Acylation of the guanidine group reduced the basicity by 4-5 orders of magnitude. Surprisingly, agonistic potency was retained or even increased. In combination with a bivalent approach, this strategy resulted in highly potent H_2R agonists. The binding mode of these compounds is far from being understood. The optimal spacer length of the most active bivalent H_2R agonists is most probably insufficient to enable simultaneous occupation of the recognition sites of putative H_2R dimers.[75] Probably, the tremendous gain in potency results from interaction with an accessory binding site at the same receptor protomer.

1.4 Functional selectivity and G-protein independent signaling

Besides G-proteins, two additional protein families are known to interact with active state GPCRs: G-protein coupled receptor kinases (GRKs) and β-arrestins.[137] Whereas originally, the role of these proteins was simply associated with desensitization, internalization and recycling of GPCRs,[138] they are nowadays considered as alternative signal transducers.[137,139] Particularly, β-arrestins are known to interact with many proteins and protein kinases, leading to the phosphorylation of numerous targets.[140,141]

Over the last decades, a growing number of experimental data supported the concept of "biased signaling" as a consequence of various active states of an individual receptor. According to the classical model, agonists are considered to have "linear efficacy", i.e. a pharmacological activity resulting from a sequence beginning with receptor occupancy and G-protein activation.[142] However, some ligands show "imbalanced efficacies" regarding the activation of different signaling pathways (**Fig. 1.14A**).[141] Such ligands proved to be antagonists on one pathway, while simultaneously being agonists on another pathway.[143,144] To consider such a behavior, the classical two-state model was extended to a multiple-state model (**Fig. 1.14B**). According to the latter, a given ligand is capable of stabilizing a unique receptor conformation, either triggering the G-protein or the β-arrestin pathway.[141,142,145,146]

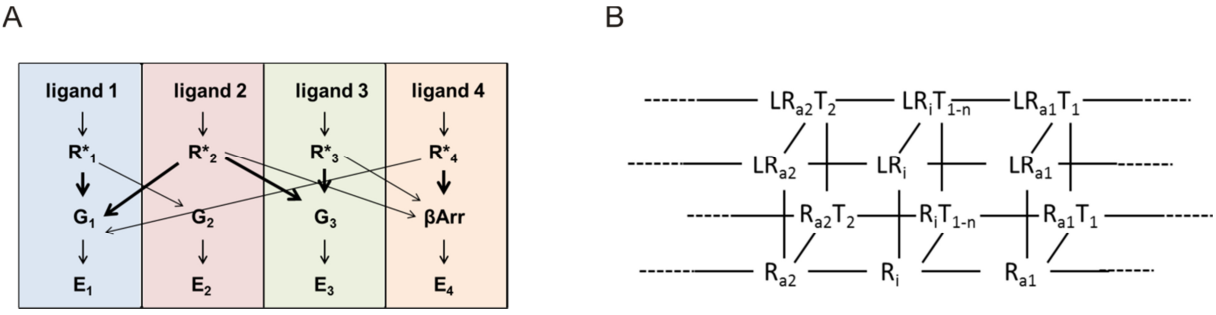

Figure 1.14. (**A**) Concept of functional selectivity: A given ligand (**1-4**) stabilizes a unique active receptor conformation (**R^*_1-R^*_4**). The distinct receptor conformations differ in their capability to interact with different G-proteins (**G_1-G_3**) and β-arrestins (**βArr**). As a result, effector systems (**E_1-E_4**) are regulated in a ligand specific manner (adopted from Seifert 2013).[146] (**B**) Multiple-state model (L = ligand; R_{an} = distinct active receptor conformations; R_i = inactive state of the receptor; T_n = distinct transducers) (adopted from Rajagopal et al. 2010)[29]

The ability of a ligand to address either G-protein signaling or β-arrestin signaling is referred to as “functional selectivity”, “biased agonism” or “collateral efficacy” (**Fig. 1.15**).[147,148] By now, functionally selective ligands were discovered for many GPCRs, e.g. for β-adrenergic receptors,[149,150] dopamine D_2 and D_3 receptors[151,152] and the histamine H_4R.[153,154] Such biased agonists harbor a great potential for the development of novel therapeutic agents with reduced adverse effects. Studies already revealed that the pharmacology of some of these functionally selective ligands was different from that of unbiased compounds.[148,155,156]

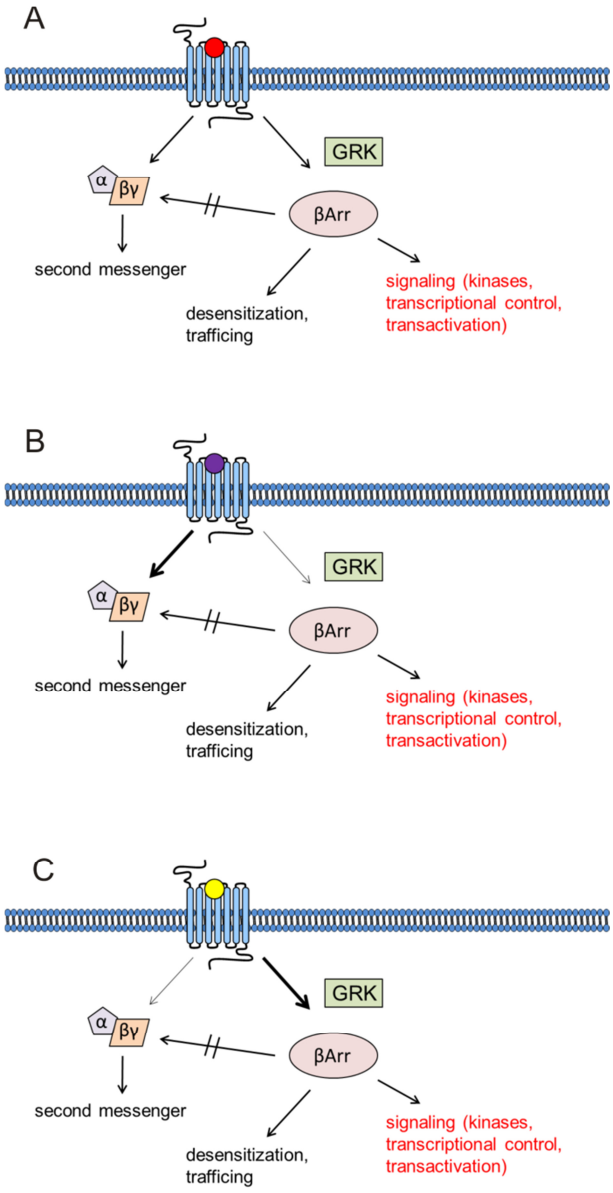

Figure 1.15. Functionally selective ligands: (**A**) Binding of an unbiased ligand leads to G-protein activation and β-arrestin recruitment in a balanced manner. (**B**) Binding of a G-protein biased ligand. (C) Binding of a β-arrestin biased ligand (βArr = β-arrestin; GRK = G-protein receptor coupled kinase) (adopted from Rajagopal et al. 2010).[29]

1.5 References

1. Lefkowitz, R. J. Historical review: A brief history and personal retrospective of seven-transmembrane receptors. *Trends Pharmacol. Sci.* **2004**, 25, 413-422.
2. Liapakis, G.; Cordomi, A.; Pardo, L. The G-protein coupled receptor family: actors with many faces (vol 18, pg 175, 2012). *Curr. Pharm. Des.* **2012**, 18, 4583-4583.
3. Sharman, J. L.; Benson, H. E.; Pawson, A. J.; Lukito, V.; Mpamhanga, C. P.; Bombail, V.; Davenport, A. P.; Peters, J. A.; Spedding, M.; Harmar, A. J.; Nc-Iuphar. IUPHAR-DB: updated database content and new features. *Nucleic Acids Res.* **2013**, 41, D1083-D1088.
4. Furchgott, R. F. Receptor mechanisms. *Annu. Rev. Pharmacol.* **1964**, 4, 21-50.
5. Dixon, R. A.; Kobilka, B. K.; Strader, D. J.; Benovic, J. L.; Dohlman, H. G.; Frielle, T.; Bolanowski, M. A.; Bennett, C. D.; Rands, E.; Diehl, R. E.; Mumford, R. A.; Slater, E. E.; Sigal, I. S.; Caron, M. G.; Lefkowitz, R. J.; Strader, C. D. Cloning of the gene and cDNA for mammalian beta-adrenergic receptor and homology with rhodopsin. *Nature* **1986**, 321, 75-79.
6. Palczewski, K.; Kumasaka, T.; Hori, T.; Behnke, C. A.; Motoshima, H.; Fox, B. A.; Le Trong, I.; Teller, D. C.; Okada, T.; Stenkamp, R. E.; Yamamoto, M.; Miyano, M. Crystal structure of rhodopsin: A G protein-coupled receptor. *Science* **2000**, 289, 739-745.
7. Warne, T.; Serrano-Vega, M. J.; Baker, J. G.; Moukhametzianov, R.; Edwards, P. C.; Henderson, R.; Leslie, A. G.; Tate, C. G.; Schertler, G. F. Structure of a beta1-adrenergic G-protein-coupled receptor. *Nature* **2008**, 454, 486-491.
8. Cherezov, V.; Rosenbaum, D. M.; Hanson, M. A.; Rasmussen, S. G.; Thian, F. S.; Kobilka, T. S.; Choi, H. J.; Kuhn, P.; Weis, W. I.; Kobilka, B. K.; Stevens, R. C. High-resolution crystal structure of an engineered human beta2-adrenergic G protein-coupled receptor. *Science* **2007**, 318, 1258-1265.
9. Haga, K.; Kruse, A. C.; Asada, H.; Yurugi-Kobayashi, T.; Shiroishi, M.; Zhang, C.; Weis, W. I.; Okada, T.; Kobilka, B. K.; Haga, T.; Kobayashi, T. Structure of the human M2 muscarinic acetylcholine receptor bound to an antagonist. *Nature* **2012**, 482, 547-551.
10. Kruse, A. C.; Hu, J.; Pan, A. C.; Arlow, D. H.; Rosenbaum, D. M.; Rosemond, E.; Green, H. F.; Liu, T.; Chae, P. S.; Dror, R. O.; Shaw, D. E.; Weis, W. I.; Wess, J.; Kobilka, B. K. Structure and dynamics of the M3 muscarinic acetylcholine receptor. *Nature* **2012**, 482, 552-556.
11. Thompson, A. A.; Liu, W.; Chun, E.; Katritch, V.; Wu, H.; Vardy, E.; Huang, X. P.; Trapella, C.; Guerrini, R.; Calo, G.; Roth, B. L.; Cherezov, V.; Stevens, R. C. Structure of the nociceptin/orphanin FQ receptor in complex with a peptide mimetic. *Nature* **2012**, 485, 395-399.
12. Wu, H.; Wacker, D.; Mileni, M.; Katritch, V.; Han, G. W.; Vardy, E.; Liu, W.; Thompson, A. A.; Huang, X. P.; Carroll, F. I.; Mascarella, S. W.; Westkaemper, R. B.; Mosier, P. D.; Roth, B. L.; Cherezov, V.; Stevens, R. C. Structure of the human kappa-opioid receptor in complex with JDTic. *Nature* **2012**, 485, 327-332.
13. Manglik, A.; Kruse, A. C.; Kobilka, T. S.; Thian, F. S.; Mathiesen, J. M.; Sunahara, R. K.; Pardo, L.; Weis, W. I.; Kobilka, B. K.; Granier, S. Crystal structure of the micro-opioid receptor bound to a morphinan antagonist. *Nature* **2012**, 485, 321-326.
14. Granier, S.; Manglik, A.; Kruse, A. C.; Kobilka, T. S.; Thian, F. S.; Weis, W. I.; Kobilka, B. K. Structure of the delta-opioid receptor bound to naltrindole. *Nature* **2012**, 485, 400-404.
15. Shimamura, T.; Shiroishi, M.; Weyand, S.; Tsujimoto, H.; Winter, G.; Katritch, V.; Abagyan, R.; Cherezov, V.; Liu, W.; Han, G. W.; Kobayashi, T.; Stevens, R. C.; Iwata, S. Structure of the human histamine H1 receptor complex with doxepin. *Nature* **2011**, 475, 65-70.
16. Lappano, R.; Maggiolini, M. G protein-coupled receptors: novel targets for drug discovery in cancer. *Nat. Rev. Drug Discov.* **2011**, 10, 47-60.

17. Wise, A.; Jupe, S. C.; Rees, S. The identification of ligands at orphan G-protein coupled receptors. *Annu. Rev. Pharmacol. Toxicol.* **2004**, 44, 43-66.
18. Fredriksson, R.; Lagerstrom, M. C.; Lundin, L. G.; Schioth, H. B. The G-protein-coupled receptors in the human genome form five main families. Phylogenetic analysis, paralogon groups, and fingerprints. *Mol. Pharmacol.* **2003**, 63, 1256-1272.
19. Pierce, K. L.; Premont, R. T.; Lefkowitz, R. J. Seven-transmembrane receptors. *Nat Rev Mol Cell Bio* **2002**, 3, 639-650.
20. Vassilatis, D. K.; Hohmann, J. G.; Zeng, H.; Li, F. S.; Ranchalis, J. E.; Mortrud, M. T.; Brown, A.; Rodriguez, S. S.; Weller, J. R.; Wright, A. C.; Bergmann, J. E.; Gaitanaris, G. A. The G protein-coupled receptor repertoires of human and mouse. *Proc. Natl. Acad. Sci. U. S. A.* **2003**, 100, 4903-4908.
21. Tang, X. L.; Wang, Y.; Li, D. L.; Luo, J.; Liu, M. Y. Orphan G protein-coupled receptors (GPCRs): biological functions and potential drug targets. *Acta Pharmacol. Sin.* **2012**, 33, 363-371.
22. Kobilka, B. K. G protein coupled receptor structure and activation. *Biochim. Biophys. Acta* **2007**, 1768, 794-807.
23. Luttrell, L. M. Reviews in molecular biology and biotechnology: transmembrane signaling by G protein-coupled receptors. *Mol. Biotechnol.* **2008**, 39, 239-264.
24. Baldwin, J. M. Structure and function of receptors coupled to G proteins. *Curr. Opin. Cell Biol.* **1994**, 6, 180-190.
25. Seifert, R., Wieland T. G Protein-Coupled Receptors as Drug Targets: Analysis of Activation and Constitutive Activity. *Wiley-VCH, Weinheim* **2005**.
26. Delean, A.; Stadel, J. M.; Lefkowitz, R. J. A ternary complex model explaines the agonist-specific binding-properties of the adenylate cyclase-coupled beta-adrenergic-receptor. *J. Biol. Chem.* **1980**, 255, 7108-7117.
27. Samama, P.; Cotecchia, S.; Costa, T.; Lefkowitz, R. J. A mutation-induced activated state of the beta 2-adrenergic receptor. Extending the ternary complex model. *J. Biol. Chem.* **1993**, 268, 4625-4636.
28. Leff, P. The two-state model of receptor activation. *Trends Pharmacol. Sci.* **1995**, 16, 89-97.
29. Rajagopal, S.; Rajagopal, K.; Lefkowitz, R. J. Teaching old receptors new tricks: biasing seven-transmembrane receptors. *Nature Reviews Drug Discovery* **2010**, 9, 373-386.
30. Kenakin, T. A Pharmacology Primer. *Elsevier* **2014**, 28.
31. Schmidt, C. J.; Thomas, T. C.; Levine, M. A.; Neer, E. J. Specificity of G-protein-beta subunit and gamma subunit interactions

    J. Biol. Chem. **1992**, 267, 13807-13810.
32. Eason, M. G.; Kurose, H.; Holt, B. D.; Raymond, J. R.; Liggett, S. B. Simultaneous Coupling of Alpha-2-Adrenergic Receptors to 2 G-Proteins with Opposing Effects - Subtype-Selective Coupling of Alpha-2c10, Alpha-2c4, and Alpha-2c2 Adrenergic-Receptors to G(I) and G(S). *J. Biol. Chem.* **1992**, 267, 15795-15801.
33. Galandrin, S.; Bouvier, M. Distinct signaling profiles of beta(1) and beta(2) adrenergic receptor ligands toward adenylyl cyclase and mitogen-activated protein kinase reveals the pluridimensionality of efficacy. *Mol. Pharmacol.* **2006**, 70, 1575-1584.
34. Mangmool, S.; Kurose, H. G(i/o) protein-dependent and -independent actions of Pertussis Toxin (PTX). *Toxins (Basel)* **2011**, 3, 884-899.
35. Wettschureck, N.; Offermanns, S. Mammalian G proteins and their cell type specific functions. *Physiol. Rev.* **2005**, 85, 1159-1204.
36. Watson, S. P.; Asazuma, N.; Atkinson, B.; Berlanga, O.; Best, D.; Bobe, R.; Jarvis, G.; Marshall, S.; Snell, D.; Stafford, M.; Tulasne, D.; Wilde, J.; Wonerow, P.; Frampton, J. The role of ITAM- and ITIM-coupled receptors in platelet activation by collagen. *Thromb. Haemost.* **2001**, 86, 276-288.
37. Wu, D. Q.; Katz, A.; Lee, C. H.; Simon, M. I. Activation of Phospholipase-C by Alpha-1-Adrenergic Receptors Is Mediated by the Alpha-Subunits of Gq Family. *J. Biol. Chem.* **1992**, 267, 25798-25802.

38. Rhee, S. G. Regulation of phosphoinositide-specific phospholipase C. *Annu. Rev. Biochem* **2001**, 70, 281-312.
39. Dhanasekaran, N.; Dermott, J. M. Signaling by the G(12) class of G proteins. *Cell. Signal.* **1996**, 8, 235-245.
40. Hooley, R.; Yu, C. Y.; Symons, M.; Barber, D. L. G alpha 13 stimulates Na+-H+ exchange through distinct Cdc42-dependent and RhoA-dependent pathways. *J. Biol. Chem.* **1996**, 271, 6152-6158.
41. Buhl, A. M.; Johnson, N. L.; Dhanasekaran, N.; Johnson, G. L. G-Alpha(12) and G-Alpha(13) Stimulate Rho-Dependent Stress Fiber Formation and Focal Adhesion Assembly. *J. Biol. Chem.* **1995**, 270, 24631-24634.
42. H. H. Dale, P. P. L. The physiological action of β-Imidazolethylamine. *J. Physiol.* **1910**, 41, 318–344.
43. D. Bovet, A. S. Action protectrice des éthers phenoliques au cours l'intoxication histaminique. *C.r. séances Soc. biol. ses. fil.* **1937**, 124, 547-549.
44. Ackermann, D. *Z Physiol Chem* **1910**, 60, 482-501.
45. Schwartz, J. C.; Arrang, J. M.; Garbarg, M.; Pollard, H.; Ruat, M. Histaminergic transmission in the mammalian brain. *Physiol. Rev.* **1991**, 71, 1-51.
46. Beaven, M. A. Factors Regulating Availability of Histamine at Tissue Receptors *Pharmacology of Histamine Receptors* **1982**, Ganellin, C.R., Parsons, M.E. (Eds.). Wright PSG, Bristol, London, Boston, 102-145.
47. Dy, M.; Schneider, E. Histamine-cytokine connection in immunity and hematopoiesis. *Cytokine Growth Factor Rev.* **2004**, 15, 393-410.
48. Riley, J. F.; West, G. B. The presence of histamine in tissue mast cells. *J. Physiol.* **1953**, 120(4), 528–537.
49. Falcone, F. H.; Zillikens, D.; Gibbs, B. F. The 21st century renaissance of the basophil? Current insights into its role in allergic responses and innate immunity. *Exp. Dermatol.* **2006**, 15, 855-864.
50. Mossner, J.; Caca, K. Developments in the inhibition of gastric acid secretion. *Eur. J. Clin. Invest.* **2005**, 35, 469-475.
51. Hill, S. J. Distribution, Properties, and Functional-Characteristics of 3 Classes of Histamine-Receptor. *Pharmacol. Rev.* **1990**, 42, 45-83.
52. Seifert, R.; Strasser, A.; Schneider, E. H.; Neumann, D.; Dove, S.; Buschauer, A. Molecular and cellular analysis of human histamine receptor subtypes. *Trends Pharmacol. Sci.* **2013**, 34, 33-58.
53. Bongers, G.; de Esch, I.; Leurs, R. Molecular Pharmacology of the Four Histamine Receptors. *Histamine in Innflammation* **2010**, 709, 11-19.
54. Simons, F. E. R.; Simons, K. J. Histamine and H-1-antihistamines: Celebrating a century of progress. *J. Allergy Clin. Immunol.* **2011**, 128, 1139-1152.
55. Barak, N. Betahistine: whats new on the agenda? *Expert Opin Inv Drug* **2008**, 17, 795-804.
56. Zingel, V.; Elz, S.; Schunack, W. Histamine Analogs .33. 2-Phenylhistamines with High Histamine H-1-Agonistic Activity. *Eur. J. Med. Chem.* **1990**, 25, 673-680.
57. Leschke, C.; Elz, S.; Garbarg, M.; Schunack, W. Synthesis and Histamine H-1 Receptor Agonist Activity of a Series of 2-Phenylhistamines, 2-Heteroarylhistamines, and Analogs. *J. Med. Chem.* **1995**, 38, 1287-1294.
58. Elz, S.; Kramer, K.; Pertz, H. H.; Detert, H.; ter Laak, A. M.; Kuhne, R.; Schunack, W. Histaprodifens: Synthesis, pharmacological in vitro evaluation, and molecular modeling of a new class of highly active and selective histamine H-1-receptor agonists. *J. Med. Chem.* **2000**, 43, 1071-1084.
59. Carman-Krzan, M.; Bavec, A.; Zorko, M.; Schunack, W. Differences in the binding characteristic and intracellular effects of specific H-1 agonists-histaprodifens in the cardiovascular tissue. *Fundam. Clin. Pharmacol.* **2001**, 15, 72-72.
60. Strasser, A.; Striegl, B.; Wittmann, H.-J.; Seifert, R. Pharmacological profile of histaprodifens at four recombinant histamine H-1 receptor species isoforms. *J. Pharm. Exp. Ther.* **2008**, 324, 60-71.

61. Menghin, S.; Pertz, H. H.; Kramer, K.; Seifert, R.; Schunack, W.; Elz, S. N-alpha-imidazolylalkyl and pyridylalkyl derivatives of histaprodifen: Synthesis and in vitro evaluation of highly potent histamine H-1-receptor agonists. *J. Med. Chem.* **2003**, 46, 5458-5470.
62. Ashford, C. A.; Heller, H.; Smart, G. A. The action of histamine on hydrochloric acid and pepsin secretion in man. *Br. J. Pharmacol. Chemother.* **1949**, 4(2), 153–156.
63. Parsons, M. E.; Ganellin, C. R. Histamine and its receptors. *Br. J. Pharmacol.* **2006**, 147, S127-S135.
64. Ash, A. S. F.; Schild, H. O. Receptors Mediating Some Actions of Histamine. *Br. J. Pharmacol. Chemother.* **1966**, 27, 427-&.
65. Black, J. W.; Parsons, E. M.; Durant, C. J.; Duncan, W. A. M.; Ganellin, C. R. Definition and Antagonism of Histamine H2-Receptors. *Nature* **1972**, 236, 385-390.
66. Hill, S. J.; Ganellin, C. R.; Timmerman, H.; Schwartz, J. C.; Shankley, N. P.; Young, J. M.; Schunack, W.; Levi, R.; Haas, H. L. International Union of Pharmacology. XIII. Classification of histamine receptors. *Pharmacol. Rev.* **1997**, 49, 253-278.
67. Johnson, C. L.; Weinstein, H.; Green, J. P. Studies on Histamine H-2 Receptors Coupled to Cardiac Adenylate-Cyclase - Blockade by H-2 and H-1 Receptor Antagonists. *Mol. Pharmacol.* **1979**, 16, 417-428.
68. Cataldi, M.; Borriello, F.; Granata, F.; Annunziato, L.; Marone, G. Histamine receptors and antihistamines: from discovery to clinical applications. *Chem. Immunol. Allergy* **2014**, 100, 214-226.
69. Dove, S.; Elz, S.; Seifert, R.; Buschauer, A. Structure-activity relationships of histamine H-2 receptor ligands. *Mini-Rev. Med. Chem.* **2004**, 4, 941-954.
70. Baumann, G.; Permanetter, B.; Wirtzfeld, A. Possible Value of H-2-Receptor Agonists for Treatment of Catecholamine-Insensitive Congestive Heart-Failure. *Pharmacol. Ther.* **1984**, 24, 165-177.
71. Baumann, G.; Felix, S. B.; Heidecke, C. D.; Riess, G.; Loher, U.; Ludwig, L.; Blomer, H. Apparent Superiority of H-2-Receptor Stimulation and Simultaneous Beta-Blockade over Conventional Treatment with Beta-Sympathomimetic Drugs in Post-Acute Myocardial-Infarction - Cardiac Effects of Impromidine - a New Specific H-2-Receptor Agonist - in the Surviving Catecholamine-Insensitive Myocardiumic. *Agents Actions* **1984**, 15, 216-228.
72. Buschauer, A. Synthesis and Invitro Pharmacology of Arpromidine and Related Phenyl(Pyridylalkyl)Guanidines, a Potential New Class of Positive Inotropic Drugs. *J. Med. Chem.* **1989**, 32, 1963-1970.
73. Ghorai, P.; Kraus, A.; Keller, M.; Götte, C.; Igel, P.; Schneider, E.; Schnell, D.; Bernhardt, G.; Dove, S.; Zabel, M.; Seifert, R.; Buschauer, A. Acylguanidines as bioisosteres of guanidines: N(G)-acylated imidazolylpropylguanidines, a new class of histamine H2 receptor agonists. *J. Med. Chem.* **2008**, 51, 7193-7204.
74. Xie, S. X.; Ghorai, P.; Ye, Q. Z.; Buschauer, A.; Seifert, R. Probing ligand-specific histamine H1- and H2-receptor conformations with NG-acylated Imidazolylpropylguanidines. *J. Pharmacol. Exp. Ther.* **2006**, 317, 139-146.
75. Birnkammer, T.; Spickenreither, A.; Brunskole, I.; Lopuch, M.; Kagermeier, N.; Bernhardt, G.; Dove, S.; Seifert, R.; Elz, S.; Buschauer, A. The bivalent ligand approach leads to highly potent and selective acylguanidine-type histamine H(2) receptor agonists. *J. Med. Chem.* **2012**, 55, 1147-1160.
76. Aurelius, J.; Martner, A.; Brune, M.; Palmqvist, L.; Hansson, M.; Hellstrand, K.; Thoren, F. B. Remission maintenance in acute myeloid leukemia: impact of functional histamine H-2 receptors expressed by leukemic cells. *Haematol-Hematol J* **2012**, 97, 1904-1908.
77. Werner, K.; Neumann, D.; Seifert, R. Analysis of the histamine H2-receptor in human monocytes. *Biochem. Pharmacol.* **2014**, 92, 369-379.
78. Romero, A. I.; Thoren, F. B.; Aurelius, J.; Askarieh, G.; Brune, M.; Hellstrand, K. Post-consolidation immunotherapy with histamine dihydrochloride and interleukin-2 in AML. *Scand. J. Immunol.* **2009**, 70, 194-205.
79. Schwartz, J. C. Histamine as a Transmitter in Brain. *Life Sci.* **1975**, 17, 503-517.

80. Arrang, J. M.; Garbarg, M.; Schwartz, J. C. Auto-Inhibition of Brain Histamine-Release Mediated by a Novel Class (H-3) of Histamine-Receptor. *Nature* **1983**, 302, 832-837.
81. Bertaccini, G.; Coruzzi, G.; Adami, M.; Pozzoli, C.; Gambarelli, E. Histamine H3 receptors: an overview. *Ital. J. Gastroenterol.* **1991**, 23, 378-385.
82. Bongers, G.; Bakker, R. A.; Leurs, R. Molecular aspects of the histamine H-3 receptor. *Biochem. Pharmacol.* **2007**, 73, 1195-1204.
83. Walter, M.; Stark, H. Histamine receptor subtypes: a century of rational drug design. *Front Biosci (Schol Ed)* **2012**, 4, 461-488.
84. Schwartz, J. C. The histamine H3 receptor: from discovery to clinical trials with pitolisant. *Br. J. Pharmacol.* **2011**, 163, 713-721.
85. Inocente, C.; Arnulf, I.; Bastuji, H.; Thibault-Stoll, A.; Raoux, A.; Reimao, R.; Lin, J. S.; Franco, P. Pitolisant, an Inverse Agonist of the Histamine H-3 Receptor: An Alternative for Narcolepsy-Cataplexy in Teenagers with Refractory Sleepiness. *Inflamm. Res.* **2014**, 63, S8-S9.
86. Kitbunnadaj, R.; Zuiderveld, O. P.; Christophe, B.; Hulscher, S.; Menge, W. M. P. B.; Gelens, E.; Snip, E.; Bakker, R. A.; Celanire, S.; Gillard, M.; Talaga, P.; Timmerman, H.; Leurs, R. Identification of 4-(1H-imidazol-4(5)-ylmethyl)pyridine (immethridine) as a novel, potent, and highly selective histamine H-3 receptor agonist. *J. Med. Chem.* **2004**, 47, 2414-2417.
87. Kitbunnadaj, R.; Hashimoto, T.; Poli, E.; Zuiderveld, O. P.; Menozzi, A.; Hidaka, R.; de Esch, I. J. P.; Bakker, R. A.; Menge, W. M. P. B.; Yamatodani, A.; Coruzzi, G.; Timmerman, H.; Leurs, R. N-substituted piperidinyl alkyl imidazoles: Discovery of methimepip as a potent and selective histamine H-3 receptor agonist. *J. Med. Chem.* **2005**, 48, 2100-2107.
88. Wijtmans, M.; Leurs, R.; de Esch, I. Histamine H-3 receptor ligands break ground in a remarkable plethora of therapeutic areas. *Expert Opin Inv Drug* **2007**, 16, 967-985.
89. Leurs, R.; Bakker, R. A.; Timmerman, H.; de Esch, I. J. The histamine H3 receptor: from gene cloning to H3 receptor drugs. *Nat. Rev. Drug Discov.* **2005**, 4, 107-120.
90. Raible, D. G.; Lenahan, T.; Fayvilevich, Y.; Kosinski, R.; Schulman, E. S. Pharmacological Characterization of a Novel Histamine-Receptor on Human Eosinophils. *Am. J. Respir. Crit. Care Med.* **1994**, 149, 1506-1511.
91. Nakamura, T.; Itadani, H.; Hidaka, Y.; Ohta, M.; Tanaka, K. Molecular cloning and characterization of a new human histamine receptor, HH4R. *Biochem. Biophys. Res. Commun.* **2000**, 279, 615-620.
92. Liu, C. L.; Ma, X. J.; Jiang, X. X.; Wilson, S. J.; Hofstra, C. L.; Blevitt, J.; Pyati, J.; Li, X. B.; Chai, W. Y.; Carruthers, N.; Lovenberg, T. W. Cloning and pharmacological characterization of a fourth histamine receptor (H-4) expressed in bone marrow. *Mol. Pharmacol.* **2001**, 59, 420-426.
93. Morse, K. L.; Behan, J.; Laz, T. M.; West, R. E.; Greenfeder, S. A.; Anthes, J. C.; Umland, S.; Wan, Y. T.; Hipkin, R. W.; Gonsiorek, W.; Shin, N.; Gustafson, E. L.; Qiao, X. D.; Wang, S. K.; Hedrick, J. A.; Greene, J.; Bayne, M.; Monsma, F. J. Cloning and characterization of a novel human histamine receptor. *J. Pharmacol. Exp. Ther.* **2001**, 296, 1058-1066.
94. Nguyen, T.; Shapiro, D. A.; George, S. R.; Setola, V.; Lee, D. K.; Cheng, R.; Rauser, L.; Lee, S. P.; Lynch, K. R.; Roth, B. L.; O'Dowd, B. F. Discovery of a novel member of the histamine receptor family. *Mol. Pharmacol.* **2001**, 59, 427-433.
95. Zhu, Y.; Michalovich, D.; Wu, H. L.; Tan, K. B.; Dytko, G. M.; Mannan, I. J.; Boyce, R.; Alston, J.; Tierney, L. A.; Li, X. T.; Herrity, N. C.; Vawter, L.; Sarau, H. M.; Ames, R. S.; Davenport, B. M.; Hieble, J. P.; Wilson, S.; Bergsma, D. J.; Fitzgerald, L. R. Cloning, expression, and pharmacological characterization of a novel human histamine receptor. *Mol. Pharmacol.* **2001**, 59, 434-441.
96. Connelly, W. M.; Shenton, F. C.; Lethbridge, N.; Leurs, R.; Waldvogel, H. J.; Faull, R. L.; Lees, G.; Chazot, P. L. The histamine H4 receptor is functionally expressed on neurons in the mammalian CNS. *Br. J. Pharmacol.* **2009**, 157, 55-63.
97. Schneider, E. H.; Neumann, D.; Seifert, R. Histamine H4-receptor expression in the brain? *Naunyn Schmiedebergs Arch. Pharmacol.* **2015**, 388, 5-9.

98. Werner, K.; Neumann, D.; Buschauer, A.; Seifert, R. No evidence for histamine h4 receptor in human monocytes. *J. Pharmacol. Exp. Ther.* **2014**, 351, 519-526.
99. Neumann, D.; Beermann, S.; Magel, L.; Jonigk, D.; Weber-Steffens, D.; Mannel, D.; Seifert, R. Problems associated with the use of commercial and non-commercial antibodies against the histamine H-4 receptor. *Naunyn Schmiedebergs Arch. Pharmacol.* **2012**, 385, 855-860.
100. Feliszek, M.; Speckmann, V.; Schacht, D.; von Lehe, M.; Stark, H.; Schlicker, E. A search for functional histamine H4 receptors in the human, guinea pig and mouse brain. *Naunyn Schmiedebergs Arch. Pharmacol.* **2015**, 388, 11-17.
101. Jablonowski, J. A.; Grice, C. A.; Chai, W. Y.; Dvorak, C. A.; Venable, J. D.; Kwok, A. K.; Ly, K. S.; Wei, J. M.; Baker, S. M.; Dsesai, P. J.; Jiang, W.; Wilson, S. J.; Thurmond, R. L.; Karlsson, L.; Edwards, J. P.; Lovenberg, T. W.; Carruthers, N. I. The first potent and selective non-imidazole human histamine H(4) receptor antagonists. *J. Med. Chem.* **2003**, 46, 3957-3960.
102. Rosethorne, E. M.; Charlton, S. J. Agonist-Biased Signaling at the Histamine H-4 Receptor: JNJ7777120 Recruits beta-Arrestin without Activating G Proteins. *Mol. Pharmacol.* **2011**, 79, 749-757.
103. Mowbray, C. E.; Bell, A. S.; Clarke, N. P.; Collins, M.; Jones, R. M.; Lane, C. A. L.; Liu, W. L.; Newman, S. D.; Paradowski, M.; Schenck, E. J.; Selby, M. D.; Swain, N. A.; Williams, D. H. Challenges of drug discovery in novel target space. The discovery and evaluation of PF-3893787: A novel histamine H4 receptor antagonist. *Bioorg. Med. Chem. Lett.* **2011**, 21, 6596-6602.
104. Thurmond, R. L.; Chen, B.; Dunford, P. J.; Greenspan, A. J.; Karlsson, L.; La, D.; Ward, P.; Xu, X. L. Clinical and Preclinical Characterization of the Histamine H-4 Receptor Antagonist JNJ-39758979. *J. Pharmacol. Exp. Ther.* **2014**, 349, 176-184.
105. Liu, W. L. Histamine H4 receptor antagonists for the treatment of inflammatory disorders. *Drug Discov. Today* **2014**, 19, 1222-1225.
106. Kiss, R.; Keseru, G. M. Novel histamine H4 receptor ligands and their potential therapeutic applications: an update. *Expert Opin. Ther. Pat.* **2014**, 24, 1185-1197.
107. Ohsawa, Y.; Hirasawa, N. The role of histamine H1 and H4 receptors in atopic dermatitis: from basic research to clinical study. *Allergology international : official journal of the Japanese Society of Allergology* **2014**, 63, 533-542.
108. Igel, P.; Geyer, R.; Strasser, A.; Dove, S.; Seifert, R.; Buschauer, A. Synthesis and structure-activity relationships of cyanoguanidine-type and structurally related histamine H4 receptor agonists. *J. Med. Chem.* **2009**, 52, 6297-6313.
109. Savall, B. M.; Edwards, J. P.; Venable, J. D.; Buzard, D. J.; Thurmond, R.; Hack, M.; McGovern, P. Agonist/antagonist modulation in a series of 2-aryl benzimidazole H-4 receptor ligands. *Bioorg. Med. Chem. Lett.* **2010**, 20, 3367-3371.
110. Strasser, A.; Wittmann, H. J.; Buschauer, A.; Schneider, E. H.; Seifert, R. Species-dependent activities of G-protein-coupled receptor ligands: lessons from histamine receptor orthologs. *Trends Pharmacol. Sci.* **2013**, 34, 13-32.
111. Yu, F.; Wolin, R. L.; Wei, J.; Desai, P. J.; McGovern, P. M.; Dunford, P. J.; Karlsson, L.; Thurmond, R. L. Pharmacological Characterization of Oxime Agonists of the Histamine H-4 Receptor. *Inflamm. Res.* **2010**, 59, S327-S327.
112. Jones, K. A.; Borowsky, B.; Tamm, J. A.; Craig, D. A.; Durkin, M. M.; Dai, M.; Yao, W. J.; Johnson, M.; Gunwaldsen, C.; Huang, L. Y.; Tang, C.; Shen, Q. R.; Salon, J. A.; Morse, K.; Laz, T.; Smith, K. E.; Nagarathnam, D.; Noble, S. A.; Branchek, T. A.; Gerald, C. GABA(B) receptors function as a heteromeric assembly of the subunits GABA(B)R1 and GABA(B)R2. *Nature* **1998**, 396, 674-679.
113. Kaupmann, K.; Malitschek, B.; Schuler, V.; Heid, J.; Froest, W.; Beck, P.; Mosbacher, J.; Bischoff, S.; Kulik, A.; Shigemoto, R.; Karschin, A.; Bettler, B. GABA(B)-receptor subtypes assemble into functional heteromeric complexes. *Nature* **1998**, 396, 683-687.
114. White, J. H.; Wise, A.; Main, M. J.; Green, A.; Fraser, N. J.; Disney, G. H.; Barnes, A. A.; Emson, P.; Foord, S. M.; Marshall, F. H. Heterodimerization is required for the formation of a functional GABA(B) receptor. *Nature* **1998**, 396, 679-682.

115. Agnati, L. F.; Ferre, S.; Lluis, C.; Franco, R.; Fuxe, K. Molecular mechanisms and therapeutical implications of intramembrane receptor/receptor interactions among heptahelical receptors with examples from the striatopallidal GABA neurons. *Pharmacol. Rev.* **2003**, 55, 509-550.
116. Hiller, C.; Kuhhorn, J.; Gmeiner, P. Class A G-protein-coupled receptor (GPCR) dimers and bivalent ligands. *J. Med. Chem.* **2013**, 56, 6542-6559.
117. Gomes, I.; Gupta, A.; Filipovska, J.; Szeto, H. H.; Pintar, J. E.; Devi, L. A. A role for heterodimerization of mu and delta opiate receptors in enhancing morphine analgesia. *Proc. Natl. Acad. Sci. U. S. A.* **2004**, 101, 5135-5139.
118. Rashid, A. J.; So, C. H.; Kong, M. M. C.; Furtak, T.; El-Ghundi, M.; Cheng, R.; O'Dowd, B. F.; George, S. R. D1-D2 dopamine receptor heterooligomers with unique pharmacology are coupled to rapid activation of G(q)/11 in the striatum. *Proc. Natl. Acad. Sci. U. S. A.* **2007**, 104, 654-659.
119. Rozenfeld, R.; Devi, L. A. Receptor heterodimerization leads to a switch in signaling: beta-arrestin2-mediated ERK activation by mu-delta opioid receptor heterodimers. *FASEB J.* **2007**, 21, 2455-2465.
120. Uberti, M. A.; Hall, R. A.; Minneman, K. P. Subtype-specific dimerization of alpha(1)-adrenoceptors: Effects on receptor expression and pharmacological properties. *Mol. Pharmacol.* **2003**, 64, 1379-1390.
121. Halazy, S. G-protein coupled receptors bivalent ligands and drug design. *Expert Opin. Ther. Pat.* **1999**, 9, 431-446.
122. Messer, W. S. Bivalent ligands for G protein-coupled receptors. *Curr. Pharm. Des.* **2004**, 10, 2015-2020.
123. Portoghese, P. S. Bivalent Ligands and the Message-Address Concept in the Design of Selective Opioid Receptor Antagonists. *Trends Pharmacol. Sci.* **1989**, 10, 230-235.
124. Erez, M.; Takemori, A. E.; Portoghese, P. S. Narcotic Antagonistic Potency of Bivalent Ligands Which Contain Beta-Naltrexamine - Evidence for Bridging between Proximal Recognition Sites. *J. Med. Chem.* **1982**, 25, 847-849.
125. Portoghese, P. S.; Larson, D. L.; Sayre, L. M.; Yim, C. B.; Ronsisvalle, G.; Tam, S. W.; Takemori, A. E. Opioid Agonist and Antagonist Bivalent Ligands - the Relationship between Spacer Length and Selectivity at Multiple Opioid Receptors. *J. Med. Chem.* **1986**, 29, 1855-1861.
126. Portoghese, P. S.; Ronsisvalle, G.; Larson, D. L.; Yim, C. B.; Sayre, L. M.; Takemori, A. E. Opioid Agonist and Antagonist Bivalent Ligands as Receptor Probes. *Life Sci.* **1982**, 31, 1283-1286.
127. Halazy, S.; Perez, M.; Fourrier, C.; Pallard, I.; Pauwels, P. J.; Palmier, C.; John, G. W.; Valentin, J. P.; Bonnafous, R.; Martinez, J. Serotonin dimers: Application of the bivalent ligand approach to the design of new potent and selective 5-HT1B/1D agonists. *J. Med. Chem.* **1996**, 39, 4920-4927.
128. Perez, M.; Pauwels, P. J.; Fourrier, C.; Chopin, P.; Valentin, J. P.; John, G. W.; Marien, M.; Halazy, S. Dimerization of sumatriptan as an efficient way to design a potent, centrally and orally active 5-HT1B agonist. *Bioorg. Med. Chem. Lett.* **1998**, 8, 675-680.
129. Kuhhorn, J.; Gotz, A.; Hubner, H.; Thompson, D.; Whistler, J.; Gmeiner, P. Development of a Bivalent Dopamine D-2 Receptor Agonist. *J. Med. Chem.* **2011**, 54, 7911-7919.
130. Huber, D.; Lober, S.; Hubner, H.; Gmeiner, P. Bivalent molecular probes for dopamine D-2-like receptors. *Biorg. Med. Chem.* **2012**, 20, 455-466.
131. Gogoi, S.; Biswas, S.; Modi, G.; Antonio, T.; Reith, M. E. A.; Dutta, A. K. Novel Bivalent Ligands for D2/D3 Dopamine Receptors: Significant Cooperative Gain in D2 Affinity and Potency. *ACS Med. Chem. Lett.* **2012**, 3, 991-996.
132. Portoghese, P. S. From models to molecules: opioid receptor dimers, bivalent ligands, and selective opioid receptor probes. *J. Med. Chem.* **2001**, 44, 2259-2269.
133. Portoghese, P. S. From models to molecules: Opioid receptor dimers, bivalent ligands, and selective opioid receptor probes. *J. Med. Chem.* **2001**, 44, 2259-2269.

134. McRobb, F. M.; Crosby, I. T.; Yuriev, E.; Lane, J. R.; Capuano, B. Homobivalent Ligands of the Atypical Antipsychotic Clozapine: Design, Synthesis, and Pharmacological Evaluation. *J. Med. Chem.* **2012**, 55, 1622-1634.
135. Bonger, K. M.; van den Berg, R. J. B. H. N.; Heitman, L. H.; IJzerman, A. P.; Oosterom, J.; Timmers, C. M.; Overkleeft, H. S.; van der Marel, G. A. Synthesis and evaluation of homo-bivalent GnRHR ligands. *Biorg. Med. Chem.* **2007**, 15, 4841-4856.
136. Kraus, A.; Ghorai, P.; Birnkammer, T.; Schnell, D.; Elz, S.; Seifert, R.; Dove, S.; Bernhardt, G.; Buschauer, A. N(G)-acylated aminothiazolylpropylguanidines as potent and selective histamine H(2) receptor agonists. *ChemMedChem* **2009**, 4, 232-240.
137. Lefkowitz, R. J.; Shenoy, S. K. Transduction of receptor signals by beta-arrestins. *Science* **2005**, 308, 512-517.
138. Lefkowitz, R. J. G protein-coupled receptors III. New roles for receptor kinases and beta-arrestins in receptor signaling and desensitization. *J. Biol. Chem.* **1998**, 273, 18677-18680.
139. Reiter, E.; Lefkowitz, R. J. GRKs and beta-arrestins: roles in receptor silencing, trafficking and signaling. *Trends Endocrinol. Metab.* **2006**, 17, 159-165.
140. Xiao, K. H.; Sun, J. P.; Kim, J.; Rajagopal, S.; Zhai, B.; Villen, J.; Haas, W.; Kovacs, J. J.; Shukla, A. K.; Hara, M. R.; Hernandez, M.; Lachmann, A.; Zhao, S.; Lin, Y. A.; Cheng, Y. S.; Mizuno, K.; Ma'ayan, A.; Gygi, S. P.; Lefkowitz, R. J. Global phosphorylation analysis of beta-arrestin-mediated signaling downstream of a seven transmembrane receptor (7TMR). *Proc. Natl. Acad. Sci. U. S. A.* **2010**, 107, 15299-15304.
141. Reiter, E.; Ahn, S.; Shukla, A. K.; Lefkowitz, R. J. Molecular Mechanism of beta-Arrestin-Biased Agonism at Seven-Transmembrane Receptors. *Annual Review of Pharmacology and Toxicology, Vol 52* **2012**, 52, 179-197.
142. Kenakin, T. New concepts in drug discovery: Collateral efficacy and permissive antagonism. *Nature Reviews Drug Discovery* **2005**, 4, 919-927.
143. Wei, H. J.; Ahn, S.; Shenoy, S. K.; Karnik, S. S.; Hunyady, L.; Luttrell, L. M.; Lefkowitz, R. J. Independent beta-arrestin 2 and G protein-mediated pathways for angiotensin II activation of extracellular signal-regulated kinases 1 and 2. *Proc. Natl. Acad. Sci. U. S. A.* **2003**, 100, 10782-10787.
144. Gesty-Palmer, D.; Chen, M. Y.; Reiter, E.; Ahn, S.; Nelson, C. D.; Wang, S. T.; Eckhardt, A. E.; Cowan, C. L.; Spurney, R. F.; Luttrell, L. M.; Lefkowitz, R. J. Distinct beta-arrestin- and G protein-dependent pathways for parathyroid hormone receptor-stimulated ERK1/2 activation. *J. Biol. Chem.* **2006**, 281, 10856-10864.
145. Venkatakrishnan, A. J.; Deupi, X.; Lebon, G.; Tate, C. G.; Schertler, G. F.; Babu, M. M. Molecular signatures of G-protein-coupled receptors. *Nature* **2013**, 494, 185-194.
146. Seifert, R. Functional selectivity of G-protein-coupled receptors: from recombinant systems to native human cells. *Biochem. Pharmacol.* **2013**, 86, 853-861.
147. Galandrin, S.; Oligny-Longpre, G.; Bouvier, M. The evasive nature of drug efficacy: implications for drug discovery. *Trends Pharmacol. Sci.* **2007**, 28, 423-430.
148. Violin, J. D.; Lefkowitz, R. J. beta-arrestin-biased ligands at seven-transmembrane receptors. *Trends Pharmacol. Sci.* **2007**, 28, 416-422.
149. Wisler, J. W.; DeWire, S. M.; Whalen, E. J.; Violin, J. D.; Drake, M. T.; Ahn, S.; Shenoy, S. K.; Lefkowitz, R. J. A unique mechanism of beta-blocker action: Carvedilol stimulates beta-arrestin signaling. *Proc. Natl. Acad. Sci. U. S. A.* **2007**, 104, 16657-16662.
150. Carter, A. A.; Hill, S. J. Characterization of isoprenaline- and salmeterol-stimulated interactions between beta 2-adrenoceptors and beta-arrestin 2 using beta-galactosidase complementation in C2C12 cells. *J. Pharmacol. Exp. Ther.* **2005**, 315, 839-848.
151. Chen, X.; Sassano, M. F.; Zheng, L. Y.; Setola, V.; Chen, M.; Bai, X.; Frye, S. V.; Wetsel, W. C.; Roth, B. L.; Jin, J. Structure-Functional Selectivity Relationship Studies of beta-Arrestin-Biased Dopamine D-2 Receptor Agonists. *J. Med. Chem.* **2012**, 55, 7141-7153.

152. Hiller, C.; Kling, R. C.; Heinemann, F. W.; Meyer, K.; Hubner, H.; Gmeiner, P. Functionally selective dopamine D2/D3 receptor agonists comprising an enyne moiety. *J. Med. Chem.* **2013**, 56, 5130-5141.
153. Thurmond, R. L.; Desai, P. J.; Dunford, P. J.; Fung-Leung, W. P.; Hofstra, C. L.; Jiang, W.; Nguyen, S.; Riley, J. P.; Sun, S. Q.; Williams, K. N.; Edwards, J. P.; Karlsson, L. A potent and selective histamine H-4 receptor antagonist with anti-inflammatory properties. *J. Pharmacol. Exp. Ther.* **2004**, 309, 404-413.
154. Nijmeijer, S.; Vischer, H. F.; Rosethorne, E. M.; Charlton, S. J.; Leurs, R. Analysis of multiple histamine H(4) receptor compound classes uncovers Galphai protein- and beta-arrestin2-biased ligands. *Mol. Pharmacol.* **2012**, 82, 1174-1182.
155. Whalen, E. J.; Rajagopal, S.; Lefkowitz, R. J. Therapeutic potential of beta-arrestin- and G protein-biased agonists. *Trends Mol. Med.* **2011**, 17, 126-139.
156. Violin, J. D.; DeWire, S. M.; Yamashita, D.; Rominger, D. H.; Nguyen, L.; Schiller, K.; Whalen, E. J.; Gowen, M.; Lark, M. W. Selectively Engaging beta-Arrestins at the Angiotensin II Type 1 Receptor Reduces Blood Pressure and Increases Cardiac Performance. *J. Pharmacol. Exp. Ther.* **2010**, 335, 572-579.

Chapter 2

Scope and Objectives

2.1 Dimeric carbamoylguanidine-type H_2 receptor ligands

A first aim of this doctoral thesis was the synthesis and the pharmacological characterization of a series of new dimeric (bivalent) H_2R agonists in which acylguanidine moieties are replaced by carbamoylguanidine groups. From the chemical point of view, the major advantage of the carbamoylguandines consists in resistance against hydrolytic cleavage compared to the acylguanidines. Hence, the stability of representative examples of carbamoylated and acylated guanidines, respectively, was compared.
With respect to confocal microscopy and investigations on the stoichiometry of ligand to receptor in case of bivalent agonist binding, a major goal of this work was the synthesis of a chain-branched dimeric ligand, enabling radio- and fluorescence labeling.

2.2 Unraveling signaling pathways of the human histamine receptors H_1R and H_2R in HEK293T CRE Luc cells

Due to a lack of data regarding functional selectivity of the H_1R and the H_2R, a second project of this thesis aimed at the development of a pharmacological tool kit for the investigation of alternative signaling pathways of the human H_1 (hH_1R) and the human H_2 receptor (hH_2R). Although preferential coupling of hH_1R and hH_2R to $G\alpha_q$ and $G\alpha_s$, respectively, had been taken for granted, alternative signaling pathways were proposed. Therefore, HEK293T cells were genetically engineered to stably co-express the firefly luciferase under the control of a cAMP response element (CRE) and the hH_1R or the hH_2R, respectively. Aiming at functional assays enabling a discrimination between different signaling pathways, the transfectants were investigated in a luciferase reporter gene assay, in the fura-2 assay and in the aequorin assay. Moreover, the application of a TR-FRET based cAMP assay was planned. In order to unravel the underlying pathways selective G-protein inhibitors were used.

Chapter 3

Dimeric carbamoylguanidine-type H_2 receptor ligands: A new class of potent and selective agonists

Note: Prior to the submission of this thesis, parts of this chapter have already been published in cooperation with partners. For detailed information on the nature of this collaboration see Acknowledgements and declaration of collaborations.

3.1 Introduction

Previously, N^G-acylated hetarylpropylguanidines were identified as potent histamine H_2 receptor (H_2R) agonists.[1-3] Surprisingly, an enormous increase in H_2R potency was achieved by linking two acylguanidine moieties. The most potent of those dimeric compounds showed up to 5000-fold potency of histamine (depending on the type of assay and the respective H_2R ortholog).[3] The first generation of N^G-acylated imidazolylpropylguanidines showed a lack of selectivity, especially towards histamine H_3 (H_3R) and histamine H_4 receptors (H_4R).[4] Selectivity for the H_2R was achieved by bioisosteric replacement of the imidazole ring by an amino(methyl)thiazole moiety.[2,3] Porthogese et al. suggested that the distance between the orthosteric binding sites of two dimerising receptor protomers is about 22 to 27 Å.[6] In an approach to explore whether the bivalent H_2R agonists bind to a receptor monomer or a receptor dimer, Birnkammer et al. investigated compounds with a spacer length between 6 and 27 Å.[3] The highest potency resided in compounds with an octa- or hexamethylene chain.[3] Due to insufficient spacer length for interaction with the orthosteric binding pockets of dimeric H_2R protomers, the gain in potency seems to result from the interaction with an additional binding site at the same receptor molecule. However, so far the binding mode of bivalent H_2R agonists is not understood, and appropriate pharmacological tools to study the mode and stoichiometry of binding are not available.

Acylguanidines turned out to undergo hydrolytic cleavage upon long-term storage in aqueous solution. Aiming at more stable dimeric H_2R agonists, we replaced the acylguanidine moieties by carbamoylguanidine groups according to a bioisosteric approach (**Fig. 3.1**). Moreover, a branched linker enabled the synthesis of radiolabeled and fluorescent derivatives. The compounds were characterized in functional and binding studies on recombinant histamine receptors. In addition, selected agonists were investigated on human monocytes.

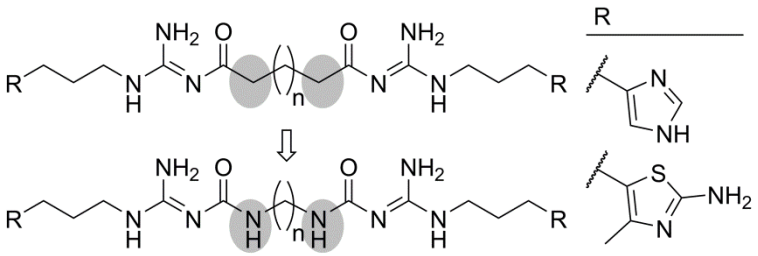

Figure 3.1. Bioisosteric replacement of the acylguanidine moieties in dimeric H_2 receptor agonists by carbamoylguanidine groups.

3.2 Chemistry

3.2.1 Homobivalent carbamoylguanidine-type H_2R ligands

The *N*-[3-(1-trityl-1*H*-imidazol-4-yl)propan-1-amine building block **3.6** (**Scheme 3.1**) was synthesized with minor modifications as previously described.[1] After esterification of urocanic acid[7] and hydrogenation of the double bond, the imidazole-NH was protected with a trityl moiety. The reduction of the ester group with $LiAlH_4$ resulted in the alcohol **3.4**, which was converted to the primary amine **3.6** by a Mitsunobu reaction.[8]

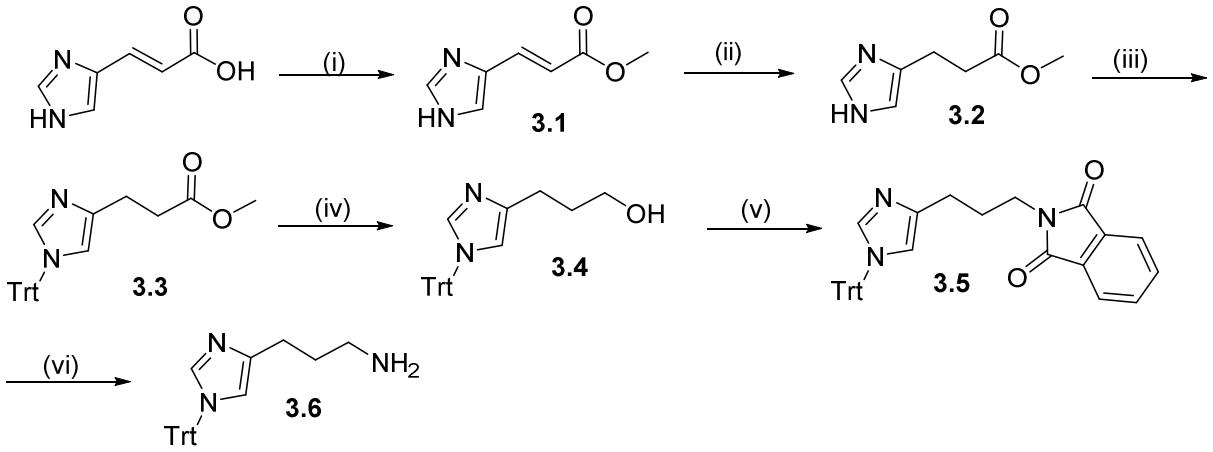

Scheme 3.1. Synthesis of the imidazolylpropylguanidine building block **3.6**. Reagents and conditions: (i) anhydrous Na_2SO_4, H_2SO_4/conc., MeOH/abs, 30 h, reflux, 78 %; (ii) H_2, Pd/C (10 %) cat., MeOH, 5 bar, 24 h, rt, 99 %; (iii) CPh_3Cl, NEt_3, MeCN, 12 h, rt, 52 %; (iv) $LiAlH_4$, THF/abs, Et_2O/abs, 2 h, reflux, 81 %; (v) phthalimide, PPh_3, DIAD, THF/abs, 24 h, rt, 68 %; (vi) $N_2H_4 \cdot H_2O$, EtOH, 1 h, reflux, 84 %

The *tert*-butyl [5-(3-aminopropyl)-4-methylthiazol-2-yl]carbamate building block **3.11** was prepared from 6-chlorohexan-2-one and phthalimide. The ketone was brominated and allowed to react with thiourea to give the thiazole **3.9**. Boc-protection gave **3.10** and subsequent hydrazinolysis resulted in the primary amine **3.11** (**Scheme 3.2**).[9]

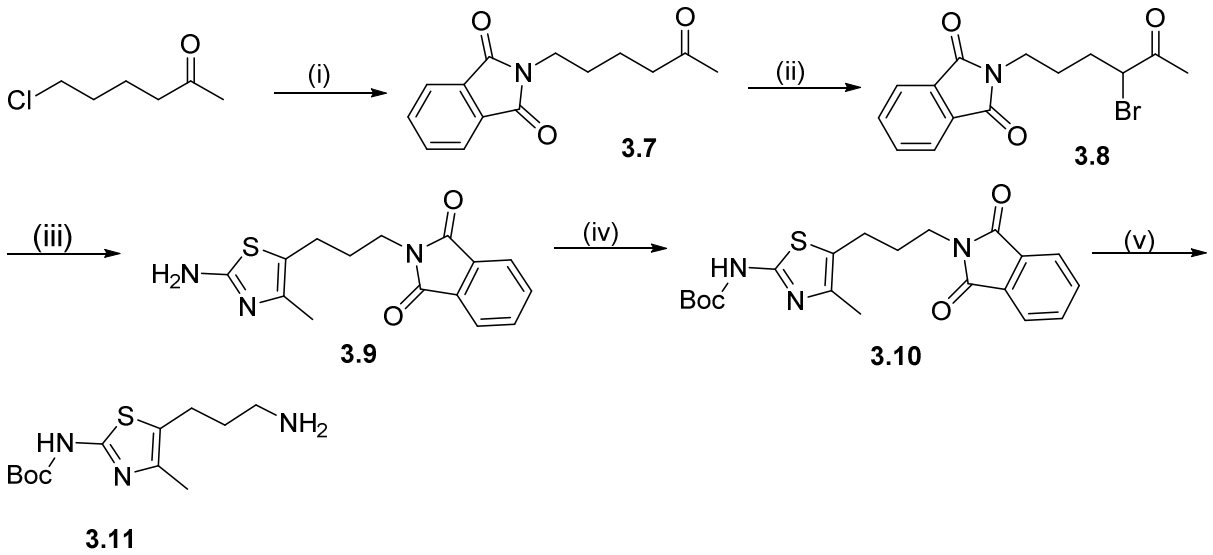

Scheme 3.2. Synthesis of the *tert*-butyl [5-(3-aminopropyl)-4-methylthiazol-2-yl]carbamate **3.11**. Reagents and conditions: (i) phthalimide, K_2CO_3, DMF, 24 h, 80 °C, 39 %; (ii) Br_2, dioxan/DCM, 1h, rt, 100 %; (iii) thiourea, DMF, 3 h, 100 °C, 62 %; (iv) Boc_2O, NEt_3, DMAP (cat.), $CHCl_3$, 24 h, rt, 79 %; (v) $N_2H_4 \cdot H_2O$, EtOH, 1 h, reflux, 53 %

The synthesis of the spacers started with the preparation of the mono-Boc protected isothiourea **3.13**, a well-established guanidinylating reagent,[10] as previously described (**Scheme 3.3**).[2]

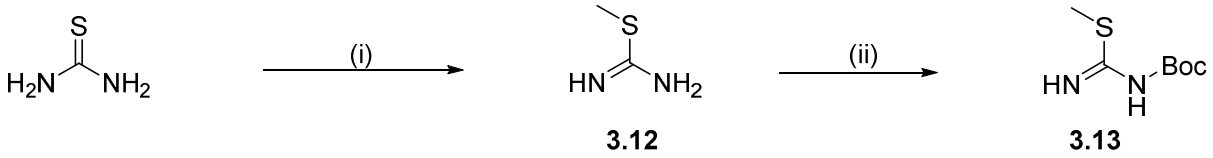

Scheme 3.3. Synthesis of the N-*tert*-butoxycarbonyl-S-methylisothiourea **3.13.** Reagents and conditions: (i) MeI (1 eq), MeOH, 1 h, reflux, 97 %; (ii) Boc_2O (1 eq), NEt_3 (1 eq), DCM, 24 h, rt, 61 %

The guanidinylating reagents **3.14-3.18** were obtained from diamines and diisocyanates in one-pot reactions[11] (**Scheme 3.4**). The diamines were treated with triphosgene to give the corresponding diisocyanates, which were allowed to react with mono-Boc-protected S-methylisothiourea **3.13**.

The dimeric ligands **3.19-3.28** were prepared by treating the building blocks **3.6, 3.11** with the guanidinylating reagents **3.14-3.18** in the presence of $HgCl_2$ and base.[12] Treating the protected carbamoylguanidine-type intermediates with TFA gave compounds **3.19-3.28** (**Scheme 3.4**), which were purified by preparative HPLC.

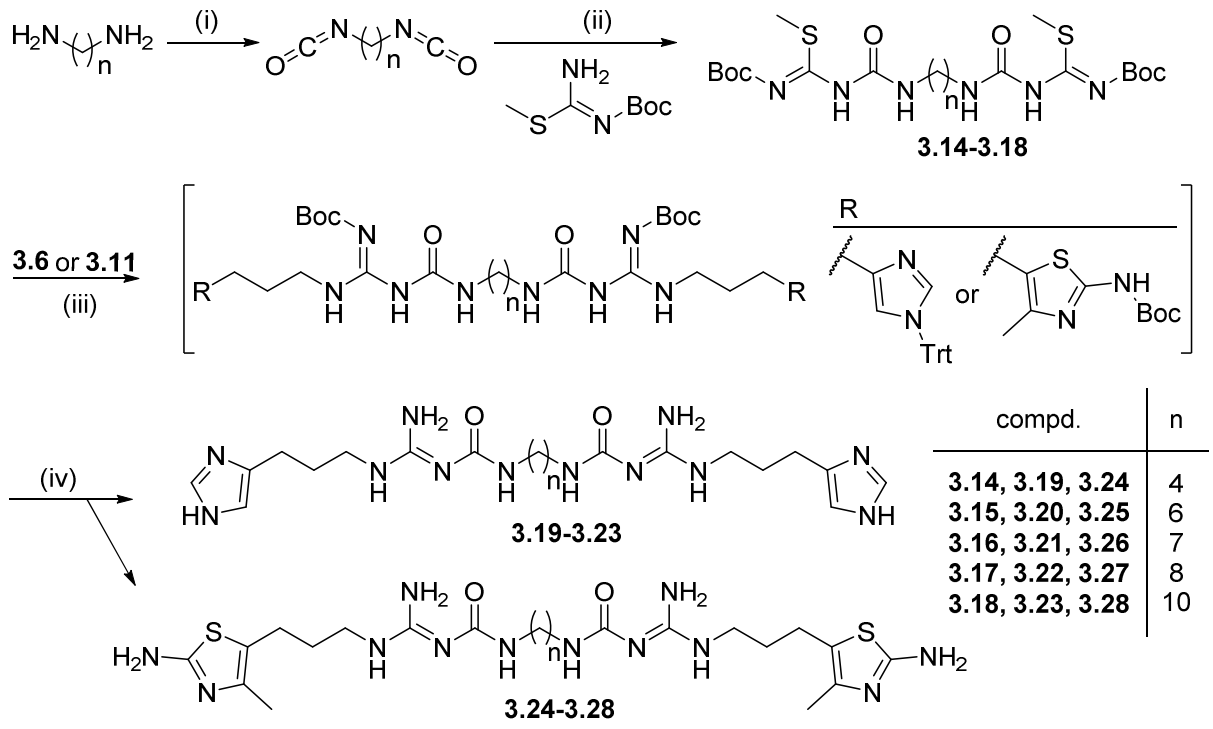

Scheme 3.4. Synthesis of the bivalent carbamoylguanidine-type ligands **3.19-3.28**. Reagents and conditions: (i) triphosgene, DIPEA, DCM abs., 30 min, 0 °C (ii) *N-tert*-butoxycarbonyl-*S*-methylisothiourea , 2.5 h, rt. **3.14**: 83 %, **3.15**: 74 %, **3.16**: 75 %, **3.17**: 74 %, **3.18**: 76 %; (iii) **3.6** or **3.11**, $HgCl_2$, NEt_3, DMF or DCM abs., 12 h, rt; (iv) 30 % TFA, DCM abs., 12 h, rt, **3.19**: 7 %, **3.20**: 10 %, **3.21**: 8 %, **3.22**: 20 %, **3.23**: 27 %, **3.24**: 14 %, **3.25**: 30 %, **3.26**: 29 %, **3.27**: 9 %, **3.28**: 9 %

3.2.2 Toward bivalent fluorescence- and radioligands

In view of radiolabeling and introduction of fluorophores, a branched linker comprising a primary amino group was synthesized. Starting from commercially available dicyclopropylketone, 1,7-dichloroheptan-4-one was obtained as recently described.[13] After nucleophilic displacement of chlorine by azides, the C=C bond was formed by a Wittig reaction[14] to yield 1-azido-4-(3-azidopropyl)-8-chlorooct-4-ene (**3.32**) (**Scheme 3.5**). Via the corresponding phthalimide (**3.33**), **3.32** was converted into the primary amine **3.34**. The amino group was Boc-protected (**3.35**) and the azide groups were reduced with $LiAlH_4$ to give the diamine **3.36**, which was converted to the diisocyanate **3.37**. The guanidinylating reagent **3.38** was prepared by analogy with the procedure for the preparation of **3.14-3.18**.

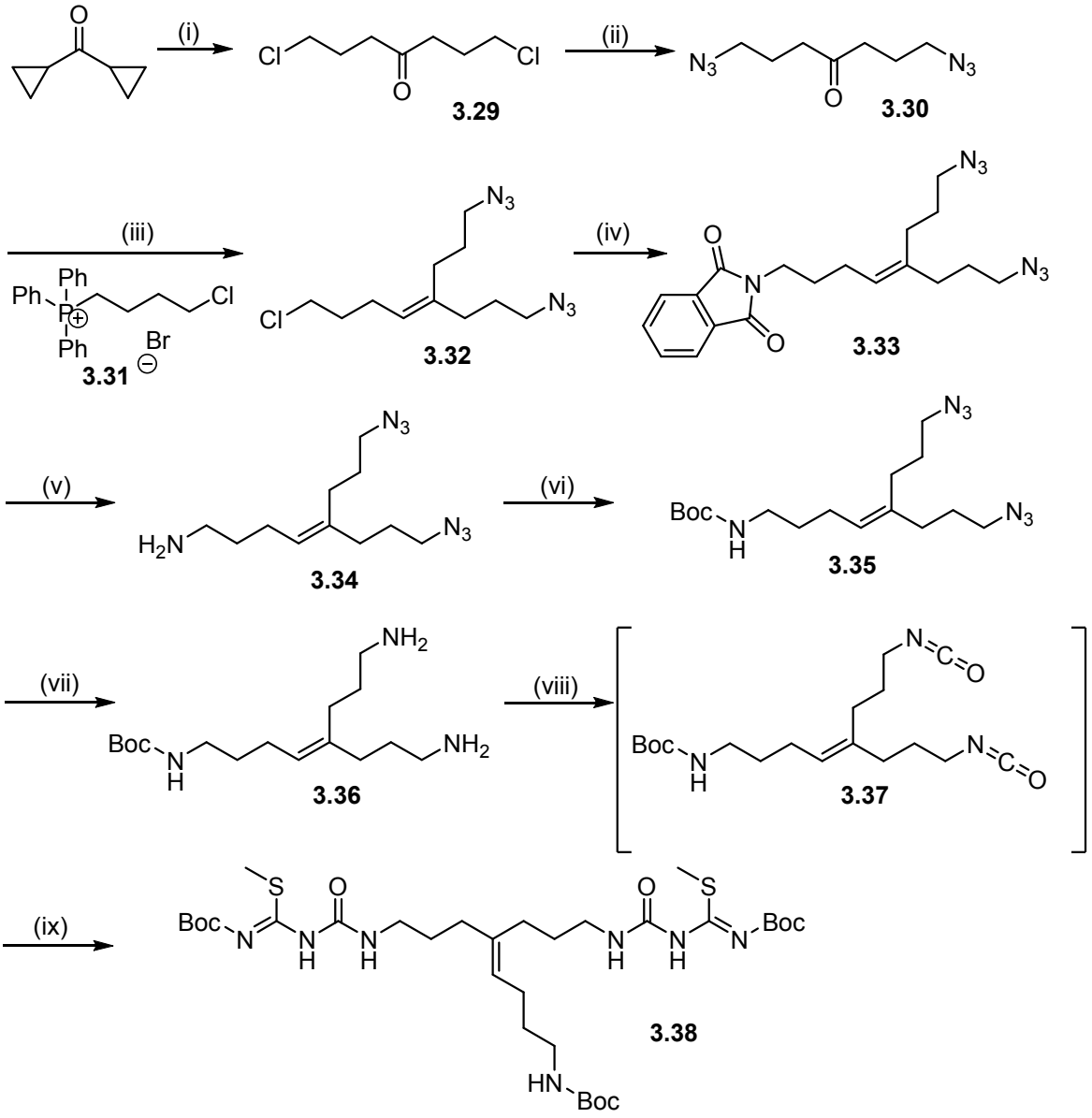

Scheme 3.5. Synthesis of the branched building block **3.38**. Reagents and conditions: (i) HCl gas, rt, 100 %; (ii) NaN_3, DMF, 12 h, rt, 79 %; (iii) *n*-BuLi, THF abs, 15 h, -72 °C → rt, 19 %; (iv) phthalimide, Cs_2CO_3, KI (cat.), DMF, 60 °C, 12 h, 57 %; (v) $N_2H_4 \cdot H_2O$, EtOH, 1 h, reflux, 88 %; (vi) Boc_2O, NEt_3, DCM, rt, 24 h, 97 %; (vii) $LiAlH_4$, Et_2O/abs, 2 h, reflux, 66 %; (viii) triphosgene, DIPEA, DCM abs., 30 min, 0 °C; (ix) *N*-tert-butoxycarbonyl-*S*-methylisothiourea, 2.5 h, rt, 44%

The precursor (**3.39**; **Scheme 3.6**) of the labeled compounds was synthesized from **3.38** according to the procedure described above for compounds **3.24-3.28** using **3.11** as building block. Compound **3.39** was coupled to three different fluorophores: the cyanine S2197 and the small pyrylium dyes Py-1 and Py-5 (**Scheme 3.6**).[15,16] S2197 provided as succinimidyl ester, was coupled to the bivalent precursor in the presence of triethylamine to give **3.40**. The pyrylium dyes reacted instantaneously in a ring transformation (color changes from blue into red) to give the positively charged N-substituted pyridinium compounds **3.41** and **3.42** (**Scheme 3.6**).[17]

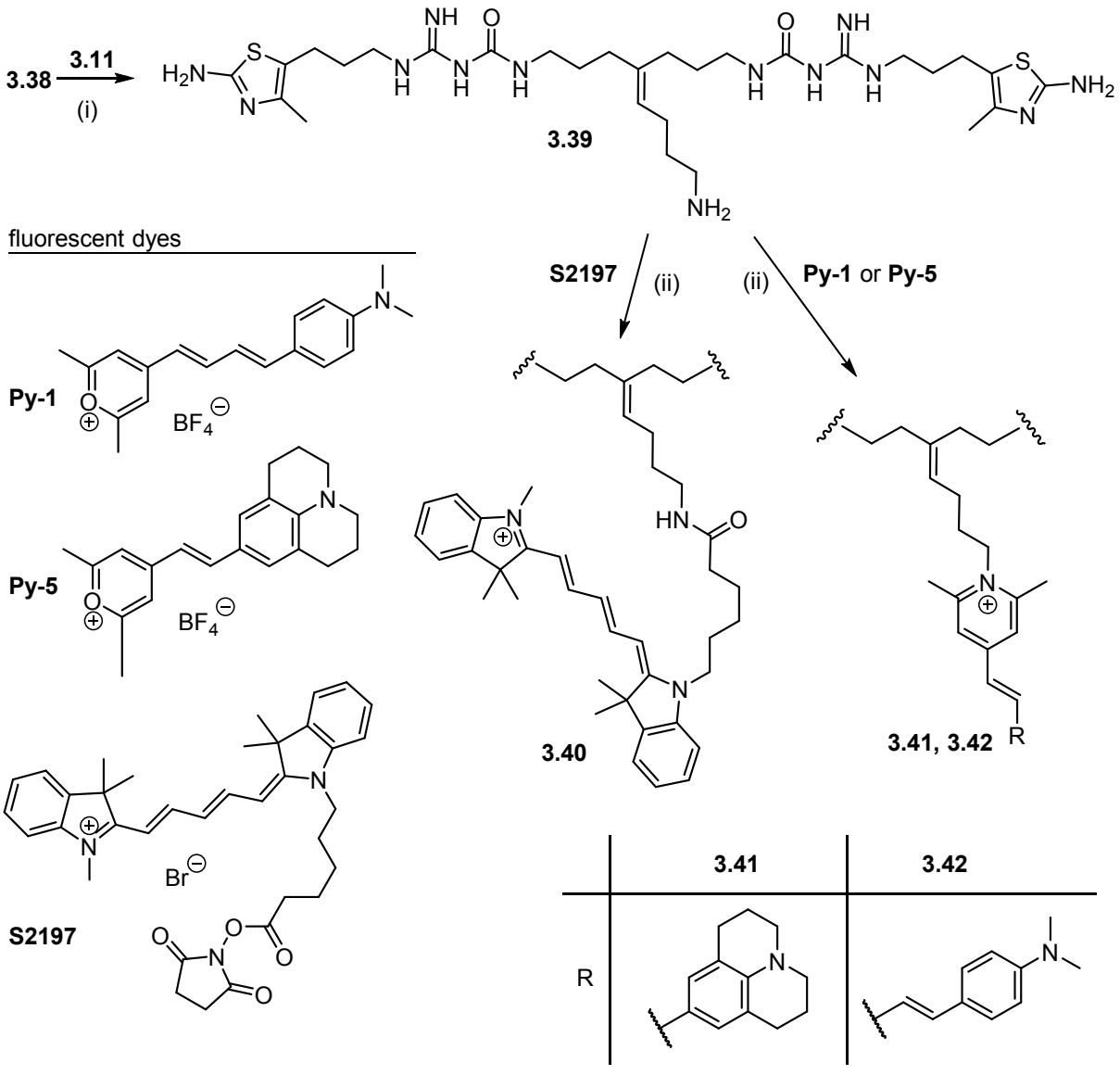

Scheme 3.6. Synthesis of compound **3.39** and preparation of the fluorescence ligands **3.40-3.42**. Reagents and conditions: (a) 1) compd. **3.11**, $HgCl_2$, NEt_3, DMF, 12 h, rt; 2) 30 % TFA, DCM abs., 12 h, rt, 21 %; (b) NEt_3, DMF, rt, 2h, **3.40**: 45 %, **3.41**: 36 %, **3.42**: 38 %

Compound **3.39** was acylated with "cold" succinimidyl propionate (cf. **3.43a**) to optimize the reaction conditions for the propionylation with tritiated succinimidyl propionate (**Scheme 3.7**). This synthetic route afforded the radioligand **3.43b** in a yield of 90 %. Purification by HPLC gave **3.43b** in a radiochemical purity of 99 % (**Fig. 3.2**) with a specific activity of 70 Ci/mmol.

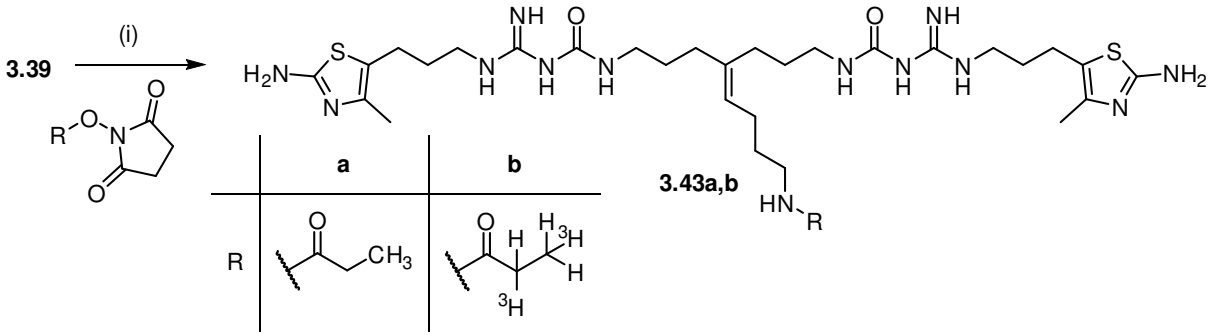

Scheme 3.7. Synthesis of the unlabeled ("cold") propionamide **3.43a** and the corresponding radiolabeled version **3.43b.** Reagents and conditions: (a) 1) NEt_3, DMF, 2 h, 81 %; 2) DIPEA, DMF, 3 h, 90 %

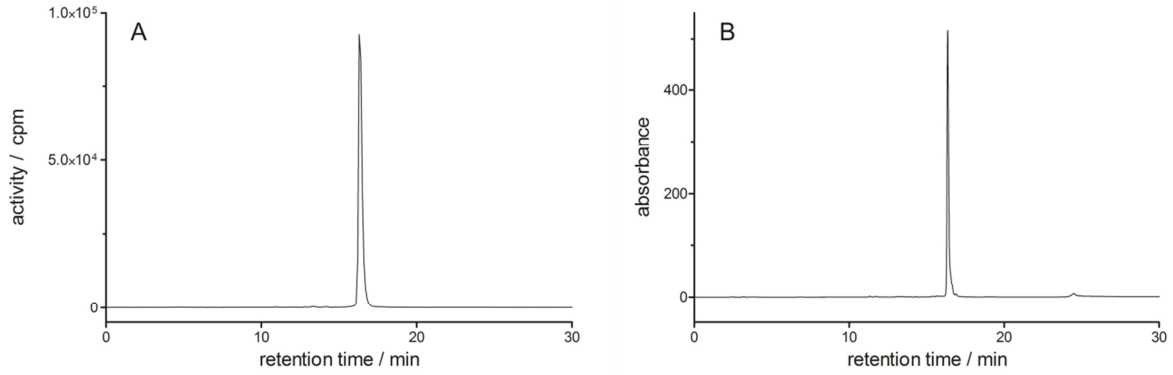

Figure 3.2. HPLC purity control with radiometric detection (**A**) and identity control (**B**) of **3.43b**: simultaneous injection of **3.43a** and **3.43b**. Conditions: eluent A: MeCN + 0.04 % TFA; eluent B: aq. 0.05 % TFA + 5 % MeCN, gradient: 0 to 20 min: A/B 5/95 to 26/74, 20 to 30 min A/B 90:10, t_R = 17,1 min

3.3 Results and Discussion

3.3.1 Stability of carbamoylguanidines compared to acylguanidines

Acylguanidines are stable at acidic pH, but tend to decompose under alkaline conditions. The decomposition becomes very fast, when an intramolecular nucleophilic attack is possible as previously demonstrated for aminoalkanoylguanidines with half-lives between 19 s and 13 h at pH 10.4.[18] Although the decomposition of acylguanidine-type H_2R agonists such as **3.44** (**Fig. 3.3A**) (provided by Dr. Anja Kraus)[3] turned out to occur at a much slower rate, hydrolytic cleavage upon long-time storage in solution has to be taken into account. For comparison, the stability of compounds **3.25** (**Fig. 3.3B**), and **3.44** as representative examples of carbamoylated and acylated guanidines, respectively, was investigated at a concentration of 100 µM in phosphate buffered saline (PBS, pH 7.4) at room temperature.

After one week, around 55 % of compound **3.44** were decomposed, whereas **3.25** proved to be stable under the same conditions.

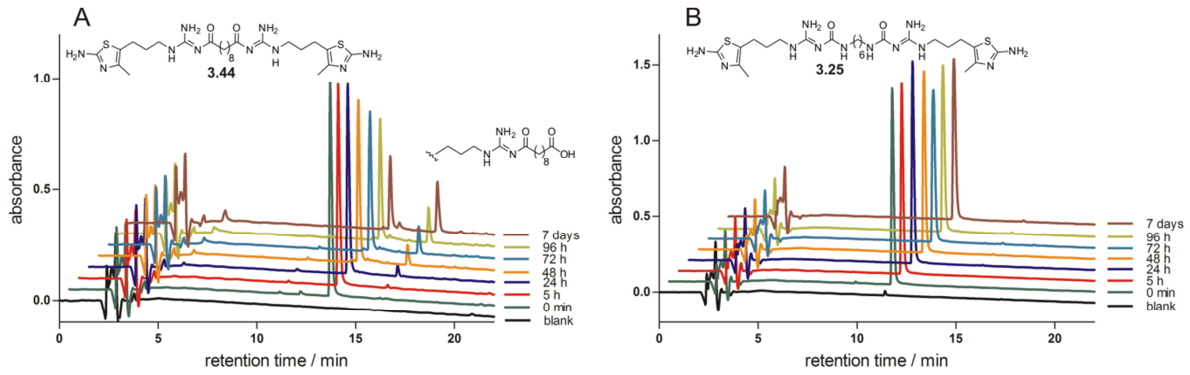

Figure 3.3. Chromatograms of the H_2R agonists **3.44** (**A**) and **3.25** (**B**) after different periods of incubation in PBS (pH 7.4) at rt.

3.3.2 Pharmacological results and discussion

The synthesized compounds were investigated on membrane preparations in the [^{35}S] GTPγS binding assay at the human (h) and at the guinea pig (gp) H_2R with regard to possible differences between species orthologs (**Table 3.1**, **Fig. 3.4**). The hH_2R as well as the gpH_2R were expressed as H_2R-$G_s\alpha_s$ fusion proteins in *Sf9* insect cells. To test the selectivity of the compounds for the H_2R compared to hH_1R, hH_3R, and hH_4R, competition binding experiments were performed using membranes of *Sf9* cells expressing the histamine receptor of interest (**Table 3.2**).

3.3.2.1 H_2R agonism in the GTPγS binding assay

The prepared bivalent ligands **3.19-3.28**, **3.39** and **3.43a** were partial or full agonists at both, the hH_2R and the gpH_2R. In agreement with previous studies on guanidine- and acylguanidine-type H_2R agonists,[2,3,19,20] higher potencies and intrinsic activities were achieved at the gpH_2R than at the hH_2R. Compound **3.22** was 2500 times more potent than histamine at the gpH_2R. Except for **3.24**, ligands bearing an imidazole ring were superior to the corresponding aminothiazoles at the hH_2R. Dimeric ligands with a spacer length of four methylene groups showed the lowest potency at the hH_2R, whereas the gpH_2R was less sensitive to variations in chain length. Interestingly, branching of the connecting chain hardly affected potency (cf. **3.39**), though the maximal response decreased. Propionylation of the primary amino group in the side chain of **3.39** resulted in regaining potency and intrinsic activity at the hH_2R (**3.43a)** (**Table 3.1**, **Fig. 3.4**).

Table 3.1. Histamine H_2 receptor agonism in the GTPγS assay[a]

	human H_2R			guinea pig H_2R		
compd.	pEC_{50} ± SEM	E_{max} ± SEM	Pot_{rel}	pEC_{50} ± SEM	E_{max} ± SEM	Pot_{rel}
HIS	5.85 ± 0.06	1.00	1.0	6.07 ± 0.14[21,b]	1.00	1.0
3.19	7.29 ± 0.08	0.97 ± 0.02	27.5	8.56 ± 0.04	0.99 ± 0.06	309.1
3.20	7.77 ± 0.02	0.88 ± 0.03	83.2	9.25 ± 0.14	0.96 ± 0.03	1512.4
3.21	8.31 ± 0.08	1.03 ± 0.06	288.4	8.45 ± 0.03	0.87 ± 0.08	239.6
3.22	8.35 ± 0.07	1.01 ± 0.07	316.0	9.47 ± 0.09	1.01 ± 0.06	2508.8
3.23	8.08 ± 0.09	0.70 ± 0.08	169.8	8.19 ± 0.07	0.95 ± 0.04	131.7
3.24	7.25 ± 0.11	0.96 ± 0.04	25.1	9.04 ± 0.13	1.04 ± 0.14	932.0
3.25	8.03 ± 0.02	0.92 ± 0.01	151.4	8.75 ± 0.15	1.09 ± 0.05	478.1
3.26	7.68 ± 0.03	0.90 ± 0.10	67.6	8.42 ± 0.19	0.97 ± 0.04	223.6
3.27	7.73 ± 0.15	0.80 ± 0.07	75.9	8.16 ± 0.07	0.80 ± 0.06	122.9
3.28	7.43 ± 0.12	0.64 ± 0.07	38.0	n.d.	n.d.	n.d.
3.39	7.49 ± 0.10	0.66 ± 0.06	43.7	8.11 ± 0.06	0.97 ± 0.06	109.5
3.43a	7.87 ± 0.12	0.73 ± 0.12	104.7	8.04 ± 0.05	0.89 ± 0.11	93.2

Table 3.1. [a] [^{35}S]GTPγS binding assay on membranes of *Sf9* cells expressing the hH_2R-$G_s\alpha_s$ and the gpH_2R-$G_s\alpha_s$. Data were analyzed by nonlinear regression and were best fit to three-parameter sigmoidal concentration-response curves. pEC_{50}: -logEC_{50}; E_{max}: maximal response relative to histamine (E_{max} = 1.0); Pot_{rel}: relative potency represents the ratio of EC_{50} values of test compound and histamine. Data shown are means ± SEM of 2-6 independent experiments, each performed in triplicate. [b] Determined in a steady-state [^{32}P]GTPase assay on *Sf9* cells expressing the gpH_2R- $G_s\alpha_s$.

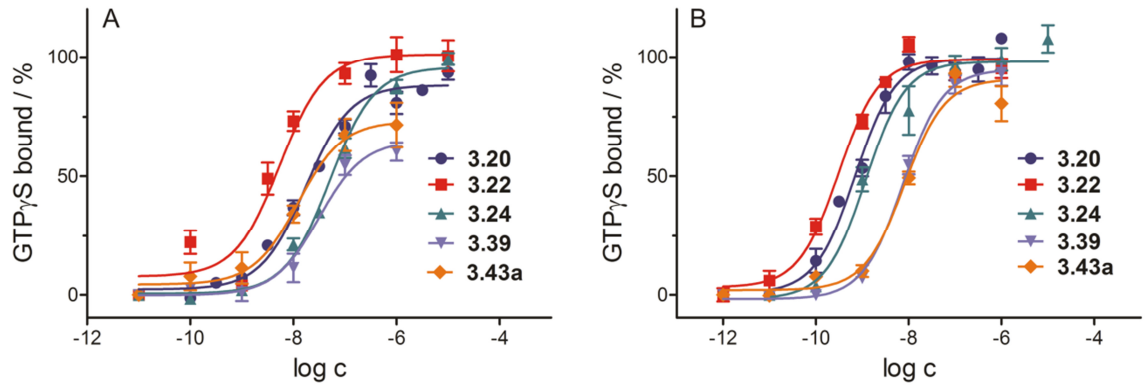

Figure 3.4. Concentration-response curves of selected agonists at hH_2R (**A**) and gpH_2R (**B**) in the GTPγS assay. The increase in GTPγS binding is referred to the maximal response to histamine (HIS) = 100 %. Data are means ± SEM of 2-6 independent experiments, each performed in triplicate.

3.3.2.2 H_2R affinities and receptor subtype selectivities

The H_2R affinity of the compounds was determined in competition binding studies. The pK_i values were in good agreement with the pEC_{50} values, in particular when [^{3}H]UR-DE257[5] was used as radioligand. Minor differences between functional and binding data became

obvious, when [^{3}H]tiotidine was used for displacement. As suggested by Kelley et al.[20] [^{3}H]tiotidine is able to address only a subpopulation of the H_2R, which might explain this phenomenon.

As expected, carbamoylguanidine-type ligands bearing two imidazole moieties were not selective for the H_2R, but also showed high affinity for the H_3R and the H_4R. By contrast, the synthesized aminothiazoles preferred the H_2R (**Table 3.2**).

Table 3.2. Binding data of the compounds **3.19-3.28**, **3.39**, **3.43a** on human histamine receptor subtypes[a]

	hH_1R	**hH_2R**	**hH_3R**	**hH_4R**
compd.	$pK_i \pm$ SEM[b]	$pK_i \pm$ SEM[c,d]	$pK_i \pm$ SEM[e,f]	$pK_i \pm$ SEM[g]
HIS	5.62 ± 0.03[22]	6.27 ± 0.04[c,19]	8.20 ± 0.04[23]	7.89 ± 0.01[24]
3.19	6.31 ± 0.10	7.57 ± 0.01[c]	8.55 ± 0.01[f]	7.02 ± 0.06
3.20	5.84 ± 0.04	7.87 ± 0.05[c]	8.16 ± 0.05[e], 8.52[f]	7.12 ± 0.04
3.21	6.60 ± 0.12	7.52 ± 0.04[d]	8.77 ± 0.02[f]	7.81 ± 0.09
3.22	6.66 ± 0.03	8.47[c], 8.52 ± 0.13[d]	8.82 ± 0.03[f]	8.27 ± 0.01
3.23	6.56 ± 0.02	7.56 ± 0.05[d]	8.21 ± 0.04[f]	7.58 ± 0.12
3.24	6.08 ± 0.03	7.76 ± 0.08[c]	6.17 ± 0.10[e], 6.17[f]	5.29 ± 0.04
3.25	6.07 ± 0.06	8.07 ± 0.05[c]	5.94 ± 0.16[e], 6.01[f]	5.69 ± 0.07
3.26	5.81 ± 0.09	7.55 ± 0.02[c]	5.76 ± 0.09[f]	5.55 ± 0.08
3.27	5.80 ± 0.06	7.17 ± 0.13[d]	6.00 ± 0.10[f]	6.26 ± 0.18
3.28	5.89 ± 0.01	7.21 ± 0.10[d]	5.81 ± 0.07[e]	5.97 ± 0.05
3.39	5.80 ± 0.08	7.59 ± 0.01[c]	6.56 ± 0.11[f]	6.08 ± 0.09
3.43a	6.36 ± 0.00	7.94 ± 0.09[c]	6.08 ± 0.08[f]	5.96 ± 0.09

Table 3.2. [a]Competition binding assay on membranes of *Sf9* cells expressing the hH_1R plus RGS4, the hH_2R-$G_s\alpha_s$, co-expressing the hH_3R plus $G\alpha_{i2}$ plus $G\beta_1\gamma_2$ or co-expressing the hH_4R plus $G\alpha_{i2}$ plus $G\beta_1\gamma_2$. Incubation period was 60 min. Data were analyzed by nonlinear regression and were best fit to 3-parameter sigmoidal concentration-response curves. Data shown are means ± SEM of 2-6 independent experiments, each performed in triplicate. [b]Displacement of 5 nM [^{3}H]mepyramine (K_d= 4.5 nM); [c]Displacement of 30 nM [^{3}H]UR-DE257 (K_d= 31 nM); [d]Displacement of 10 nM tiotidine (K_d= 19.7 nM); [e]Displacement of 15 nM [^{3}H]histamine (K_d= 12.6 nM); [f]Displacement of 3 nM [^{3}H]*N*$^\alpha$-methylhistamine (K_d= 3 nM); [g]Displacement of 10 nM histamine (K_d= 10 nM); Note: Representative compounds were investigated for functional activity at the hH_1R, hH_3R and hH_4R. In agreement with previous studies[1-3] on bivalent H_2R ligands, the carbamoylated imidazolylpropylguanidines behaved as agonists in the [^{35}S]GTPγS assay (Sf9 membranes) at the H_3R and the H_4R respectively, whereas the corresponding amino(methyl)thiazolylpropylguanidines proved to be H_3R and H_4R antagonists and were antagonists at the hH_1R (luciferase assay, HEK293 cells). hH_1R, $pK_b \pm$ SEM: **3.21**: 6.48 ± 0.14; **3.22**: 6.29 ± 0.21; **3.25**: 5.71 ± 0.06; **3.27**: 5.69 ± 0.13; **3.43a**: 5.32 ± 0.13. hH_3R, $pK_b \pm$ SEM: **3.25**: 5.57 ± 0.05; **3.27**: 5.86 ± 0.01; **3.43a**: 5.87 ± 0.06. hH_4R: **3.21**: pEC_{50} = 8.00 ± 0.04, E_{max} = 0.65 ± 0.03; **3.22**: pEC_{50} = 8.04 ± 0.09, E_{max} = 0.86 ± 0.08; **3.25**: pK_b = 5.30 ± 0.02; **3.27**: pK_b = 6.12 ± 0.11; **3.43a**: pK_b = 5.09 ± 0.22.

3.3.2.3 Investigation of the fluorescence ligands **3.40-3.42** and the radioligand **3.43b**

The compounds **3.40-3.42** were investigated in a flow cytometric binding assay[25] at HEK293T cells, transfected with the hH_2R. None of these compounds bound in a saturable manner (**Fig 3.5**).

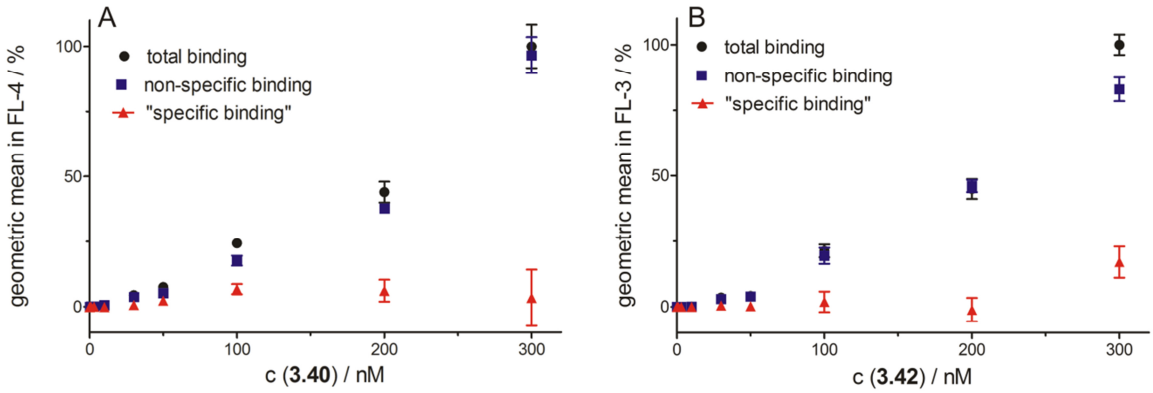

Figure 3.5. Flow cytometric binding assay on HEK293T CRE Luc hH_2R cells with ligands **3.40** (**A**) and **3.42** (**B**) as examples

Confocal microscopy with **3.42** revealed that the fluorescence ligands enter the HEK293T cells in a receptor-independent manner (**Fig 3.6**).

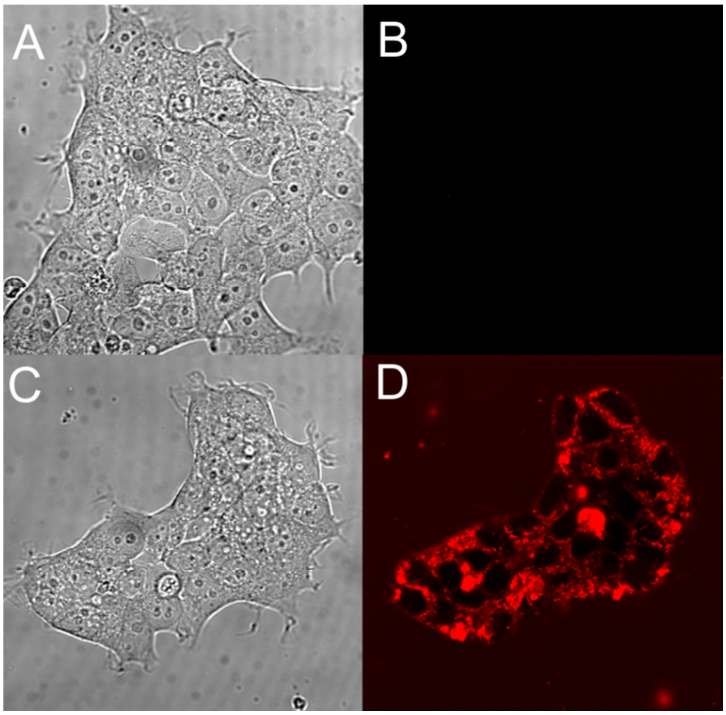

Figure 3.6. Confocal microscope images of HEK293T cells (not transfected with the hH_2R) after 20 min of incubation, at room temperature, with the fluorescent ligand **3.42**. 40000 cells were seeded 2 days prior to microscopy in Leibovitz L15 supplemented with 5 % FCS. **A**) Transmitted light; **B**) Autofluorescence; **C**) Transmitted light **D**) 500 nM of **3.42**. Images were acquired with a Zeiss Axiovert 200 M microscope; Plan Apochromat 60x/1.4W, 488 nm/ LP 560 nm.

Similarly, it was impossible to perform saturation binding studies with the radioligand **3.43b** on *Sf9* membranes (**Fig. 3.7**) and HEK293T (**Fig. 3.8**) cells because of high unspecific binding. Interestingly, lower unspecific binding was observed in the presence of competitors structurally similar to **3.43a**, hinting at reversible binding to non-H_2R sites at the cell membrane. Nevertheless, non-H_2R mediated internalization of **3.43b** into HEK293T cells is conceivable.

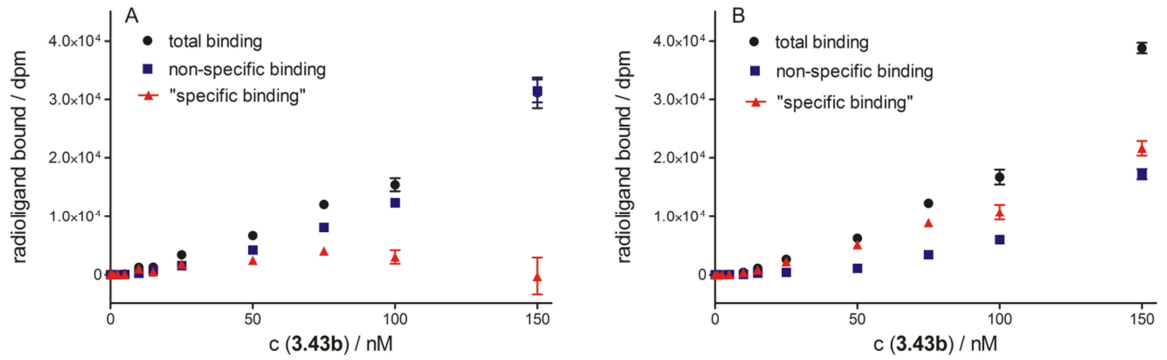

Figure 3.7. Concentration-dependent binding of **3.43b** to membranes of *Sf9* cells expressing the hH_2R-$G_s\alpha_s$ fusion protein. Non-specific binding was determined in the presence of 100 µM famotidine as competitor (**A**) and 10 µM **3.43a** as competitor (**B**).

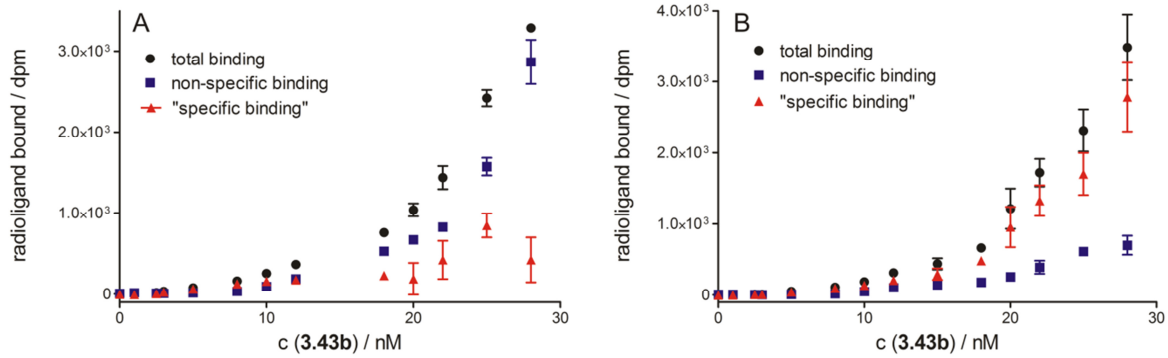

Figure 3.8. Concentration-dependent binding of **3.43b** to HEK293T cells expressing the hH_2R. Non-specific binding was determined in the presence of 100 µM famotidine as competitor (**A**) and 10 µM **3.43a** as competitor (**B**).

Previously, it was shown that the cholesterol content of *Sf9* insect cell membranes is 20-fold lower than in membranes of higher eukaryotic cells. Gimpl et al. demonstrated that the addition of cholesterol improved the specific binding of oxytocin to its receptor.[26]

By analogy with this approach, the *Sf9* cell membranes membranes were treated with cholesterol prior to investigating the binding of the radioligand **3.43b**. Surprisingly, the addition of cholesterol resulted in saturable binding (**Fig. 3.9A**). However, unfortunately, there was no difference between membranes of *Sf9* cells expressing the hH_2R and wild-type *Sf9* membranes (**Fig. 3.9B**), again suggesting that the radioligand binds in a reversible manner to off-targets in the cell membrane. Thus, radioligand **3.43b** proved to be inappropriate for H_2R quantification.

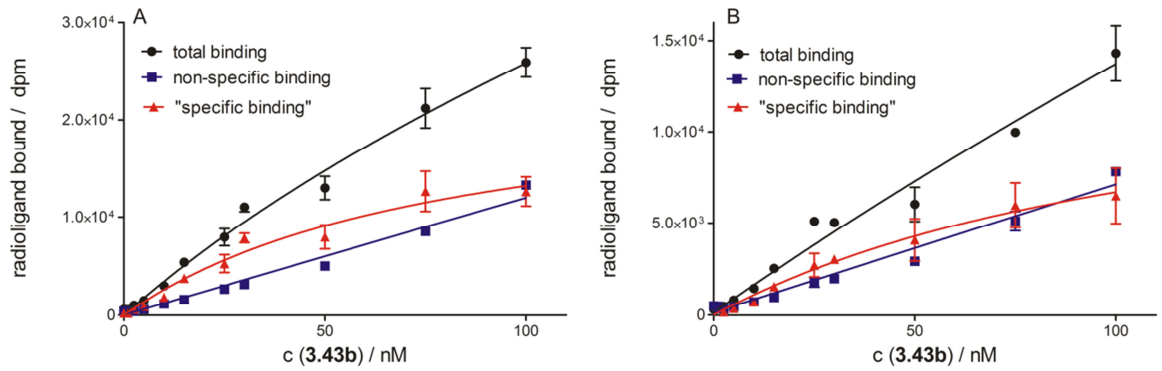

Figure 3.9. Concentration-dependent binding of **3.43b to cholesterol treated membranes** of *Sf9* cells expressing the hH_2R-$G_s\alpha_s$ fusion protein (**A**) and to wild-type membranes of *Sf9* cells (**B**). Non-specific binding was determined in the presence of 10 µM **3.43a** as competitor.

In spite of that, affinities determined for various H_2R ligands in competition binding experiments with **3.43b** (membranes of *Sf9* cells expressing the hH_2R), were in the range of K_i values determined by displacement of [^{3}H]UR-DE257[5] (**Fig. 3.10**). However, it should be noted that, due to the low signal-to-noise ratio, the data determined with **3.43b** as radioligand are less reliable.

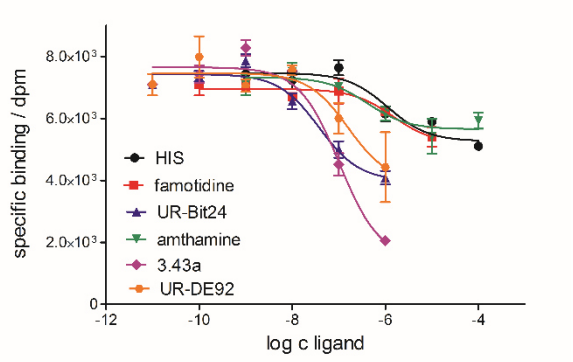

Figure 3.10. Displacement of the radioligand **3.43b** (c = 12 nM; K_d= 10.7 nM) by different H_2R ligands. K_d value of the radioligand was set to the K_i value of the "cold" version **3.43a**. The assay was performed on *Sf9* membranes expressing the hH_2R-$G_s\alpha_s$ fusion protein. Data shown are representative displacement curves.

Table 3.3. pK_i values determined with **3.43b** in comparison with **UR-DE257**[5]

compd.	pK_i value determined with **3.43b**[b]	pK_i value determined with **UR-DE257**[c]
HIS	6.46 ± 0.18	6.27 ± 0.04[5]
famotidine	6.32 ± 0.15	6.87 ± 0.05[5]
UR-Bit24[3]	8.12 ± 0.22	8.15 ±0.07[5]
amthamine	6.59 ± 0.12	6.61 ±0.07[5]
3.43a	7.33 ± 0.13	7.94 ± 0.09
UR-DE92[5]	7.81 ± 0.68	7.55 ± 0.03[5]

[a]Competition binding assay on *Sf9* membranes expressing the hH_2R-$G_s\alpha_s$. The incubation period was 60 min. Data were analyzed by nonlinear regression and were best fit to 3-parameter sigmoidal concentration-response curves. Data shown are means ± SEM of 2-3 independent experiments, each performed in triplicate. [b]Displacement of 12 nM **3.43b** (K_d = 10.7 nM); [c]Displacement of 30 nM [^{3}H]UR-DE257 (K_d = 31 nM);

3.3.2.4 Investigation of H_2R agonists in human monocytes[a]

[a] Note: These experiments were performed by Kristin Werner in the laboratory of Professor Dr. Roland Seifert (Institute of Pharmacology, Medical School of Hannover, Carl-Neuberg-Str.1, D-30625 Hannover, Germany).

Acute myeloid leukemia (AML) is an indication for post-consolidation therapy with histamine to prevent relapse.[26, 27] It is assumed that histamine inhibits oxygen radical formation via H_2R mediated inhibition of NADPH oxidase, resulting in the protection of T cells and NK cells.[26] Since histamine activates all four histamine receptor subtypes, the treatment is accompanied by serious side effects like itch, erythema, decrease in blood pressure and gastrointestinal problems.[26, 27] Patients could benefit from selective H_2R stimulation due to reduction of side effects mediated by the other histamine receptor subtypes.

Compounds **3.20** and **3.25** were studied at the H_2R in human monocytes regarding functional responses such as stimulation of cAMP formation and inhibition of fMLP-induced (formyl peptide) production of reactive oxygen species (ROS) (**Fig. 3.11**, **Table 3.4**). To avoid cell lysis as observed for such cationic amphilic compounds depending on the chain length of the linker (cf. section **3.3.2.7**), compounds **3.20** and **3.25**, which are among the most potent H_2R agonists and proved to be nontoxic (cf. **Fig 3.12**) under the assay conditions, were selected.

In a recently published study, it was shown that H_2R agonists increase cAMP levels in a concentration-dependent manner in human monocytes.[27] In accordance with these results, compounds **3.20** and **3.25** induced cAMP accumulation (**Fig. 3.11A**). Additionally, both ligands inhibited the fMLP-induced ROS production in a concentration-dependent manner *via* H_2R stimulation **(Fig 3.11B**).

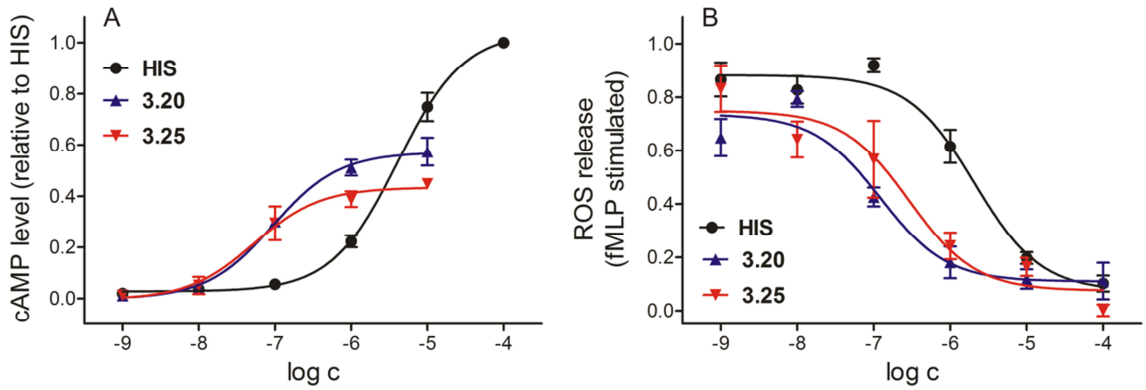

Figure 3.11. Effects of histamine (**HIS**), **3.20** and **3.25** on cAMP accumulation (**A**) and fMLP-induced ROS production (**B**) in human monocytes. Samples were analyzed by HPLC-MS/MS. A: Data were normalized to the maximal effect of HIS and represent means ± SEM from three independent experiments. B: Data were normalized to the ROS release induced by fMLP and are expressed as means ± SEM from four different experiments performed in triplicate. **Note**: The influence of H_2R agonists on ROS production had to be studied in an indirect way, i. e. after stimulation of the cells with fMLP (1 µM). In accordance with previous studies,[27] the maximal effect of fMLP (set to 1.0 in Fig. **3.11B**) was not fully restored in the presence of very low concentrations of histamine or H_2R agonists. So far, we have no explanation for this phenomenon, which only minimally affects the inflections points of the concentration-response curves. In Table **3.4** the maximal responses (E_{max}) of **3.20** and **3.25** are given relative to the amplitude of the concentration-response curve of histamine defined as E_{max} = 1.0.

Table 3.4. Potencies and efficacies in the cAMP assay and in the reactive oxygen species (ROS) assay in human monocytes[a]

	cAMP assay		ROS assay	
compd.	pEC_{50}	E_{max}	pIC_{50}	E_{max}
HIS	5.39 ± 0.06	1.00	5.68 ± 0.13	1.00
3.20	7.03 ± 0.11	0.57 ± 0.03	6.91 ± 0.19	0.78 ± 0.07
3.25	7.27 ± 0.19	0.44 ± 0.04	6.54 ± 0.27	0.83 ± 0.10

Table 3.4. Data were analyzed by nonlinear regression and were best fit to 3-parameter sigmoidal concentration-response curves. The maximal responses (E_{max} values) of **3.20** and **3.25** are referred to the efficacy of histamine defined as E_{max} = 1.00. Data shown are means ± SEM of three to four independent experiments.

Cytotoxicity of compounds **3.20** and **3.25** on monocytes was assessed by ethidium bromide / acridine orange (EBAO) staining. Acridine orange stains living and dead cells, whereas ethidium bromide only stains dead cells. Under the fluorescence microscope living cells appear green and dead cells orange.

The monocytes from three different donors were incubated with the respective dimeric ligand for 2 h. The respective compounds at a concentration of 100 µM did not induce cell death (**Fig. 3.12**).

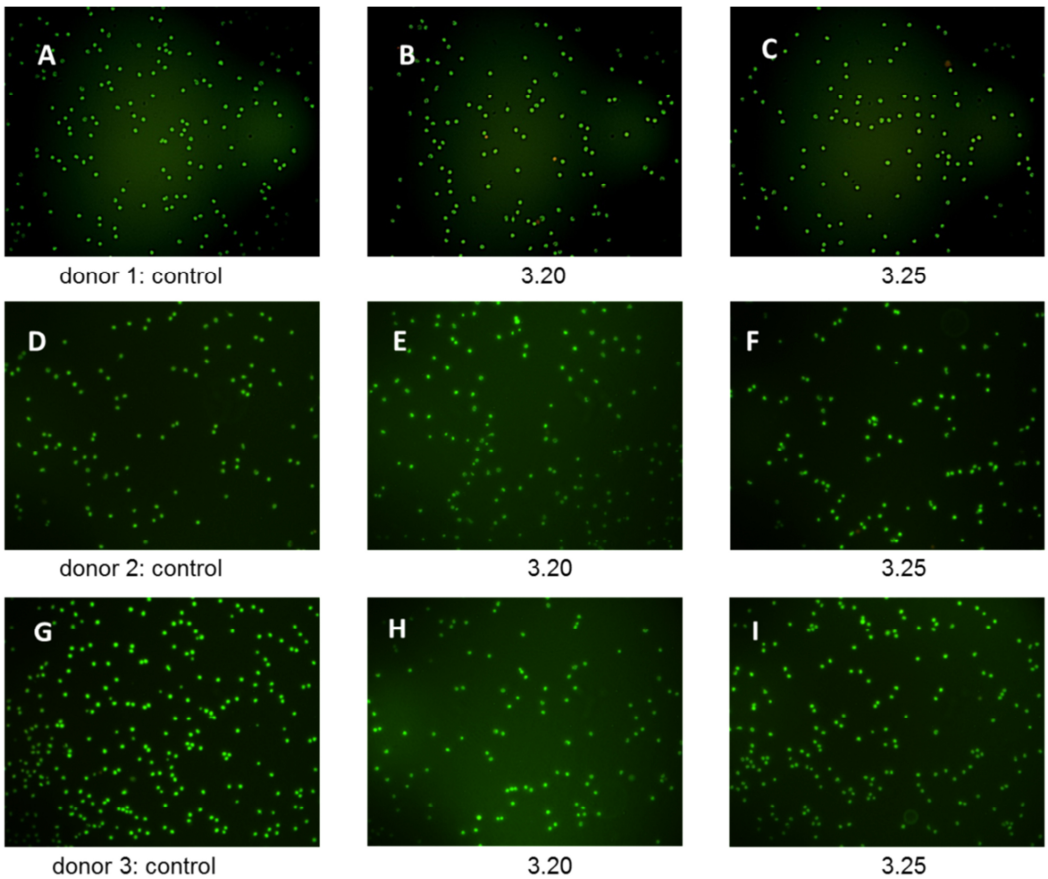

Figure 3.12. EBAO staining of human monocytes. Monocytes were incubated with 100 µM of compounds **3.20** [B, E, H] and **3.25** [C, F, I] for 2 h. Untreated cells served as control [A, D, G] (objective 20x). Cytotoxicity studies have been performed with monocytes of two female [A – C, D – F] and one male [G – I] caucasian.

3.3.2.5 Stability of selected carbamoylguanidines in plasma

With respect to future in vivo studies, **3.20** (**Fig. 3.13**) and **3.25** (**Fig 3.14**) were investigated regarding their stability in mouse plasma. Both compounds were stable during the incubation period of 24 h.

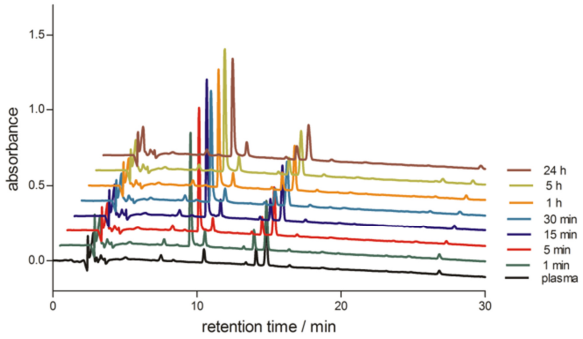

Figure 3.13. Stability of **3.20** in plasma. Compound **3.20** was incubated in murine plasma over 24 h at 37 °C, and the samples were analyzed by HPLC (UV detection at 210 nm).

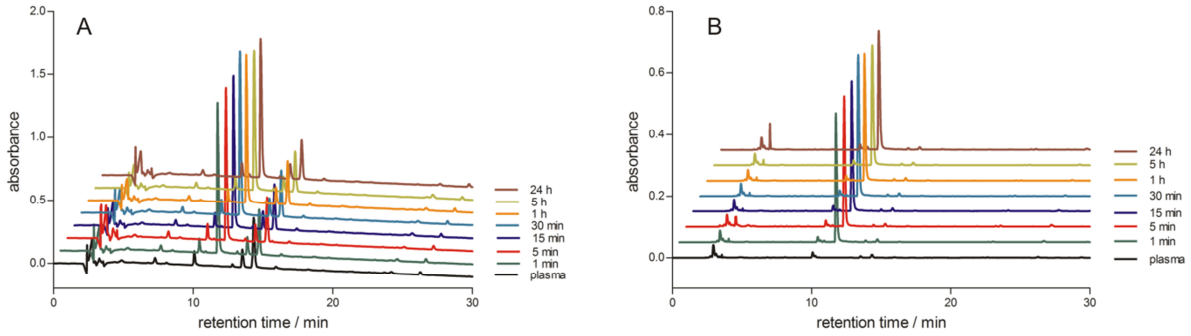

Figure 3.14. Stability of **3.25** in plasma. Compound **3.25** was incubated in murine plasma over 24 h at 37 °C, and the samples were analyzed by HPLC (UV detection at 210 nm (**A**) and 260 nm (**B**)).

3.3.2.6 Plasma protein binding

3.3.2.6.1 Equilibrium dialysis

Prior to the determination of plasma protein binding, recovery studies were performed with **3.19** (**Fig. 3.15A**) and **3.24 (Fig 3.15B)**. Unfortunately, only around 40 % of the compounds were recovered, most probably due to adsorption to the regenerated cellulose membrane. Thus, equilibrium dialysis turned out to be an inappropriate method for the determination of plasma protein binding of the dimeric ligands.

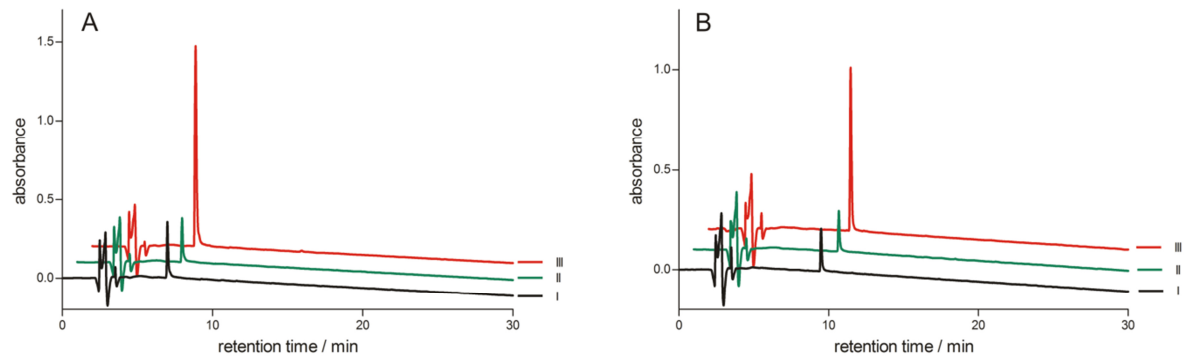

Figure 3.15. Recovery studies for **3.19 (A)** and **3.24 (B)** after dialysis for 24 h**.** HPLC analysis, UV detection at 210 nm. **I)** dialysis chamber 1: 200 µM solution of the tested compounds; **II)** dialysis chamber 2: PBS; **III)** 200 µM solution of the tested compounds

3.3.2.6.2 Ultrafiltration

Prior to plasma protein binding studies, control experiments were performed to determine the ability of the compounds to pass the membrane (**Fig. 3.16**). For each compound, this recovery value was considered in the calculation of plasma protein binding.

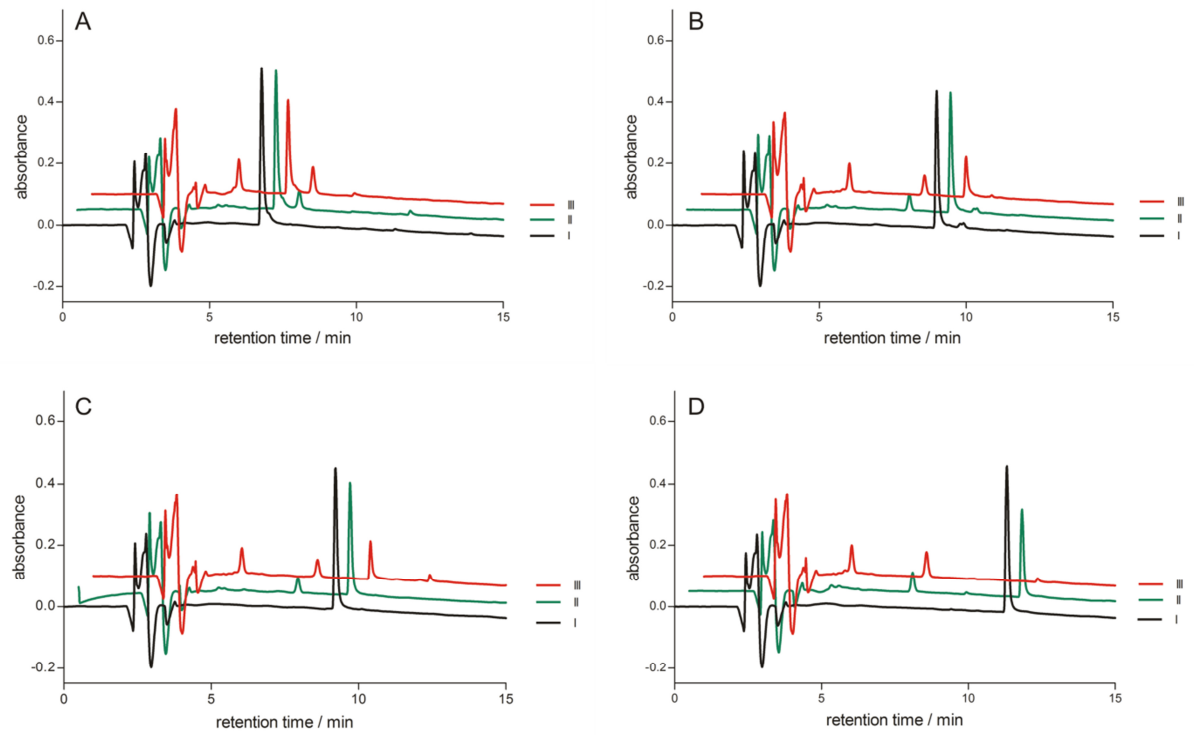

Figure 3.16. Determination of plasma protein binding for compounds **3.19 (A)**, **3.20 (B)**, **3.24 (C)**, **3.25 (D)**. HPLC analysis, UV detection at 210 nm. **I**) 100 µM solution of the tested compounds; **II**) solution **I** after filtration (recovery); **III**) 100 µM solution of the tested compounds after incubation in 600 µM BSA and filtration (plasma protein binding)

Table 3.5. Extent of plasma protein binding of selected compounds determined by ultrafiltration

compd.	recovery (without BSA)	plasma protein binding
3.19	87 %	33 %
3.20	89 %	75 %
3.24	80 %	64 %
3.25	61 %	96 %

In summary, the plasma protein binding strongly depended on the lipophilicity of the compounds. The most hydrophilic compound **3.19** showed the lowest extent of plasma protein binding, whereas **3.25**, the most lipohilic compound in this series, exhibited the highest amount of plasma protein binding. These results should be taken into account for future in vivo studies.

3.3.2.7 Cytotoxicity in the crystal violet based chemosensitivity assay

Representative compounds (**3.19**, **3.23**, **3.24** and **3.28**) were investigated for cytotoxicity against HEK293T cells in a kinetic crystal violet based chemosensitivity assay over an incubation period of approximately 140 h and compared to vinblastin as reference(**Fig. 3.17**).

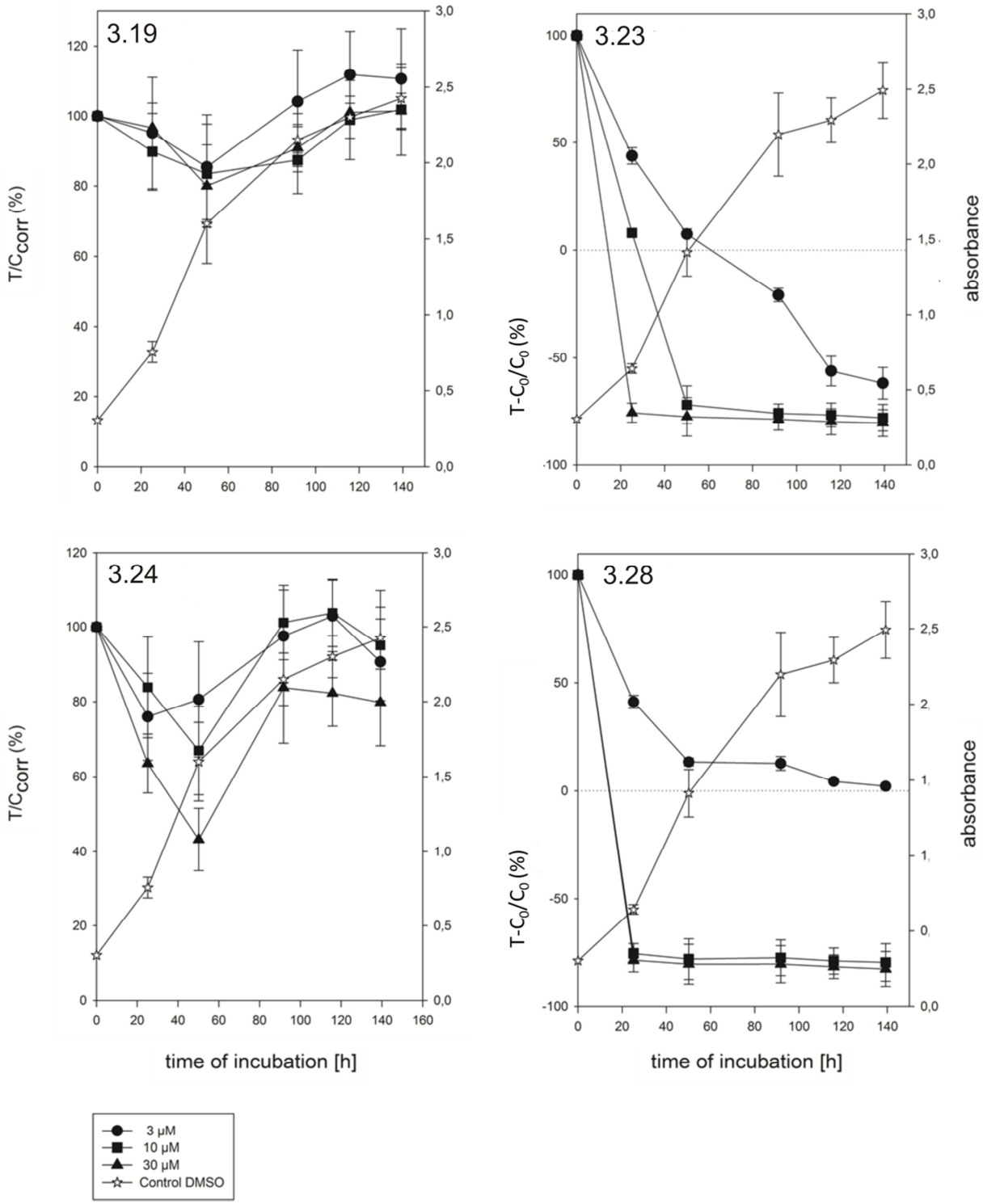

Figure 3.17. Effect of **3.19 (A)**, **3.23 (B)**, **3.24 (C)** and **3.28 (D)** on HEK293T cells in the crystal violet assay

The cytotoxic effect of the bivalent ligands strongly depended on the length of the spacer. After initial cell damage, the two dimeric ligands **3.19** and **3.24**, with a spacer length of four methylene groups, showed no cytotoxic effect up to a concentration of 30 µM. By contrast, **3.23** and **3.28,** with a spacer length of 10 methylene groups, showed strong cytotoxic to cytocidal effects even at the lowest concentration of 3 µM. Due to their polar basic pharmacophore and their lipophilic spacers, the dimeric ligands are of cationic amphiphilic

nature, implying a potential interaction with biological membranes. In accordance with previous data,[28,29] cytotoxicity increased with the chain length of the spacer.

3.4 Summary and conclusion

The exchange of the acylguanidine moieties in bivalent H_2R agonists by carbamoylguanidine groups resulted in compounds with retained potencies and intrinsic activities. Achieving up to 2500 times the potency of histamine these compounds are among the most potent H_2R agonists known so far. Unfortunately, H_2R binding studies with fluorescence and radiolabeled ligands derived from the chain-branched precursor **3.39** failed due to pronounced cellular accumulation and high non-specific binding, respectively. In this respect, the results underline the fact that, regardless of high affinity of the "cold" form, applicability of the corresponding labeled version as a molecular tool cannot be taken for granted. Aminothiazoles were superior to the corresponding imidazoles in terms of histamine receptor subtype selectivity. Due to high potency and stability against hydrolytic cleavage, the new H_2R agonists are promising pharmacological tools for investigations on the biological role of the H_2R and are of potential value for in vivo studies on histamine receptors in the CNS. Regarding the properties of plasma protein binding and cytotoxicity, compounds bearing a short spacer should be favored in future for in vivo studies. In human monocytes the investigated compounds revealed high H_2R agonist potency, suggesting this class of compounds to point a way to selective H_2R agonists as potential agents for the treatment of AML.

3.5 Experimental section

3.5.1 General Experimental conditions

Unless otherwise indicated, chemicals and solvents were from commercial suppliers and were used as received. The fluorescence dye S2197 was from FEW Chemicals GmbH (Bitterfeld-Wolfen, Germany), the pyrylium dyes Py-1 and Py-5 were kindly provided by Prof. Dr. O. S. Wolfbeis (Institute of Analytical Chemistry, Chemo- and Biosensors, University of Regensburg, Germany). All of the solvents were of analytical grade or were distilled prior to use. THF and Et_2O were distilled over sodium, DCM was stored over $CaCl_2$ and was afterwards distilled from P_2O_5. For column chromatography silica gel 60 (Merck, 0.04-0.063 mm) was used. Reactions were monitored by thin layer chromatography (TLC) on Merck silica gel 60 F254 aluminium sheets, and spots were visualized with UV light at 254 nm, iodine vapor or ninhydrin spray. NMR spectra were recorded on a Bruker Avance 300 (^{1}H: 300 MHz, ^{13}C: 75.5 MHz) and a Bruker Avance 600 (^{1}H: 600 MHz, ^{13}C: 150.9 MHz) (Bruker, Karlsruhe, Germany) with deuterated solvents from Deutero (Kastellaun, Germany). LRMS was performed on a Finnigan ThermoQuest TSQ 7000 Instrument (Thermo Scientific, Waltham, MA) using an ESI source. HRMS was performed on an Agilent 6540 UHD Accurate-Mass Q-TOF LC/MS system (Agilent Technologies, Santa Clara, CA) using an ESI or an APCI source. Melting points (mp) were measured on a Büchi B-540 apparatus using an open capillary and are uncorrected. Preparative HPLC was performed with a system from Knauer (Berlin, Germany) consisting of two K-1800 pumps, a K-2001 detector and the column was either a Eurospher-100 C18 (250 × 32 mm, 5 µm), a Nucleodur 100-5 C18 (250 × 21 mm, 5 µm) (Macherey-Nagel, Düren, Germany) or in case of the fluorescence ligands a Phenomenex Kinetex (250 × 21 mm, 5 µm) (Phenomenex, Aschaffenburg, Germany). As mobile phase, mixtures of acetonitrile and 0.1 % aqueous TFA were used. The temperature was 30 °C, and UV detection was carried out at 220 nm. Prior to lyophilisation (Christ alpha 2-4 LD freeze dryer (Osterode, Germany), equipped with a RZ 6 rotary vane vacuum pump (Vacuubrand, Wertheim, Germany), acetonitrile was removed under reduced pressure. Analytical HPLC was performed on a system from Thermo Separation Products equipped with an SN400 controller, a P4000 pump, an AS3000 autosampler, and a Spectra Focus UV/Vis detector. The column was either a Eurospher-100 C18 (250 × 4 mm, 5.0 µm; Knauer, Berlin, Germany) or a YMC C8 Column (250 x 4.6 mm, 5.0 µm); YMC Europe GmbH, Dinslaken, Germany), thermostated at 30 °C. As mobile phase, mixtures of MeCN /aqueous TFA were used. Gradient (unless otherwise indicated): MeCN/TFA (0.05%) (v/v) 0 min: 5:95, 30 min: 40/60, 31-41 min: 90:10; flow rate = 0.75 mL/min, t_0 = 2.95 min (Eurospher), t_0 = 2.55 min (YMC); capacity factor k= $(t_R-t_0)/t_0$. Absorbance was detected at 210 nm. Compound purities were calculated as the percentage peak area of the analyzed compound by UV detection at 210 nm. UV Spectra were recorded with a Cary Eclipse spectrofluorimeter (Varian, Mulgrave, Victoria, Australia).

3.5.2 Chemistry: Experimental Protocols and Analytical data

(E)-Methyl 3-(1*H*-imidazol-4-yl)propenoate (3.1).[7] Urocanic acid (10.0 g, 72.40 mmol) and Na_2SO_4 (2.0 g, 14.08 mmol) were dissolved in 100 mL of anhydrous MeOH. Under external cooling H_2SO_4 conc. (6 mL) was added. The mixture was heated to reflux for 30 h and the solvent was removed under reduced pressure. The residue was dissolved in a small amount of water, and the solution was neutralized with saturated $NaHCO_3$ solution. The mixture was

extracted with EA. After drying over Na_2SO_4, the solvent was evaporated. The crude product was used in the next step without further purification (R_f= 0.25 for DCM/MeOH 4.5:0.5). The product was obtained as a white solid (8.57 g, 78 %); mp = 94.6-103.5 °C. ^{1}H NMR (300 MHz, [D_4]MeOH) δ (ppm) 3.75 (s, 3H), 6.39 (s, 1H), 6.45 (s, 1H), 7.42 (s, 1H), 7.77 (s, 1H). MS (ESI; MeOH) m/z (%) 153 (100) $[M+H]^+$, 121 (8) $[M+H\text{-}MeOH]^+$. HRMS (ESI): m/z $[M+H]^+$ calculated for $C_7H_9N_2O_2^+$: 153.0659, found 153.0658; $C_7H_8N_2O_2$ (152.15).

Methyl 3-(1*H*-imidazol-4-yl)propanoate (3.2).[30] To a solution of **3.1** (8.27 g, 54.35 mmol) in MeOH 1.0 g of Pd/C (10 %) was added at room temperature under stirring. The mixture was hydrogenated at 5 bar for 24 h. Afterwards, Pd/C was filtrated off, and the solvent was removed under reduced pressure. The procedure afforded the product as yellow oil (8.32 g, 99 %). The crude product was used in the next step without further purification (R_f = 0.25 in DCM/MeOH 4.5:0.5, detection with iodine). ^{1}H NMR (300 MHz, $CDCl_3$) δ (ppm) 2.66 (t, 2H, *J* 7.2 Hz), 2.92 (t, 2H, *J* 7.2 Hz,), 3.66 (s, 3H), 6.79 (s, 1H), 7.54 (s, 1H). MS (ESI; MeOH) m/z (%) 309 (1) $[2M+H]^+$, 155 (100) $[M+H]^+$, 123 (16) $[M+H\text{-}MeOH]^+$. HRMS (ESI): m/z $[M+H]^+$ calculated for $C_7H_{11}N_2O_2^+$: 155.0815, found 155.0830; $C_7H_{10}N_2O_2$ (154.17).

Methyl 3-(1-trityl-1*H*-imidazol-4-yl)propanoate (3.3).[31] To a suspension of **3.2** (8.32 g, 53.98 mmol) and NEt_3 (19.52 mL, 140.82 mmol) in 120 mL MeCN a solution of trityl chloride (13.57 g, 48.68 mmol) in MeCN was added dropwise under external cooling. The mixture was stirred for 12 h at room temperature. After removing the solvent under reduced pressure, water (300 mL) was added, and the suspension was stirred for 1 h. The solid was filtrated off and recrystallized from dry EtOH yielding **3.3** (10.10 g, 52 %) as a white solid (R_f = 0.9 in EA/7N NH_3 4.5:0.5). mp= 145-146 °C (lit.[28] mp 131 °C). ^{1}H-NMR (300 MHz, $CDCl_3$) δ (ppm) 2.66 (t, 2H, *J* 7.4 Hz), 2.87 (t, 2H, *J* 7.5 Hz), 3.62 (s, 3H), 6.55 (s, 1H), 7.08 – 7.37 (m, 15H). MS (ESI; MeOH) m/z (%) 397 (69) $[M+H]^+$, 243 (100) $[Trt^+]$. HRMS (ESI): m/z $[M+H]^+$ calculated for $C_{26}H_{25}N_2O_2^+$: 397.1911, found 397.1918; $C_{26}H_{24}N_2O_2$ (396.48).

3-(1-Trityl-1*H*-imidazol-4-yl)propan-1-ol (3.4).[31] Compound **3.4** (8.32 g, 20.98 mmol) was added in portions to a mechanically stirred suspension of $LiAlH_4$ (1.52 g, 24.97 mmol) in freshly distilled THF under argon and external cooling. After the addition was complete, the mixture was allowed to warm to room temperature and heated to reflux for 2 h. The reaction was carefully quenched with 0.1 N NaOH. The residue was filtrated, and the solution was extracted with DCM. After drying over Na_2SO_4, the solvent was removed under reduced pressure, and the residue was purified by column chromatography ($CHCl_3$/MeOH 95:5) to obtain **3.4** as a white solid (6.26 g, 81 %) (R_f = 0.33 in DCM/MeOH 9.5:0.5). mp= 119.5-125.5 °C. (lit.[28] mp 138 °C). ^{1}H-NMR (300 MHz, $CDCl_3$) δ (ppm) 1.79-1.94 (m, 2H), 2.67 (t, 2H, *J* 6.7 Hz), 3.72 (t, 2H, *J* 5.7 Hz), 6.54 (s, 1H), 7.11-7.35 (m, 15H). MS (ESI; MeOH) m/z (%) 369 (89) $[M+H]^+$, 243 (100) $[Trt]^+$. HRMS (ESI): m/z $[M+H]^+$ calculated for $C_{25}H_{25}N_2O^+$: 369.1961, found 369.1964. $C_{25}H_{24}N_2O$ (368.47).

2-[3-(1-Trityl-1*H*-imidazol-4-yl)propyl]isoindoline-1,3-dione (3.5).[28,32] **3.4** (6.26 g, 16.99 mmol), phthalimide (2.50 g, 16.99 mmol) and triphenylphosphine (4.46 g, 17.00 mmol) were suspended in anhydrous THF and cooled to 0 °C. DIAD (3.44 g, 17.01 mmol) was added slowly. After complete addition of DIAD, the mixture was allowed to warm to room temperature, and stirring was continued for 3 h. The precipitate was filtered off and

recrystallized from THF/MeCN (50:50) yielding compound **3.5** as a white solid (5.75 g, 68 %) (R_f = 0.71 in EA/PE 4:1). mp = 215.9-220.8 °C (lit.[33] 217-219 °C). ^{1}H-NMR (300 MHz, $CDCl_3$) δ (ppm) 1.96- 2.10 (m, 2H), 2.63 (t, J 7.7 Hz, 2H), 3.72 (t, J 7.1 Hz, 2H), 6.61 (s, 1H), 7.10-7.77 (m, 6H). 7.29-7.38 (m, 9H), 7.66-7.72 (m, 2H), 7.78-7.85 (m, 2H). MS (ESI; MeOH) m/z (%) 243 (26) [Trt$^+$], 498 (100) [M+H]$^+$, 1017 [2M+Na]$^+$. HRMS (ESI): m/z [M+H]$^+$ calculated for $C_{33}H_{28}N_3O_2^+$: 468.2176, found 468.2176; $C_{33}H_{27}N_3O_2$ (497.60)

3-(1-Trityl-1*H*-imidazol-4-yl)propan-1-amine (3.6).[34] A mixture of **3.5** (5.50 g, 11.05 mmol) and hydrazine monohydrate (3.60 g, 71.89 mmol) in EtOH was heated to reflux for 1 h. After removable of insoluble material, the filtrate was evaporated. The residue was purified by column chromatography (eluent: DCM:MeOH:NH_3 95:4:1). Compound **3.6** was obtained as a yellowish oil that solidified (3.41g, 84 %) (R_f = 0.13 in DCM/7N NH_3 4.5:0.5). mp = 108.1-112.9 °C (lit.[32] mp 106-108 °C). ^{1}H-NMR (300 MHz, $CDCl_3$) δ (ppm) 1.62- 1.78 (m, 2H), 2.46 (t, 2H, *J* 7.2 Hz), 2.67 (t, 2H, *J* 6.7 Hz), 6.39 (s, 1H), 6.94-7.19 (m, 15H). MS (ESI; MeOH) m/z (%) 368 (23) [M+H]$^+$, 243 (100) [Trt$^+$]. HRMS (ESI): m/z [M+H]$^+$ calculated for $C_{25}H_{26}N_3^+$: 368.2121, found 368.2124; $C_{25}H_{25}N_3$ (367.49).

2-(5-Oxohexyl)-1,3-dihydro-2*H*-isoindol-1,3-dione (3.7).[35] 6-Chlorohexan-2-one (13.30 g, 98.81 mmol) and phthalimide (8.20 g, 55.73 mmol) were dissolved in DMF. The mixture was heated to 80 °C for 24 h. After cooling to room temperature, the solvent was reduced in vacuo. The residue was suspended in water and extracted with $CHCl_3$. The combined organic layers were dried over Na_2SO_4 and evaporated under reduced pressure. The crude product was purified by column flash chromatography (eluent: DCM/MeOH 20:1) yielding compound **3.7** as a white solid (9.50 g, 39 %) (R_f = 0.15 in EE/PE 1:8); mp = 74.6 -78.6 °C (lit.[28] mp 73-75 °C). ^{1}H-NMR (300 MHz, $CDCl_3$) δ (ppm) 1.54- 1.84 (m, 4H), 2.13 (s, 3H), 2.49 (t, 2H, *J* 7.0 Hz), 3.69 (t, 2H, *J* 6.8 Hz), 7.67 (m, 2H), 7.79- 7.88 (m, 2H). MS (APCI; MeOH) m/z (%) 246 (100) [M+H]$^+$. HRMS (APCI): m/z [M+H]$^+$ calculated for $C_{14}H_{16}NO_3^+$: 246.1124, found: 246.1126. $C_{14}H_{15}NO_3$ (245.27).

2-(4-Bromo-5-oxohexyl)-1,3-dihydro-2*H*-isoindol-1,3-dione (3.8).[35] To a solution of **3.7** (6.26 g, 25.52 mmol) in dioxan and DCM (1.5:1), bromine (4.08 g, 25.54 mmol) was added slowly. Thereafter, the mixture was stirred at room temperature for 1 h. Subsequently, the mixture was washed twice with water and extracted with EA. The organic layer was dried over Na_2SO_4, and the solvent was removed under reduced pressure. The crude product **3.8** was obtained as a yellow oil (8.27, 100 %) and used in the next step without further purification (R_f = 0.55 in EA/PE 1:2). ^{1}H-NMR (300 MHz, $CDCl_3$) δ (ppm) 1.54-1.84 (m, 4H), 2.33 (m, 3H), 3.65-3.67 (m, 2H), 4.24-4.35 (m, 1H), 7.66-7.70 (m, 2H), 7.78-7.82 (m, 2H). MS (APCI; MeOH) m/z (%) 324 (100) [M+H]$^+$. HRMS (APCI): m/z [M+H]$^+$ calculated for $C_{14}H_{15}BrNO_3^+$: 324.0230, found: 324.0230. $C_{14}H_{14}BrNO_3$ (324.17).

2-[3-(2-Amino-4-methylthiazol-5-yl)propyl]-1,3-dihydro-2*H*-isoindol-1,3-dione (3.9).[35] To a solution of **3.8** (8.27 g, 25.51 mmol) in 50 mL of DMF, a solution of thiourea (1.94 g, 25.51 mmol in 50 mL of DMF) was added. Subsequently, the mixture was heated to 100 °C for 3 h. The mixture was allowed to cool to room temperature, and DMF was removed in vacuo. A

mixture of EA/MeOH (1:1) was added, and the suspension was stirred for 30 min. Afterwards, the residue was filtered off, and washed with PE and EA, yielding compound **3.9** (4.79 g, 62 %); (R_f = 0.45 in EA:PE 4:1). ^{1}H-NMR (300 MHz, $CDCl_3$) δ (ppm) 1.95-2.10 (m, 2H), 2.25 (s, 3H), 2.76 (m, 2H), 3.76 (t, 2H, *J* 7.1 Hz), 7.68-7.76 (m, 2H), 7.80-7.91(m, 2H). MS (ESI; MeOH) m/z (%) 302.09 (1) $[M+H]^+$.HRMS (ESI): m/z $[M+H^+]^+$ calculated for $C_{15}H_{16}N_3O_2S^+$: 302.0958, found: 302.0962. $C_{15}H_{15}N_3O_2S$ (301.36).

***tert*-Butyl 4-methyl-5-[3-(1,3-dioxo-1,3-dihydro-2*H*-isoindol-2-yl)propyl]thiazol-2-yl-carbamate (3.10)**.[35] To compound **3.9** (4.79 g, 15.89 mmol), dissolved in $CHCl_3$, Boc_2O (3.81 g, 17.48 mmol), NEt_3 (1.93 g, 19.07 mmol) and DMAP (cat.) were added. The mixture was stirred at room temperature overnight. The solvent was removed under reduced pressure, and the crude product was purified by flash chromatography (eluent: PE/EA 2:3). This afforded compound **3.10** as a colorless foam-like solid (5.04 g, 79 %) (R_f = 0.40 in EA/PE 1:1). ^{1}H-NMR (300 MHz, $CDCl_3$) δ (ppm) 1.52 (s, 9H), 1.91-2.02 (m, 2H), 2.21 (s, 3H), 2.63-2.77 (m, 2H), 3.68- 3.78 (m, 2H), 7.66-7.75 (m, 2H), 7.80-7.88 (m, 2H). HRMS (ESI): m/z $[M+H^+]^+$ calculated for $C_{20}H_{24}N_3O_4S^+$: 402.1482, found: 402.1487. $C_{20}H_{23}N_3O_4S$ (401.48).

***tert*-Butyl 5-(3-aminopropyl)-4-methylthiazol-2-ylcarbamate (3.11)**.[2] To a solution of **3.10** (5.04 g, 12.55 mmol) in 100 mL of EtOH, hydrazine monohydrate (2.01 g, 40.15 mmol) was added, and the mixture was heated to reflux for 1 h. The mixture was allowed to cool to room temperature, and solid material was removed by filtration. The solvents were evaporated under reduced pressure, and the residue was purified by column chromatography (eluent: DCM/MeOH/NH_3 95:4:1). Compound **3.11** was obtained as a yellow glassy solid (1.81 g, 53 %). ^{1}H-NMR (300 MHz, $[D_4]$MeOH) δ (ppm) 1.53 (s, 9H), 1.70-1.83 (m, 2H), 2.17 (s, 3H), 2.67-2.74 (m, 4H). MS (ESI; MeOH) m/z (%) 272 (100) $[M+H]^+$, 216 (52) $[M+H\text{-}C_4H_8]^+$, 172 (23) $[M+H\text{-Boc}]^+$, 108 (85), $[M+2H\text{-}C_4H_8]^{2+}$. HRMS (ESI): m/z $[M+H]^+$ calculated for $C_{12}H_{22}N_3O_2S^+$: 272.1427, found 272.1430; $C_{12}H_{21}N_3O_2S$ (271.38).

S-Methylthiouronium iodide (3.12).[36] Thiourea (9.20 g, 120.86 mmol) and methyl iodide (17.0 g, 119.77 mmol) were heated to reflux for 1 h in MeOH. Afterwards, the solvent was evaporated under reduced pressure, the crude product was suspended with Et_2O, sucked off and washed twice with Et_2O. Compound **3.12** was obtained as a white solid (25.11 g, 97 %). mp = 119.1-120.5 °C (lit.[37] mp 117 °C). ^{1}H-NMR (300 MHz, $[D_6]$DMSO) δ (ppm) 2.57 (s, 3H), 8.88 (s, 4H). MS (ESI; MeOH) m/z (%) 91 (100) $[M+H]^+$. HRMS (ESI): m/z $[M+H]^+$ calculated for $C_2H_7N_2S^+$: 91.0324, found 91.0325; $C_2H_6N_2S$ x I (218.06).

***N*-*tert*-Butoxycarbonyl-S-methylisothiourea (3.13)**.[36] To a solution of **3.12** (25.11 g, 115.69 mmol) in DCM, NEt_3 (11.74 g, 116.00 mmol) and Boc_2O (25.37 g, 116.24 mmol) were added. The mixture was stirred for 24 h and subsequently washed with brine and water. The organic layer was dried over Na_2SO_4, and the solvent was removed under reduced pressure. The crude product was purified by flash chromatography (eluent: PE/EA 4:1). This afforded compound **3.13** as a white solid (13.43 g, 61 %) (R_f = 0.26 in PE/EA 4:1). mp = 82.1-85.0 °C (lit.[36] mp 76-78 °C) ^{1}H-NMR (300 MHz, $[D_6]$DMSO) δ (ppm) 1.39 (s, 9H), 2.30 (s, 3H), 8.55

(s, 2H). MS (ESI; MeOH) m/z (%) 191 (10) $[M+H]^+$, 135 (100) $[M+H-C_4H_8]^+$. HRMS (ESI): m/z $[M+H]^+$ calculated for $C_7H_{15}N_2O_2S^+$: 191.0849, found 191.0849; $C_7H_{14}N_2O_2S$ (190.26).

***N*¹,*N*⁴-Bis{[(*tert*-butoxycarbonylamino)(methylsulfanyl)methylene]aminocarbonyl}-butane-1,4-diamine** (**3.14**)**.** To a solution of *N*-*tert*-butoxycarbonyl-*S*-methylisothiourea (855 mg, 4.50 mmol) NEt_3 (30 µL, 0.22 mmol) in DCM was added dropwise a solution of 1,4-diisocyanatobutane (300 mg, 2.14 mmol) in DCM. The solution was stirred for 2.5 h at room temperature. The solvent was removed under reduced pressure and the crude product was purified by column chromatography (eluent: DCM/EA 15:1) (R_f = 0.19 in Hex/EA 3:2). The product **3.14** was obtained as a white solid (928 mg, 83 %). mp= 144.9–146.1 °C. ^{1}H-NMR (300 MHz, $CDCl_3$) δ (ppm) 1.47 (s, 18H), 1.55- 1.65 (m, 4H), 2.29 (s, 6H), 3.22-3.26 (m, 4H), 5.62 (t, 2H, *J* 6.0 Hz), 12.27 (s, 2H); ^{13}C-NMR (75 MHz, $CDCl_3$) δ (ppm) 14.4, 27.3, 28.1, 39.8, 82.7, 151.2, 162.1, 167.6. MS (ESI) m/z (%) 521 (100) $[M+H]^+$. HRMS (ESI): m/z $[M+H]^+$ calculated for $C_{20}H_{37}N_6O_6S_2^+$: 521.2211, found 521.2214; $C_{20}H_{36}N_6O_6S_2$ (520.67).

***N*¹,*N*⁶-Bis{[(*tert*-butoxycarbonylamino)(methylsulfanyl)methylene]aminocarbonyl}-hexane-1,6-diamine (3.15).** To a solution of *N*-*tert*-butoxycarbonyl-*S*-methylisothiourea (700 mg, 3.68 mmol) and NEt_3 (30 µL, 0.22 mmol) in DCM, a solution of 1,6-diisocyanatohexane (340 mg, 2.02 mmol) in DCM was added dropwise. The solution was stirred for 2.5 h at room temperature. The solvent was removed under reduced pressure, and the crude product was purified by column chromatography (eluent: DCM/EA 15:1) (R_f = 0.29 in Hex/EA 3:2). The product **3.15** was obtained as a white solid (820 mg, 74 %). Mp = 128.8–133.6 °C**.** ^{1}H-NMR (300 MHz, $CDCl_3$) δ (ppm) 1.34-1.39 (m, 4H), 1.46 (s, 18H), 1.50-1.56 (m, 4H), 2.29 (s, 6H), 3.17-3.24 (m, 4H), 5.55 (t, 2H, *J* 5.8 Hz), 12.30 (s, 2H); ^{13}C-NMR (75 MHz, $[D_4]$MeOH) δ (ppm) 14.4, 26.7, 28.1, 29.7, 40.1, 82.7, 151.2, 162.1, 167.4. MS (ESI) m/z (%) 549 (100) $[M+H]^+$. HRMS (ESI): m/z $[M+H]^+$ calculated for $C_{22}H_{41}N_6O_6S_2^+$: 549.2524, found 549.2525; $C_{22}H_{40}N_6O_6S_2$ (548.72).

General procedure for the synthesis of the guanidinylating reagents (3.16-3.18).

The respective diamine was dried overnight in vacuo, and the reactions were carried out in an argon-purged two-necked round bottom flask. The diamines (1 eq) were dissolved in freshly distilled DCM (8 mL), and DIPEA (5.6 eq) was added. This mixture was added dropwise under external cooling to a solution of triphosgene (1 eq) in anhydrous DCM over a period of 30 min. *N*-*tert*-Butoxycarbonyl-*S*-methylisothiourea (4 eq) was added, and stirring was continued for 2.5 h. The solvent was removed under reduced pressure and the crude product was purified by column chromatography (eluent DCM/ EA 15:1).

***N*¹,*N*⁷-Bis{[(*tert*-butoxycarbonylamino)(methylsulfanyl)methylene]aminocarbonyl}-heptane-1,7-diamine (3.16).** The title compound was prepared from heptane-1,7-diamine (262 mg, 2.01 mmol), DIPEA (1963 µL, 11.27 mmol), triphosgene (596 mg, 2.01 mmol) in anhydrous DCM and *N*-*tert*-butoxycarbonyl-*S*-methylisothiourea (1530 mg, 8.08 mmol) according to the general procedure (R_f = 0.29 in Hex/ EA 3:2). The product **3.16** was obtained as a colorless glassy solid (855 mg, 75 %). ^{1}H-NMR (300 MHz, $CDCl_3$) δ (ppm) 1.33 (m, 6H), 1.46 (s, 18H), 1.49 (overlap with *tert*-Bu, 4H), 2.29 (s, 6H), 3.16-3.23 (m, 4H), 5.55 (t, 2H, *J* 5.0 Hz), 12.31 (s, 2H); ^{13}C-NMR (75 MHz, $CDCl_3$) δ (ppm) 14.4, 26.9, 28.1, 29.1,

29.7, 40.2, 82.6, 151.2, 162.0, 167.3. MS (ESI) m/z (%) 563 (100) $[M+H]^+$. HRMS (ESI): m/z $[M+H]^+$ calculated for $C_{23}H_{43}N_6O_6S_2^+$: 563.2680, found 563.2690; $C_{23}H_{42}N_6O_6S_2$ (562.75).

***N*¹,*N*⁸-Bis{[(*tert*-butoxycarbonylamino)(methylsulfanyl)methylene]aminocarbonyl}-octane-1,8-diamine (3.17).** The title compound was prepared from octane-1,8-diamine (400 mg, 2.77 mmol), DIPEA (2701 µL, 15.50 mmol), triphosgene (823 mg, 2.77 mmol) and *N*-*tert*-butoxycarbonyl-S-methylisothiourea (2108 mg, 11.08 mmol) according to the general procedure (R_f = 0.34 in Hex/ EA 3:2). The product **3.17** was obtained as a white solid (1183 mg, 74 %). Mp = 116.4-119.2 °C. ^{1}H-NMR (300 MHz, $CDCl_3$) δ (ppm) 1.32 (m, 8H), 1.47 (s, 18H), 1.50 (m, 4H), 2.29 (s, 6H), 3.17-3.24 (m, 4H), 5.53 (t, 2H, *J* 5.6 Hz), 12.32 (s, 2H); ^{13}C-NMR (75 MHz, $CDCl_3$) δ (ppm) 14.4, 27.0, 28.2, 29.3, 29.8, 40.3, 82.7, 151.3, 162.1, 167.4. MS (ESI) m/z (%) 577 (100) $[M+H]^+$. HRMS (ESI): m/z $[M+H]^+$ calculated for $C_{24}H_{45}N_6O_6S_2^+$: 577.2837, found 577.2845; $C_{24}H_{44}N_6O_6S_2$ (576.77).

***N*¹,*N*¹⁰-Bis{[(*tert*-butoxycarbonylamino)(methylsulfanyl)methylene]aminocarbonyl}-decane-1,10-diamine (3.18)**. The title compound was prepared from decane-1,10-diamine (300 mg, 1.74 mmol), DIPEA (1697 µL, 9.74 mmol), triphosgene (517 mg, 1.74 mmol) and *N*-*tert*-butoxycarbonyl-S-methylisothiourea (1325 mg, 6.97 mmol) according to the general procedure (R_f = 0.35 in Hex/ EA 3:2). The product **3.18** was obtained as a colorless glassy solid (798 mg, 76 %). ^{1}H-NMR (300 MHz, [D$_4$]MeOH) δ (ppm) 1.33 (m, 12H), 1.48-1.54 (m, 22H), 2.32 (s, 6H), 3.14 (t, 4H, *J* 7.0 Hz); ^{13}C-NMR (75 MHz, [D$_4$]MeOH) δ (ppm) 14.4, 28.0, 28.2, 30.4, 30.6, 41.0, 83.6, 152.1, 163.7, 167.2. MS (ESI) m/z (%) 605 (100) $[M+H]^+$. HRMS (ESI): m/z $[M+H]^+$ calculated for $C_{26}H_{49}N_6O_6S_2^+$: 605.3150, found 605.3154; $C_{26}H_{48}N_6O_6S_2$ (604.83).

General procedure for the synthesis of the bivalent carbamoylguanidine-type ligands (3.19-3.28).

The guanidinylating reagents (**3.14-3.18**) (1 eq) and 2.1 eq of 3-(1-trityl-1*H*-imidazol-4-yl)propan-1-amine (**3.6**) or *tert*-butyl 5-(3-aminopropyl)-4-methylthiazol-2-ylcarbamate (**3.11**) were dissolved in DMF (unless indicated otherwise). NEt_3 (5 eq) and $HgCl_2$ (4 eq) were added to the mixture, and stirring was continued for 12 h. The precipitate was centrifuged, washed with DMF (unless otherwise indicated) and centrifuged for a second time. The bis(Boc)-bis(trityl)- (cf. imidazoles) or tetrakis(Boc)-protected intermediate (cf. amino-thiazoles) was extracted with EA (unless indicated otherwise), purified by column chromatography (eluent: DCM/MeOH 100:1 to 50:1), and dried in vacuo. Subsequently, deprotection was performed by stirring with 30 % TFA in DCM for 12 h. The obtained carbamoylguanidine (cf. **3.19-3.28**) was purified by preparative HPLC.

1-(Amino{[3-(1*H*-imidazol-4-yl)propyl]amino}methylene)-3-{4-[3-(amino{[3-(1*H*-imidazol-4-yl)propyl]amino}methylene)ureido]butyl}urea (3.19). The title compound was prepared from **3.14** (175 mg, 0.336 mmol), amine **3.6** (260 mg, 0.708 mmol), NEt_3 (233 µL, 1.67 mmol) and $HgCl_2$ (365 mg, 1.34 mmol) according to the general procedure, yielding **3.19** as a white fluffy, hygroscopic solid (21.88 mg, 7 %): RP-HPLC: 99 %, (t_R = 11.75 min, k = 2.99); UV_{max} 204 nm. ^{1}H-NMR (600 MHz, [D$_4$]MeOH) δ (ppm) 1.57 (m, 4H), 2.03 (tt, 4H, ^2J 7.0 Hz, ^3J 7.6 Hz), 2.84 (t, 4H, *J* 7.7 Hz), 3.23 (m, 4H), 3.36 (t, 4H, *J* 6.9 Hz), 7.36 (s, 2H), 8.80 (d, 2H, *J*

1.2 Hz); ^{13}C-NMR (151 MHz, [D$_4$]MeOH, trifluoroacetate) δ (ppm) 22.6, 27.7, 28.2, 40.3, 41.4, 117.1, 134.4, 135.0, 155.6, 156.0, 163.3, 163.5. MS (ESI) m/z (%) 475 (29) [M+H]$^+$, 238 (75) [M+2H]$^{2+}$. HRMS (ESI): m/z [M+H]$^+$ calculated for $C_{20}H_{35}N_{12}O_2^+$: 475.3000, found 475.3003; $C_{20}H_{34}N_{12}O_2$ x 4 TFA (930.64).

1-(Amino{[3-(1*H*-imidazol-4-yl)propyl]amino}methylene)-3-{6-[3-(amino{[3-(1*H*-imidazol-4-yl)propyl]amino}methylene)ureido]hexyl}urea (**3.20**)**.** The title compound was prepared from **3.15** (175 mg, 0.319 mmol), amine **3.6** (250 mg, 0.680 mmol), NEt_3 (222 µL, 1.60 mmol) and $HgCl_2$ (346 mg, 1.27 mmol) according to the general procedure, yielding **3.20** as a white fluffy hygroscopic solid (36.00 mg, 12 %): RP-HPLC: 98 %, (t_R = 15.18 min, k = 4.15); UV_{max} 205 nm. ^{1}H-NMR (600 MHz, [D$_4$]MeOH) δ (ppm) 1.36-1.38 (m, 4H), 1.52-1.58 (m, 4H), 2.03 (tt, 4H, ^2J 7.1 Hz, ^3J 7.5 Hz), 2.84 (t, 4H, *J* 7.7 Hz), 3.20 (t, 4H, *J* 7.1 Hz,), 3.37 (t, 4H, *J* 6.9 Hz), 7.37 (s, 2H), 8.81 (d, 2H, *J* 1.3 Hz); ^{13}C-NMR (151 MHz, [D$_4$]MeOH, trifluoroacetate) δ (ppm) 22.5, 27.4, 28.2, 30.3, 40.7, 41.4, 117.1, 134.3, 135.0, 155.5, 156.0. MS (ESI) m/z (%) 617 (4) [M+H+TFA]$^+$, 503 (22) [M+H]$^+$, 252 (84) [M+2H]$^{2+}$. HRMS (ESI): m/z [M+H]$^+$ calculated for $C_{22}H_{39}N_{12}O_2^+$: 503.3313, found 503.3314; $C_{22}H_{38}N_{12}O_2$ x 4 TFA (958.70).

1-(Amino{[3-(1*H*-imidazol-4-yl)propyl]amino}methylene)-3-{7-[3-(amino{[3-(1*H*-imidazol-4-yl)propyl]amino}methylene)ureido]heptyl}urea (**3.21**)**.** The title compound was prepared from **3.16** (106 mg, 0.188 mmol), amine **3.6** (145 mg, 0.395 mmol), NEt_3 (128 µL, 0.92 mmol) and $HgCl_2$ (201 mg, 0.74 mmol) according to the general procedure, yielding **3.21** as a white fluffy hygroscopic solid (15.30 mg, 8 %): RP-HPLC: 97 %, (t_R = 16.65 min, k = 4.65); UV_{max} 205 nm. ^{1}H-NMR (600 MHz, [D$_4$]MeOH) δ (ppm) 1.36 (m, 6H), 1.54 (m, 4H), 2.03 (tt, 4H, ^2J 7.0 Hz, ^3J 7.5 Hz), 2.84 (t, 4H, *J* 7.7 Hz), 3.19 (t, 4H, *J* 7.1 Hz), 3.36 (t, 4H, *J* 6.9 Hz), 7.36 (s, 2H), 8.80 (d, 2H, *J* 1.1 Hz); ^{13}C-NMR (151 MHz, [D$_4$]MeOH, trifluoroacetate) δ (ppm); 22.5, 27.7, 28.2, 29.9, 30.4, 40.7, 41.4, 117.1, 134.3, 134.9, 155.5, 156.1. MS (ESI) m/z (%) 517 (13) [M+H]$^+$, 259 (41) [M+2H]$^{2+}$. HRMS (ESI): m/z [M+H]$^+$ calculated for $C_{23}H_{41}N_{12}O_2^+$: 517.3473, found 517.3473; $C_{23}H_{40}N_{12}O_2$ x 4 TFA (972.72).

1-(Amino{[3-(1*H*-imidazol-4-yl)propyl]amino}methylene)-3-{8-[3-(amino{[3-(1*H*-imidazol-4-yl)propyl]amino}methylene)ureido]octyl}urea (**3.22**)**.** Compound **3.17** (175 mg, 0.303 mmol) and amine **3.6** (234 mg, 0.637 mmol) were dissolved in DCM. NEt_3 (210 µL, 1.51 mmol) and $HgCl_2$ (330 mg, 1.21 mmol) were added to the mixture. The mixture was centrifuged and the precipitate was washed with DCM and centrifuged for a second time. The solvent was removed under reduced pressure. Purification by column chromatography (eluent: DCM/MeOH 100:1 to 50:1) yielded **3.22** as a white fluffy hygroscopic solid (58.62 mg, 20 %): RP-HPLC: 96 %, (t_R = 18.80 min, k = 5.38); UV_{max} 205 nm. ^{1}H-NMR (600 MHz, [D$_4$]MeOH) δ (ppm) 1.35 (m, 8H), 1.46-1.66 (m, 4H), 2.03 (tt, 4H, ^2J 7.0 Hz, ^3J 7.5 Hz), 2.86 (t, 4H, *J* 7.7 Hz), 3.19 (t, 4H, *J* 7.0 Hz), 3.39 (t, 4H, *J* 6.4 Hz), 7.39 (s, 2H), 8.83 (d, 2H, *J* 0.9 Hz); ^{13}C-NMR (151 MHz, [D$_4$]MeOH, trifluoroacetate) δ (ppm) 22.5, 27.8, 28.2, 30.2, 30.4, 40.8, 41.5, 117.1, 134.3, 134.9, 155.3, 155.9. MS (ESI) m/z (%) 531 (15) [M+H]$^+$, 266 (47) [M+2H]$^{2+}$. HRMS (ESI): m/z [M+H]$^+$ calculated for $C_{24}H_{43}N_{12}O_2^+$: 531.3626, found 531.3625; $C_{24}H_{42}N_{12}O_2$ x 4 TFA (986.75).

1-(Amino{[3-(1*H*-imidazol-4-yl)propyl]amino}methylene)-3-{10-[3-(amino{[3-(1*H*-imidazol-4-yl)propyl]amino}methylene)ureido]decyl}urea (3.23). The title compound was prepared from **3.18** (150 mg, 0.248 mmol), amine **3.6** (191 mg, 0.520 mmol), NEt_3 (172 µL, 1.24 mmol) and $HgCl_2$ (270 mg, 0.99 mmol) according to the general procedure, yielding **3.23** as a white fluffy hygroscopic solid (68.83 mg, 27 %): RP-HPLC: 91 %, (t_R = 22.73 min, k = 6.71); UV_{max} 205 nm. ^{1}H-NMR (600 MHz, [D$_4$]MeOH) δ (ppm) 1.32 (m, 12H), 1.49-1.57 (m, 4H), 2.02 (tt, 4H, ^2J 7.0 Hz, ^3J 7.6 Hz), 2.83 (t, 4H, *J* 7.7 Hz), 3.18 (t, 4H, *J* 7.0 Hz), 4H), 3.36 (t, 4H, *J* 6.9 Hz), 7.36 (s, 2H), 8.80 (d, 2H, *J* 0.7 Hz); ^{13}C-NMR (151 MHz, [D$_4$]MeOH, trifluoroacetate) δ (ppm) 22.5, 27.8, 28.1, 30.3, 30.4, 30.5, 40.8, 41.4, 117.0, 134.3, 134.9, 155.4, 156.0. MS (ESI) m/z (%) 559 (10) $[M+H]^+$, 280 (27) $[M+2H]^{2+}$. HRMS (ESI): m/z $[M+H]^+$ calculated for $C_{26}H_{47}N_{12}O_2^+$: 559.3939, found 559.3935; $C_{26}H_{46}N_{12}O_2$ x 4 TFA (1014.80).

1-(Amino{[3-(2-amino-4-methyl-thiazol-5-yl)propyl]amino}methylene)-3-{4-[3-(amino{[3-(2-amino-4-methyl-thiazol-5-yl)propyl]amino}methylene)ureido]butyl}urea (3.24). Compound **3.14** (200 mg, 0.384 mmol) and amine **3.11** (216 mg, 0.796 mmol) were dissolved in DCM. NEt_3 (265 µL, 1.80 mmol) and $HgCl_2$ (412 mg, 1.52 mmol) were added to the mixture. The mixture was centrifuged and the precipitate was washed with DCM and centrifuged for a second time. The solvent was removed under reduced pressure and the product was purified by column chromatography (eluent: DCM/MeOH 100:1 to 50:1), yielding **3.24** as a white fluffy hygroscopic solid (53.34 mg, 14 %): RP-HPLC: 99 %, (t_R = 15.61 min, k = 4.29); UV_{max} 205 nm and 265 nm. ^{1}H-NMR (600 MHz, [D$_4$]MeOH) δ (ppm) 1.57 (m, 4H), 1.90 (tt, 4H, ^2J 7.0 Hz, ^3J 7.3 Hz), 2.18 (s, 6H), 2.72 (t, 4H, *J* 7.6 Hz), 3.23 (m, 4H), 3.33 (t, 4H, *J* 6.9 Hz); ^{13}C-NMR (151 MHz, [D$_4$]MeOH, trifluoroacetate) δ (ppm) 11.4, 23.6, 27.7, 29.9, 40.34, 41.4, 118.4, 132.6, 155.6, 156.0, 170.3. MS (ESI) m/z (%) 567 (34) $[M+H]^+$, 284 (58) $[M+2H]^{2+}$. HRMS (ESI): m/z $[M+H]^+$ calculated for $C_{22}H_{39}N_{12}O_2S_2^+$: 567.2755, found 567.2760; $C_{22}H_{38}N_{12}O_2S_2$ x 4 TFA (1022.83).

1-(Amino{[3-(2-amino-4-methyl-thiazol-5-yl)propyl]amino}methylene)-3-{6-[3-(amino{[3-(2-amino-4-methyl-thiazol-5-yl)propyl]amino}methylene)ureido]hexyl}urea (3.25). Compound **3.15** (175 mg, 0.319 mmol) and amine **3.11** (177 mg, 0.652 mmol) were dissolved in DCM. NEt_3 (215 µL, 1.55 mmol) and $HgCl_2$ (378 mg, 1.24 mmol) were added to the mixture. The mixture was centrifuged and the precipitate was washed with DCM and centrifuged for a second time The solvent was removed under reduced pressure and the product was purified by column chromatography (eluent: DCM/MeOH 100:1 to 50:1), yielding **3.25** as a white fluffy hygroscopic solid (99.34 mg, 30 %): RP-HPLC: 99 %, (t_R = 18.12 min, k = 5.15); UV_{max} 203 nm and 265 nm. ^{1}H-NMR (600 MHz, [D$_4$]MeOH) δ (ppm) 1.37 (m, 4H), 1.48-1.62 (m, 4H), 1.89 (tt, 4H, ^2J 7.0 Hz, ^3J 7.4 Hz), 2.18 (s, 6H), 2.72 (t, 4H, *J* 7.5 Hz), 3.20 (t, 4H, *J* 6.9 Hz), 3.33 (t, 4H, *J* 6.8 Hz, overlap with solvent). ^{13}C-NMR (75 MHz, [D$_4$]MeOH, trifluoroacetate) δ (ppm) 11.4, 23.6, 27.4, 29.9, 30.3, 40.6, 41.4, 118.4, 132.6, 155.5, 156.0, 170.3. MS (ESI) m/z (%) 595 (23) $[M+H]^+$, 298 (38) $[M+2H]^{2+}$. HRMS (ESI): m/z $[M+H]^+$ calculated for $C_{24}H_{43}N_{12}O_2S_2^+$: 595.3068, found 595.3068; $C_{24}H_{42}N_{12}O_2S_2$ x 4 TFA (1050.88).

1-(Amino{[3-(2-amino-4-methyl-thiazol-5-yl)propyl]amino}methylene)-3-{7-[3-(amino{[3-(2-amino-4-methyl-thiazol-5-yl)propyl]amino}methylene)ureido]heptyl}urea (**3.26**)**.** The title compound was prepared from **3.16** (175 mg, 0.311 mmol), **3.11** (177 mg, 0.652 mmol),

NEt_3 (215 µL, 1.55 mmol) and $HgCl_2$ (338 mg, 1.24 mmol) according to the general procedure, yielding **3.26** as a white fluffy hygroscopic solid (95.46 mg, 29 %): RP-HPLC: 99 %, (t_R = 19.85 min, k = 5.74); UV_{max} 204 nm and 264 nm. ^{1}H-NMR (600 MHz, [D$_4$]MeOH) δ (ppm) 1.36 (s, 6H), 1.51-1.57 (m, 4H), 1.90 (tt, 4H, ^2J 7.2 Hz, ^3J 7.4 Hz), 2.18 (s, 6H), 2.72 (t, 4H, *J* 7.6 Hz), 3.19 (t, 4H, *J* 7.1 Hz), 3.33 (t, 4H, *J* 6.9 Hz); ^{13}C-NMR (151 MHz, [D$_4$]MeOH, trifluoroacetate) δ (ppm) 11.4, 23.6, 27.7, 29.9, 30.0, 30.4, 40.8, 41.4, 118.4, 132.7, 155.5, 156.0, 170.3. MS (ESI) m/z (%) 609 (23) $[M+H]^+$, 305 (50) $[M+2H]^{2+}$. HRMS (ESI): m/z $[M+H]^+$ calculated for $C_{25}H_{45}N_{12}O_2S_2^+$: 609.3224, found 609.3226; $C_{25}H_{44}N_{12}O_2S_2$ x 4 TFA (1064.91).

1-(Amino{[3-(2-amino-4-methyl-thiazol-5-yl)propyl]amino}methylene)-3-{8-[3-(amino{[3-(2-amino-4-methyl-thiazol-5-yl)propyl]amino}methylene)ureido]octyl}urea (**3.27).** The title compound was prepared from **3.17** (130 mg, 0.225 mmol), **3.11** (128 mg, 0.472 mmol), NEt_3 (156 µL, 1.12 mmol) and $HgCl_2$ (244 mg, 0.90 mmol) according to the general procedure, yielding **3.27** as a white fluffy hygroscopic solid (21.77 mg, 9 %): RP-HPLC: 98 %, (t_R = 21.69 min, k = 6.36); UV_{max} 204 nm and 264 nm. ^{1}H-NMR (600 MHz, [D$_4$]MeOH) δ (ppm) 1.34 (m, 8H), 1.50-1.56 (m, 4H), 1.90 (tt, 4H, ^2J 7.0 Hz, ^3J 7.4 Hz), 2.18 (s, 6H), 2.72 (t, 4H, *J* 7.6 Hz), 3.19 (t, 4H, *J* 7.1 Hz), 3.33 (t, 4H, *J* 6.9 Hz). ^{13}C-NMR (151 MHz, [D$_4$]MeOH, trifluoroacetate) δ (ppm) 11.4, 23.6, 27.8, 29.9, 30.3, 30.4, 40.8, 41.4, 118.4, 132.6, 155.5, 156.0, 170.3. MS (ESI) m/z (%) 623 (11) $[M+H]^+$, 312 (21) $[M+2H]^{2+}$. HRMS (ESI): m/z $[M+H]^+$ calculated for $C_{26}H_{47}N_{12}O_2S_2^+$: 623.3381, found 623.3375; $C_{26}H_{46}N_{12}O_2S_2$ x 4 TFA (1078.94).

1-(Amino{[3-(2-amino-4-methyl-thiazol-5-yl)propyl]amino}methylene)-3-{10-[3-(amino-{[3-(2-amino-4-methyl-thiazol-5-yl)propyl]amino}methylene)ureido]decyl}urea (**3.28).** The title compound was prepared from **3.18** (150 mg, 0.248 mmol), **3.11** (141 mg, 0.519 mmol), NEt_3 (172 µL, 1.24 mmol) and $HgCl_2$ (269 mg, 0.99 mmol) according to the general procedure, yielding **3.28** as a white fluffy hygroscopic solid (24.25 mg, 9 %): RP-HPLC: 99 %, (t_R = 25.49 min, k =7.65); UV_{max} 205 nm and 263 nm. ^{1}H-NMR (600 MHz, [D$_4$]MeOH) δ (ppm) 1.32 (m, 12H), 1.50-1.56 (m, 4H), 1.90 (tt, 4H, ^2J 7.0 Hz, ^3J 7.3 Hz), 2.18 (s, 6H), 2.72 (t, 4H, *J* 7.1 Hz), 3.19 (t, 4H, *J* 7.1 Hz), 3.33 (t, 4H, *J* 6.9 Hz). ^{13}C-NMR (151 MHz, [D$_4$]MeOH, trifluoroacetate) δ (ppm) 11.5, 23.6, 27.8, 29.9, 30.3, 30.4, 30.6, 40.8, 41.4, 118.4, 132.7, 155.5, 156.0, 170.3. MS (ESI) m/z (%) 651 (4) $[M+H]^+$, 326 (17) $[M+2H]^{2+}$, 218 (27) $[M+3H]^{3+}$, 163 (42) $[M+4H]^{4+}$. HRMS (ESI): m/z $[M+H]^+$ calculated for $C_{28}H_{51}N_{12}O_2S_2^+$: 651.3694, found 651.3684; $C_{28}H_{50}N_{12}O_2S_2$ x 4 TFA (1106.99).

1,7-Dichloroheptan-4-one (3.29).[13] HCl gas (1fold excess) was passed through dicyclopropyl ketone (15.00 g, 136.16 mmol) for 30 min. After stirring for 3 h, HCl gas was passed through the mixture for another 30 min. The crude product was obtained as a brown oil (24.93 g, 100 %) and was used in the next step without any further purification. ^{1}H-NMR (300 MHz, $CDCl_3$): δ (ppm) 2.02 (m, 4H), 2.61 (t, 4H, *J* 7.0 Hz), 3.55 (t, 4H, *J* 6.3 Hz). ^{13}C-NMR (75 MHz, [D$_4$]MeOH) δ (ppm) 27.6, 40.3, 45.2, 210.7. MS (APCI; MeOH) m/z (%) 183 (100). HRMS (APCI): m/z $[M+H]^+$ calculated for $C_7H_{13}Cl_2O^+$: 183.0337, found 183.0337. $C_7H_{12}Cl_2O$ (183.08).

1,7-Diazidoheptan-4-one (3.30). To a solution of 1,7-dichloroheptan-4-one (**3.29**) (3.40 g, 18.57 mmol) in 50 mL DMF, sodium azide (3.62 g, 55.68 mmol) was added and stirred overnight at 60 °C. After cooling and addition of water (500 mL), the mixture was extracted with EA (3 x 100 mL). The combined organic phases were dried over sodium sulfate. Filtration and evaporation of the solvent yielded a yellow oil (2.87 g, 79 %). The crude product **3.30** was used in the next step without any further purification. ^{1}H-NMR (300 MHz, $CDCl_3$) δ (ppm) 1.86 (m, 4H), 2.52 (t, 4H, *J* 7.1 Hz), 3.31 (t, 4H, *J* 6.6 Hz). ^{13}C-NMR (75 MHz, $CDCl_3$) δ (ppm) 22.6, 39.0, 50.4, 208.2. MS (ESI; MeOH) m/z (%) 219 (46) [M+Na$^+$], 197 (2) [M+H]$^+$, 169 (100) [M+H-N_2]$^+$. HRMS (ESI): m/z [M+H]$^+$ calculated for $C_7H_{13}N_6^+$: 197.1145, found 197.1138. $C_7H_{12}N_6$(196.11).

(4-Chlorobutyl)triphenylphosphonium bromide (3.31).[38] Triphenylphosphine (38.24 g, 0.14 mol) and 1-bromo-4-chlorobutane (25 g, 0.15 mol) were dissolved in anhydrous toluene (500 mL), and the mixture was heated to reflux overnight. The reaction mixture was cooled to room temperature. The white solid was filtered off, washed with toluene and hexane and dried in vacuo (38.68 g, 61 %); mp = 229-231 °C. ^{1}H-NMR (300 MHz, $CDCl_3$) δ (ppm) 1.77-1.90 (m, 2H), 2.21-2.30 (m, 2H), 3.66-3.77 (m, 2H), 3.71 (t, 2H, *J* 6.4 Hz), 3.94-4.04 (m, 2H), 7.66-7.92 (bm, 15H). MS (ESI) m/z (%) 353 (100) [M]$^+$. HRMS (ESI): m/z [M]$^+$ calculated for $C_{22}H_{23}ClP^+$: 353.1220, found 353.1222. $C_{22}H_{23}ClP^+$ Br^-(433.02).

1-Azido-4-(3-azidopropyl)-8-chlorooct-4-ene (3.32). (4-Chlorobutyl)triphenylphosphonium bromide (**3.31**) (2.50 g, 5.76 mmol) was suspended in anhydrous THF (20 mL) under an atmosphere of argon and the mixture was cooled to -72 °C. n-Butyllithium (1.6 M in n-hexane, 3.60 mL, 5.76 mmol) was added to the suspension and the mixture was allowed to warm up to -10 °C over a period of 45 min. The temperature was kept at -10 °C for 1.5 h and then cooled again to -72 °C. 1,7-diazidoheptan-4-one (1.13 g, 5.76 mmol) was added and the mixture was allowed to warm up to room temperature over a period of 60 min, stirring was continued overnight. After filtration of solid material and evaporation of the solvent, the product was purified by column chromatography using mixtures of Hex and EA as eluent (R_f = 0.45 for Hex /EA 4:1), affording **3.32** as yellow oil (300 mg, 19 %). ^{1}H-NMR (300 MHz, [D_4]MeOH) δ (ppm) 1.61-1.74 (m, 4H), 1.76-1.86 (m, 2H), 2.07-2.26 (bm, 6H), 3.26-3.31 (overlap with solvent, m, 4H), 3.56 (t, 2H, *J* 6.5 Hz), 5.23 (t, 1H, *J* 7.3 Hz). ^{13}C-NMR (75 MHz, $CDCl_3$) δ (ppm) 25.0, 27.0, 27.4, 27.6, 32.7, 33.6, 44.6, 51.0, 51.2, 125.3, 138.0. MS (ESI) m/z (%) 243 (100) [M+H-N_2]$^+$. HRMS (ESI): m/z [M+H-N_2]$^+$ calculated for $C_{11}H_{20}ClN_4^+$: 243.1376, found 243.1374; $C_{11}H_{19}ClN_6$ (270.76).

2-[8-Azido-5-(3-azidopropyl)oct-4-en-1-yl]isoindoline-1,3-dione (3.33). To a solution of **3.32** (1.89 g, 6.98 mmol) and phthalimide (1.54 g, 10.47 mmol) in 40 mL DMF, Cs_2CO_3 (5.00g, 15.34 mmol) and catalytic traces of KI were added. The mixture was stirred at 60 °C overnight. After cooling 400 mL 5 % NaOH were added and the product was extracted with EA. The combined organic phases were dried over Na_2SO_4. After filtration and evaporation, the crude product was purified by column chromatography using mixtures of Hex and EA as eluent (R_f = 0.45 for Hex/EA 2:1), affording **3.33** (1.51 g, 57 %) as yellow oil. ^{1}H-NMR (300 MHz, $CDCl_3$) δ (ppm) 1.56-1.58 (m, 4H), 1.69-1.78 (m, 2H), 1.96-2.15 (m, 6H), 3.24 (td, 4H, ^{2}J 6.8, ^{3}J 2.9), 3.65-3.73 (m, 2H), 5.21 (t, 1H, *J* 7.1 Hz), 7.75-7.67 (m, 2H), 7.80-7.87 (m, 2H). ^{13}C-NMR (75 MHz, $CDCl_3$) δ (ppm) 25.1, 26.9, 27.2, 27.3, 28.7, 33.4, 37.7, 50.9, 51.1,

123.2, 125.7, 132.1, 133.9, 137.3, 168.4. MS (ESI) m/z (%) 404 (31) [M+Na$^+$], 354 (100) [M+H-N_2]$^+$. HRMS (ESI): m/z [M+H-N_2]$^+$ calculated for $C_{19}H_{24}N_5O_2^+$: 354.1925, found 354.1925; $C_{19}H_{23}N_7O_2$ (381.44).

8-Azido-5-(3-azidopropyl)oct-4-en-1amine (3.34). A mixture of **3.33** (1.00 g, 2.62 mmol) and hydrazine (0.50 g, 15.60 mmol) in ethanol was heated to reflux for 1h. Solid material was removed by filtration. After removing the solvent in vacuo, the product was purified by column chromatography (eluent: EA/MeOH/NH_3 9/0.8/0.2 to EA/MeOH/NH_3 8/1.5/0.5), (R_f = 0.14 for DCM / 7 N NH_3 in MeOH 4:1). Compound **3.34** was obtained as yellow oil (580 mg, 88 %). ^{1}H-NMR (300 MHz, $CDCl_3$) δ (ppm) 1.45-1.54 (m, 2H), 1.58-1.85 (m, 6H), 1.99-2.13 (m, 6H), 2.70 (t, 2H, *J* 7.1 Hz), 3.26 (td, 4H, ^2J 6.8, ^3J 2.4) 5.20 (t, 1H, *J* 7.1). ^{13}C-NMR (75 MHz, $CDCl_3$) δ (ppm) 25.2, 27.3, 27.5, 33.3, 33.6, 39.5, 41.6, 51.0, 51.2, 126.6, 136.7. MS (ESI) m/z (%) 252 (100) [M+H]$^+$. HRMS (ESI): m/z [M+H$^+$]$^+$ calculated for $C_{11}H_{22}N_7^+$: 252.1931, found 252.1925; $C_{11}H_{21}N_7$ (251.34).

***tert*-Butyl [8-azido-5-(3-azidopropyl)oct-4-en-1-yl]carbamate (3.35).** A solution of di-*tert*-butyldicarbonat (756 mg, 3.46 mmol) in DCM was added dropwise to an external cooled solution of number 8-azido-5-(3-azidopropyl)oct-4-en-1amine (**3.34**) (870 mg, 3.46 mmol) and NEt_3 (480 µL, 3.46 mmol) in DCM over a period of 1h. The mixture was stirred at room temperature for 24h. The solvent was removed in vacuo. The product was purified by column chromatography (eluent: Hex/EA 10/90 to Hex/EA 50/50), (R_f = 0.23 for Hex/EA 3:2) and obtained as pale yellowish oil (1.18 g, 97 %). ^{1}H-NMR (300 MHz, $CDCl_3$) δ (ppm) 1.44 (s, 9H), 1.47-1.59 (m, 2H), 1.59-1.73 (m, 4H), 2.00-2.12 (m, 6H), 3.11 (t, 2H, *J* 6.9 Hz), 3.23-3.30 (m, 4H), 4.54 (s, 1H), 5.19 (t, 1H, *J* 7.1 Hz). ^{13}C-NMR (75 MHz, $CDCl_3$) δ (ppm) 25.1, 26.8, 27.3, 27.4, 28.5, 30.3, 33.5, 40.3, 51.0, 51.1, 79.1, 126.3, 137.0, 156.0. MS (ESI) m/z (%) 374 (26) [M+Na$^+$], 324 (25) [M+H-N_2]$^+$, 268 (100) (M+H-C_4H_8]$^+$. HRMS (ESI): m/z [M+Na$^+$] calculated for $C_{16}H_{29}N_7O_2Na^+$: 374.2275, found 374.2282; $C_{16}H_{29}N_7O_2$ (351.45).

***tert*-Butyl [8-amino-5-(3-aminopropyl)oct-4-en-1-yl]carbamate (3.36).** A solution of **3.35** (200 mg, 0.57 mmol) in anhydrous diethyl ether was dropped to a stirred suspension of $LiAlH_4$ (100 mg, 2.63 mmol) in anhydrous diethyl ether over 1 h. The mixture was heated to reflux for an additional hour. After cooling and quenching with a solution of 2 g Seignette salt in 12 g water (pH = 9-10), the organic phase was washed twice with 0.1 M KOH and the solvent was evaporated in vacuo. The crude product was used in the next step without any further purification (113 mg, 66 %). ^{1}H-NMR (300 MHz, [D_4]MeOH) δ (ppm) 1.42 (s, 9H), 1.47-1.57 (m, 6H), 1.63 (s, 4H), 1.98-2.06 (m, 6H), 2.66 (td, 4H, ^2J 7.1, ^3J 2.5), 3.05-3.12 (m, 2H), 4.67 (s, 1H), 5.11 (t, 1H *J* 7.0 Hz). ^{13}C-NMR (75 MHz, $CDCl_3$) δ (ppm) 25.1, 27.4, 28.5, 30.4, 32.2, 32.4, 34.2, 40.4, 42.0, 42.3, 79.1, 124.4, 139.3, 156.1. MS (ESI) m/z (%) 300 (40) [M+H]$^+$, 244 (51) [M+H-C_4H_8]$^+$, 200 (100) [M+H-Boc]$^+$. HRMS (ESI): m/z [M+H$^+$]$^+$ calculated for $C_{16}H_{34}N_3O_2^+$: 300.2646, found 300.2649; $C_{16}H_{33}N_3O_2$ (299.45).

***tert*-Butyl ({3-[4-({3-[(tert-butoxycarbonylimino)(methylsulfanyl)methyl]ureido}propyl)-8-(tert-butoxycarbonylamino)oct-4-en-1-yl]ureido}(methylsulfanyl)methylene)carbamate (3.38).** The title compound was prepared from **3.36** (122 mg, 0.41 mmol), DIEA (393 µL, 2.3 mmol) and triphosgene (122 mg, 0.41 mmol), giving *tert*-butyl [8-isocyanato-5-(3-isocyanatopropyl)oct-4-en-1-yl]carbamate (**3.37**) as intermediate. Compound **3.37** was not isolated but allowed to react with *N*-Boc-*S*-methylisothiourea (310 mg, 1.63 mmol) according to the general procedure for the synthesis of the guanidinylating reagents **(3.14-3.18)**. **3.38** was obtained as a yellowish oil (R_f = 0.37 in DCM) (131 mg, 44 %). ^{1}H-NMR (300 MHz, [D_4]MeOH) δ (ppm) 1.43 (s, 9H), 1.48-1.54 (m, 20H), 1.59-1.66 (m, 4H), 2.03-2.07 (m, 4H), 2.08-2.12 (m, 2H), 2.33 (d, 6H, *J* 2.1 Hz), 3.03 (t, 2H, *J* 7.0 Hz), 3.14 (m, 4H), 5.22 (t, 1H, *J* 7.1 Hz). ^{13}C-NMR (75 MHz, $CDCl_3$) δ (ppm) 14.4, 26.1, 28.2, 28.8, 29.1, 29.3, 31.2, 35.1, 40.8, 41.1, 83.6, 126.3, 139.8, 152.2, 163.7, 163.72, 167.2, 167.3. MS (ESI) m/z (%) 754 (14) [M+Na$^+$], 732 (100) [M+H]$^+$, 266 (69) [M+2H-2Boc]$^{2+}$. HRMS (ESI): m/z [M+H$^+$]$^+$ calculated for $C_{32}H_{58}N_7O_8S_2^+$: 732.3794, found 732.3794; $C_{32}H_{57}N_7O_8S_2$ (731.97).

1-(8-Amino-4-{[3-(amino{[3-(2-amino-4-methyl-thiazol-5-yl)propyl]amino}methylene)ureido]propyl}oct-4-enyl)-3-[(amino{[3-(2-amino-4-methyl-thiazol-5-yl)propyl]amino}methylene)]urea (**3.39).** The title compound was prepared from **3.38** (111 mg, 0.15 mmol), **3.11** (86 mg, 0.317 mmol), NEt_3 (105 µL, 0.76 mmol) and $HgCl_2$ (165 mg, 0.60 mmol) according to the general procedure for the synthesis of the bivalent carbamoylguanine-type ligands (**3.19-3.28**), yielding **3.39** as a white fluffy hygroscopic solid (34.80 mg, 21 %). RP-HPLC: 96 %, (t_R = 17.19 min, k = 4.83); UV_{max} 204 nm and 263 nm. ^{1}H-NMR (600 MHz, [D_4]MeOH) δ (ppm) 1.59-1.67 (m, 4H), 1.70 (m, 2H), 1.90 (tt, 4H, ^2J 7.0 Hz, ^3J 7.3 Hz), 2.05-2.17 (bm, 6H), 2.18 (s, 6H), 2.72 (t, 4H, *J* 7.6 Hz), 2.90-2.94 (m, 2H), 3.19 (m, 4H), 3.34 (t, 4H, *J* 6.8 Hz, overlap with solvent), 5.23 (t, 1H, *J* 7.1 Hz). ^{13}C-NMR (151 MHz, [D_4]MeOH, trifluoroacetate) δ (ppm) 11.4, 23.6, 25.6, 28.1, 28.8, 28.9, 29.1, 29.9, 34.7, 40.41, 40.44, 40.8, 41.4, 118.4, 125.3, 132.6, 140.6, 155.6, 156.0, 170.3. MS (ESI) m/z (%) 678 (10) [M+H]$^+$, 340 (23) [M+2H]$^{2+}$. HRMS (ESI): m/z [M+H]$^+$ calculated for $C_{29}H_{52}N_{13}O_2S_2^+$: 678.3803, found 678.3806. $C_{29}H_{51}N_{13}O_2S_2$ x 5 TFA (1248.03).

General procedure for the synthesis of the bivalent fluorescence ligands (3.40-3.42)

The reactions were carried out in a 1.5-mL Eppendorf reaction vessel. The amine precursor **3.39** (2 eq) was dissolved in 30 µL DMF and NEt_3 (15 eq) was added. The fluorescence dyes (1 eq) were dissolved in 20 µL DMF and this solution was added to the mixture, the cup was rinsed two times with DMF (20 µL and 10 µL). The mixture was stirred for 2 h at room temperature and then the reaction was stopped by adding 20 µL of 10 % TFA. The crude products were purified by preparative HPLC.

2-{(1*E*,3*E*)-5-[(*Z*)-1-(5-amino-12-{3-[3-(amino{[3-(2-amino-4-methylthiazol-5-yl)propyl]amino}methylene)ureido]propyl}-1-(2-amino-4-methylthiazol-5-yl)-7,18-dioxo-4,6,8,17-tetraazatricosa-5,12-dien-23-yl)-3,3-dimethylindolin-2-ylidene]penta-1,3-dien-1-yl}-1,3,3-trimethyl-3*H*-indol-1-ium trifluoroacetate (3.40). The title compound was prepared from **3.39** (1.60 mg, 1.28 µmol), S2197 (422 µg, 0.64 µmol) and NEt_3 (1.33 µL, 9.60 µmol) according to the general procedure, yielding **3.40** as a dark blue solid (490 µg, 45 %): RP-HPLC: 99 %, (t_R = 24.83 min, k = 7.42) (eluent: MeCN/TFA (0.05% aq.) 10:90, 30 min:

60/40, 31 min: 80:20, -41 min; flow rate = 0.75 mL/min). MS (ESI) m/z (%) 1143.8 (1) $[M]^+$, 571.9 (34) $[M+H]^{2+}$, 381.6 (100) $[M+2H]^{3+}$, 296.6 (24) $[M+4H+MeOH]^{4+}$. $C_{63}H_{88}F_3N_{15}O_5S_2$ x 4 TFA (1713.70).

1-{8-[3-(amino{[3-(2-amino-4-methylthiazol-5-yl)propyl]amino}methylene)ureido]-5-{3-[3-(amino{[3-(2-amino-4-methylthiazol-5-yl)propyl]amino}methylene)ureido]propyl}oct-4-en-1-yl}-2,6-dimethyl-4-[(*E*)-2-(2,3,6,7-tetrahydro-1*H*,5*H*-pyrido[3,2,1-ij]quinolin-9-yl)vinyl]pyridin-1-ium trifluoroacetate (3.41). The title compound was prepared from **3.39** (1.50 mg, 1.20 µmol), Py-1 (236 µg, 0.60 µmol) and NEt_3 (1.25 µL, 9.00 µmol) according to the general procedure, yielding **3.41** as a red solid (332 µg, 36 %): RP-HPLC: 93 %, (t_R = 23.11 min, k = 6.84) (eluent: MeCN/TFA (0.05% aq.) 10:90, 30 min: 60/40, 31 min: 80:20, -41 min; flow rate = 0.75 mL/min). MS (ESI) m/z (%) 965.7 (1) $[M]^+$, 483.2 (82) $[M+H]^{2+}$, 336.1 (100) $[M+2H+MeCN]^{3+}$, 322.4 (15) $[M+2H]^{3+}$. $C_{52}H_{73}F_3N_{14}O_4S_2$ x 4 TFA (1536.45).

1-{8-[3-(amino{[3-(2-amino-4-methylthiazol-5-yl)propyl]amino}methylene)ureido]-5-{3-[3-(amino{[3-(2-amino-4-methylthiazol-5-yl)propyl]amino}methylene)ureido]propyl}oct-4-en-1-yl}-4-{(1E,3E)-4-[4-(dimethylamino)phenyl]buta-1,3-dien-1-yl}-2,6-dimethylpyridin-1-ium trifluoroacetate (3.42). The title compound was prepared from **3.39** (2.00 mg, 1.60 µmol), Py-5 (294 µg, 0.80 µmol) and NEt_3 (1.66 µL, 12 µmol) according to the general procedure, yielding **3.42** as a red solid (462 µg, 38 %): RP-HPLC: 96 %, (t_R = 19.68 min, k = 5.68) (eluent: MeCN/TFA (0.05% aq.) 10:90, 30 min: 60/40, 31 min: 80:20, -41 min; flow rate = 0.75 mL/min). MS (ESI) m/z (%) 939.6 (1) $[M]^+$, 470 (90) $[M+H]^{2+}$, 327 (100) $[M+2H+MeCN]^{3+}$, 313 (11) $[M+2H]^{3+}$. $C_{50}H_{71}F_3N_{14}O_4S_2$ x 4 TFA (1510.41).

***N*-{8-[3-(amino{[3-(2-amino-4-methylthiazol-5-yl)propyl]amino}methylene)ureido]-5-{3-[3-(amino{[3-(2-amino-4-methylthiazol-5-yl)propyl]amino}methylene)ureido]propyl}oct-4-en-1-yl}propionamide (3.43a).** The reaction was carried out in a 1.5-mL Eppendorf reaction vessel. Compound **3.39** (13.62 µmol, 17.00 mg) was dissolved in 30 µL DMF and NEt_3 (102.20 µmol, 14.14 µL) was added. Succinimidyl propionate (16.36 µmol, 2.80 mg) was dissolved in 20 µL DMF and this solution was added to the mixture. The cup was rinsed a second time with 10 µL DMF and the reaction mixture was stirred for 2 h at room temperature. The reaction was stopped by adding 20 µL of 10 % TFA. The crude product was purified by preparative HPLC, yielding **3.43a** as a white fluffy hygroscopic solid (13.18 mg, 81 %): RP-HPLC: 94 %, (t_R = 21.77 min, k = 7.54) (YMC C8 column); UV_{max} 204 nm and 264 nm. ^{1}H-NMR (600 MHz, [D$_4$]MeOH) δ (ppm) 1.12 (t, 3H, *J* 7.6 Hz), 1.54 (tt, 2H, ^2J 7.0 Hz, ^3J 7.4 Hz), 1.62 (m, 4H), 1.90 (tt, 4H, ^2J 7.3 Hz, ^3J 7.4 Hz), 2.03-2.11 (bm, 6H), 2.16-2.21 (m, 8H), 2.72 (t, 4H, *J* 7.6 Hz), 3.14-3.20 (m, 6H), 3.33 (t, 4H, *J* 6.9 Hz), 5.23 (t, 1H, *J* 7.1 Hz). ^{13}C-NMR (151 MHz, [D$_4$]MeOH, trifluoroacetate) δ (ppm) 10.6, 11.4, 23.6, 26.1, 27.9, 28.8, 29.1, 29.2, 30.2, 30.7, 34.7, 40.1, 40.4, 40.8, 41.4, 118.4, 126.6, 132.6, 139.3, 155.5, 156.0, 170.3, 177.0. MS (ESI) m/z (%) 734.4 (10) $[M+H]^+$, 367.7 (23) $[M+2H]^{2+}$, 245.5 (77) $[M+3H]^{3+}$. HRMS (ESI): m/z $[M+H]^+$ calculated for $C_{32}H_{56}N_{13}O_3S_2^+$: 734.4065, found 734.4068. $C_{32}H_{55}N_{13}O_3S_2$ x 4 TFA (1190.08).

***N*-{8-[3-(amino{[3-(2-amino-4-methylthiazol-5-yl)propyl]amino}methylene)ureido]-5-{3-[3-(amino{[3-(2-amino-4-methylthiazol-5-yl)propyl]amino}methylene)ureido]propyl}oct-4-en-1-yl}-2,3-ditritiopropionamide (3.43b).**

Succinimidyl [2,3-$^{3}H_2$]propionate was from Hartmann Analytic (Braunschweig, Germany), provided in EA (a_s = 2.96 TBq/mmol, 80 Ci/mmol; a_v = 18.5 GBq/mL, 5 mCi/mL). The reaction was carried out in a 1.5 mL Eppendorf reaction vessel. The precursor **3.39** (0.375 µmol, 468 µg) was dissolved in a mixture of 50 µL DMF and DIPEA (5.625 µmol, 0.96 µL). This mixture was added to the solved succinimidyl [2,3-^{3}H]propionate (41.46 nmol, 3.32 mCi). The EA was removed in a vacuum concentrator for about 45 min. Afterwards 9 µL EA and 1 µL DIPEA were added, and the mixture was stirred for 3 h with a magnetic stirrer at room temperature. 80 µL 2 % of aq. TFA and 280 µL Millipore water were added. The product was isolated with a Waters HPLC system (column: YMC – Triart C18 (250 x 6.0mm x 5 µm). Eluent: mixtures of MeCN and 0.04% TFA (A) and 0.05 % aq. TFA (B), gradient 0 to 20 min A/B 5:95 to 30/70. The retention time of the radioligand was 18.4 min and the eluates were collected in a 1.5-mL reaction vessel. The combined fractions were concentrated in a vacuum concentrator to a volume of around 600 µL.

Quantification: The concentration of the radioligand was determined by a 4 point calibration with **3.43a**. The solutions for the calibration were prepared freshly prior to the injection. All of the solutions were prepared separately in mobile phase from a 20 µM solution of **3.43a**. Eluent: mixtures of MeCN and 0.04 % TFA (A) and 0.05 % aq. TFA (B), gradient: 0 to 20 min A/B 5:95 to 26/74 (column: Phenomenex Luna C18 (150 x 4.6mm x 3µm). The molarity of the solution of **3.43b** was calculated from the peak areas of the standards.

Determination of the specific activity: 10 aliquots of the diluted radioligand in mobile phase were counted in 3 mL of Rotiszint eco plus (Roth, Karlsruhe, Germany) in a LS 6500 liquid scintillation counter (Beckmann-Coulter, München). The calculated specific activity was 2.60 tBq/mmol (70.15 Ci/mmol). The concentration was adjusted to 1 mCi/ml by adding 1291 µL of a mixture of Millipore water and EtOH (60 : 40). This yielded in a concentration of 14.25 µM.
The radioligand was obtained in a yield of 90 % (37.34 nmol, 44.41 µg) with a radiochemical purity of 99 %. $C_{32}H_{55}N_{13}O_3S_2$ x 4 TFA (1190.08).

3.5.3 Pharmacological Protocols

3.5.3.1 GTPγS binding assay

[^{35}S]GTPγS was from PerkinElmer Life Science (Boston, USA) or Hartmann Analytic (Braunschweig, Germany). *Sf9* membranes expressing the hH_2R-$G_s\alpha_s$ or the gpH_2R- $G_s\alpha_s$ were thawed and sedimented by centrifugation at 13.000 g (4 °C) for 10 min. The membranes were resuspended in cold (4 °C) binding buffer BB (12.5 mM $MgCl_2$, 1 mM EDTA and 75 mM Tris/HCl, pH 7.4) so that the final concentration was 1 µg of protein per 1 µL BB. Experiments were performed in 96-well plates (PP microplates 96 well, Greiner Bio-One, Frickenhausen, Germany) in a total volume of 100 µL, containing 10 µg of membrane, 1 µM GDP, 0.05 % BSA, 20 nCi [^{35}S]GTPγS and the investigated ligands at various concentration (dissolved in water). During the incubation period of 90 min, at room temperature, the plates were shaken at 250 rpm. Afterwards, bound [^{35}S]GTPγS was separated from free [^{35}S]GTPγS by filtration through GF/C filters using a 96-well Brandel harvester (Brandel Inc., Unterföhring, Germany). Filter- bound radioactivity was either quantified by liquid scinitillation counting or the filters were dried overnight and MeltiLex solid scintillator was melted onto the filtermats. Scintillation counting was performed with the MicroBeta21450 PlateCounter (Perkin Elmer, Rodgau, Germany).

3.5.3.2 Competition binding experiments

[^{3}H]mepyramine, [^{3}H]tiotidine, [^{3}H]histamine and [^{3}H]*N*$^{\alpha}$-Methylhistamine were from Hartmann analytic (Braunschweig, Germany). *Sf9* membranes (general procedures for the generation of recombinant baculoviruses, culture of *Sf9* cells and membrane preparation have been described elsewhere[39]) were thawed and sedimented by centrifugation at 13.000 g and 4 °C for 10 min. The membranes were resuspended in cold (4 °C) binding buffer (BB: 12.5 mM $MgCl_2$, 1 mM EDTA and 75 mM Tris/HCl, pH 7.4) so that the final concentration was 2-6 µg of protein per 1 µL BB. Experiments were performed in 96-well plates (PP microplates 96 well, Greiner Bio-One, Frickenhausen, Germany) in a total volume of 100 µL containing 20-60 µg of membrane, 0.05 % BSA, the respective radioligand and the investigated ligands at various concentrations (dissolved in water). During the incubation period of 60 min at room temperature, the plates were shaken at 250 rpm. Afterwards, bound radioligand was separated from free radioligand by filtration through, PEI covered, GF/C filters using a 96-well Brandel harvester (Brandel Inc., Unterföhring, Germany). After two washing steps with binding buffer, filter pieces were punched and transferred into untapped 96-well sample plates 1450-401 (Perkin Elmer, Rodgau, Germany). Each well was supplemented with 200 µL of scintillation cocktail (Rotiscint Eco plus, Roth, Karlsruhe, Germany) and incubated in the dark for 12 h. Radioactivity was measured with a Micro Beta2 1450 scintillation counter (Perkin Elmer, Rodgau, Germany).

3.5.3.3 Studies on human monocytes

The present study was approved by the Ethics Committee of the Hannover Medical School. Monocytes were isolated from peripheral blood of healthy human volunteers using density gradient centrifugation and magnetic activated cell sorting. To study the H_2R mediated responses in human monocytes, increases in cAMP levels were analyzed *via* reversed

phase HPLC coupled to mass spectrometry (HPLC-MS/MS). For this purpose, 5 × 10^5 cells were treated with the ligands (1 nM – 100 µM) in the presence of 100 µM IBMX at 37 °C for 10 min. Inhibition of fMLP-induced production of ROS was investigated using the lucigenin chemiluminescence assay: 1 × 10^5 cells loaded with the chemiluminescence dye lucigenin were pre-incubated with the ligands (1 nM – 100 µM) at 37 °C for 5 min. After adding fMLP (1 µM), the chemiluminescence was recorded at 37 °C for 60 min. These methods have been described in detail in Werner et al.[27]

3.5.3.4 EBAO staining

Cytotoxicity of the compounds was assessed by ethidium bromide / acridine orange (EBAO) staining. Monocytes (2.5 × 10^5 cells/ml) were incubated with 100 µM of compounds **3.20** and **3.25** in RPMI-medium supplemented with 10 % (v/v) bovine calf serum, 100 U/ml penicillin, 100 µg/ml streptomycin, 2 mM L-glutamine and 1 % (v/v) NEA at 37 °C in a humidified atmosphere with 5 % (v/v) CO_2. After 2 h cells were stained with 50 µg/ml EBAO solution and cell viability was determined by fluorescence microscopy using a Zeiss Axiovert 200 M microscope (Carl Zeiss, Jena, Germany).

3.5.3.5 Stability in plasma

Mouse plasma was prepared as previously described.[40] The stock solutions of the compounds (10 mM) were prepared in water and were diluted 5:100 in mouse plasma. The samples were vortexed and incubated at 37 °C. At different periods of time an aliquot was taken and deproteinated with two parts of ice-cold acetonitrile. The samples were shaken for 24 h at 700 rpm. Afterwards, they were centrifuged for 5 min at 13.000 g. Finally, 60 µL of the supernatant were diluted 1:5 with 0.05 % aq. TFA and filtered (Phenex-NY 4 mm Syringe Filters 0.2 µm; Phenomenex; Aschaffenburg, Germany). Prior to HPLC analysis the samples were stored at -20 °C. HPLC analysis was performed as described before (cf. section **3.5.1**) (column: Eurospher-100). Gradient mode: MeCN/TFA (0.05%) (v/v) 0 min: 10:90, 30 min: 60/40, 31-41 min: 80:20; flow rate = 0.75 mL/min.

3.5.3.6 Plasma protein binding

3.5.3.6.1 Recovery after equillibrium dialysis

Dialysis was performed with DispoEquilbrium Dialyzer with a molecular weight cut off of 5000 Da (Harvard Apparatus, Hollliston, USA). Recoveries tests were determined as follows: The compounds were diluted in PBS (pH 7.4) to a final concentration of 200 µM. 70 µL of this solution were added to the sample chamber. The second chamber was filled with PBS. The samples were shaken at 500 rpm and incubated at 37 °C for 24 h. Afterwards, the amount of compound in both samples was determined by HPLC analysis. HPLC analysis was performed as described before (cf. section **3.5.1**) (column: Eurospher-100). Gradient mode: MeCN/TFA (0.05%) (v/v) 0 min: 10:90, 30 min: 60/40, 31-41 min: 80:20; flow rate = 0.75 mL/min.

3.5.3.6.2 Ultrafiltration

Ultrafiltration was performed with Nanosep® Centrifugal Devices (modified polyethersulfone membrane) from Pall GmbH (Dreieich, Germany) with a molecular weight cut off of 10000 Da. Prior to plasma protein binding studies, recovery studies were performed. Therefore, 250 µL of a 100 µM test solution in PBS were incubated in the centrifugal devices at 37 °C for one hour. After centrifugation (10 min, 16.000 g), 40 µL of this solution were analyzed by analytical HPLC. Moreover, 40 µL of the non-incubated solution were analyzed by HPLC, and the two peak areas were compared. Plasma protein binding was performed with a solution of 600 µM BSA (analytical grade, Sigma Aldrich) in PBS. The test compounds were diluted in the BSA solution to a final concentration of 100 µM. This mixture was incubated in the centrifugal devices at 37 °C for one hour. Thereafter, it was centrifuged (10 min, 16.000 g) and 40 µL of the filtrate were analyzed by analytical HPLC. HPLC analysis was performed as described before (cf. section **3.5.1**) (column: Eurospher-100). Gradient mode: MeCN/TFA (0.05%) (v/v) 0 min: 10:90, 15 min: 35/65; flow rate = 0.75 mL/min.

3.5.3.7 Crystal violet based chemosensitivity assay

The assay was performed as previously described.[41] Accordingly, HEK293T cells in DMEM were seeded into 96 well plates (Greiner, Frickenhausen, Germany) at a density of 15 cells per microscopic field (magnification: 320-fold). The cells were allowed to attach overnight, and the test compounds were added at the desired concentrations. As a control, cells were treated with medium containing only the respective solvent. After various incubation periods the cells were fixed with 1 % glutardialdehyde solution and stored at 4 °C. At the end of the assay, cells were stained with crystal violet. Prior to measurement, excess dye was removed by washing the cells with water, and cell-bound dye was extracted with 70 % EtOH. Absorbance was measured at 580 nm using a GENios Pro microplate reader (Tecan, Salzburg, Austria). Drug effects were expressed as corrected T/C- values, according to following equation:

$$\frac{T}{C}\ corr.(\%) = \frac{T - Co}{C - Co} \times 100$$

Where T = mean absorbance of treated cells, C = mean absorbance of controls and C_0 = mean absorbance of the cells when the test compounds were added (t = 0).

When the absorbance was less than that at t = 0, the cytocidal effect was calculated according to following equation:

$$cytocidal\ effect\ (\%) = \frac{Co - T}{Co} \times 100$$

3.6 References

1. Ghorai, P.; Kraus, A.; Keller, M.; Götte, C.; Igel, P.; Schneider, E.; Schnell, D.; Bernhardt, G.; Dove, S.; Zabel, M.; Seifert, R.; Buschauer, A. Acylguanidines as bioisosteres of guanidines: N(G)-acylated imidazolylpropylguanidines, a new class of histamine H2 receptor agonists. *J. Med. Chem.* **2008**, 51, 7193-7204.
2. Kraus, A.; Ghorai, P.; Birnkammer, T.; Schnell, D.; Elz, S.; Seifert, R.; Dove, S.; Bernhardt, G.; Buschauer, A. N(G)-acylated aminothiazolylpropylguanidines as potent and selective histamine H(2) receptor agonists. *ChemMedChem* **2009**, 4, 232-240.
3. Birnkammer, T.; Spickenreither, A.; Brunskole, I.; Lopuch, M.; Kagermeier, N.; Bernhardt, G.; Dove, S.; Seifert, R.; Elz, S.; Buschauer, A. The bivalent ligand approach leads to highly potent and selective acylguanidine-type histamine H(2) receptor agonists. *J. Med. Chem.* **2012**, 55, 1147-1160.
4. Ghorai, P.; Kraus, A.; Birnkammer, T.; Geyer, R.; Bernhardt, G.; Dove, S.; Seifert, R.; Elz, S.; Buschauer, A. Chiral NG-acylated hetarylpropylguanidine-type histamine H2 receptor agonists do not show significant stereoselectivity. *Bioorg. Med. Chem. Lett.* **2010**, 20, 3173-3176.
5. Baumeister, P.; Erdmann, D.; Biselli, S.; Kagermeier, N.; Elz, S.; Bernhardt, G.; Buschauer, A. [3H]UR-DE257: Development of a tritium-labeled squaramide-type selective histamine H2 receptor antagonist. *ChemMedChem* **2015**, 10, 83-93.
6. Portoghese, P. S. From models to molecules: Opioid receptor dimers, bivalent ligands, and selective opioid receptor probes. *J. Med. Chem.* **2001**, 44, 2259-2269.
7. Pirrung, M. C.; Pei, T. Synthesis of (+/-)-Homohistidine. *J. Org. Chem.* **2000**, 65 (7), 2229-2230.
8. Mitsunobu, O.; Yamada, M.; Mukaiyama, T. Preparation of esters of phosphoric acid by the reaction of trivalent phosphorus compounds with diethyl azodicarboxylate in the presence of alcohols. *Bull. Chem. Soc. Jpn.* **1967**, 40, 935-939.
9. Kraus, A. Highly Potent, Selective Acylguanidine-Type Histamine H2 Receptor Agonists: Synthesis and Structure-Activity Relationships. *Doctoral Thesis, University of Regensburg* **2007**.
10. Gers, T.; Kunce, D.; Markowski, P.; Izdebski, J. Reagents for efficient conversion of amines to protected guanidines. *Synthesis* **2004**, 37-42.
11. Keller, M.; Erdmann, D.; Pop, N.; Pluym, N.; Teng, S.; Bernhardt, G.; Buschauer, A. Red-fluorescent argininamide-type NPY Y1 receptor antagonists as pharmacological tools. *Bioorg. Med. Chem.* **2011**, 19, 2859-2878.
12. Kim, K. S.; Qian, L. G. Improved method for the preparation of guanidines. *Tetrahedron Lett.* **1993**, 34, 7677-7680.
13. Garcia-Delgado, N.; Bertrand, S.; Nguyen, K. T.; van Deursen, R.; Bertrand, D.; Reymond, J. L. Exploring alpha7-Nicotinic Receptor Ligand Diversity by Scaffold Enumeration from the Chemical Universe Database GDB. *ACS Med. Chem. Lett.* **2010**, 1, 422-426.
14. Wittig, G.; Schöllkopf, U. Über Triphenyl-phosphin-methylene als olefinbildende Reagenzien. *Chem. Ber.* **1954**, 87, 1318-1330.
15. Craig, D. B.; Wetzl, B. K.; Duerkop, A.; Wolfbeis, O. S. Determination of picomolar concentrations of proteins using novel amino reactive chameleon labels and capillary electrophoresis laser-induced fluorescence detection. *Electrophoresis* **2005**, 26, 2208-2213.
16. Wetzl, B. K.; Yarmoluk, S. M.; Craig, D. B.; Wolfbeis, O. S. Chameleon labels for staining and quantifying proteins. *Angew. Chem. Int. Ed. Engl.* **2004**, 43, 5400-5402.
17. Caro, B.; Le Guen-Robin, F.; Salmain, M.; Jaouen, G. 4-benchrotrenyl pyrylium salts as protein organometallic labelling reagents. *Tetrahedron* **2000**, 56, 257-263.
18. Brennauer, A.; Keller, M.; Freund, M.; Bernhardt, G.; Buschauer, A. Decomposition of 1-(x-aminoalkanoyl)guanidines under alkaline conditions. *Tetrahedron Lett.* **2007**, 48, 6996-6999.

19. Xie, S. X.; Ghorai, P.; Ye, Q. Z.; Buschauer, A.; Seifert, R. Probing ligand-specific histamine H1- and H2-receptor conformations with NG-acylated Imidazolylpropylguanidines. *J. Pharmacol. Exp. Ther.* **2006**, 317, 139-146.
20. Kelley, M. T.; Bürckstümmer, T.; Wenzel-Seifert, K.; Dove, S.; Buschauer, A.; Seifert, R. Distinct interaction of human and guinea pig histamine H2-receptor with guanidine-type agonists. *Mol. Pharmacol.* **2001**, 60, 1210-1225.
21. Preuss, H.; Ghorai, P.; Kraus, A.; Dove, S.; Buschauer, A.; Seifert, R. Point mutations in the second extracellular loop of the histamine H2 receptor do not affect the species-selective activity of guanidine-type agonists. *Naunyn Schmiedebergs Arch. Pharmacol.* **2007**, 376, 253-264.
22. Pertz, H. H.; Gornemann, T.; Schurad, B.; Seifert, R.; Strasser, A. Striking differences of action of lisuride stereoisomers at histamine H-1 receptors. *Naunyn-Schmiedeberg's Arch. Pharmacol.* **2006**, 374, 215-222.
23. Schnell, D.; Strasser, A.; Seifert, R. Comparison of the pharmacological properties of human and rat histamine H(3)-receptors. *Biochem. Pharmacol.* **2010**, 80, 1437-1449.
24. Brunskole, I.; Strasser, A.; Seifert, R.; Buschauer, A. Role of the second and third extracellular loops of the histamine H(4) receptor in receptor activation. *Naunyn Schmiedebergs Arch. Pharmacol.* **2011**, 384, 301-317.
25. Schneider, E.; Mayer, M.; Ziemek, R.; Li, L.; Hutzler, C.; Bernhardt, G.; Buschauer, A. A simple and powerful flow cytometric method for the simultaneous determination of multiple parameters at G-protein-coupled receptor subtypes. *ChemBioChem* **2006**, 7, 1400-1409.
26. Gimpl, G.; Klein, U.; Reilander, H.; Fahrenholz, F. Expression of the human oxytocin receptor in baculovirus-infected insect cells: high-affinity binding is induced by a cholesterol-cyclodextrin complex. *Biochemistry* **1995**, 34, 13794-13801.
27. Werner, K.; Neumann, D.; Seifert, R. Analysis of the histamine H2-receptor in human monocytes. *Biochem. Pharmacol.* **2014**, 92, 369-379.
28. Birnkammer, T. Highly potent and selective acylguanidinetype histamine H2 receptor agonists: synthesis and structure-activity relationships of mono-and bivalent ligands. *Doctoral Thesis, University of Regensburg* **2011**.
29. Ertel, M. Ambivalence of Drug Metabolism: Exploration of Cilazapril and Candesartan Prodrugs for Transdermal Delivery and Search for Toxic Reactive Intermediates of N^G-Acylated Hetarylpropylguanidines. *Doctoral Thesis, University of Regensburg* **2011**.
30. Schunack, W. Äther und Ester des 4-(2-Hydroxyaethyl)-imidazols und Ester der 4-Imidazolpropionsäure 4. Mitt. über Struktur-Wirkungs-Beziehungen bei Histaminanaloga. *Arch.Pharm. (Weinheim)* **1974**, 307 (7), 517-523.
31. Stark, H.; Purand, K.; Huls, A.; Ligneau, X.; Garbarg, M.; Schwartz, J. C.; Schunack, W. [125I]iodoproxyfan and related compounds: a reversible radioligand and novel classes of antagonists with high affinity and selectivity for the histamine H3 receptor. *J. Med. Chem.* **1996**, 39, 1220-1226.
32. Igel, P. Synthesis and structure-activity relationships of N^G-acylated arylalkylguanidines and related compounds as histamine receptor ligands: Searching for selective H4R agonists. *Doctoral Thesis, University of Regensburg* **2008**.
33. Bertinaria, M.; Di Stilo, A.; Tosco, P.; Sorba, G.; Poli, E.; Pozzoli, C.; Coruzzi, G.; Fruttero, R.; Gasco, A. 3-(1H-imidazol-4-yl)propyl guanidines containing furoxan moieties: A new class of H-3-antagonists endowed with NO-donor properties. *Biorg. Med. Chem.* **2003**, 11, 1197-1205.
34. Wolin, R.; Connolly, M.; Afonso, A.; Hey, J. A.; She, H.; Rivelli, M. A.; Willams, S. M.; West, R. E., Jr. Novel H3 receptor antagonists. Sulfonamide homologs of histamine. *Bioorg. Med. Chem. Lett.* **1998**, 8, 2157-2162.
35. Eriks, J. C.; van der Goot, H.; Sterk, G. J.; Timmerman, H. Histamine H2-receptor agonists. Synthesis, in vitro pharmacology, and qualitative structure-activity relationships of substituted 4- and 5-(2-aminoethyl)thiazoles. *J. Med. Chem.* **1992**, 35, 3239-3246.

36. Brennauer, A. Acylguanidines as bioisosteric groups in argininamide-type neuropeptide Y $Y_1$and Y_2 receptor antagonists: synthesis, stability and pharmacological activity. *Doctoral Thesis, University of Regensburg* **2006**.
37. Bernthsen, A.; Klinger, H. Über Sulfinverbindungen des Thioharnstoffs. *Chem. Ber.* **1878**, 65, 1192.
38. Pearson, W. H.; Lin, K. C. The intramolecular cycloaddition of azides with omega-chloroalkenes - a facile rout to (-) swainsonine and other indolizidine alkaloids. *Tetrahedron Lett.* **1990**, 31, 7571-7574.
39. Pop, N.; Igel, P.; Brennauer, A.; Cabrele, C.; Bernhardt, G.; Seifert, R.; Buschauer, A. Functional reconstitution of human neuropeptide Y (NPY) Y-2 and Y-4 receptors in Sf9 insect cells. *J. Recept. Signal Transduct.* **2011**, 31, 271-285.
40. Bauer, S.; Ochoa-Puentes, C.; Sun, Q.; Bause, M.; Bernhardt, G.; Konig, B.; Buschauer, A. Quinoline carboxamide-type ABCG2 modulators: indole and quinoline moieties as anilide replacements. *ChemMedChem* **2013**, 8, 1773-1778.
41. Bernhardt, G.; Reile, H.; Birnböck, H.; Spruss, T.; Schönenberger, H. Standardized kinetic microassay to quantify differential chemosensitivity on the basis of proliferative activity. *J. Cancer Res. Clin. Oncol.* **1992**, 118, 35-43.

Chapter 4

Unraveling signaling pathways of the human histamine receptors H_1R and H_2R in HEK293T CRE Luc cells

4.1 Introduction

The histamine H_1R is a GPCR that interacts with $G\alpha_q$ proteins to activate PLC. The activation of PLC results in the formation of IP_3 and subsequent mobilization of intracellular Ca^{2+}.[1] It is worth mentioning that in some tissues histamine is capable of stimulating receptor independent inositol phospholipid hydrolysis.[2-5] The H_2R canonically couples to the $G\alpha_s$ protein, resulting in an increase in intracellular cAMP due to the activation of AC.[1] In addition to activation of PLC and AC, respectively, both receptors have been reported to trigger differential signaling pathways.[6-8]

In several cells, histamine induces an increase in intracellular Ca^{2+} mediated by the H_2R.[6] It was shown, for example in HL-60 promeylocytes that the histamine mediated Ca^{2+} signal was predominantly induced by the H_2R.[8] Another study on transfected rat hepatoma cells reported that the H_2R is linked to both, the adenylate cyclase and the $[Ca^{2+}]_i$ signaling system.[9]

In addition to the inositol phospholipid pathway, the H_1R is known to activate other signaling pathways. In this context it was shown that stimulation of the H_1R in CHO and HEK293 cells led to an increase in cAMP.[7,10,11] Furthermore, Fitzsimons et al. demonstrated that an activation of the H_1R increased cAMP levels in benign papilloma in mice.[12]

In order to investigate differences in H_1R- and H_2R signaling, HEK293T cells were genetically engineered, stably expressing the firefly luciferase under the control of a cAMP response element (CRE) and the hH_1R or the hH_2R, respectively. The transfectants were investigated in functional assays that allowed for the identification of the underlying pathways.

Alternative signaling pathways resulting in CRE binding protein (CREB) phosphorylation are shown in **Fig. 4.1**.

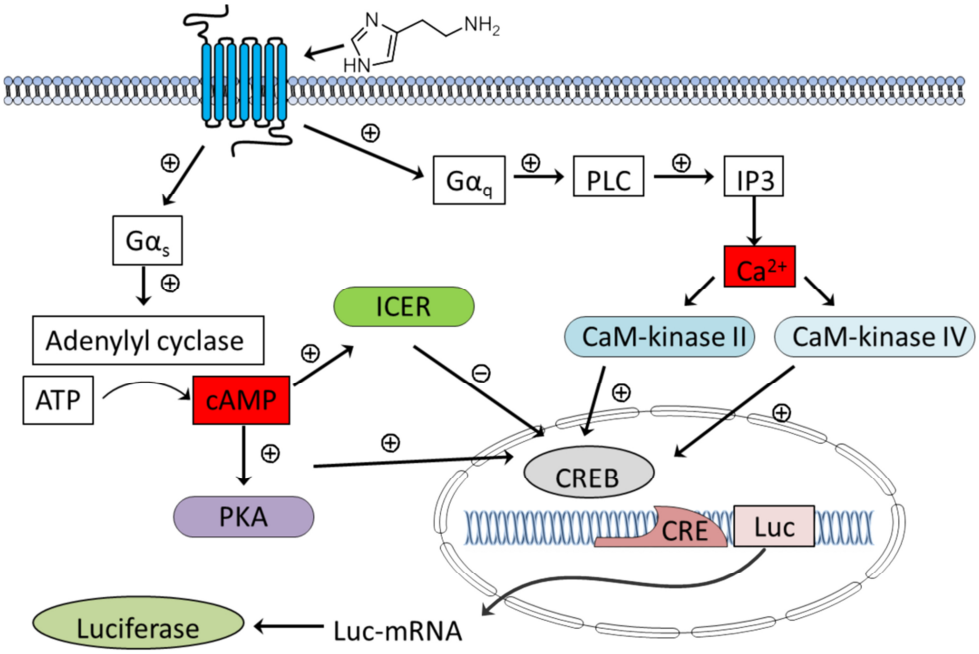

Figure 4.1. Alternative signaling pathways resulting in the phosphorylation of the cAMP response element binding protein (CREB).

4.2 Materials and Methods

All chemicals were from commercial suppliers. The $G\alpha_q$ inhibitor UBO-QIC was from the Institute of Pharmaceutical Biology in Bonn (Germany), and the stock solution (10 mM) was prepared in DMSO. Pertussis toxin (PTX) was from List. Biologicals (Campbell, USA) (stock solution: 0.5 µg/µL in water), Rp-cAMP-S, Rp-8-Br-cAMP-S (stock solutions: 10 mM in water) and gallein (stock solution: 10 mM in DMSO) were from Santa Cruz Biotechnology (Heidelberg, Germany) and forskolin (stock solution: 10 mM in DMSO) was from Sigma Aldrich (Taufkirchen, Germany). The Lance®cAMP assay kit was from Perkin Elmer (Boston, USA).

4.2.1 Cell culture

HEK293T CRE Luc cells stably expressing either the hH_1R or the hH_2R were cultured in Dulbecco`s Modified Eagle Medium (DMEM) (Sigma-Aldrich) containing L-glutamine (Sigma-Aldrich), 4500 mg/L glucose, 3.7 g/L $NaHCO_3$ (Merck, Darmstadt, Germany), 110 mg/L sodium pyruvate (Serva, Heidelberg, Germany), 10 % fetal calf serum (FCS) (Biochrom, Berlin, Germany) and the selection antibiotics G418 (600 µg/mL) (Biochrom) and hygromycin b (250 µg/mL) (MoBiTec GmbH, Göttingen, Germany). DMEM for cells expressing mtAeq contained additional zeocin (400 µg/mL) (InvivoGen SAS, Toulouse, France). Cells were incubated in culture flasks from Sarstedt (Nümbrecht, Germany) at 37 °C in water saturated atmosphere containing 5 % CO_2. For passaging, the cells were treated with 0.05 % trypsin / 0.02 % EDTA (PAA, Pasching, Austria) in phosphate buffered saline (KCl 2.7 mM; KH_2PO_4 1.5 mM; NaCl 137 mM; Na_2HPO_4 5.6 mM; NaH_2PO_4 1.1 mM in Millipore water, pH 7.4, all chemicals were from Merck). After detachment, the cells were resuspended in 5 mL DMEM, the suspension was centrifuged (10 min, 300 g) and the cells were diluted with fresh medium twice a week.

4.2.2 Stable transfection of HEK293T CRE Luc cells with the pcDNA3.1(+)-hH1R vector

The pcDNA3.1(+)-hH_1R vector was from Missouri S&T cDNA Resource Center (Rolla, USA). The parental HEK293T CRE Luc cell line was kindly provided by Dr. Uwe Nordemann.[13] One day before transfection, the cells were detached with 5 mL trypsin and 5 mL DMEM supplemented with 10 % FCS. The suspension was centrifuged (300 g, 10 min) and resuspended in medium. Afterwards, 2 mL of the cell suspension were seeded into a 6-well flat bottom plate (Sarstedt, Nümbrecht, Germany) at a density of 500,000 per mL. The next day, prior to transfection, the plasmid was linearized with *Pvu*I (New England Biolabs, Frankfurt am Main, Germany) for 2 h at 37 °C. The linearized vector was purified with a PCR purification KIT (Quiagen, Leipzig, Germany) according to the manufacturer's instructions. An amount of 2 µg of DNA was diluted with serum-free DMEM, and 6 µL of the transfection kit FuGene HD (Roche Diagnostics GmbH, Mannheim, Germany) were added. After vortexing, the mixture was incubated for 15 min before it was added to the cells. The medium was removed after 32 h, and the cells were pooled into a 25-cm^2 culture flask with DMEM containing 10 % FCS and hygromycin b. After another 24 h, the medium was replaced by fresh medium, supplemented with G418.

4.2.3 Stable transfection of HEK293T CRE Luc cells with the pcDNA3.1(+)-hH_2R vector

The transfection was performed according to section **4.2.2**. The pcDNA3.1(+)-hH_2R vector was from Missouri S&T cDNA Resource Center (Rolla, USA).

4.2.4 Stable transfection of HEK293T CRE Luc hH_1R cells with the pcDNA3.1(-)mtAEQ plasmid

The transfection was performed according to section **4.2.2** with minor modifications. The medium was removed 24 h after transfection, and the cells were pooled in a 75-cm^2 culture flask with DMEM + 10 % FCS. Selection was started the next day by adding medium containing hygromycin, G418 and zeocin. The pcDNA3.1(-)mtAEQ vector was kindly provided by Dr. Ralf Ziemek.[14]

4.2.5 Stable transfection of HEK293T CRE Luc hH_2R cells with the pcDNA3.1(-)mtAEQ vector

The transfection was performed according to section **4.2.2**.

4.2.6 Stable transfection of HEK293T CRE Luc-SF-hH_4R-His_6 with pGL4.29[luc2P/CRE/Hygro] plasmid

The cells were kindly provided by Dr. Uwe Nordemann.[13]

4.2.7 Whole cell radioligand binding assay

The whole cell radioligand binding assay was performed as described previously[15] with minor modifications. Cells were grown in a 75-cm^2 flask to a confluency of around 80 %. They were detached with 5 mL of trypsin and resuspended in 5 mL of Leibovitz´s L15 medium (Invitrogen, Darmstadt, Germany). After centrifugation, the cells were resuspended in Leibovitz´s L15 at a density between 1.0 mio – 2.25 mio per mL. In case of the H_1R, unspecific binding was detected in the presence of 3 µM azelastine. As radioligand [^{3}H]mepyramine (specific activity: 20 Ci $mmol^{-1}$) (Hartmann Analytics, Braunschweig, Germany) was used. For saturation binding experiments performed with HEK CRE Luc hH_2R cells, unspecific binding was detected in the prescence of 10 µM famotidine and [^{3}H]UR-DE257 (specific activity: 63 Ci $mmol^{-1}$)[16] was used as radioligand. For economic reasons, [^{3}H]UR-DE257 was diluted with unlabeled UR-DE257. Samples were completed by adding 80 µL of the cell suspension. The plates were shaken at 250 rpm at room temperature for 60 min. After the incubation period, unbound radioligand was separated by filtration through PEI coated GF/C filters using a 96-well Brandel harvester (Brandel Inc., Unterföhring, Germany). After two washing steps with cold binding buffer, filter pieces were punched out and transferred into 96-well sample plates 1450-401 (Perkin Elmer, Rodgau, Germany). Each well was supplemented with 200 µL of scintillation cocktail (Rotiscint Eco plus, Roth, Karlsruhe, Germany). The plate was sealed with permanent plateseal (Perkin Elmer, Rodgau, Germany) and incubated in the dark for 12 h. Radioactivity was measured with a

Micro Beta2 1450 scintillation counter (Perkin Elmer, Rodgau, Germany). Data were analyzed with GraphPadPrism 5, and specific binding was calculated by subtraction of non-specific binding from the total binding.

4.2.8 Luciferase reporter gene assay

The assay was performed as previously described with minor modifications.[13] One day prior to the experiments, the cells were adjusted to a density of approximately 800,000 per mL in DMEM without phenol red (Sigma Aldrich) supplemented with 5 % FCS. 160 µL of the cell suspension were seeded into flat bottom 96-well plates (Greiner, Frickenhausen, Germany) per well. In case of pertussis toxin (PTX), the cell suspension contained 0.5 µg/mL of PTX. The cells were allowed to attach overnight. After addition of 20 µL of the respective inhibitor, the cells were pre-incubated for 2 hours (UBO-QIC and gallein) or one hour (Rp-cAMP-S and Rp-8-Br-cAMP-S), respectively, at 37 °C and in water saturated atmosphere containing 5 % CO_2. Afterwards, 20 µL of a 10 fold concentrated histamine solution were added, and the cells were incubated for another 5 h. All wells contained the same amount of DMSO or water.

The medium was discarded, and 80 µL of lysis buffer (25 mM Tricine (Sigma Aldrich); Glycerol 10 % (v/v) (Merck); EGTA, 2 mM (Sigma Aldrich); 1 % (v/v) Triton^{TM} X-100 (Serva); $MgSO_4 \times 7\ H_2O$, 5 mM (Merck); DTT, 1 mM (Sigma), the pH was adjusted to 7.8 with HCl) were added to each well. The plates were shaken at 600 rpm for 15 min. Afterwards, 40 µL of the lysate were transferred into white 96-well plates (Greiner, Frickenhausen, Germany). Luminescence was measured with a GENios Pro microplate reader (Tecan, Salzburg, Austria). Light emission was induced by injecting 80 µL of the assay buffer (25 mM Gly-Gly, (Sigma Aldrich); $MgSO_4 \times 7\ H_2O$, 15 mM; KH_2PO_4, 15 mM (Merck); EGTA, 4 mM; ATP disodium salt, 2 mM (Sigma Aldrich); DTT, 2 mM; D-luciferin potassium salt, 0.2 mg/mL (Synchem, Felsberg, Germany); pH was adjusted to 7.8 with HCl). Luminescence [RLU] was measured for 10 s. The data were analyzed with GraphPadPrism 5 and best fitted to 3-parameters sigmoidal concentration-response curves. pK_b values were calculated according to the Cheng-Prusoff equation.[17]

4.2.9 Fura-2 Ca^{2+} assay

The assay was performed as described previously.[18] After detachment of the cells with trypsin/EDTA and DMEM, the cells were centrifuged at 300 g for 10 min. The medium was discarded, and the cells were counted. To three volumes of the cell suspension, prepared in loading buffer (HEPES (Serva), 25 mM; NaCl, 120 mM; KCl, 5 mM; $MgCl_2$, 2 mM; $CaCl_2$,1.5 mM; glucose 10 mM; pH was adjusted to 7.4), one volume of loading dispersion (1 mLof loading dispersion contained: 2 % BSA (Serva); 5 µL of Pluronic (Sigma); 4 µL of Fura-2 (VWR, Ismaning, Germany) was added, so that the final cell density was 1.0 mio cells per mL. The suspension was incubated in the dark for 30 min. Thereafter, the suspension was centrifuged, the cells were resuspended in loading buffer and allowed to stand in the dark for another 30 min. The cells were washed twice with loading buffer and adjusted to a final density of 1.0 mio cells per mL. The assay was performed either in acrylic cuvettes (VWR) using an LS50 B spectrofluorimeter (Perkin Elmer)[18] or in transparent 96-well microplates (Greiner) using a GENios Pro microplate reader.[15] Assays in the antagonist mode were always performed in cuvettes, and the cells were preincubated with the respective antagonist for 15 min. The data were analyzed with GraphPadPrism 5 and were best fitted to 3-

parameter sigmoidal concentration-response curves. pK_b values were calculated according to the Cheng-Prusoff equation.[17]

4.2.10 Aequorin assay

The assay was performed as described previously.[14] Cells were detached with trypsin/EDTA and DMEM without phenol red and centrifuged at 300 g for 10 min. Thereafter, they were adjusted to a density of 10 mio per mL in DMEM without phenol red, and coelenterazin (Biotrend, Köln, Germany) was added, so that the final concentration was 2 µM. The suspension was incubated in the dark for 2 h. The cell suspension was diluted 1:20 with loading buffer (cf. **4.2.9**), and the suspension was incubated in the dark under gentle stirring for additional 3 h. In the agonist mode, 18 µL (10-fold concentrated) of the test compound (diluted in loading buffer) were added in a white 96-well plate (Greiner), and luminescence was measured for 43 s with a GENios Pro microplate reader by injecting 162 µL of the cell suspension. Subsequently, 20 µL of a 1 % Triton 100-X solution was injected, and light emission was recorded for additional 22 s. In the antagonist mode, 2 µL (100-fold concentrated) of the respective antagonist were incubated with 178 µL of the cell suspension for 15 min. Luminescence was measured by injecting 20 µL of agonist solution (10-fold concentrated) for 43 s and subsequent addition of 20 µL of a 1 % Triton X-100 for additional 22 s. The fractional luminescence was calculated by dividing the area of the first peak (injection of the cell suspension, respectively agonist solution) by the sum of the total area of peak 1 and peak 2 (Triton X-100 injection) using Sigma Plot 11.0 software. The data were analyzed with GraphPadPrism 5 and were best fitted to 3-parameter sigmoidal concentration-response curves. pK_b values were calculated according to the Cheng-Prusoff equation.[17]

4.2.11 cAMP assay

The Lance cAMP assay was performed according to the manufacturer´s (Perkin Elmer, Rodgau, Germany) instruction with minor modifications. The kit contains a Europium complex and a cAMP-specific antibody labeled with an Alexa dye. Furthermore, the kit includes biotinylated cAMP and cAMP standards. The Europium-labeled cAMP tracer complex is formed by the tight interaction between biotin-cAMP and Eu-streptavidin. In this arrangement Eu-streptavidin can be excited at wavelengths of 320 or 340 nm and the energy is transferred to the Alexa dye. Time-resolved fluorescence energy transfer (TR-FRET) can be measured at a wavelength of 665 nm. In the presence of cAMP the FRET emission at 665 nm will decrease in a concentration dependent manner.

The cells were detached with trypsin and DMEM + 5 % FCS and were centrifuged (300 g, 10 min). The cells were washed with PBS + 0.1 % BSA and centrifuged again. The cells were resuspended in PBS + 0.1 % BSA + 0.05 mmol/l IBMX (Sigma Aldrich) and adjusted to the required cell number (cf. **4.3.1.5.1.2**). The antibody was added to the cell suspension (1:100), 5 µL of the antibody/cell mixture were dispensed into white 96-well plates (Greiner), and 5 µL of the test compounds diluted in PBS + 0.1 % BSA were added. Prior to incubation at room temperature in the dark for 1 h, the plate was centrifuged at 200 g for 1 min. After 45 min, the detection mix was prepared (cf. **table 4.1**) and incubated for 15 min. Subsequently, the samples were completed by adding 5 µL of detection buffer and the plate was incubated in the dark for one additional hour.

Table 4.1. Preparation of the detection mix

solution 1	1 µL of Eu-W8044 labeled streptavidin (Eu-SA) to 85 µL of cAMP detection buffer
solution 2	1 µL of biotin-cAMP to 4 µL of detection buffer
solution 3	5 µL of solution **1** to 615 µL of detection buffer (vortex)
detection mix	solution **3** to solution **2**

TR-FRET was measured in a GENios Pro microplate reader (instrument settings cf. **4.3.1.5.1.1**).

4.3 Results and Discussion

4.3.1 Investigation of HEK293T CRE Luc cells expressing the hH_1R

4.3.1.1 Saturation binding assay using HEK293T CRE Luc hH_1R cells

Receptor expression was confirmed by saturation binding assays using whole cells. The quantitative analysis of the saturation binding resulted in around 500,000 receptors per cell for the HEK293T hH_1R (**Fig. 4.2A**). The obtained K_d value of 7.8 ± 2.8 nM was in the same range as data determined on *Sf*9 membranes.[19] The corresponding Scatchard plot was linear, indicating that the radioligand binds to a single binding site (**Fig 4.2B**).

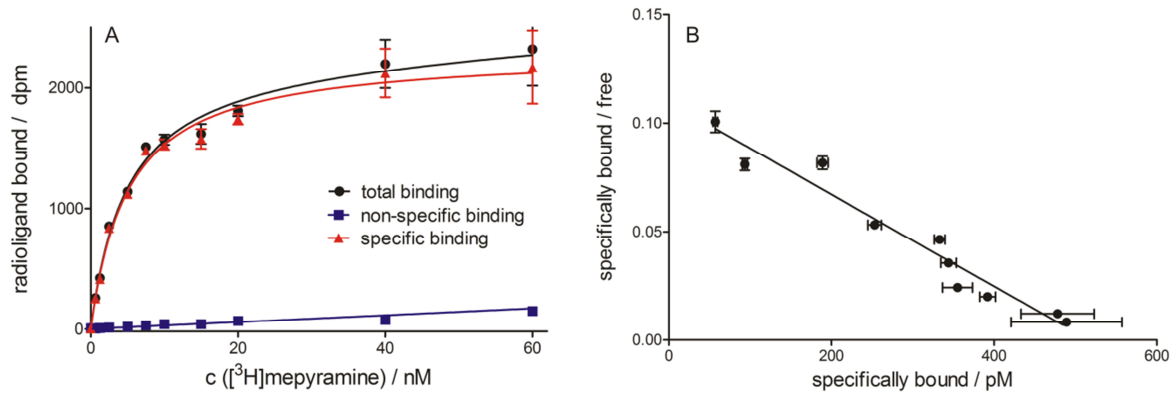

Figure 4.2. (**A**) Representative saturation binding experiment on HEK293T CRE Luc hH_1R cells, performed in triplicate. Non-specific binding of [^{3}H]mepyramine was determined in the presence of 3 µM azelastine. (**B**) The corresponding Scatchard plot of the saturation binding experiment was best fitted by linear regression (r^2= 0.95).

4.3.1.2 Luciferase reporter gene assay using HEK293T CRE Luc hH_1R cells

Reporter gene assays are available for $G\alpha_{q/11}$, $G\alpha_{i/o}$ and $G\alpha_s$ coupled receptors. Upon stimulation of GPCRs, the Gα subunit dissociates from the Gβγ dimer and both of them influence second messengers. These second messengers often regulate gene transcription.[20]

To discriminate between different signaling pathways, HEK293T cells were stably transfected with a CRE-linked firefly luciferase and the hH_1R or hH_2R (cf. section **4.3.2.2**), respectively.

It is well known that an activation of the cAMP pathway leads to the stimulation of gene expression due to the phosphorylation of CREB by PKA.[21,22] However, the activation of CREB can also be induced in a cAMP independent manner by an increase in the intracellular Ca^{2+} concentration, particularly *via* Ca^{2+}-calmodulin-dependent kinase (CAM kinase) IV, and to a lesser extent, by CAM kinases I and II.[23-25] In fact, the activation of the hH_1R in HEK293T CRE Luc cells by histamine induced an increase in the expression of luciferase (**Fig. 4.3A**). The pEC_{50} value was 6.87 ± 0.06, which is in good agreement with reported data from different assays.[26] The response to histamine was inhibited by the H_1R antagonist azelastine (**Fig. 4.3B**). The pK_b value of azelastine was 8.34 ± 0.08 and in accordance with data from other functional assays,[27] confirming that the transcription of the luciferase is mediated by the H_1R (cf. section **5.3.4**/**5.3.5**).

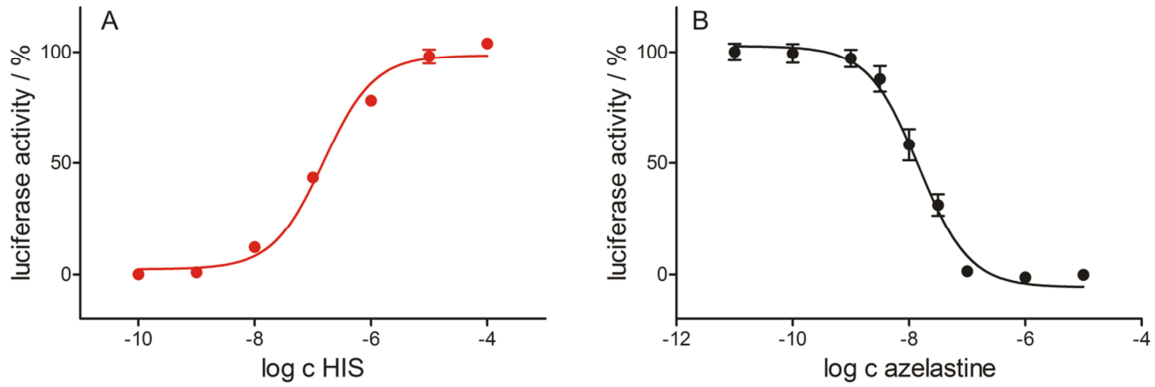

Figure 4.3. Luciferase activity in HEK293T CRE Luc hH_1R cells induced by histamine (HIS) (**A**) and inhibition of the HIS signal by azelastine (**B**). The response was normalized to the maximal effect induced by HIS**.** Data are means ± SEM of 3-4 independent experiments, each performed in triplicate.

4.3.1.2.1 Effect of $G\alpha_q$ inhibition on the H_1R dependent luciferase activity

To verify the involvement of $G\alpha_q$, the selective $G\alpha_q$ inhibitor UBO-QIC, a cyclic depsipeptide from Ardisia crenata sims,[28] was investigated (**Fig 4.4**). UBO-QIC is structurally closely related to YM254890.[28] Presumably, these compounds inhibit the GDP-GTP exchange in $G\alpha_q$.[29]

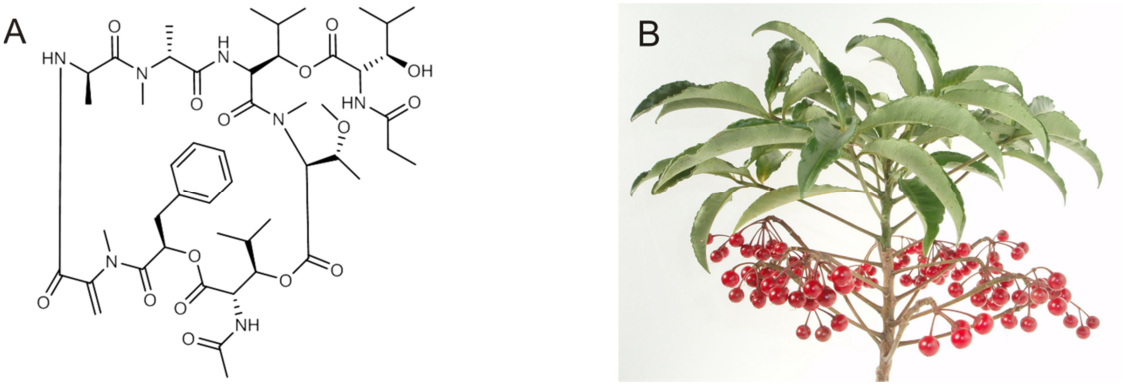

Figure 4.4. (**A**) Chemical structure of the $G\alpha_q$ inhibitor UBO-QIC from *Ardisia crenata* Sims (**B**) (adopted from Wikipedia).

In the presence of 1 µM UBO-QIC the concentration-response curve of histamine was rightward shifted and the maximal response was reduced by approximately 50 % (**Fig. 4.5**). The depression of the maximum effect of histamine (100 µM) was the same (50 %) in the presence of 10 µM UBO-QIC (data not shown), indicating that a further reduction of luciferase activity cannot be achieved by UBO-QIC at concentrations >1 µM. These results suggest that $G\alpha_q$-mediated activation of Ca^{2+}-calmodulin-dependent kinases is not the only pathway triggered by H_1R activation.

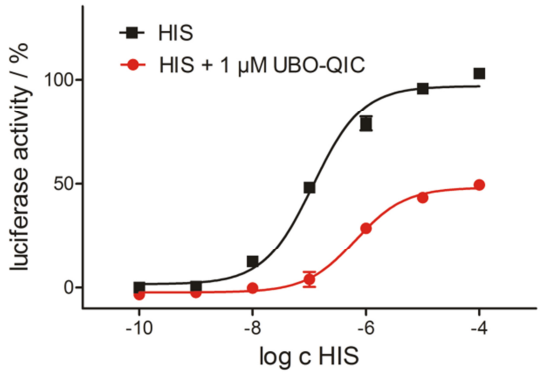

Figure 4.5. Luciferase activity in HEK293T CRE Luc hH_1R cells in the absence and presence of the $G\alpha_q$ inhibitor UBO-QIC. The response was normalized to the maximal effect induced by histamine (HIS). Data are means ± SEM of 3 independent experiments, each performed in triplicate.

4.3.1.2.2 Effect of pertussis toxin on the H_1R dependent luciferase activity

Besides the inhibition of the ACs, depending on the particular receptor and the cell type, activation of the $G_{i/o}$ family can result in an increase or decrease in the intracellular concentration of Ca^{2+},[30] presumably mediated by the βγ subunit. In case of the H_4R, it was shown that the increase in intracellular Ca^{2+} was induced *via* the activation of PLC.[31] By contrast, the activation of the H_3R leads to a decrease in intracellular Ca^{2+}, presumably *via* the inhibition of P/Q-, N-type Ca^{2+} channels.[32,33]

As the inhibition of the H_1R mediated luciferase signal by UBO-QIC was incomplete, the involvement of the G_i protein was studied with pertussis toxin (PTX). $G_{i\alpha1}$, $G_{i\alpha2}$ and $G_{i\alpha3}$ are PTX-sensitive G-proteins, whereas $G_{Z\alpha}$ is insensitive to pertussis toxin.[34] The A-protomer of the toxin ADP-ribosylates the $G\alpha_i$ subunit resulting in uncoupling of the receptor.[35,36]

Surprisingly, in HEK293T CRE Luc hH_1R cells, the maximum luciferase activity upon stimulation by histamine was increased in the presence of PTX (**Fig 4.6**).

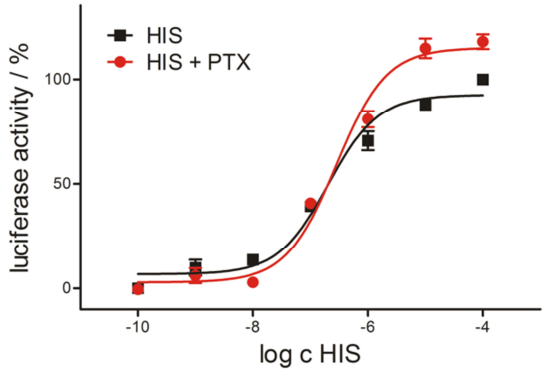

Figure 4.6. Luciferase activity in HEK293T CRE Luc hH_1R cells in the absence and presence of the G_i inhibitor PTX. The response was normalized to the maximal effect induced by HIS. Data are means ± SEM of 3 independent experiments, each performed in triplicate.

Unraveling the effect of PTX on the luciferase activity in the reporter gene assay is complicated due to the fact that both second messengers, Ca^{2+} and cAMP, are influenced by the G_i complex, and have contrary effects on the phosphorylation of CREB. With regard to cAMP, an inhibition of G_i is expected to result in an increase in luciferase activity. By contrast the influence of G_i inhibition on the intracellular Ca^{2+} concentration cannot be predicted.

Indeed, there are hints that coupling of the H_1R to G_i proteins in HEK293T CRE Luc cells is rather unlikely. Firstly, it was shown that the inhibition of the βγ subunit had no influence on the histamine-mediated luciferase expression (cf. section **4.3.1.2.4**). In case of G_i involvement, one would expect either an increase or a decrease in the luciferase expression due to the alteration of the Ca^{2+} concentration *via* the βγ dimer. Secondly, a G_i-mediated increase in Ca^{2+} can be excluded, as it was shown that the increase in intracellular Ca^{2+} is only mediated by the G_q protein (cf. section **4.3.1.4**).

In principle, the increased luciferase expression in PTX-treated cells might reflect a certain constitutive activity of $G\alpha_i$ proteins. If so, inhibition of those proteins is expected to result in an increase in cAMP production, i. e., the basal luciferase activity of PTX-treated cells should be higher than the basal value of untreated cells. However, this does not apply for this experiment.

A more likely explanation for the increased maximum effect in the luciferase assay is that PTX influences cellular responses in a G_i protein independent manner. For example, PTX is known to induce an increase in the cytoplasmic Ca^{2+} concentration.[36-39]

Regardless of the possible explanation discussed above, coupling of the H_1R to G_i proteins in HEK293T CRE Luc cells cannot be ruled out.

In order to verify that PTX was used at a sufficiently high concentration, HEK293T CRE Luc hH_4R[13] cells were treated 0.5 µg/ml with PTX. The next day, the PTX-intoxicated cells were stimulated with forskolin (FSK) (**Fig 4.7**) and histamine, whereas the non PTX-treated cells were incubated only with FSK (**Fig. 4.8**).

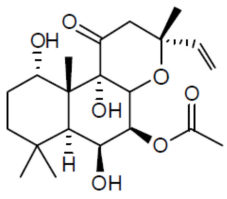

Figure 4.7. Chemical structure of forskolin (FSK), a diterpene from ***Coleus forskohli*** **Briq**.[40]

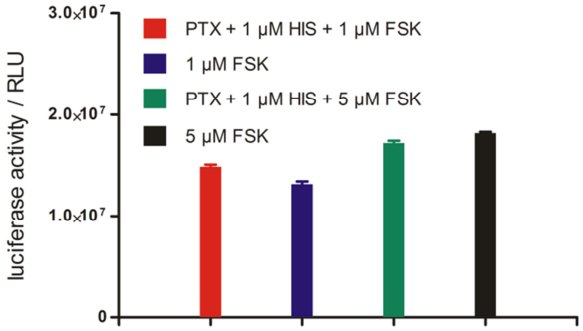

Figure 4.8. Representative luciferase assay at HEK293T CRE Luc hH_4R cells in the absence and presence of PTX. Experiment was performed twice in triplicate.

The luciferase expression was in the same range in PTX-treated and untreated cells, respectively, indicating that the G_i signaling pathway was completely blocked with PTX at a concentration of 0.5 µg/mL.

4.3.1.2.3 Effect of protein kinase A inhibitors on the H_1R dependent luciferase activity

To investigate, whether the H_1R is capable of coupling to $G\alpha_s$ proteins, the effect of the protein kinase A (PKAI and PKAII) inhibitors Rp-cAMP-S and Rp-8-Br-cAMP-S (**Fig. 4.9**) was studied.

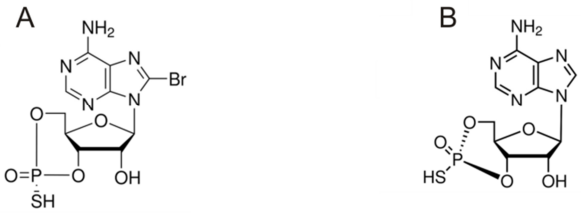

Figure 4.9. Chemical structures of the PKA inhibitors Rp-8-Br-cAMP-S (**A**) and Rp-cAMP-S (**B**).

These inhibitors are cell-permeable cAMP analogs and act as competitive antagonists of cAMP by interacting with the cAMP binding site of the PKA.[41] Due to rather low affinity, the compounds were used at a concentration of 100 µM.

In the presence of 100 µM Rp-cAMP-S and 100 µM Rp-8-Br-cAMP-S, the maximum luciferase signal was reduced by around 50 %. In combination with UBO-QIC the transcription of the luciferase was almost completely inhibited (**Fig. 4.10**), suggesting that the luciferase expression is, at least in part mediated by cAMP.

However, it should be noted that the inhibitors are used at a high concentration, hence their selectivity cannot be taken for granted.

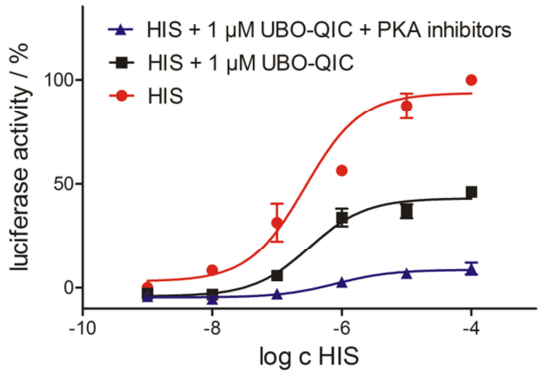

Figure 4.10. Luciferase assay on HEK293T CRE Luc hH_1R cells in the absence and presence of 100 µM Rp-cAMP-S, 100 µM Rp-8-Br-cAMP-S and 1 µM UBO-QIC. The response was normalized to the maximal effect induced by HIS. Data are means ± SEM of 2 independent experiments, each performed in triplicate.

4.3.1.2.4 Effect of the Gβγ inhibitor gallein on the H_1R dependent luciferase activity

Previously, it was shown that the Gβγ dimer is capable of interacting with effector proteins. For instance, Gβγ can interfere with the cAMP pathway by activating AC,[42] and it is also known to influence intracellular Ca^{2+} by interacting with PLC and Ca^{2+} channels.[30,32]

The influence of the Gβγ subunit on the phosphorylation of CREB was studied by using gallein (**Fig. 4.11**/**4.12**). Gallein is supposed to be a reversible inhibitor of Gβγ with a K_d value of 422 nM.[43]

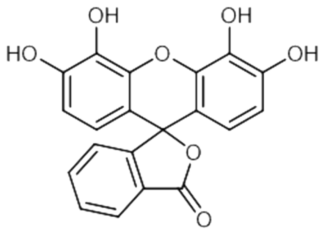

Figure 4.11. Chemical structure of the Gβγ inhibitor gallein.

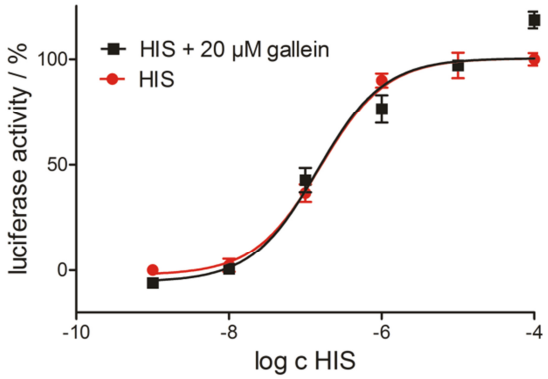

Figure 4.12. Luciferase activity in HEK293T CRE Luc hH_1R cells in the absence and presence of gallein (20 µM). The response was normalized to the maximal effect induced by HIS. Data are means ± SEM of 2 independent experiments, each performed in triplicate.

Gallein had no influence on the luciferase assay performed with HEK293T CRE Luc hH_1R cells, suggesting that the Gβγ dimer is not involved in the phosphorylation of CREB.

4.3.1.3 Investigation of hH_1R expressing HEK293T cells in the fura-2 assay

Changes in Ca^{2+} levels can be measured in a fura-2 assay. Fura-2 is a fluorescent dye that shows a shift of the excitation maximum upon binding of Ca^{2+} ions. Accordingly, this assay was used to verify whether the hH_1R and the hH_2R (cf. section **4.3.2.3**), respectively, induce a Ca^{2+} signal upon stimulation.

As expected due to $G\alpha_q$ coupling, the stimulation of the hH_1R in HEK293T CRE Luc cells by histamine led to an increase in intracellular Ca^{2+} in a concentration dependent manner (**Fig. 4.13A**). Histamine was about 10 times more potent (pEC_{50} = 7.34 ± 0.11) than on cells natively expressing the H_1R, e.g. U373-MG cells. The histamine induced Ca^{2+} response was antagonized by H_1R antagonist diphenhydramine (pK_b = 7.37 ± 0.17) (**Fig. 4.13B**).

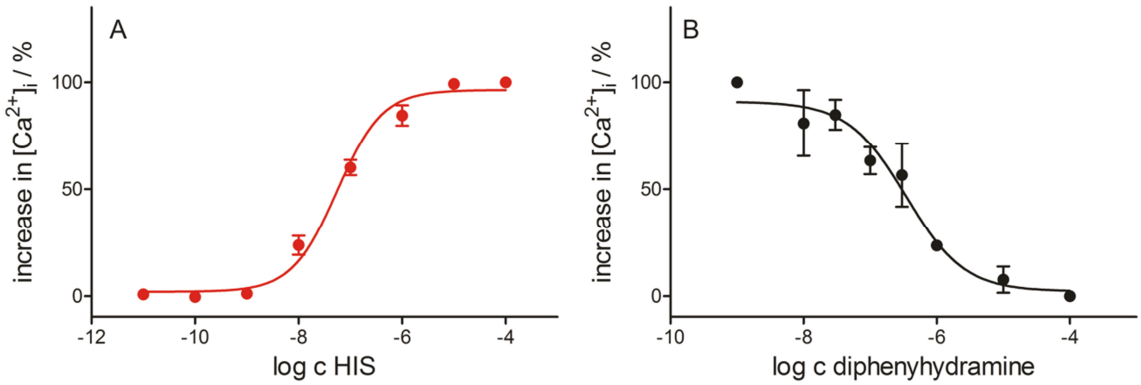

Fig 4.13. (**A**) Intracellular increase in Ca^{2+} in HEK293T CRE Luc hH_1R cells induced by histamine. (**B**) Inhibition of the histamine induced signal by diphenhydramine. The response was normalized to the maximal effect induced by HIS. Data are means ± SEM of 2-4 independent experiments, each performed in triplicate.

4.3.1.4 Investigation of hH_1R expressing HEK293T cells in the aequorin assay

The aequorin assay is another assay to measure changes in the intracellular Ca^{2+} concentration. For this purpose, the HEK293T CRE Luc cells, expressing the hH_1R or the hH_2R (cf. section **4.3.2.4**), were additionally transfected with mitochondrially targeted apoaeqorin (mtAEQ). The advantage of the aequorin assay in comparison to the fura-2 assay is that the cells can be easily pre-incubated with the desired receptor antagonist or inhibitor of signaling. Previously, it was shown that cytoplasmatically and mitochondrially expressed apoaeqorin provide the same functional data.[44]

In agreement with the fura-2 assay, the stimulation of the hH_1R in HEK293T CRE Luc cells by histamine led to an increase in intracellular Ca^{2+} (pEC_{50} 6.94 ± 0.15) (**Fig. 4.14A**). As expected, the histamine induced signal was antagonized by mepyramine (**Fig. 4.14B**).

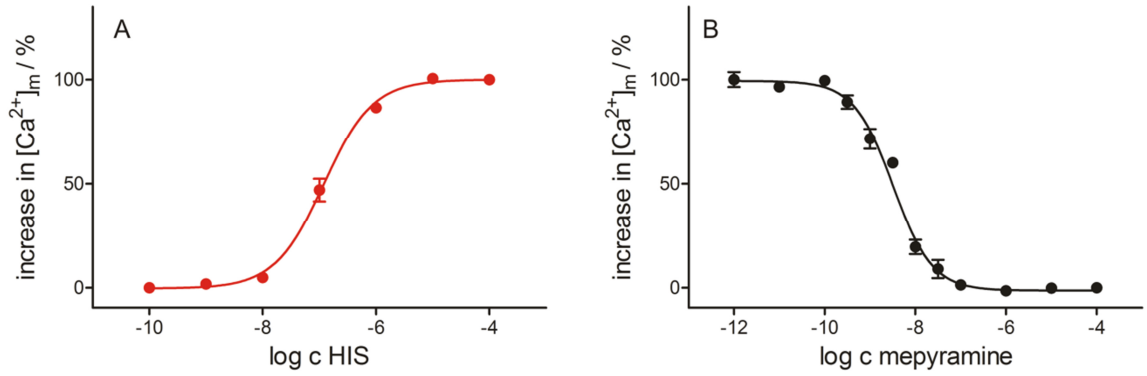

Fig 4.14. (**A**) Aequorin assay on HEK293T CRE Luc hH_1R cells with histamine ($[Ca^{2+}]_m$ = mitochondrial calcium concentration). (**B**) Inhibition of the Ca^{2+} signal by mepyramine. The response was normalized to the maximal effect induced by HIS. Data are means ± SEM of 4 independent experiments, each performed in triplicate.

When the cells were treated with UBO-QIC (1 µM) prior to stimulation of the H_1R, the Ca^{2+} signal was completely blocked (**Fig 4.15**), confirming $G\alpha_q$ coupling of the hH_1R.

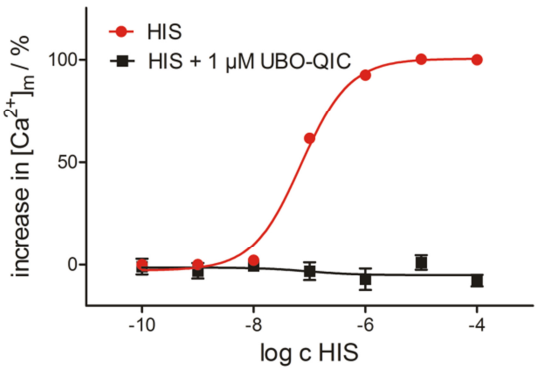

Fig 4.15. Aequorin assay on HEK293T CRE Luc hH_1R cells in the presence and absence of the $G\alpha_q$ inhibitor UBO-QIC ($[Ca^{2+}]_m$ = mitochondrial calcium concentration). The response was normalized to the maximal effect induced by HIS. Data are means ± SEM of 2 independent experiments, each performed in triplicate.

4.3.1.5 Investigation of hH_1R expressing HEK293T cells in a cAMP assay

The transfected cells were investigated in view of their ability to induce a cAMP signal upon stimulation of the respective receptor, using a Lance®cAMP assay from Perkin Elmer. The principle of the assay is shown in **Fig 4.16**.

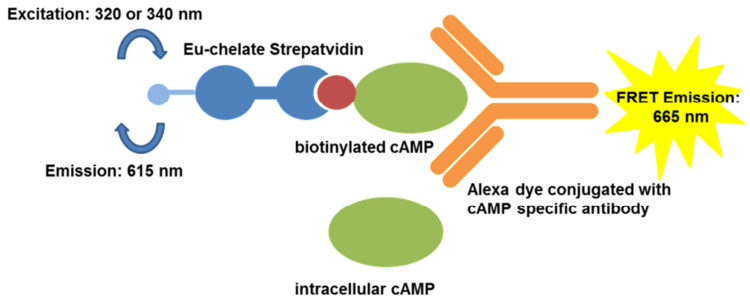

Fig 4.16. Principle of the Lance cAMP assay

4.3.1.5.1 Optimization of cAMP assay parameters

4.3.1.5.1.1 Instrument settings of the GENios Pro microplate reader

Appropriate instrument settings of the microplate reader were determined by registering a cAMP standard curve (**Fig. 4.17**). For this purpose, cAMP standards were incubated for one hour in the dark with antibody solution (1:100). Thereafter, detection buffer was added, and the samples were incubated for an additional hour. Afterwards, the TR-FRET was measured at the microplate reader.

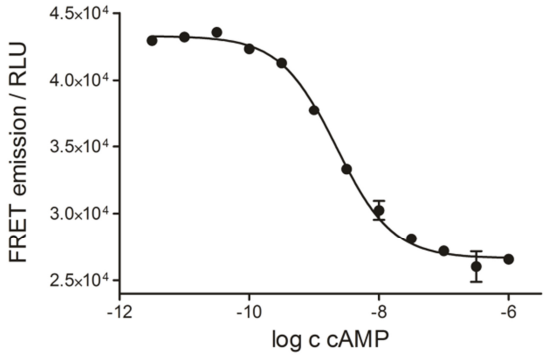

Figure 4.17. cAMP standard curve obtained with the Lance cAMP assay.

Instrument settings: excitation wavelength 340 nm (+/- 10 nm), emission wavelength 670 nm (+/- 25 nm), mirror: dichroic 3, lag time: 50 µs, integration time: $2 \cdot 10^3$ µs, optimal gate.

The pEC_{50} value of cAMP determined in this experiment was 8.67 ± 0.04, which was in perfect agreement with the pEC_{50} values indicated by Perkin Elmer (pEC_{50} 8.43 – 8.66).

4.3.1.5.1.2 Optimization of the cell number

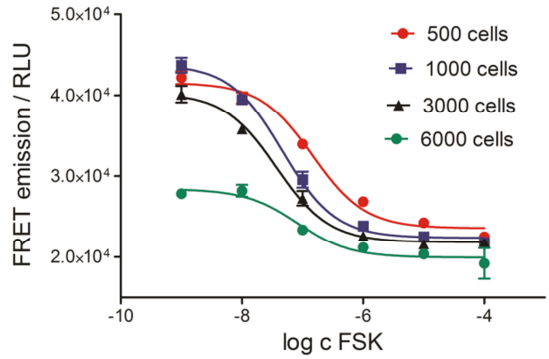

Figure 4.18. Concentration-response curves of FSK on HEK293T CRE Luc hH_2R cells as a function of cell number.

Concentration-response curves of forskolin were constructed using different numbers of HEK293T CRE Luc hH_2R cells per well (**Fig. 4.18**). As the highest signal-to-noise ratio was obtained with a cell number of 1000 cells per well, the following assays were performed accordingly.

4.3.1.5.1.3 cAMP assay on HEK293T CRE Luc hH_1R cells

Unfortunately, it was impossible to produce a cAMP signal upon stimulation of the H_1R probably due to the low signal-to-noise ratio in this assay. Even if there is evidence to suggest that the H_1R is capable of inducing a cAMP signal after stimulation (cf. section **4.3.1.2.3**), it should be taken into account that there might be another pathway involved in the phosphorylation of CREB.

4.3.2 Investigation of HEK293T CRE Luc cells expressing the hH_2R

4.3.2.1 Saturation binding assay using HEK293T CRE Luc hH_2R cells

Receptor expression was verified by saturation binding assays. The quantitative analysis of the saturation binding resulted in around 2.5 million receptors per cell (**Fig. 4.19A).** The K_d value of 54.9 ± 8.1 nM for [^{3}H]UR-DE257 was in the same range as data determined on *Sf*9 membranes.[16] The corresponding Scatchard plot was linear, indicating that the radioligand binds to a single binding site (**Fig 4.19B**).

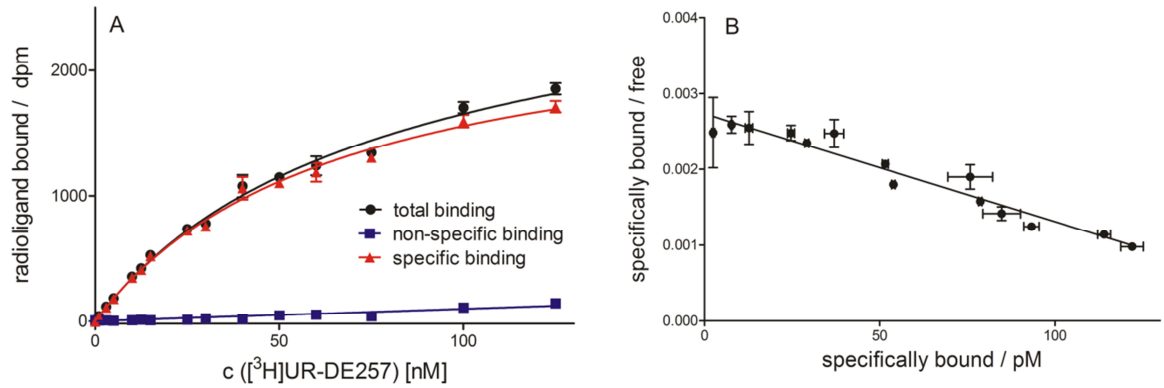

Figure 4.19. (**A**) Representative saturation binding experiment on HEK293T CRE Luc hH_2R cells, performed in triplicate. Non-specific binding of [^{3}H]UR-DE257 was determined in the presence of 10 µM famotidine. The radioligand was diluted 1:20 with unlabeled UR-DE257. (**B**) The corresponding scatchard plot of the saturation binding experiment was best fitted by linear regression (r^2 = 0.90).

4.3.2.2 Luciferase reporter gene assay using HEK293T CRE Luc hH_2R cells

Agonist binding to a G_s-coupled receptor results in an increase in intracellular cAMP and hence in the activation of PKA. Subsequently, the catalytic unit of PKA enters the nucleus and phosphorylates CREB. Upon phosphorylation, CREB binds to CRE and activates the transcription of luciferase.[22]

In the luciferase reporter gene assay the hH_2R revealed high constitutive activity, probably due to a very high expression level of the receptor (2.5 million receptors per cell, cf. section **4.3.2.1**). The high basal levels were reduced by adding different concentrations of FSK, presumably *via* the activation of the inducible cyclic AMP early repressor (ICER). In this setting, histamine amplified the luciferase signal (**Fig. 4.20**), suggesting that this is not a cAMP-mediated response, but rather a Ca^{2+} mediated effect. It was recently shown that in certain cell lines, the cAMP response element modulator (CREM) expression was mediated by cAMP.[45] The translation product of a short isoform of CREM is termed ICER. ICER binds to CRE and acts as a potent repressor of gene transcription.[46]

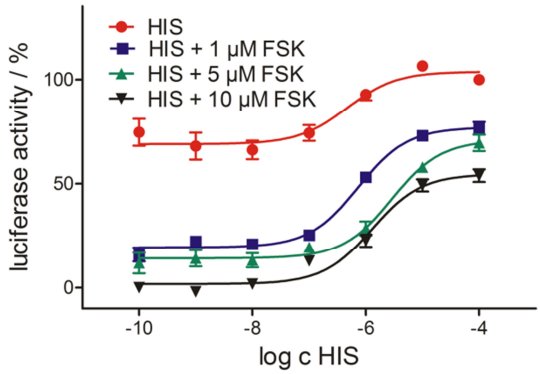

Figure 4.20. Luciferase activity in HEK293T CRE Luc hH_2R using different concentrations of forskolin. The response was normalized to the maximal effect induced by HIS. Data are means ± SEM of 5 independent experiments, each performed in triplicate.

In an approach to reduce the constitutive activity of the H_2R, the standard antagonists famotidine, ranitidine and cimetidine were investigated. All three compounds tested acted as inverse agonists (**Fig 4.21**). The pEC_{50} values were in the same order of magnitude as the pK_i values reported,[15] suggesting that the luciferase expression was mediated by the H_2R.

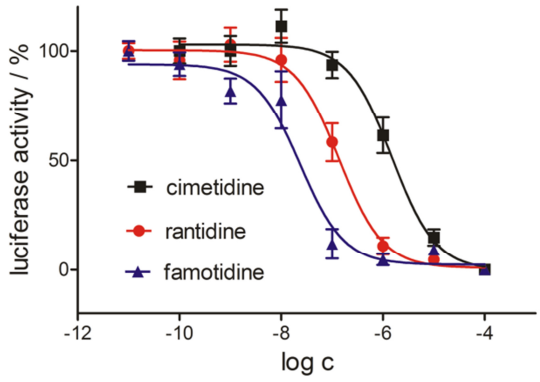

Figure 4.21. Inverse agonistic effect of famotidine, ranitidine and cimetidine in the luciferase reporter gene assay at HEK CRE Luc hH_2R cells. Data are means ± SEM of 3 independent experiments, each performed in triplicate.

Due to the high constitutive activity of the H_2R in this assay system, the signal-to-noise ratio was very poor (cf. **Fig. 4.20**). However, partial inhibition of the receptors with famotidine reduced the constitutive activity and allowed for the activation of the receptor with histamine (**Fig 4.22**).

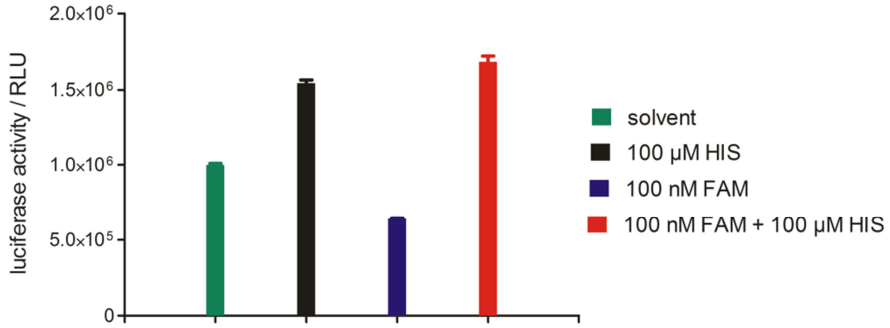

Figure 4.22. Comparison of the signal-to-noise ratio in the absence and presence of 100 nM famotidine. Results shown are representative data.

4.3.2.2.1 Effect of $G\alpha_q$ inhibition on the H_2R dependent luciferase activity

To verify the hypothesis that the expression of luciferase is in part mediated by Ca^{2+}, and to clarify, if the Ca^{2+} signal is triggered by IP_3, the influence of the $G\alpha_q$ inhibitor UBO-QIC was investigated (**Fig 4.23**).

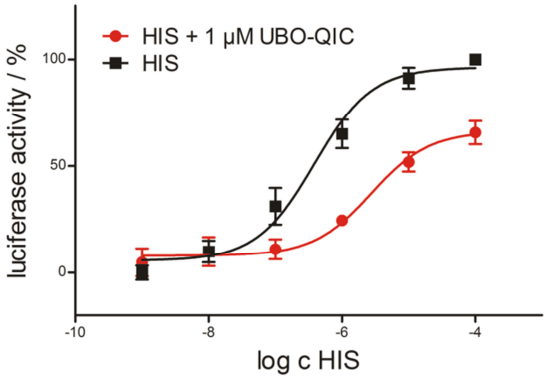

Figure 4.23. Luciferase activity in HEK293T CRE Luc hH_2R cells in the absence and presence of the $G\alpha_q$ inhibitor UBO-QIC. The response was normalized to the maximal effect induced by HIS. Data are means ± SEM of 3 independent experiments, each performed in triplicate.

Interestingly, in the presence of 1 µM of the $G\alpha_q$ protein inhibitor UBO-QIC the maximal response was reduced by approximately 35 % and the curve was rightward-shifted, suggesting $G\alpha_q$ to be involved in the H_2R stimulated luciferase expression. Increasing the inhibitor concentration to 10 µM did not result in a further reduction of the maximal response (data not shown).

4.3.2.2.2 Effect of protein kinase A inhibitors on the H_2R stimulated luciferase activity

Supposed that the H_2R is capable of coupling to $G\alpha_s$ and $G\alpha_q$ proteins, the luciferase expression should be completely inhibited in the presence of both, a $G\alpha_q$ inhibitor UBO-QIC and a PKA inhibitor such as Rp-cAMP-S or Rp-8-Br-cAMP-S. Therefore, the HEK293T CRE

Luc hH_2R cells were pre-incubated with the respective inhibitors and afterwards stimulated with 100 µM histamine (**Fig. 4.24**).

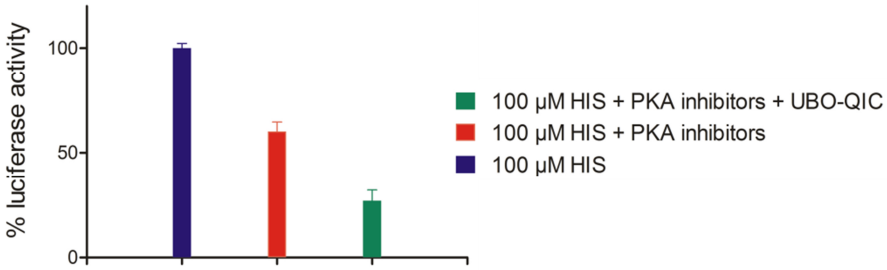

Figure 4.24. Luciferase activity in HEK CRE Luc hH_2R cells in the presence or absence of Rp-cAMP-S, Rp-8-Br-cAMP-S and UBO-QIC. The response was normalized to the maximal effect induced by HIS. Data are means ± SEM of 3 independent experiments, each performed in duplicate or triplicate. Increasing the signal-to-noise ratio was achieved by accessorily adding 100 nM famotidine.

In the presence of 100 µM Rp-cAMP-S and Rp-8-Br-cAMP-S, the luciferase signal was reduced by around 44 %. Cells additionally treated with UBO-QIC showed no complete inhibition, but 32 % of the luciferase expression compared to the control, suggesting pathways other than the $G\alpha_q$ and $G\alpha_s$ mediated ones to be involved as well.

4.3.2.2.3 Effect of pertussis toxin on the H_2R stimulated luciferase activity

To further investigate, whether the Ca^{2+} signal is at least, in part, mediated by G_i, the effect of PTX was studied (**Fig 4.25**).

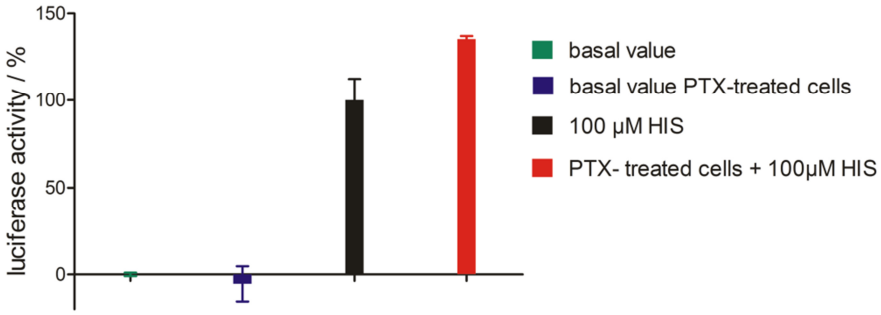

Figure 4.25. Luciferase activity in HEK293T CRE Luc hH_2R cells in the absence and presence of the $G\alpha_i$ inhibitor PTX. The response was normalized to the maximal effect induced by HIS in the absence of PTX. Data are means ± SEM of 2 independent experiments, each performed in triplicate. The high constitutive activity of the hH_2R in HEK CRE Luc cells was reduced by accessorily adding 100 nM famotidine into each well.

In agreement with the inhibition of the $G\alpha_i$ subunit in HEK293T CRE Luc hH_1R cells (cf. section **4.3.1.2.2**), the transcription of luciferase was higher in PTX-intoxicated cells compared to the non-pertussis treated cells.

A reason for the increased luciferase expression in PTX-treated cells may be the PTX-mediated increase in intracellular Ca^{2+} (cf. section **4.3.1.2.2**).[36-39]

4.3.2.2.4 Effect of the Gβγ inhibitor gallein on the H_2R dependent luciferase activity

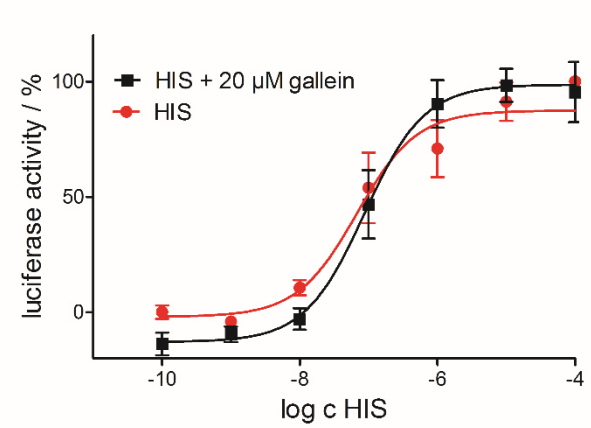

Figure 4.26. Luciferase activity in HEK293T CRE Luc hH_2R cells in the absence and presence of gallein (20 µM). The response was normalized to the maximal effect induced by HIS. Data are means ± SEM of 3 independent experiments, each performed in triplicate.

To investigate the contribution of Gβγ to the hH_2R stimulated luciferase activity, the cells were pre-incubated with gallein (**Fig 4.26**).

Gallein did not significantly influence the transcription of luciferase, suggesting that the Gβγ subunits are not involved in CREB phosphorylation.

4.3.2.3 Investigation of hH_2R expressing HEK293T cells in the fura-2 assay

Indeed, the activation of the hH_2R resulted in a Ca^{2+} signal as well (**Fig. 4.27A**). The pEC_{50} value of histamine of 5.89 ± 0.11 was perfectly in agreement with the pEC_{50} value for histamine obtained with HEK293-hH_2R-qs5 cells in the fura-2 assay.[15] The effect of histamine was completely suppressed by famotidine (**Fig. 4.27B**), confirming that the Ca^{2+} response was mediated by the H_2R.

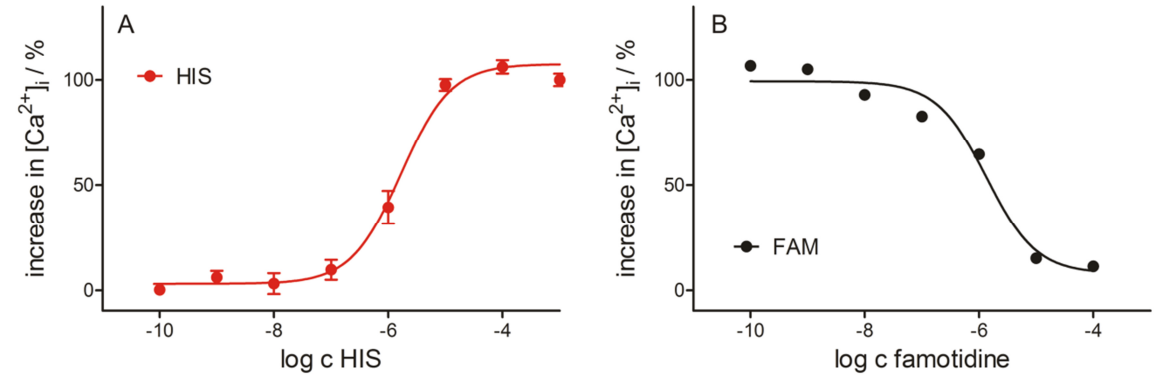

Fig 4.27. (**A**) Intracellular increase in Ca^{2+} in HEK293T CRE Luc hH_2R cells induced by HIS. (**B**) Inhibition of the HIS induced signal by famotidine. The response was normalized to the maximal effect induced by HIS. Data are means ± SEM of 4 independent experiments, each performed in triplicate (**A**); inhibition with famotidine was only performed once.

4.3.2.4 Investigation of hH_2R expressing HEK293T cells in the aequorin assay

The stimulation of the H_2R in HEK293T CRE Luc cells by histamine led to an increase in intracellular Ca^{2+} in a concentration dependent manner (pEC_{50} 5.47 ± 0.13) (**Fig. 4.28A**). Unfortunately, the signal-to-noise ratio was very low. Nevertheless, it was possible to antagonize the histamine induced Ca^{2+} response by famotidine (**Fig 4.28B**).

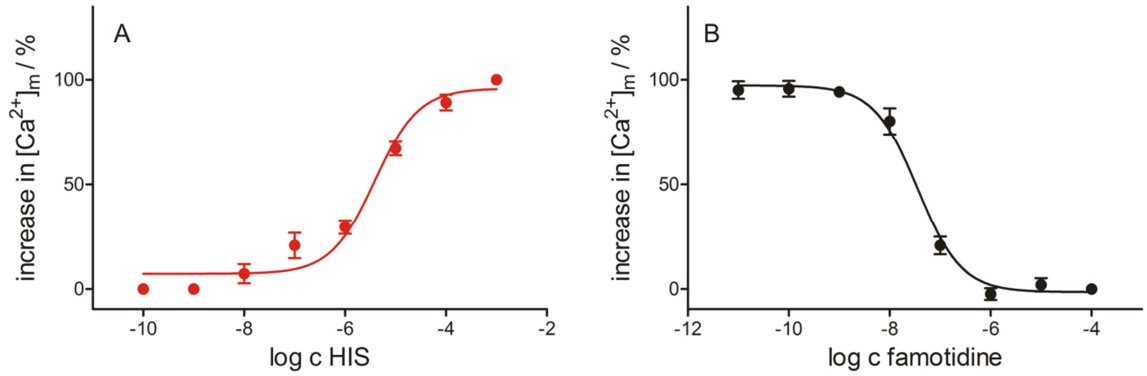

Fig 4.28. (**A**) Aequorin assay on HEK293T CRE Luc hH_2R cells with HIS ($[Ca^{2+}]_m$ = mitochondrial calcium concentration). (**B**) Inhibition of the Ca^{2+} signal by famotidine. The response was normalized to the maximal effect induced by HIS. Data are means ± SEM of 3-4 independent experiments, each performed in triplicate.

In the presence of UBO-QIC, the H_2R mediated Ca^{2+} signal was completely blocked (**Fig. 4.29**). These data suggest that the H_2R, at least in genetically engineered cells, is capable of activating $G\alpha_q$ proteins.

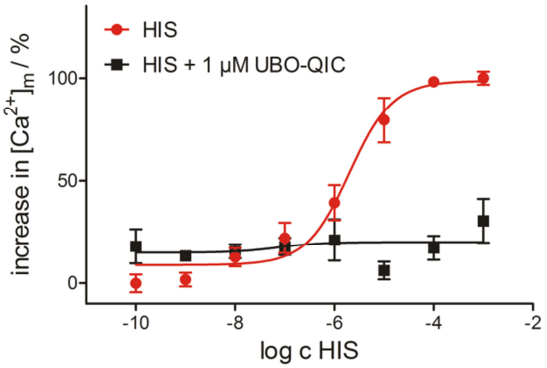

Fig 4.29. Aequorin assay on HEK293T CRE Luc hH_2R cells in the presence and absence of the $G\alpha_q$ inhibitor UBO-QIC ($[Ca^{2+}]_m$ = mitochondrial calcium concentration). The response was normalized to the maximal effect induced by HIS. Data are means ± SEM of 2 independent experiments, each performed in triplicate.

4.3.2.5 Investigation of hH_2R expressing HEK293T cells in a cAMP assay

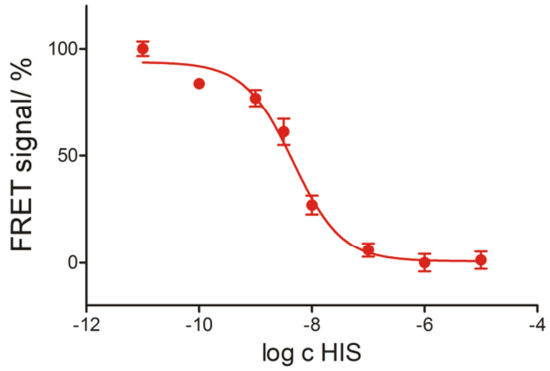

Figure 4.30. cAMP assay on HEK293T CRE Luc hH_2R cells. The response was normalized to the maximal effect induced by HIS. Data are means ± SEM of 3 independent experiments, each performed in triplicate.

As expected, the activation of the H_2R led to an increase in intracellular cAMP in a concentration dependent manner (**Fig 4.30**). The pEC_{50} value determined for histamine was 8.32 ± 0.13 corresponding to more than 100 times higher potency compared to other assays. This discrepancy may be attributed to the very high H_2R expression level. Recently, it was reported that the pEC_{50} value, obtained in a cAMP assay on hH_2R transfected HEK cells strongly depends on the receptor density.[7]

4.4 Summary and conclusion

HEK293T CRE Luc cells were stably transfected with the cDNA encoding the hH_1R or the hH_2R, respectively.

H_1 receptor. The stimulation of the H_1R by histamine led to an expression of luciferase, presumably *via* the activation of CAM kinase IV. The inhibition of the $G\alpha_q$ protein with UBO-QIC resulted in a reduction, but not in a complete inhibition of luciferase expression. In the presence of a combination of the $G\alpha_q$ inhibitor and PKA inhibitors (Rp-cAMP-S or Rp-8-Br-cAMP-S), the luciferase transcription was almost completely inhibited. PTX increased the luciferase activity. Unfortunately, this effect could not be analyzed in detail due to the high complexity of cell signaling and crosstalk. A potential contribution of the Gβγ dimer was taken into account. However, the Gβγ inhibitor gallein did not show any effect in the luciferase reporter gene assay. Additionally, as demonstrated in an aequorin assay, the H_1R mediated increase in intracellular Ca^{2+} is completely blocked by UBO-QIC and, thus, only mediated by $G\alpha_q$. A quantitative detection of a cAMP signal in the LANCE cAMP assay failed, probably due to a low signal-to-noise ratio. It cannot be ruled out that the activation of the hH_1R in genetically modified HEK293T cells is associated with additional pathways.

H_2 receptor. The investigation of the HEK293T CRE Luc hH_2R cells revealed that the H_2R is capable of activating $G\alpha_q$, at least in H_2R overexpressing cells. The luciferase expression was reduced in the presence of UBO-QIC. Additionally, inhibiting PKAI and PKAII resulted in a further decrease in the luciferase transcription. The hypothesis that the H_2R additionally activates $G\alpha_q$ is supported by the results of fura-2 and aequorin assays, where histamine induced a Ca^{2+} signal. The Ca^{2+} signal is not mediated by $G\alpha_i$, but via $G\alpha_q$, as UBO-QIC completely inhibited the Ca^{2+} response in the aequorin assay. There was no hint to a contribution of the Gβγ complex to the transcription of luciferase, as gallein did not induce any effect in the luciferase reporter gene assay. It should be taken into consideration that a third signaling pathway is involved in the H_2R mediated cellular response, most notably because it was impossible to entirely inhibit the luciferase expression in the presence of a combination of UBO-QIC plus Rp-cAMP-S or Rp-8-Br-cAMP-S.

In summary, the genetically engineered HEK293T CRE Luc cells transfected with the receptor of choice provide a powerful pharmacological toolkit for the investigation of GPCRs and functionally selective ligands in a reporter gene assay and enabling the determination of both the Ca^{2+} and the cAMP mediated response (cf. graphical summary in **Fig 4.31**).

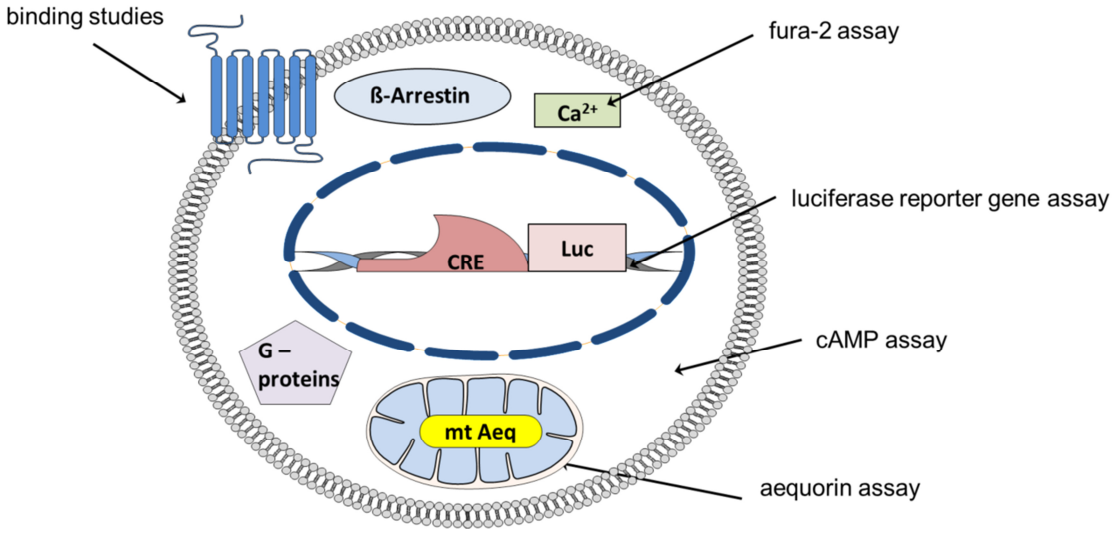

Figure 4.31. Genetically engineered HEK293T cells as a versatile assay platform

Furthermore, such cells should be useful with respect to the deconvolution of holistic readouts from label-free assays, where the identification of the underlying pathways is a major challenge.

4.5 References

1. Hill, S. J.; Ganellin, C. R.; Timmerman, H.; Schwartz, J. C.; Shankley, N. P.; Young, J. M.; Schunack, W.; Levi, R.; Haas, H. L. International Union of Pharmacology. XIII. Classification of histamine receptors. *Pharmacol. Rev.* **1997**, 49, 253-278.
2. Seifert, R.; Hageluken, A.; Hoer, A.; Hoer, D.; Grunbaum, L.; Offermanns, S.; Schwaner, I.; Zingel, V.; Schunack, W.; Schultz, G. The H1 receptor agonist 2(3-chlorophenyl)histamine activates Gi proteins in HL-60 cells through a mechanism that is independent of known histamine-receptor subtypes. *Mol. Pharmacol.* **1994**, 45, 578-586.
3. Bailey, S. J.; Lippe, I. T.; Holzer, P. Effect of the tachykinin antagonist, [D-Pro4, D-Trp7,9,10] substance P-(4-11), on tachykinin- and histamine-induced inositol phosphate generation in intestinal smooth muscle. *Naunyn Schmiedebergs Arch. Pharmacol.* **1987**, 335, 296-300.
4. Claro, E.; Garcia, A.; Picatoste, F. Histamine-stimulated phosphoinositide hydrolysis in developing rat brain. *Mol. Pharmacol.* **1987**, 32, 384-390.
5. Donaldson, J.; Hill, S. J. Histamine-induced inositol phospholipid breakdown in the longitudinal smooth muscle of guinea-pig ileum. *Br. J. Pharmacol.* **1985**, 85, 499-512.
6. Kuhn, B.; Schmid, A.; Harteneck, C.; Gudermann, T.; Schultz, G. G proteins of the Gq family couple the H2 histamine receptor to phospholipase C. *Mol. Endocrinol.* **1996**, 10, 1697-1707.
7. Esbenshade, T. A.; Kang, C. H.; Krueger, K. M.; Miller, T. R.; Witte, D. G.; Roch, J. M.; Masters, J. N.; Hancock, A. A. Differential activation of dual signaling responses by human H1 and H2 histamine receptors. *J. Recept. Signal Transduct. Res.* **2003**, 23, 17-31.
8. Seifert, R.; Hoer, A.; Schwaner, I.; Buschauer, A. Histamine increases cytosolic Ca2+ in HL-60 promyelocytes predominantly via H2 receptors with an unique agonist/antagonist profile and induces functional differentiation. *Mol. Pharmacol.* **1992**, 42, 235-241.
9. Delvalle, J.; Wang, L.; Gantz, I.; Yamada, T. Characterization of H2 histamine receptor: linkage to both adenylate cyclase and [Ca2+]i signaling systems. *Am. J. Physiol.* **1992**, 263, G967-972.
10. Leurs, R.; Traiffort, E.; Arrang, J. M.; Tardivel-Lacombe, J.; Ruat, M.; Schwartz, J. C. Guinea pig histamine H1 receptor. II. Stable expression in Chinese hamster ovary cells reveals the interaction with three major signal transduction pathways. *J. Neurochem.* **1994**, 62, 519-527.
11. Sanderson, E. M., Iredale, P.A., Hill, S.J. Role of Ca2+ ions in the stimulation of cAMP accumulation by histamine in CHO-K1 cells transfected with the bovine H1-receptor. (Abstract)

    Br. J. Pharmacol. **1996**, 117: 7P.
12. Fitzsimons, C.; Molinari, B.; Duran, H.; Palmieri, M.; Davio, C.; Cricco, G.; Bergoc, R.; Rivera, E. Atypical association of H1 and H2 histamine receptors with signal transduction pathways during multistage mouse skin carcinogenesis. *Inflamm. Res.* **1997**, 46, 292-298.
13. Nordemann, U.; Wifling, D.; Schnell, D.; Bernhardt, G.; Stark, H.; Seifert, R.; Buschauer, A. Luciferase reporter gene assay on human, murine and rat histamine H4 receptor orthologs: correlations and discrepancies between distal and proximal readouts. *PLoS One* **2013**, 8, e73961.
14. Ziemek, R.; Schneider, E.; Kraus, A.; Cabrele, C.; Beck-Sickinger, A. G.; Bernhardt, G.; Buschauer, A. Determination of affinity and activity of ligands at the human neuropeptide Y Y4 receptor by flow cytometry and aequorin luminescence. *J. Recept. Signal Transduct. Res.* **2007**, 27, 217-233.
15. Mosandl, J. Radiochemical and luminescence-based binding and functional assays for human histamine receptors using genetically engineered cells *Doctoral Thesis, University of Regensburg* **2009**.

16. Baumeister, P.; Erdmann, D.; Biselli, S.; Kagermeier, N.; Elz, S.; Bernhardt, G.; Buschauer, A. [3H]UR-DE257: Development of a tritium-labeled squaramide-type selective histamine H2 receptor antagonist. *ChemMedChem* **2015**, 10, 83-93.
17. Cheng, Y.; Prusoff, W. H. Relationship between the inhibition constant (K1) and the concentration of inhibitor which causes 50 per cent inhibition (I50) of an enzymatic reaction. *Biochem. Pharmacol.* **1973**, 22, 3099-3108.
18. Muller, M.; Knieps, S.; Gessele, K.; Dove, S.; Bernhardt, G.; Buschauer, A. Synthesis and neuropeptide Y Y1 receptor antagonistic activity of N,N-disubstituted omega-guanidino- and omega-aminoalkanoic acid amides. *Arch. Pharm. (Weinheim)* **1997**, 330, 333-342.
19. Strasser, A.; Striegl, B.; Wittmann, H.-J.; Seifert, R. Pharmacological profile of histaprodifens at four recombinant histamine H-1 receptor species isoforms. *J. Pharm. Exp. Ther.* **2008**, 324, 60-71.
20. Hill, S. J.; Baker, J. G.; Rees, S. Reporter-gene systems for the study of G-protein-coupled receptors. *Curr. Opin. Pharmacol.* **2001**, 1, 526-532.
21. Zhang, X.; Odom, D. T.; Koo, S. H.; Conkright, M. D.; Canettieri, G.; Best, J.; Chen, H.; Jenner, R.; Herbolsheimer, E.; Jacobsen, E.; Kadam, S.; Ecker, J. R.; Emerson, B.; Hogenesch, J. B.; Unterman, T.; Young, R. A.; Montminy, M. Genome-wide analysis of cAMP-response element binding protein occupancy, phosphorylation, and target gene activation in human tissues. *Proc. Natl. Acad. Sci. U. S. A.* **2005**, 102, 4459-4464.
22. Montminy, M. R.; Gonzalez, G. A.; Yamamoto, K. K. Regulation of cAMP-inducible genes by CREB. *Trends Neurosci.* **1990**, 13, 184-188.
23. Matthews, R. P.; Guthrie, C. R.; Wailes, L. M.; Zhao, X.; Means, A. R.; McKnight, G. S. Calcium/calmodulin-dependent protein kinase types II and IV differentially regulate CREB-dependent gene expression. *Mol. Cell. Biol.* **1994**, 14, 6107-6116.
24. Sheng, M.; Thompson, M. A.; Greenberg, M. E. CREB: a Ca(2+)-regulated transcription factor phosphorylated by calmodulin-dependent kinases. *Science* **1991**, 252, 1427-1430.
25. Berridge, M. J.; Lipp, P.; Bootman, M. D. The versatility and universality of calcium signalling. *Nat. Rev. Mol. Cell Biol.* **2000**, 1, 11-21.
26. Seifert, R.; Strasser, A.; Schneider, E. H.; Neumann, D.; Dove, S.; Buschauer, A. Molecular and cellular analysis of human histamine receptor subtypes. *Trends Pharmacol. Sci.* **2013**, 34, 33-58.
27. Seifert, R.; Wenzel-Seifert, K.; Burckstummer, T.; Pertz, H. H.; Schunack, W.; Dove, S.; Buschauer, A.; Elz, S. Multiple differences in agonist and antagonist pharmacology between human and guinea pig histamine H1-receptor. *J. Pharmacol. Exp. Ther.* **2003**, 305, 1104-1115.
28. Fujioka, M.; Koda, S.; Morimoto, Y.; Biemann, K. Structure of FR900359, a cyclic depsipeptide from ardisia-crenata sims. *J. Org. Chem.* **1988**, 53, 2820-2825.
29. Takasaki, J.; Saito, T.; Taniguchi, M.; Kawasaki, T.; Moritani, Y.; Hayashi, K.; Kobori, M. A novel Galphaq/11-selective inhibitor. *J. Biol. Chem.* **2004**, 279, 47438-47445.
30. Krauss, G. Biochemistry of Signal Transduction and Regulation. *Wiley-VCH, Weinheim* **2014**.
31. Hofstra, C. L.; Desai, P. J.; Thurmond, R. L.; Fung-Leung, W. P. Histamine H4 receptor mediates chemotaxis and calcium mobilization of mast cells. *J. Pharmacol. Exp. Ther.* **2003**, 305, 1212-1221.
32. Wettschureck, N.; Offermanns, S. Mammalian G proteins and their cell type specific functions. *Physiol. Rev.* **2005**, 85, 1159-1204.
33. Bongers, G.; Bakker, R. A.; Leurs, R. Molecular aspects of the histamine H-3 receptor. *Biochem. Pharmacol.* **2007**, 73, 1195-1204.
34. Seifert, R.; Wenzel-Seifert, K. Constitutive activity of G-protein-coupled receptors: cause of disease and common property of wild-type receptors. *Naunyn Schmiedebergs Arch. Pharmacol.* **2002**, 366, 381-416.
35. Burns, D. L. Subunit structure and enzymic activity of pertussis toxin. *Microbiol. Sci.* **1988**, 5, 285-287.

36. Mangmool, S.; Kurose, H. G(i/o) protein-dependent and -independent actions of Pertussis Toxin (PTX). *Toxins (Basel)* **2011**, 3, 884-899.
37. Macintyre, E. A.; Tatham, P. E.; Abdul-Gaffar, R.; Linch, D. C. The effects of pertussis toxin on human T lymphocytes. *Immunology* **1988**, 64, 427-432.
38. Sommermeyer, H.; Resch, K. Pertussis toxin B-subunit-induced Ca2(+)-fluxes in Jurkat human lymphoma cells: the action of long-term pre-treatment with cholera and pertussis holotoxins. *Cell. Signal.* **1990**, 2, 115-128.
39. Lauckner, J. E.; Hille, B.; Mackie, K. The cannabinoid agonist WIN55,212-2 increases intracellular calcium via CB1 receptor coupling to Gq/11 G proteins. *Proc. Natl. Acad. Sci. U. S. A.* **2005**, 102, 19144-19149.
40. Kavitha, C.; Rajamani, K.; Vadivel, E. Coleus forskohlii: A comprehensive review on morphology, phytochemistry and pharmacological aspects. *Journal of Medicinal Plants Research* **2010**, 4, 278-285.
41. Gjertsen, B. T.; Mellgren, G.; Otten, A.; Maronde, E.; Genieser, H. G.; Jastorff, B.; Vintermyr, O. K.; Mcknight, G. S.; Doskeland, S. O. Novel (Rp)-Camps Analogs as Tools for Inhibition of Camp-Kinase in Cell-Culture - Basal Camp-Kinase Activity Modulates Interleuktin-1-Beta Action. *J. Biol. Chem.* **1995**, 270, 20599-20607.
42. Federman, A. D.; Conklin, B. R.; Schrader, K. A.; Reed, R. R.; Bourne, H. R. Hormonal stimulation of adenylyl cyclase through Gi-protein beta gamma subunits. *Nature* **1992**, 356, 159-161.
43. Lehmann, D. M.; Seneviratne, A. M.; Smrcka, A. V. Small molecule disruption of G protein beta gamma subunit signaling inhibits neutrophil chemotaxis and inflammation. *Mol. Pharmacol.* **2008**, 73, 410-418.
44. Stables, J.; Green, A.; Marshall, F.; Fraser, N.; Knight, E.; Sautel, M.; Milligan, G.; Lee, M.; Rees, S. A bioluminescent assay for agonist activity at potentially any G-protein-coupled receptor. *Anal. Biochem.* **1997**, 252, 115-126.
45. Molina, C. A.; Foulkes, N. S.; Lalli, E.; Sassone-Corsi, P. Inducibility and negative autoregulation of CREM: an alternative promoter directs the expression of ICER, an early response repressor. *Cell* **1993**, 75, 875-886.
46. Kemp, D. M.; George, S. E.; Kent, T. C.; Bungay, P. J.; Naylor, L. H. The effect of ICER on screening methods involving CRE-mediated reporter gene expression. *J. Biomol. Screen.* **2002**, 7, 141-148.

Chapter 5

Application of the established luciferase reporter gene assay for the functional investigation of hH_1R ligands

5.1 Introduction

Over the past decade, numerous recombinant expression assay systems were established for H_xRs in our workgroup.[1-4] With respect to the H_1R, for example, in an approach to develop a cell based assay for the H_1R, potentially applicable to high throughput screening, the fura-2 assay was adapted to the microtitre format.[5] This approach succeeded only partially, since screening of agonists became possible, whereas the assays did not work reliably in case of antagonists.

The aim of this sub-project was to explore the applicability of the established luciferase reporter gene assay (cf. chapter 4) to the functional investigation of H_1R ligands. In reporter gene assays, signal amplification may occur due to the distal readout. Agonists may be more potent in the luciferase reporter gene assay compared to assays with a more proximal readout.[6] Therefore, the results obtained from the luciferase assay were compared to reported functional and binding data.

5.2 Material and Methods

All chemicals were from commercial suppliers, unless otherwise indicated.

5.2.1 Cell culture

Cells were cultured as described in section **4.2.1**.

5.2.2 Stable transfection of HEK293T CRE Luc cells with the pcDNA3.1(+)-hH_1R vector

The transfection is described in section **4.2.2**.

5.2.3 Luciferase reporter gene assay

The assay is described in section **4.2.8**. After addition of 20 µL of the 10 fold concentrated test compound (in water, DMEM or DMF; cf. section **5.3.3**), the samples were completed by adding 20 µL of DMEM to a total volume of 200 µL. The cells were incubated at 37 °C in water saturated atmosphere containing 5 % CO_2 for 5 hours.

5.2.4 Crystal violet based chemosensitivity assay

The assay was performed as described in section **3.5.3.7**.

5.2.5 Selected test compounds

5.2.5.1 H_1R agonists

All selected H_1R agonists (**Fig. 5.1**), except for histamine, were synthesized in the laboratory of Professor Dr. Sigurd Elz (Institute of Pharmacy, University of Regensburg). The stock

solutions (10 mM) were prepared with water, except for the histaprodifen derivatives (stock solutions in 30 % DMSO or 100 % DMF).

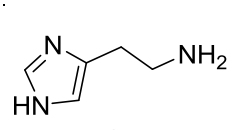

HIS

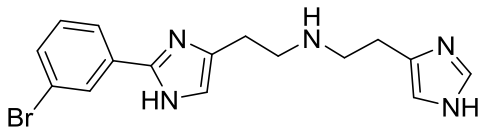

N[a]-imidazolylethyl substituted 2- phenylhistamine (5.1)

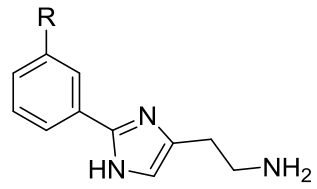

2-phenylhistamines

compd.	R
5.2	H
5.3	Br
5.4	CF_3

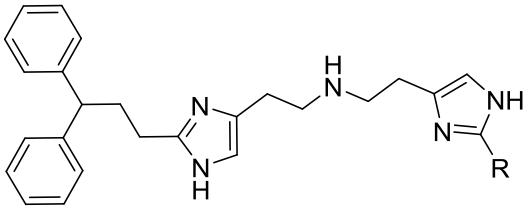

histaprodifen derivatives

compd.	R
5.5	H
5.6	
5.7	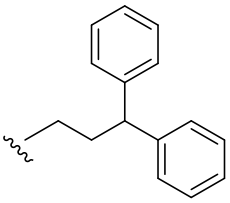

Figure 5.1. Chemical structures of the selected H_1R agonists

5.2.5.2 H_1R antagonists

The antidepressants, antipsychotic and antihistaminic compounds were from Sigma Aldrich (Taufkirchen, Germany), RBI (Natick, USA) or Biotrend (Köln, Germany) (**Fig. 5.2**). The stock solutions (10 mM) were prepared with water, except for clozapine (stock solution in 0.1 M HCl) and fexofenadine (stock solution in 50 % DMSO or 50 % DMF). The H_1R was activated by 300 nM HIS. pK_b values were calculated according to the Cheng-Prusoff equation.[7]

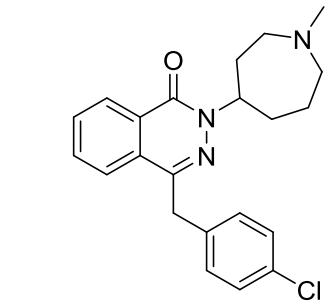

azelastine (5.8)

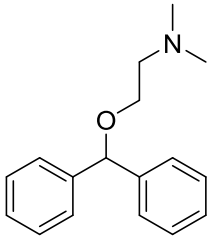

diphenhydramine (5.9)

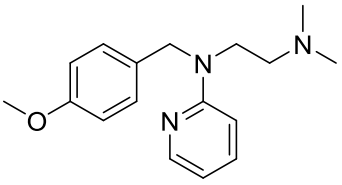

mepyramine (5.10)

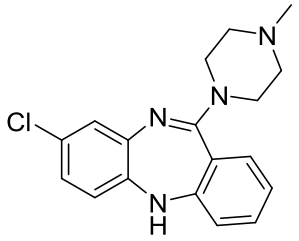

clozapine (5.11)

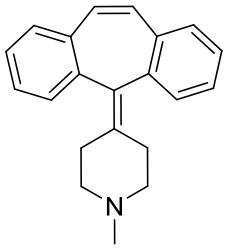

cyproheptadine (5.12)

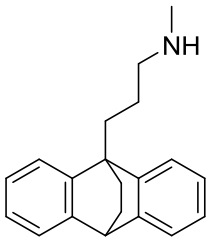

maprotiline (5.13)

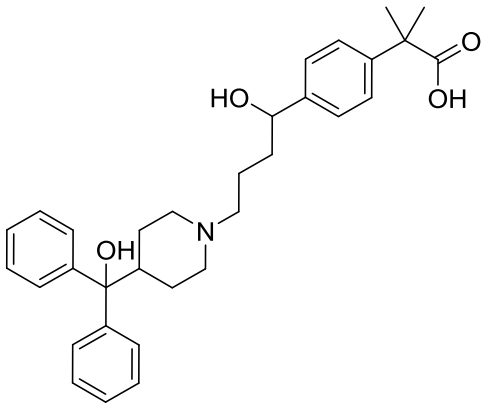

fexofenadine (5.14)

Figure 5.2. Chemical structures of the selected H_1R antagonists

5.3 Results and Discussion

5.3.1 Quantification of hH_1 receptors per cell

Receptor expression was verified by saturation binding assays using whole HEK CRE Luc hH_1R cells as described in section **4.3.1.1** Approximately 500,000 hH_1R were expressed per cell.

5.3.2 Optimization of the incubation period

In case of HEK CRE Luc H_4R cells, the optimal incubation period was determined for 5 h.[6] Likewise, 5 h seemed to be an appropriate incubation period for HEK CRE Luc hH_1R cells. By analogy to the HEK CRE Luc hH_4R cells, a maximum was reached after 8 h of incubation

and sustained over 30 h (data not shown). Nevertheless, an incubation period of 5 h was chosen, due to the potential risk of receptor internalisation after longer incubation periods.

5.3.3 Effect of the solvent on the luciferase activity

Due to the fact that not all of the selected compounds were soluble in water, the effects of DMSO (**Fig. 5.3A**) and DMF (**Fig. 5.3B**) were investigated.

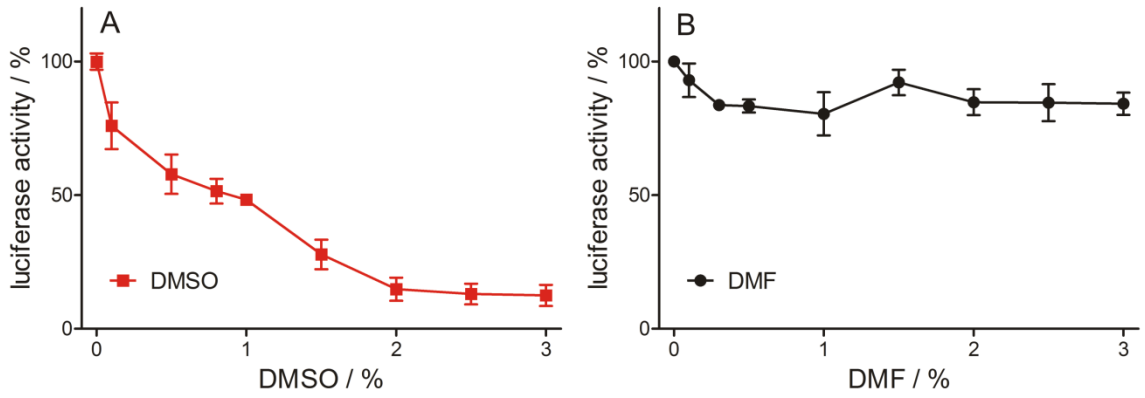

Figure 5.3. Influence of DMSO (**A**) and DMF (**B**) on the luciferase signal. Cells were incubated with the respective solvent and 10 µM HIS. The luciferase activity induced by 10 µM HIS was set to 100 %. Data are means ± SEM of 2 independent experiments, each performed in triplicate.

DMSO at a concentration of 0.1 % reduced the maximum luciferase signal by approximately 24 %, whereas in the presence of 2 % DMSO the signal was almost completely suppressed. In search for an alternative to DMSO, the effect of DMF was investigated. In contrast to DMSO, up to a final concentration of 3 % DMF the reduction of the maximum luminescence signal was only around 14 %. Therefore, DMSO was replaced by DMF as solvent.

5.3.4 Functional characterization of H_1R ligands

A variety of structurally different agonists and antagonists (cf. section **5.2.5**) was studied in the luciferase reporter gene assay. The pEC_{50} values of all investigated agonists were in agreement with data from literature (**Table 5.1**).

The pEC_{50} values determined for histamine and **5.1** were comparable to the pEC_{50} values determined in the steady-state GTPase assay. By contrast, the pEC_{50} values of the phenylhistamine derivatives **5.2**, **5.3** and **5.4,** obtained in the luciferase reporter gene assay, correlated better with the pK_i values of these compounds. As suggested by Seifert et al.,[8] the structurally related compound 2-(3-chlorophenyl)histamine directly activates G_i proteins in HL-60 cells which might explain the low potency of the 2-phenylhistamines in the luciferase reporter gene assay. Indeed, direct activation of G_i proteins in HEK293T CRE Luc cells could not be confirmed for the tested phenylhistamine derivatives in HEK CRE Luc cells (data not shown).

Table 5.1. Potencies of H_1 receptor agonists determined in the luciferase reporter gene assay compared to functional and binding data reported in literature

	luciferase reporter gene assay[a]		**steady-state GTPase assay**[b,9]		**competition binding**[b,9]
compd.	pEC_{50} ± SEM	E_{max} ± SEM	pEC_{50} ± SEM	E_{max} ± SEM	pK_i ± SEM
HIS	6.87 ± 0.06	1.00	6.92 ± 0.07	1.00	5.62 ± 0.03[10]
5.1	7.49 ± 0.08	1.05 ± 0.03	7.75 ± 0.11	0.94 ± 0.06	6.43 ± 0.08
5.2	5.12 ± 0.15	0.56 ± 0.07	6.14 ± 0.06	0.72 ± 0.04	5.36 ± 0.13
5.3	5.46 ± 0.17	0.56 ± 0.05	6.75 ± 0.03	0.62 ± 0.01	5.86 ± 0.09
5.4	5.81 ± 0.06	0.62 ± 0.02	6.71 ± 0.04	0.61 ± 0.02	5.83 ± 0.10

[a]Luciferase reporter gene assay on HEK CRE Luc hH_1R cells. Data were analyzed by nonlinear regression and were best fit to three-parameter sigmoidal concentration-response curves. pEC_{50}: $-logEC_{50}$; E_{max}: maximal response relative to histamine (E_{max} = 1.0). Data shown are means ± SEM of 2-5 independent experiments, each performed in triplicate. [b]Data were taken from Straßer et al. (2009); pEC_{50} and pK_i values determined on *Sf9* insect cell membranes.

In case of the H_1R antagonists, the determined pK_b values were in good agreement with both functional and binding data from literature (**Table 5.2**).

Table 5.2. H_1 receptor antagonism determined in the luciferase reporter gene assay compared to functional and binding data reported in literature

	luciferase reporter gene assay[a]	**steady-state GTPase assay**[b,9]	**competition binding**[c,9]
compd.	pK_b ± SEM	pK_b ± SEM	pK_i ± SEM
5.8	8.34 ± 0.08	8.77 ± 0.04[3]	-
5.9	7.88 ± 0.13*	7.81 ± 0.05[11]	7.78 ± 0.03[12]
5.10	8.13 ± 0.10	8.24 ± 0.08[3]	8.33 ± 0.03[12]
5.11	8.51 ± 0.06	8.36 ± 0.12[11]	8.58 ± 0.16[11]
5.12	8.55 ± 0.11	8.72 ± 0.03[3]	-
5.13	8.47 ± 0.12	8.54 ± 0.16[11]	8.86 ± 0.07[11]
5.14	7.47 ± 0.03	-	7.45 ± 0.07[12]

[a]Luciferase reporter gene assay on HEK CRE Luc hH_1R cells. Data were analyzed by nonlinear regression and were best fit to 3-parameter sigmoidal concentration-response curves. pK_b values were calculated according to the Cheng-Prusoff equation (c(HIS) = 300 nM; *1 µM, EC_{50} (HIS) = 134 nM) . Data are means ± SEM of 2-4 independent experiments, each performed in triplicate. [b]Data were taken from Appl et al. (2012) or Seifert et al. (2003); pK_b values determined on *Sf9* insect cells, expressing the hH_1R and co-expressing RGS4. [c]Data were taken from Appl et al. (2012) or Wittmann et al. (2009) on *Sf9* insect cells co-expressing the hH_1R and RGS4.

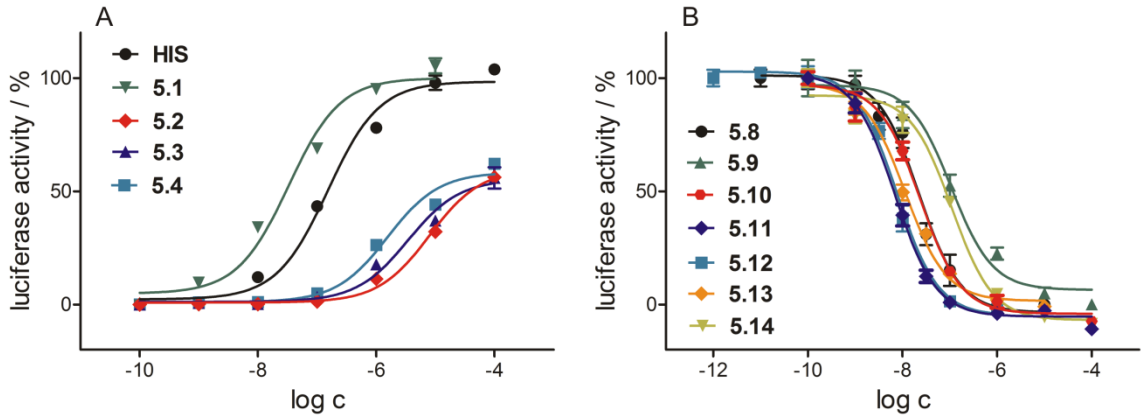

Figure 5.4. Concentration-response curves of H_1R agonists (**A**) and antagonists (**B**) in the luciferase reporter gene assay.

Unfortunately, it was not possible to quantify the hH_1R agonist potencies of the histaprodifen derivatives in the luciferase reporter gene assay (**Fig. 5.5**), most probably due to cytolysis caused by these amphiphilic compounds (cf. section **5.3.5**).

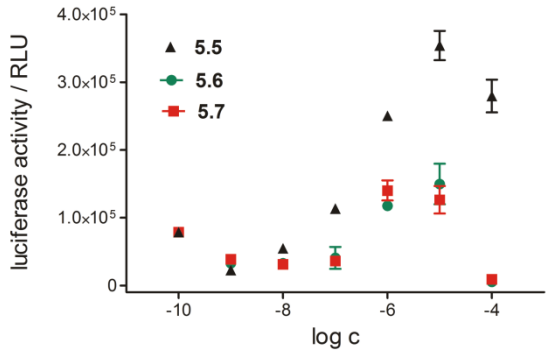

Figure 5.5. Effects of the histaprodifen derivatives **5.5**, **5.6** and **5.7** in the luciferase reporter gene assay (data from two representative experiments).

Bakker et al.[13] characterized **5.9** as an inverse agonist at the H_1R. By contrast, in the present study, **5.9** acted as a neutral antagonist (**Fig 5.6**). It should be stressed that in HEK CRE Luc hH_1R cells the H_1R was devoid of constitutive activity.
Constitutive activity of a receptor can vary depending on the cell systems.[14] However, the most likely explanation for this difference is that Bakker et al. used cells co-expressing the H_1R and the $G\alpha_q$ protein, as constitutive activity can be modulated by co-expressed G-proteins.[15]

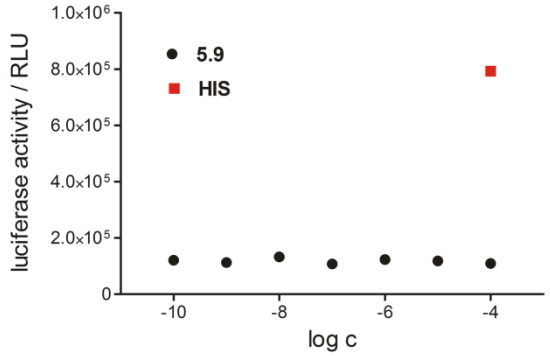

Figure 5.6. Luciferase activity in HEK CRE Luc hH_1R cells in the presence of compd. **5.9** (representative experiment). The luciferase activity remained unaffected at increasing concentrations of **5.9**. Constitutive of the H_1R was not detectable in this cellular system.

5.3.5 Characterization of histaprodifen derivatives in the crystal violet based chemosensitivity assay

To elucidate why the histaprodifen derivatives did not induce a luciferase signal at higher concentrations, the compounds were investigated in a crystal violet based chemosensitivity assay on HEK CRE Luc hH_1R cells (**Fig 5.7**).

Regardless of considerably longer incubation periods in the chemosensitivity assay, the results provided an explanation for the behavior of the compounds in the luciferase reporter gene assay (cf. **Fig 5.5**). Compound **5.5** were not cytotoxic up to a concentration of 10 µM, whereas compounds **5.6** and **5.7** revealed strong cytocidal effects at a concentration of 10 µM. Additionally, at a concentration of 1 µM, **5.6** was less toxic than **5.7**. These observations correlate with the amphiphilic character of these compounds and their potential to interact with cell membranes.

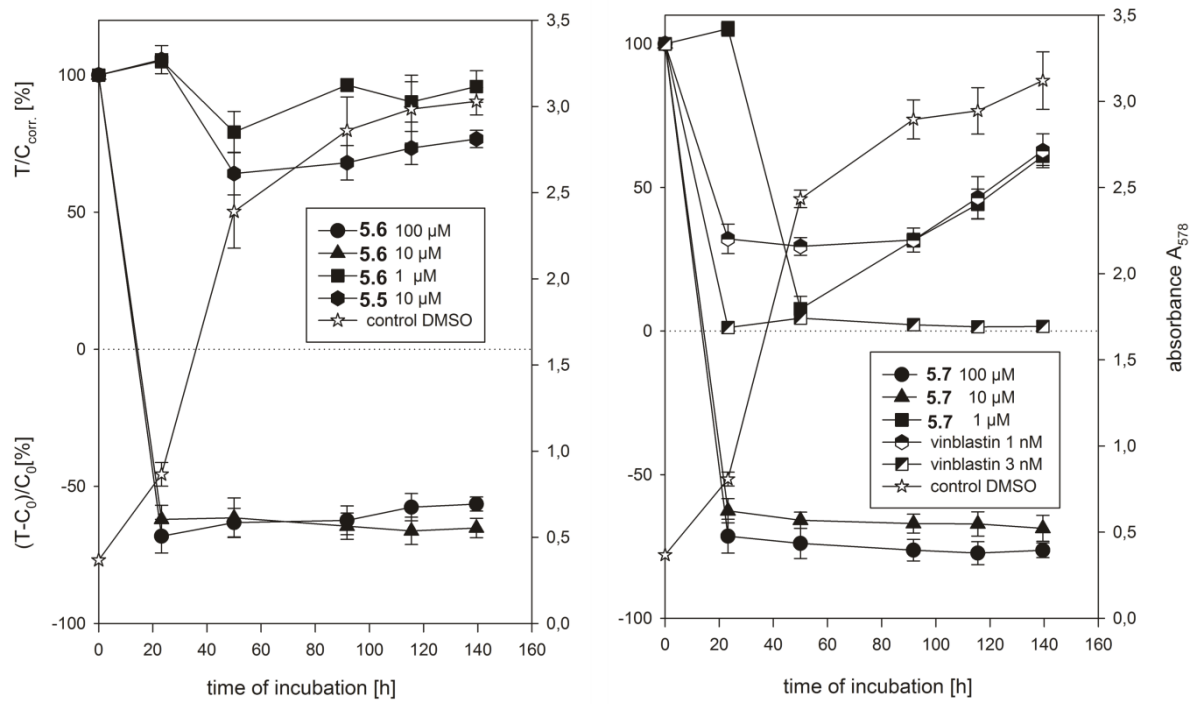

Figure 5.7. Cytotoxicity of **5.5**, **5.6** and **5.7** on HEK293T CRE Luc hH$_1$R cells in the crystal violet assay. Vinblastin and DMSO as positive and negative controls.

5.4 Summary and conclusion

HEK293T CRE Luc cells were stably co-transfected with the human H$_1$R, and the luciferase reporter gene assay was successfully established. By analogy with the luciferase assay for the H$_3$R and the H$_4$R, respectively, an incubation period of 5 h was chosen for the HEK CRE Luc hH$_1$R cells. In contrast to studies on cells co-transfected with the cDNAs encoding receptor and Gα_q proteins, respectively, the H$_1$R did not display constitutive activity in this system.

The established luciferase assay was successfully used for the characterization of structurally different agonists and antagonists. Furthermore, the reliability and accuracy of the assay were proven by comparing the results to data from literature.

5.5 References

1. Kelley, M. T.; Bürckstümmer, T.; Wenzel-Seifert, K.; Dove, S.; Buschauer, A.; Seifert, R. Distinct interaction of human and guinea pig histamine H2-receptor with guanidine-type agonists. *Mol. Pharmacol.* **2001**, 60, 1210-1225.
2. Schnell, D.; Strasser, A.; Seifert, R. Comparison of the pharmacological properties of human and rat histamine H(3)-receptors. *Biochem. Pharmacol.* **2010**, 80, 1437-1449.
3. Seifert, R.; Wenzel-Seifert, K.; Burckstummer, T.; Pertz, H. H.; Schunack, W.; Dove, S.; Buschauer, A.; Elz, S. Multiple differences in agonist and antagonist pharmacology between human and guinea pig histamine H1-receptor. *J. Pharmacol. Exp. Ther.* **2003**, 305, 1104-1115.
4. Schneider, E. H.; Seifert, R. Sf9 cells: a versatile model system to investigate the pharmacological properties of G protein-coupled receptors. *Pharmacol. Ther.* **2010**, 128, 387-418.
5. Mosandl, J. Radiochemical and luminescence-based binding and functional assays for human histamine receptors using genetically engineered cells *Doctoral Thesis, University of Regensburg* **2009**.
6. Nordemann, U.; Wifling, D.; Schnell, D.; Bernhardt, G.; Stark, H.; Seifert, R.; Buschauer, A. Luciferase reporter gene assay on human, murine and rat histamine H4 receptor orthologs: correlations and discrepancies between distal and proximal readouts. *PLoS One* **2013**, 8, e73961.
7. Cheng, Y.; Prusoff, W. H. Relationship between the inhibition constant (K1) and the concentration of inhibitor which causes 50 per cent inhibition (I50) of an enzymatic reaction. *Biochem. Pharmacol.* **1973**, 22, 3099-3108.
8. Seifert, R.; Hageluken, A.; Hoer, A.; Hoer, D.; Grunbaum, L.; Offermanns, S.; Schwaner, I.; Zingel, V.; Schunack, W.; Schultz, G. The H1 receptor agonist 2(3-chlorophenyl)histamine activates Gi proteins in HL-60 cells through a mechanism that is independent of known histamine-receptor subtypes. *Mol. Pharmacol.* **1994**, 45, 578-586.
9. Strasser, A.; Wittmann, H. J.; Kunze, M.; Elz, S.; Seifert, R. Molecular basis for the selective interaction of synthetic agonists with the human histamine H1-receptor compared with the guinea pig H1-receptor. *Mol. Pharmacol.* **2009**, 75, 454-465.
10. Pertz, H. H.; Gornemann, T.; Schurad, B.; Seifert, R.; Strasser, A. Striking differences of action of lisuride stereoisomers at histamine H1 receptors. *Naunyn Schmiedebergs Arch. Pharmacol.* **2006**, 374, 215-222.
11. Appl, H.; Holzammer, T.; Dove, S.; Haen, E.; Strasser, A.; Seifert, R. Interactions of recombinant human histamine H(1)R, H(2)R, H(3)R, and H(4)R receptors with 34 antidepressants and antipsychotics. *Naunyn Schmiedebergs Arch. Pharmacol.* **2012**, 385, 145-170.
12. Wittmann, H. J.; Seifert, R.; Strasser, A. Contribution of binding enthalpy and entropy to affinity of antagonist and agonist binding at human and guinea pig histamine H(1)-receptor. *Mol. Pharmacol.* **2009**, 76, 25-37.
13. Bakker, R. A.; Nicholas, M. W.; Smith, T. T.; Burstein, E. S.; Hacksell, U.; Timmerman, H.; Leurs, R.; Brann, M. R.; Weiner, D. M. In vitro pharmacology of clinically used central nervous system-active drugs as inverse H(1) receptor agonists. *J. Pharmacol. Exp. Ther.* **2007**, 322, 172-179.
14. Seifert, R.; Wenzel-Seifert, K. Constitutive activity of G-protein-coupled receptors: cause of disease and common property of wild-type receptors. *Naunyn Schmiedebergs Arch. Pharmacol.* **2002**, 366, 381-416.
15. Burstein, E. S.; Spalding, T. A.; Brann, M. R. Pharmacology of muscarinic receptor subtypes constitutively activated by G proteins. *Mol. Pharmacol.* **1997**, 51, 312-319.

Chapter 6

Summary

Previously, our workgroup applied the bivalent ligand approach for the H_2R by linking two acylguanidine moieties. This led to highly potent and selective H_2R agonists. However, the acylguandines turned out to decompose upon long-term storage in aqueous solution, in particular under alkaline conditions. Based on this preceding work, the medicinal chemistry part of this thesis deals with the synthesis of stable bivalent H_2R agonists in which the acylguanidine group was replaced by a bioisosteric carbamoylguanidine moiety. With respect to studying the mode and stoichiometry of binding of such bivalent compounds, the synthesis of a chain-branched dimeric ligand, enabling radio- and fluorescence labeling was considered.

The prepared compounds were investigated in GTPγS binding assays on recombinant human and guinea pig H_2R and by radioligand competition binding on human H_1, H_2, H_3 and H_4 receptors expressed in *Sf9* insect cells. Moreover, representative compounds were studied on human monocytes, with regard to cAMP formation and the inhibition of fMLP induced reactive oxygen species.

The bivalent carbamoylguanidine-type H_2R ligands proved to be high affinity H_2R agonists, equipotent with the corresponding carba analogs, the acylguanidines. Achieving up to 2500 times the potency of histamine, these compounds are among the most potent H_2R agonists known so far. Unlike the imidazole-type compounds, the bioisosteric aminothiazoles proved to be selective for the H_2R over the other histamine receptor subtypes. Although the “cold” version of a synthesized propionamide derivative proved to be a potent and selective H_2R agonist, the corresponding tritiated analog, due to a high degree of unspecific binding, was not applicable to saturation binding studies, making the determination of the number of binding sites impossible. Unfortunately, the fluorescently labeled ligands entered the cells in an H_2R-independent manner.

In human monocytes the investigated compounds induced cAMP accumulation and inhibited the fMLP-induced ROS production in a highly potent manner so that such compounds represent a good starting point for the development of selective H_2R drugs for the treatment of AML.

The bioisosteric and bivalent approach led to highly potent, selective and stable H_2R agonists that proved to be useful pharmacological tools for functional studies on recombinant receptors and native cells. Regarding the bioanalytical and toxicological properties of the bivalent ligands, compounds bearing a short spacer should be preferred for future in-vivo studies.

The second part of this work aimed at the establishment of cell-based functional assays for the discrimination between alternative signaling pathways activated by H_xR stimulation. For this purpose, HEK293T CRE Luc cells were stably transfected with the cDNA encoding the hH_1R or the hH_2R, respectively. The transfectants were investigated in a luciferase reporter gene assay, in a fura-2 assay and in an aequorin assay. Moreover, a TR-FRET based cAMP assay was applied.

The activation of the H_1R led to an increase in the transcription of luciferase. In the presence of the selective $G\alpha_q$ inhibitor UBO-QIC the luciferase expression was reduced, whereas in combination with UBO-QIC and PKA inhibitors (Rp-cAMP-S and Rp-8-Br-cAMP-S) the luciferase activity was almost completely inhibited. The data obtained from the luciferase reporter gene assay suggested that the luciferase expression, mediated by the H_1R, was at

least in part mediated by cAMP. Furthermore, it was shown that cells preincubated with UBO-QIC were no longer capable of triggering a Ca^{2+} signal in the aequorin assay, upon activation of the H_1R. Detection of a cAMP signal failed most probably due to a low signal-to-noise ratio, hence it should be taken into consideration that the activation of the hH_1R is associated with additional pathways.

The H_2R revealed high constitutive activity in the luciferase reporter gene assay, probably due to a high expression level of the receptor in the cells. In the presence of UBO-QIC the luciferase activity was reduced. Additionally, it was shown in both Ca^{2+} assays that the activation of the H_2R led to a $G\alpha_q$ mediated Ca^{2+} response.

The data indicate that, regardless of preferential coupling of hH_1R and hH_2R to $G\alpha_q$ and $G\alpha_s$, respectively, both receptors are capable of triggering differential signaling pathways, at least in genetically modified cells. In general, the stably co-transfected HEK293T CRE Luc cells represent a powerful pharmacological toolkit for:

- The identification of alternative signaling pathways.
- The investigation of GPCRs and the pharmacological characterization of functionally selective ligands.
- The deconvolution of signals from label-free assays.

Chapter 7

Appendix

7.1 NMR spectra of compounds **3.19** and **3.24**

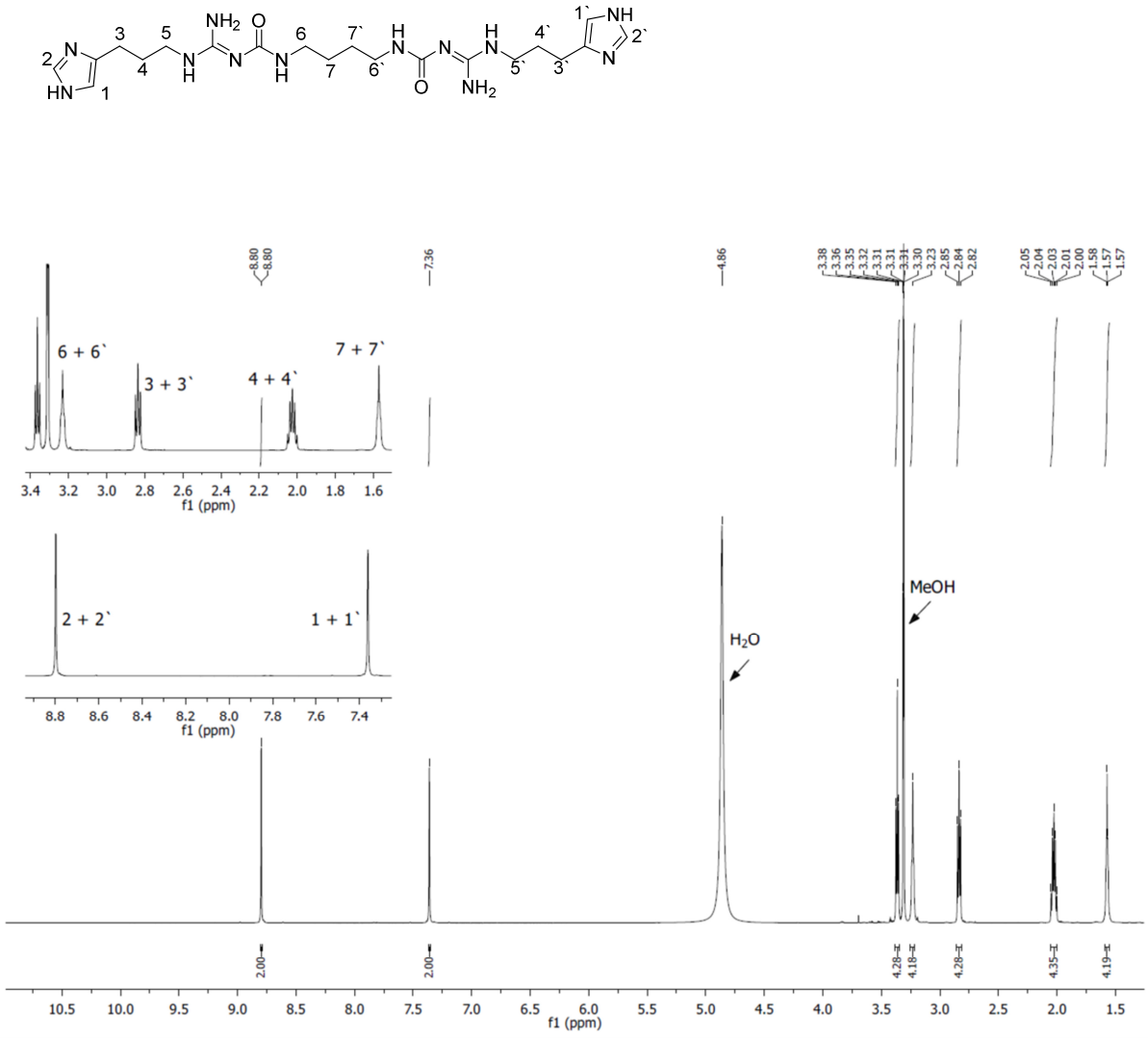

Figure 7.1. ^{1}H NMR spectrum of **3.19**

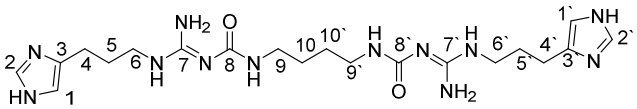

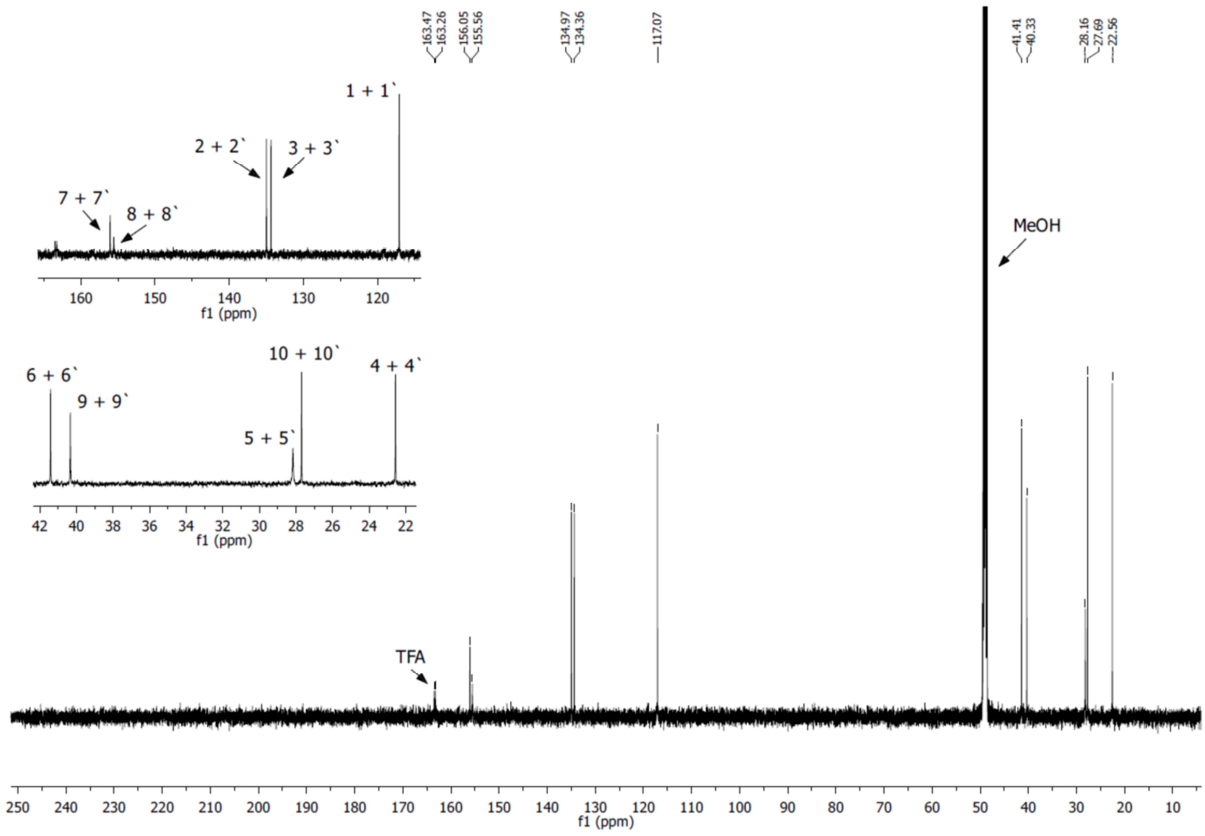

Figure 7.2. ^{13}C NMR spectrum of **3.19**

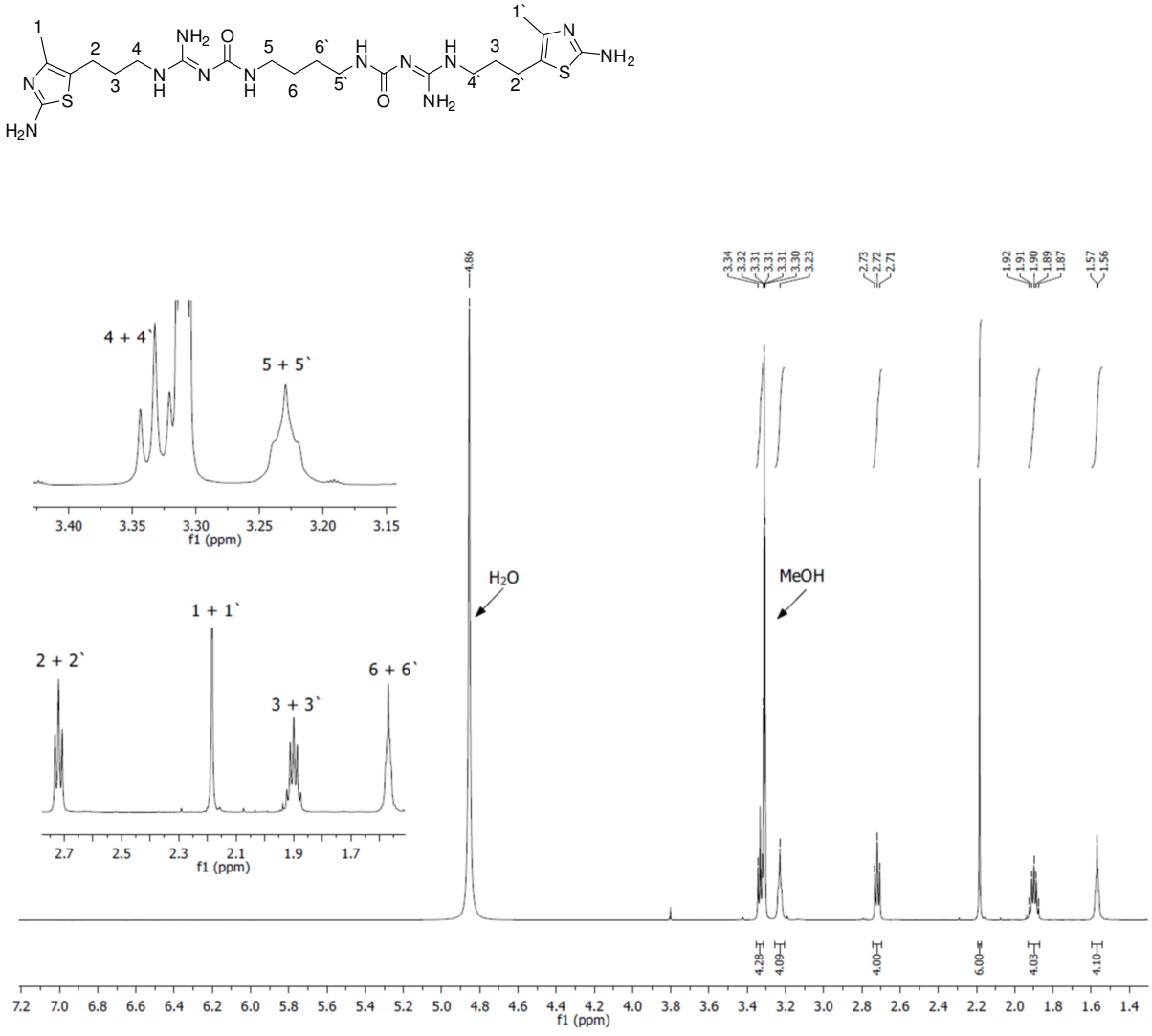

Figure 7.3. ^{1}H NMR spectrum of **3.24**

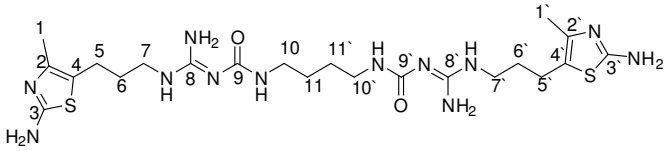

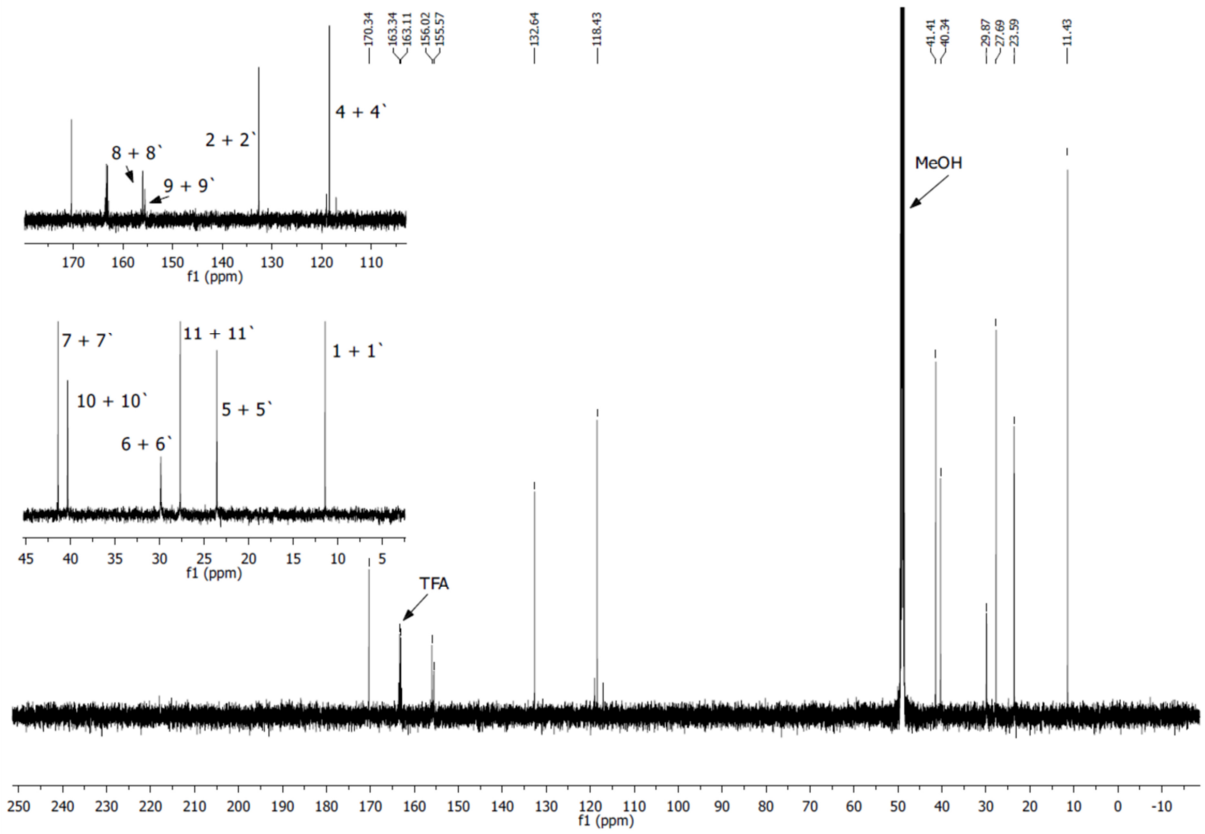

Figure 7.4. ^{13}C NMR spectrum of **3.24**

7.2 RP-HPLC chromatograms of compounds **3.19-3.28**, **3.39-3.42**, and **3.43a**

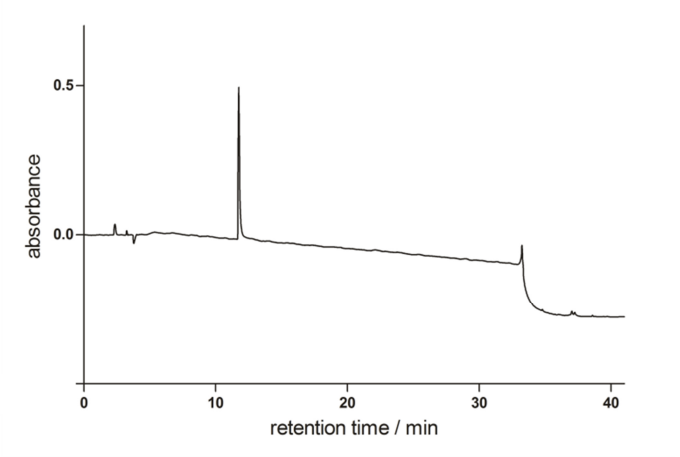

Figure 7.5. Chromatogram of **3.19**

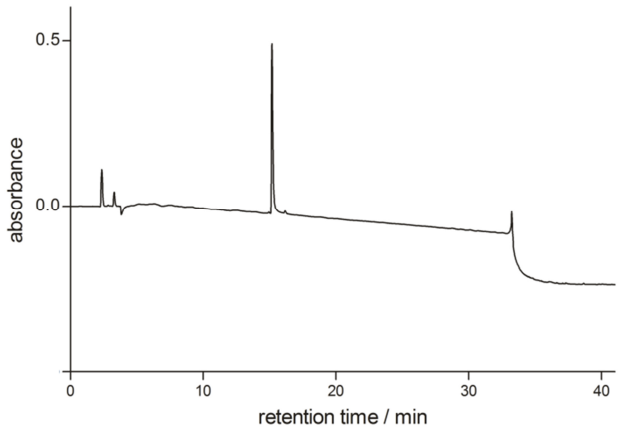

Figure 7.6. Chromatogram of **3.20**

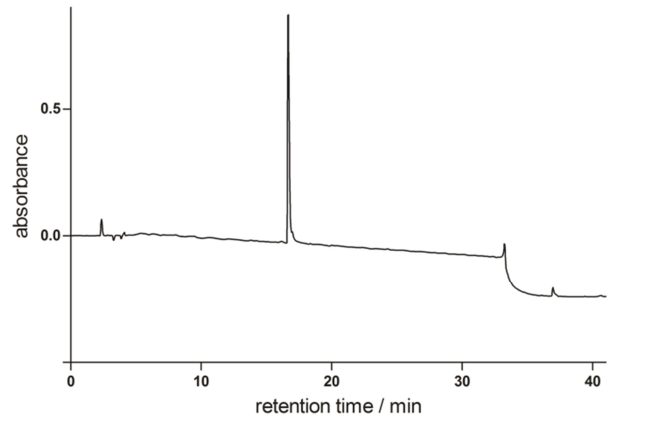

Figure 7.7. Chromatogram of **3.21**

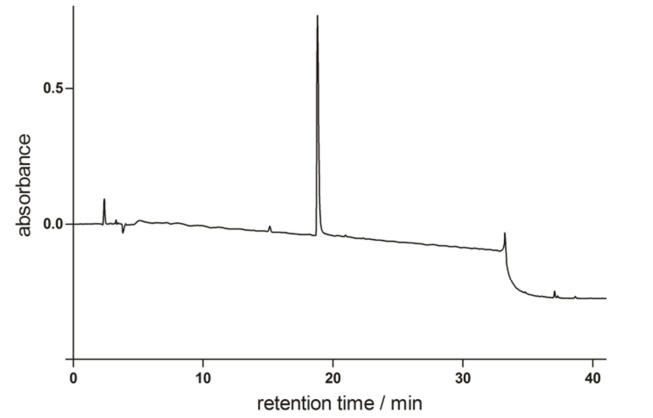

Figure 7.8. Chromatogram of **3.22**

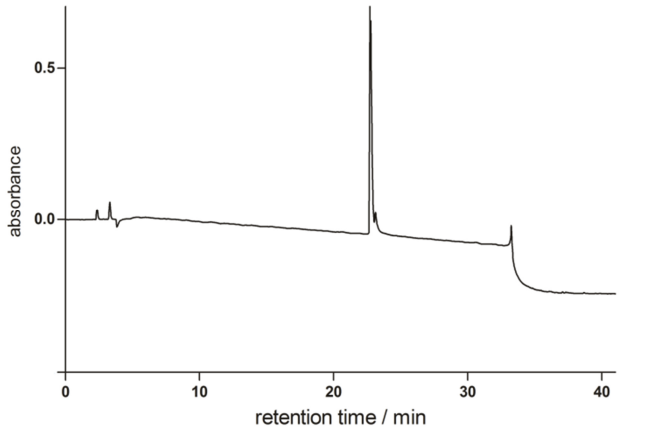

Figure 7.9. Chromatogram of **3.23**

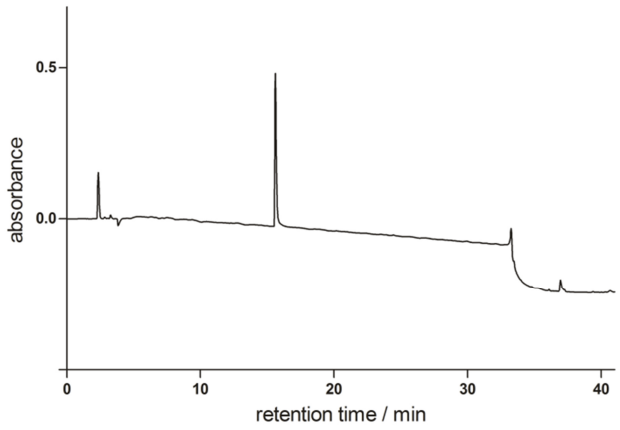

Figure 7.10. Chromatogram of **3.24**

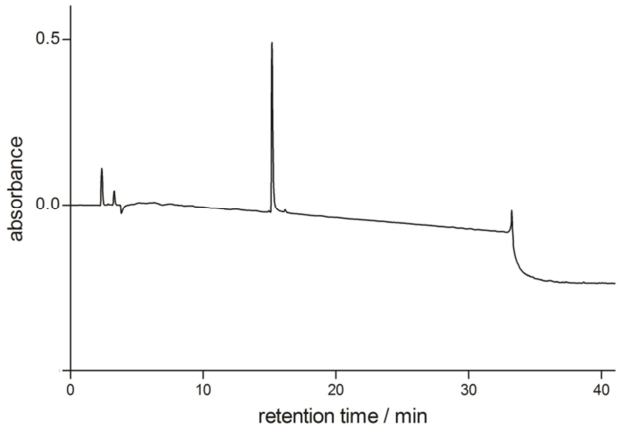

Figure 7.11. Chromatogram of **3.25**

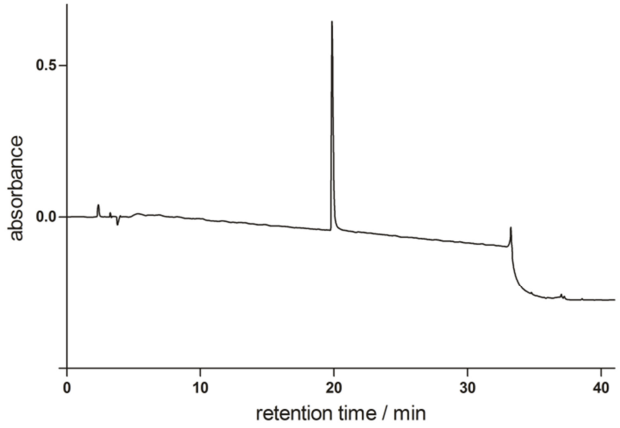

Figure 7.12. Chromatogram of **3.26**

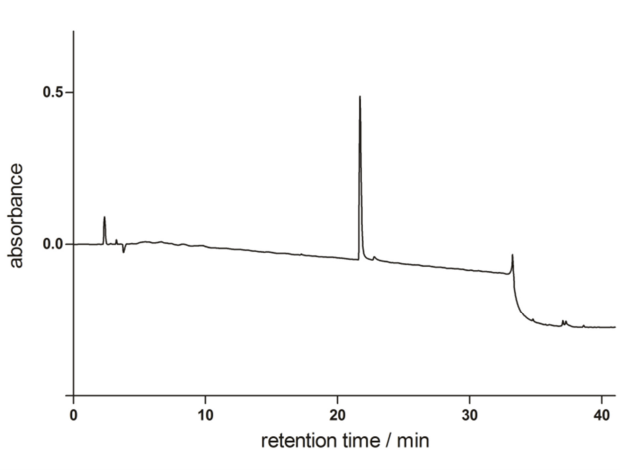

Figure 7.13. Chromatogram of **3.27**

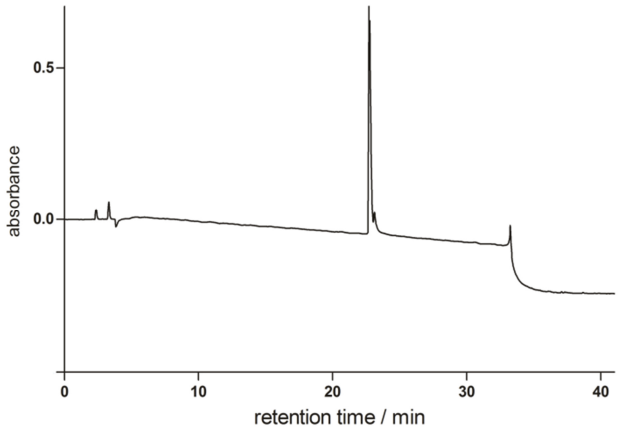

Figure 7.14. Chromatogram of **3.28**

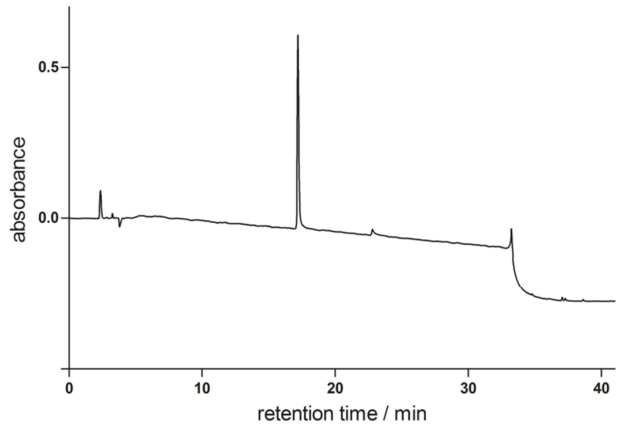

Figure 7.15. Chromatogram of **3.39**

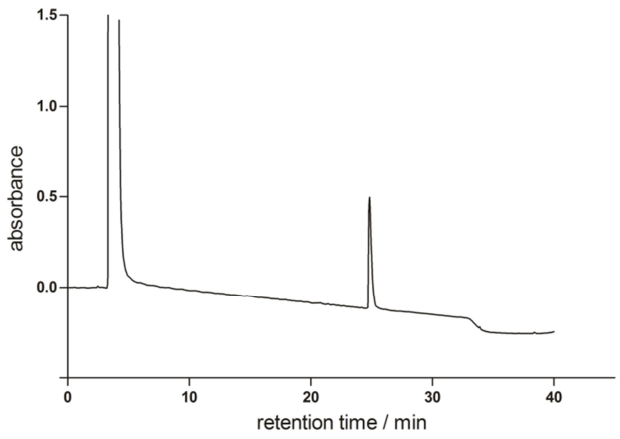

Figure 7.16. Chromatogram of **3.40**

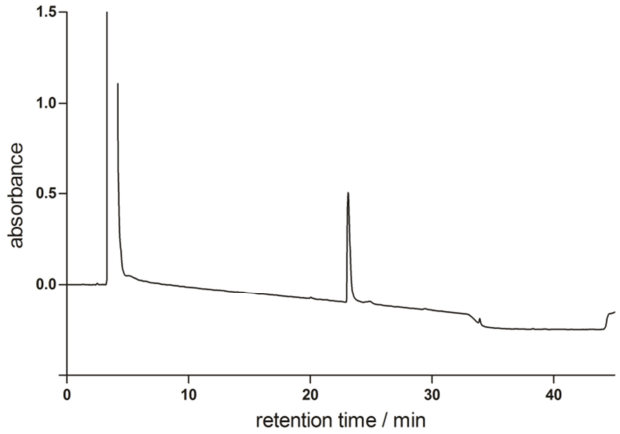

Figure 7.17. Chromatogram of **3.41**

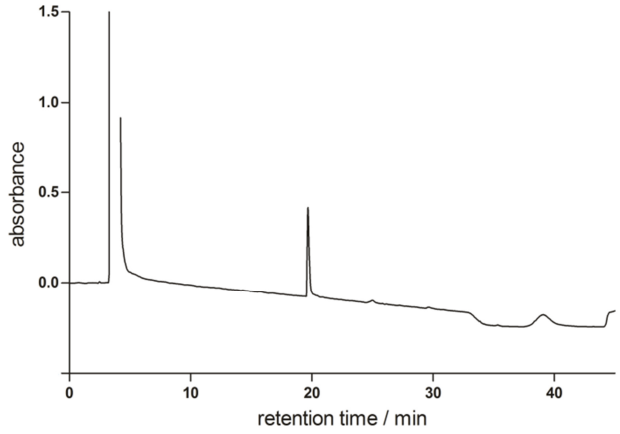

Figure 7.18. Chromatogram of **3.42**

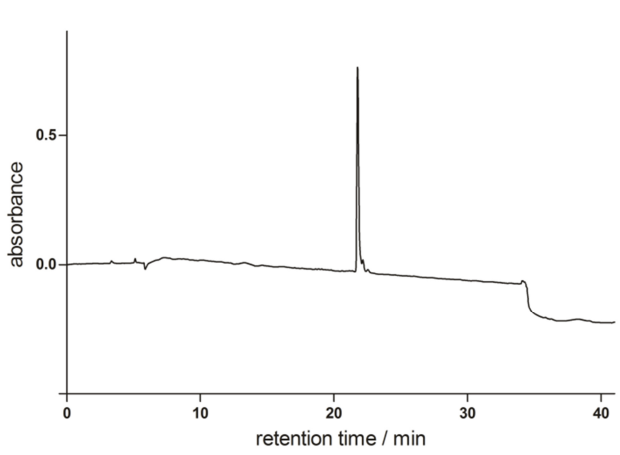

Figure 7.19. Chromatogram of **3.43a**

Abbreviations

Å	Ångström
abs	absolute
AC	adenylyl cyclase
ADP	adenosine diphosphate
α_{1B}-AR	α_{1B} adrenoceptor
α_{1D}-AR	α_{1D} adrenoceptor
AML	acute myeloid leukemia
EBAO	ethidium bromide/acridin orange
APCI	atmospheric-pressure chemical ionization
aq.	aqueos
ATP	adenosine triphosphate
BB	binding buffer
Boc	*tert*-butoxycarbonyl
BSA	bovine serum albumin
CaM-kinase	calcium/calmodulin-dependent protein kinase
cAMP	cyclic adenosine monophosphate
CHO	chinese hamster ovary
CNS	central nervous system
conc	concentrated
CRE	cAMP response element
CREB	cAMP response element binding protein
CREM	cAMP response element modulator
d	day(s) or doublet
D_1R	dopamine 1 receptor
D_2R	dopamine 2 receptor
DAO	diamine oxidase
DCM	dichloromethane
δ-OR	δ opioid receptor
DIAD	diisopropyl azodicarboxylate
DIPEA	diisopropylethylamine
DMAP	4-(dimethylamino)pyridine
DMEM	Dulbecco's modified eagle medium
DMF	dimethylformamide
DMSO	dimethylsulfoxide
DTT	dithiothreitol

EA	ethylacetate
EC_{50}	molar concentration of the agonist causing 50 % of the maximal response
ECL	extracellular loop
EDTA	ethylenediaminetetraacetic acid
EGTA	ethylenglycol-bis(aminoethylether)-N,N,N′,N′-tetraessigsäure
E_{max}	maximal response relative to histamine (1.00)
eq	equivalents
ESI	electrospray ionisation
Et_2O	diethyl ether
EtOH	ethanol
FCS	fetal calf serum
fMLP	formyl-methionyl-leucyl-phenylalanine
FRET	fluorescence resonance energy transfer
FSK	forskolin
GABA	γ-aminobutyric acid
GDP	guanosine diphosphate
GF/C	a glass fibre filter grade
gp	guinea pig
GPCR	G-protein coupled receptor
GRK	G-protein coupled receptor kinase
GTP	guanosine triphosphate
GTPγS	guanosine 5'-thiotriphosphate
h	hour(s) or human
H_1R	histamine H_1 receptor
H_2R	histamine H_2 receptor
H_2R-$G_s\alpha_s$	fusion protein of the H_2R and the short splice variant of $G_s\alpha$
H_3R	histamine H_3 receptor
H_4R	histamine H_4 receptor
HDC	histidine decarboxylase
HEK	human embryonic kidney
hex	hexane
HIS	histamine
HL60	human promyelocytic leukemia cells
HNMT	histamine *N*-methyltransferase
HPLC	high performance liquid chromatography
HRMS	high resolution mass spectrometry

H_xR	histamine receptors
IBMX	3-isobutyl-1-methylxanthine
ICER	inducible cAMP early repressor
IL2	Intracellular loop 2 or interleukin 2
IP_3	inositol-1,4,5-trisphosphate
J	coupling constant
k	capacity factor
κ-OR	κ opioid receptor
K_d	dissociation constant (saturation binding)
Luc	luciferase
m	multiplet
M_2R	muscarinic M_2 receptor
M_3R	muscarinic M_3 receptor
MeCN	acetonitrile
MeOD	deuterated methanol
MeOH	methanol
min	minute(s)
mp	melting point
m-RNA	Messenger ribonucleic acid
mtAeq	mitochondrial targeted aequorin
μOR	μ opioid receptor
NADPH	nicotinamide adenine dinucleotide phosphate
n-BuLi	*n*-butyllithium
NHS	N-hydroxysuccinimide
NK cells	natural killer cells
NMR	nuclear magnetic resonance
PBS	phoshpate buffered saline
PCR	polymerase chain reaction
PE	petrol ether
pEC_{50}	negative decadic logarithm of the molar concentration of the agonist causing 50 % of the maximal response
PEI	polyethyleneimine
pK_a	negative decadic logarithm of the acid dissociation constant
PKA	protein kinase A
pK_b	negative decadic logarithm of the dissociation constant (functional assay)
pK_i	negative decadic logarithm of the dissociation constant (competition

	binding)
PLA_2	phospholipase A2
PLC	phospholipase C
Pot_{rel}	relative potency
ppm	parts per million
PTX	pertussis toxin
q	quartet
R	receptor
RGS	regulator of G-protein signaling
ROS	reactive oxygen species
s	singulet
SEM	standard error of the mean
Sf9	Spodoptera frugiperda
$ß_1$-AR	β1 adrenoceptor
$ß_2$-AR	β2 adrenoceptor
t	triplet
TFA	trifluoroacetic acid
THF	tetrahydrofuran
TM	transmembrane
t_0	dead time
t_R	retention time
TR-FRET	time-resolved fluorescence resonance energy transfer

Ich erkläre hiermit an Eides statt, dass ich die vorliegende Arbeit ohne unzulässige Hilfe Dritter und ohne Benutzung anderer als der angegebenen Hilfsmittel angefertigt habe; die aus anderen Quellen direkt oder indirekt übernommenen Daten und Konzepte sind unter Angabe des Literaturzitats gekennzeichnet.

Regensburg,

Nicole Plank